Antibacterial Compounds from Bacteria Isolated from Hot Springs Water in Saudi Arabia

Thesis submitted by

Omaish Salman O. ALQAHTANI

for the PhD degree in Pharmacy

University College London

December 2020

I

Declaration

"I, Omaish Alqahtani, confirm that the work presented in this thesis is my own. Where information has been derived from other sources, I confirm that this has been indicated in the thesis."

_____

Abstract

Recently, the emergence of antimicrobial-resistant bacterial infections has been considered one of the global health crises that threaten communities. The rise and dissemination of resistance within bacterial pathogens make the effectiveness of antibiotics decline gradually over time. As a result, the search for novel antibiotics from different natural sources has increased. Some microorganisms are able to produce secondary metabolites for protection. Bacteria, for example, have the ability to yield antibiotics. One important habitat that has yet to be fully exploited for antibiotic-producing bacteria is geothermal springs. Hot springs have been used for spas as well as for treating dermatological infections.

Thirty-two water samples were collected from six different hot springs in Saudi Arabia. Several biological and microbiological assays were used to assess the antibacterial activities of samples against antimicrobial-resistant- and susceptible-bacterial strains and identify the genus and species of antibiotic-producing bacteria. Moreover, chromatographic and spectroscopic techniques were utilized to isolate the active compounds, and aid structural elucidation.

The cross-streak assay's findings illustrated that there were 14 bacteria with antimicrobial activities against most of the resistant- and susceptible-bacterial strains. 16S rRNA gene sequencing demonstrated that all antibiotic-producing bacteria to be *Bacillus* species; *Bacillus paralicheniformis* (6), *Bacillus licheniformis* (2), *Bacillus pumilus* (5) and *Bacillus cereus* (1). Seven compounds were isolated from these bacteria: five of which were known and two compounds were novel. The outcomes of MIC assay showed that all isolated compounds had mild to moderate antibacterial activities (between 128 µg/mL and 512 µg/mL in compared to the control) against all tested strains except for one

compound (cholesterol **(OM2)**), which had no activity. The other known compounds were phenylacetic acid **(OM7)**, isovaleric acid **(OM4)**, ethyl-4-ethoxybenzoate **(OM5)** and *N*-acetyltryptamine **(OM1)**. The two new compounds were N^1-(*N,N*-dimethylcarbamimidoyl)-N^1-methylterephthalamide **(OM3)** that belongs to the guanidine class of antibiotics, which are commonly isolated from microbes and 3-methyl-*2H,7H*-pyrano[*2,3-b*]pyran-2,7-dione **(OM6),** coumarin-like structures, which are also known for their antibacterial activities.

In summary, this is the first study to investigate antibiotic-producing bacteria from hot thermal springs in Saudi Arabia. Screening revealed the propensity to isolate *Bacillus* spp., which are known to produce antibiotics in other habitats, particularly soil and aquatic environments. New compounds of known antibacterial classes could be isolated illustrating the potential of hot thermal springs as a source of discovering antibiotics.

Impact statement

Lately, the universal health crisis that threatens communities has been attributed to the emergence of resistant bacterial infections. The occurrence of multidrug resistance is considered as a global economic and healthcare crisis; it is also regarded as one of the top 3 threats to international public health listed by the World Health Organization. Searching for novel antibiotics from different natural sources is an effective way to tackle the resistant pathogens. Bacteria are regarded as an essential source for discovering novel antibiotics, specifically from harsh environments, but thermal springs have yet to be fully exploited.

In this study, compounds were isolated from different *Bacillus* species found in hot springs in Saudi Arabia, two of which were novel compounds. These agents demonstrated mild to moderate antibacterial activities.

This thesis provides new insight into the potential of thermal springs to yield antibiotic-producing bacteria. The findings suggest that the isolated compounds could provide a suitable scaffold for the design and development of compounds that are able to inhibit the bacterial growth of pathogenic multidrug-resistant strains.

Acknowledgments

I would like to express my sincere appreciation and heartfelt gratitude to my primary supervisor Prof. Simon Gibbons for his keen and continuous interest, valuable suggestion, support and guidance throughout this project.

My sincere gratitude also goes to my secondary supervisor Dr. Paul Stapleton for his assistance, knowledge and expertise in microbiology throughout this project.

Many thanks to Prof. Michael Munday for his supervision and assistance during this project's last year.

Many thanks to Prof. Matthew Todd and Dr. Jeoffrey Wells for their assistance during this project's last year.

 I am greatly indebted to my colleagues and lab mates for their valuable assistance during the project.

My special thank goes to Najran University for the sponsorship that made this work possible and also for the opportunity to study this programme at this university.

My big thanks to my family and friends who supported me directly or indirectly throughout my study.

Table of contents

List of Figures

List of Tables

Abbreviations

A	Absorbance
A.	*Acinetobacter*
ABC	ATP-Binding Cassette family
AHL	Acyl Homoserine Lactone
AMR	Anti-Microbial Resistance
ATP	Adenosine TriPhosphate
B.	*Bacillus*
bp	Base Pair
°C	Celsius
C.	*Calderobacterium*
D.	*Deinococcus*
CDC	Centers for Disease Control and Prevention
CFU	Cell for unit
CM	Cytoplasmic Membrane
DAP	diaminopimelic acid
DNA	Deoxyribonucleic acid
$	Dollar (USA)
E. coli	*Escherichia Coli*
ECDC	European Center for Disease Prevention and Control
ESBL	Extended-Spectrum Beta-Lactamases
g	Gram
G20	Group of Twenty
h	Hours
H.	*Hydrogenobacter*
H_2S	Hydrogen sulfide
K.	*Klebsiella*
Kb	Kilo of Base pair
km	Kilometer
KSA	Kingdom of Saudi Arabia
LPS	Lipopolysaccharide
M	Meter
MATE	Multidrug and Toxic compounds Extrusion family
MDR	Multi-Drug Resistance
MDR-TB	Multi-Drug Resistant Tuberculosis
MFS	Major Facilitator Superfamily
mL	Milliliter
mg	Milligram
min.	Minute

MIC	**Minimum inhibitory concentration**
mRNA	**Messenger RiboNucleic Acid**
MRSA	**Methicillin Resistant-*S. aureus***
MTT	**3-(4,5 dimethylthizol-2-yl)-2,5-diphenyltetrazolium bromide**
NAM	**N-acetylmuramic acid**
NAG	**N-acetylglucosamine**
nm	**Nanometer**
NTS	**Non-Typhoidal *Salmonella***
OM	**Outer Membrane**
P.	***Pseudomonas***
pbp	**penicillin-binding protein**
PBS	**Phosphate buffer saline**
PMF	**Proton Motive Force**
R&D	**Research and Development**
RND	**Resistance-Nodulation-Division family**
rRNA	**Ribosomal RiboNucleic Acid**
S. aureus	***Staphylococcus aureus***
SCC*mec*	**staphylococcal cassette chromosome *mec* gene**
SMF	**Submerged Fermentation**
SMR	**Small Multidrug Resistance family**
SPE	**Solid Phase Extraction**
Spp.	**Species**
SSF	**Solid-State Fermentation**
%	**Percentage**
T.	***Thermotoga***
tRNA	**Transfer RiboNucleic Acid**
µg	**Microgram**
µL	**Microliter**
µm	**Micrometer**
µM	**Micromolar**
UK	**United Kingdom**
UN	**United nations**
USA	**United States of America**
VRE	**Vancomycin-Resistant Enterococci**
WHO	**World Health Organization**
WGS	**Whole Genome Sequencing**
XDR	**Extensively-Drug Resistance**
XDR-TB	**Extensively Drug-Resistant Tuberculosis**

1 Introduction

1.1 An overview of antibiotic resistance

The definition of antibiotic resistance can be made from two different viewpoints; clinical and microbiological definitions. Microbiologically, bacteria can be classified into resistant or susceptible depending on the likelihood of curing the infections they produce (Martinez, 2014). Clinically, antibiotic resistance is a level of antibiotic activity associated with a high possibility of a therapeutic failure (MacGowan and Macnaughton, 2017). It is thought that antibiotic resistance has an ancient origin before using antibiotics. For example, various antimicrobial resistance genes dating back over 30,000 years were discovered from permafrost sediments in the Yukon Territory in Canada in 2011 by a research team from McMaster University (Rolain *et al.*, 2016). Furthermore, genes encoding for β-lactamases were found in one Alaskan soil, where anthropogenic actions are minimum (Marti *et al.*, 2014). In addition, DNA isolated from Beringian permafrost (30,000-year-old) included resistance genes for glycopeptides, tetracyclines and β-lactams, emphasizing that antibiotic resistance existed before the use of antibiotics in medicine and agriculture (Skandalis *et al.*, 2021). In fact, it is estimated that the genesis of natural product antibiotics ranges from 40 million to 2 billion years, which suggests that antibiotic resistance might be ancient (Cruz-Loya *et al.*, 2019).

Recently, the emergence of antimicrobial-resistant bacterial infections has been considered one of the global health crises that threaten communities (Khameneh *et al.*, 2016). The emergence and dissemination of resistance within bacterial pathogens make antibiotics' effectiveness decline gradually over time (Rossolini *et al.*, 2014). Globally, 700,000 patients die from drug-resistant infections each year (Singh *et al.*, 2021).

In May 2016, the Review on Antimicrobial Resistance published a report that estimates that the current annual deaths due to antimicrobial-resistant infections may expand to 10 million by 2050 if no action is taken (Balcázar, 2020). This might lead to a rise in the cost of lost worldwide production to the US $100 trillion from now until that time (Robinson *et al.*, 2016). This may imply how dangerous antibiotic resistance will be in the future in both the medical and economic sectors. From an economic standpoint, the medical costs of antimicrobial resistance for each patient per year are between $18,000 and $29,000 in the USA alone (Thabit *et al.*, 2015). Furthermore, the latest reports, published by the World Economic Forum Global Risks, have highlighted that antibiotic resistance is regarded as the biggest menace to human health (Blair *et al.*, 2015). Moreover, it is estimated that 2.4 million people will die from the drug-resistant infections in North America, Australia and Europe during the next 30 years and this might cost up to $3.5 billion per a year according to the latest report by Organization for Economic Co-operation and Development (OECD) (Singh *et al.*, 2021).

In the USA in 2017, 35,000 people died directly because of antibiotic-resistant infections; however, 2.8 million people have severe infections with pathogens resistant to at least one antibiotic utilized for curing these infections based on the Centers for Disease Control and Prevention (CDC) (Skandalis *et al.*, 2021). Depending on recent data from the European Medicines Agency and the European Centre for Disease Prevention and Control, 25,000 European people die from infections caused by antibiotic-resistant bacteria every year (Balcázar, 2020).

It has become evident that the extended use and misuse of antimicrobial agents in human and veterinary medicine as well as in agriculture have led to the spread of highly resistant bacterial strains worldwide (Tyrrell *et al.*, 2019). As an example, the WHO

demonstrated that *Campylobacter* resistance to many antibacterial drugs is probably connected to the consumption of infected poultry in several regions of the world in 2013 (Lobanovska and Pilla, 2017). Additionally, self-medication, poor prescription by doctors, overuse of antibiotics in husbandry and agriculture as well as not finishing an antibiotic course prescribed by the doctor are examples of misuse of antibiotics (Kolivand and Kolivand, 2017). Moreover, poor hygiene and sanitation in hospitals and communities, inter-species gene transmission and the growing rate of universal trade, travel and disease transmission play a pivotal role in facilitating the spread of resistant bacteria around the world (Mweetwa *et al.*, 2021).

Self-medication is regarded as an essential source for making bacteria resistant to antibacterial agents in humans and can be defined as the use of antibiotics without prescription or the taking of another person's advice who is not a medical practitioner (Rather *et al.*, 2017). According to Alghadeer *et al.* (2018), the purchase of antibiotics without prescription is expected to be around 47% in Southern Europe, 30% in Eastern Europe, 58% in Asia, 39% in the Middle East and 25% in South America. These numbers indicate how antibiotics are used around the world without any control or supervision. Furthermore, antimicrobial agents are one of the most popular prescribed drugs utilized in human medicine, even though approximately 50% are considered unnecessary (Holmes *et al.*, 2016). Consequently, antimicrobial resistance has spread worldwide because of the misuse and overuse of antibiotics (Holmes *et al.*, 2016). Additionally, the easy access and low cost of antibiotics have aided in their misuse and overuse (Fernandes and Martens, 2017).

The WHO has listed seven bacteria of international concern*; Klebsiella pneumoniae*, *Escherichia. coli*, *Staphylococcus aureus*, non-typhoidal *Salmonella* (NTS),

Neisseria gonorrhoeae, *Shigella* species and *Streptococcus pneumoniae* (Chaudhary, 2016). For instance, there are 19,000 deaths a year just in the USA due to methicillin-resistant *Staphylococcus aureus* (MRSA) (Khameneh *et al*., 2016). Moreover, trends in the resistance of *Enterococcus faecium*, *Acinetobacter baumannii*, *Enterobacter* spp. and *Pseudomonas aeruginosa* represent an exceptionally worrying trend around the globe (Aminov, 2017).

One of the challenges in the production of effective antimicrobial agents is that antibiotic resistance has evolved over time from resistance to one class of antibiotics to multidrug-resistance and extreme-drug-resistance (Marti *et al*., 2014). The occurrence of multidrug-resistance is considered a global economic and healthcare crisis; it is also regarded as one of the top 3 threats (cancer and cardiovascular diseases) to international public health that has been listed by the WHO (Brooks and Brooks, 2014). This threat has also been confirmed by different global organizations such as the WHO, ECDC and CDC (Roca *et al*., 2015). Based on the WHO, *Klebsiella pneumoniae* has shown resistance against cephalosporins and carbapenems as well as *Escherichia coli* against antibiotics such as cephalosporins and fluoroquinolones (Tanwar *et al*., 2014). In addition, it has been found that multi-resistant *E. coli* has a higher mortality rate in comparison to susceptible *E. coli* (MacGowan and Macnaughton, 2017). These are some examples of MDR in the world.

It is believed that the most significant risk of multidrug resistance comes from Gram-negative organisms, on which new antibiotics remain poorly active. (Pidot *et al*., 2014). For instance, increasing levels of resistance to polymyxin B and colistin in Gram-negative bacteria have been reported from various countries worldwide, including Greece, Italy, Saudi Arabia and South Korea (Laxminarayan *et al*., 2013). *P. aeruginosa*

is considered the first bacterium that exhibited XDR and MDR phenotypes to all classes of anti-pseudomonal agents besides polymyxins (Rossolini *et al.*, 2014). Moreover, 400,000 people were infected with multidrug-resistant pathogens, which led to approximately 25,000 deaths in 2007 in Europe (Hwang and Gums, 2016). 480,000 new cases of multidrug-resistant tuberculosis (MDR-TB) were discovered in 2013 as well as extensively drug-resistant tuberculosis (XDR-TB) has been found in 100 countries based on World Health Organization data (WHO) (Chellat *et al.*, 2016).

In addition, increasing antimicrobial resistance has affected the efficacy and safety of immunosuppressive chemotherapy and surgical procedures; for instance, 26.8% of organisms that cause infections after chemotherapy as well as 50.9% of bacteria that cause surgical site infections are resistant to standard prophylactic antibiotics in the USA (Friedman *et al.*, 2016).

The resistance to sulfonamides **(Figure 1.1)** in the late 1930s and penicillin **(Figure 1.1)** in the 1940s were considered the first cases of antimicrobial resistance (Alanis, 2005). Antimicrobial resistance can be found in both the community and hospital, which leads to the appearance of resistant pathogens. Infections from the community are deemed as a source of death for patients. However, health-associated infections are a public health issue that could threaten life (Khameneh *et al.*, 2016). As an example, roughly 90% of hospital-acquired infections are caused by bacteria (Fair and Tor, 2014).
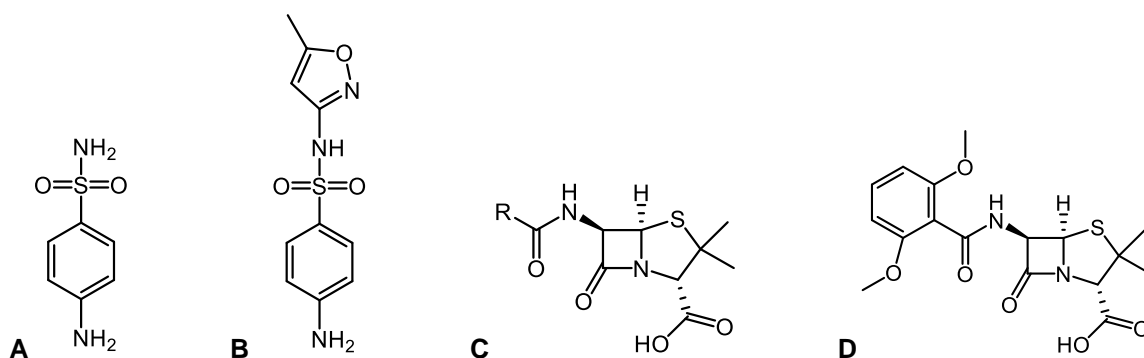
Figure 1.1: Some examples of sulfonamides and penicillins.
A: Sulfanilamide, **B:** Sulfamethoxazole, **C:** Penicillin, **D:** Methicillin.

Antibiotic resistance can be evolved through four main genetic 'reactors', which are illustrated in **Table 1.1.**

Table 1.1: The main genetic reactors for antibiotics resistance (Ghernaout and Elboughdiri, 2020).

Reactor	Example
The primary reactor	Human microbiota Animal microbiota
The secondary reactor	Farms Aquaculture Hospitals Long-term care facilities
The tertiary reactor	Wastewater Effluents Compost toilets Lagoons Biological residues Sewage treatment plants
The fourth reactor	Soil sediments Groundwater environments Surface

One of the main issues in discovering new antibiotics is that pharmaceutical companies' interest and investment have decreased (Zheng *et al.*, 2018). This is because of the rediscovering of known antibiotics (Iorio *et al.*, 2018), the lack of benefits (Rolain *et al.*, 2016) as well as the cost for discovering a novel drug has become more challenging

(Mak and Pichika, 2019). As an example, it is appreciated that the price to develop a new antibiotic drug is approximately $2.6 billion (Jacobs, 2019).

Searching for novel antibiotics from different natural sources has increased as well as an increasing level of research on how bacteria resist drugs in order to understand the mechanism of bacterial resistance and to find suitable treatments (Alrumman *et al.*, 2018). Moreover, educational initiatives, development of therapies, political agendas and legislation are fundamental to alleviate antibiotic resistance's increasing rate (Frieri *et al.*, 2017). For example, Jim O'Neill and colleagues proposed a ten-point plan to the UK government in order to decrease antimicrobial resistance; these points are categorized in **Table 1.2**.

Table 1.2: The proposed plan for decreasing antimicrobial resistance (Lobanovska and Pilla, 2017).

Points	Examples
1- Prevent the spread of infection	Reduction of infection in hospitals and care settings. Expansion of the access to clean water and appropriate sanitation.
2- Public Awareness	Public health programs across the countries.
3- Rapid new diagnostics	Support research and innovation in this area.
4- Use of alternative antimicrobials	Vaccines. Bacteriophage therapy, engineered bacteria, antimicrobial peptides.
5- Reduction of antibiotic use in agriculture	Restriction on the use of highly critical antibiotics in farming. Prevention of antibiotic dissemination into environment.
6- Recognition of researchers in infectious disease	Clear career paths and rewards for scientists in the field.
7- Global surveillance	Major surveillance programs including USA Global Health Security Agenda, UK Fleming Fund, WHO Global AMR Surveillance System. Easy data accessibility around the world.
8- A better investment for new drugs	Governments should find new ways to reward innovation. The link between profit and volume of sales should be reduced.
9- Global Coalition for real action	Joint efforts from G20 and UN are needed. Step change plan to fight AMR has to be redesigned.
10- Global Innovation Fund	Link and expand major initiatives. Fund different projects (e.g., R&D that might lack commercial imperative).

In recent years, many strategies have been established to delay and fight the increasing concerns of antimicrobial resistance such as preventing the misuse of antibiotics, implementing antimicrobial stewardship programs and promoting the discovery of new antimicrobial agents (Hwang and Gums, 2016). Enhancement of antimicrobial therapy, dissipation of antibiotic resistance, reducing hospital expenses and diminishing the occurrence of adverse events are the aims for the majority antimicrobial stewardship systems (Hwang and Gums, 2016).

1.1.1   Types of antibiotic resistance

Generally, bacterial resistance to antibiotics can be classified into three types: intrinsic, acquired and adaptive resistance (Brooks and Brooks, 2014).

1.1.1.1 Intrinsic resistance

Intrinsic resistance can be defined as the ability of bacteria to fight a specific antibiotic's action because of innate structural features; the absence of a target of a specific antibiotic is an example of this kind of intrinsic resistance (Blair *et al.*, 2015). An example of this is *Mycoplasma*, which is resistant to cell wall acting antibacterial drugs due to the absence of a cell wall (Ramalingam, 2015). Additionally, *Pseudomonas aeruginosa* is resistant to several antibiotics because of their low membrane permeability (Purro *et al.*, 2018). Furthermore, the existence of an outer membrane in Gram-negative pathogens makes them resistant to a large number of antibiotics (Courvalin, 2016). Intrinsic resistance does not have the ability to spread horizontally among bacteria; in contrast, it can spread clonally within a bacterial species or among a subpopulation that has a general evolutionary history (Agersø *et al.*, 2019). Moreover, intrinsic resistance relies on the biological properties of bacteria and is specific for some bacteria. For example, *E. coli* demonstrates intrinsic resistance to vancomycin (Khameneh *et al.*,

2016). Additionally, the bacterial genome contains genes that are able to produce a resistance phenotype such as proto-resistance (putative resistance) or quasi-resistance (no/weak phenotype) (Shao *et al.*, 2018). Proto-resistance genes are genes that might have other functions in the cell with little antibiotic resistance capability but have potential to convert to a resistance element whose role is to detoxify antimicrobial drugs (Morar and Wright, 2010). Proto-resistance genes have the ability to provide phenotypic resistance by changes in expression and/or mutation (Perry *et al.*, 2014). Proto-resistance genes might share common ancestry so that resistance genes can act as proto-resistance genes for another drug group such as obtaining the function of aminoglycoside acetyltransferase with quinolone proto-resistance genes (Perry *et al.*, 2014). To clear this, an enzyme that confers resistance to aminoglycosides antibiotics has an ability to expand its activity to quinolone antibiotics without any impact on the aminoglycoside acetyltransferase ability.

1.1.1.2 Acquired resistance

Acquired resistance depends on the mutation of chromosomal DNA and the acquisition of resistance genes from other bacteria (Khameneh *et al.*, 2016). These resistance genes can be found in specific parts of DNA called transposons (O'Neill *et al.*, 2020). Some transposons may include a specific, more complicated DNA fragment called integron (El-Demerdash *et al.*, 2018). Generally, integrons might be carried in plasmids or be chromosomally-integrated, as in the case of *Salmonella enterica* serotype Typhimurium DT 104 (SCENIHR, 2009).

In addition to transposons, plasmids and integrons may also include resistance genes that are able to be transferred to other bacteria, whether of different or similar species (Allen *et al.*, 2010). As Lekunberri *et al.* (2017) stated, the recombination and

acquisition of foreign DNA can be achieved through mobile genetic elements such as plasmids, transposons, bacteriophages, integrative conjugative elements and insertion sequences. An insertion sequence can be defined as a short DNA sequence that works as a transposable element (Ramalingam, 2015). From these elements, a transmissible plasmid is considered the most active mediator that is utilized for horizontal gene transfer by a procedure called conjugation (Khameneh *et al.*, 2016). Acquired resistance can be done by mutation or horizontal transfer of resistance genes between species and strains (Toma and Deyno, 2015).

1.1.1.3 Adaptive resistance

Adaptive resistance is environmentally provoked genetic changes that contain the transformation from a planktonic (floating or drifting) life cycle to a sessile (attached or immobilized) biofilm life cycle (Brooks and Brooks, 2014). Changes such as nutrient concentration changes may cause temporary changes in gene and protein expression levels, which contribute to bacterial resistance (Garneau-Tsodikova and Labby, 2016). Furthermore, bacterial biofilms are regarded as an example of adaptive resistance (Garneau-Tsodikova and Labby, 2016).

Biofilms can be defined as complicated microbial clusters attached to abiotic or biotic surfaces (Soto, 2013). These aggregations of bacteria can live together with a highly structured arrangement and in an organized community (Marti *et al.*, 2014). A bacteria biofilm is composed of proteins, polysaccharides and extracellular DNA (Frieri *et al.*, 2017). Bacterial biofilms can be protected from killing by biocides, antibiotics, immune responses, ultraviolet radiations and adverse conditions such as oxidation, drying, and certain metallic cations (Ramos *et al.*, 2018). It is thought that 65% of all bacterial infections is attributed to the presence of bacterial biofilms (Soto, 2013). Bacteria in

biofilms can communicate with each other by a phenomenon called quorum sensing (Frieri *et al.*, 2017).

Quorum sensing is considered a cell-to-cell communication system that is responsible for the infection, colonization, regulation of virulence factors, biofilm formation, invasion and antibiotic resistance within bacterial populations (Martinez-Klimova *et al.*, 2017). Quorum sensing can be done by two mechanisms: the first being the detection of signals via a cytosolic transcription factor such as acyl homoserine lactone (AHL) derivatives, whereas the other is mediated by auto-inducing signal-like peptides (Nigam *et al.*, 2014). Generally, there are three approaches to suppress quorum sensing: suppression of receptor/ligand interactions, inhibition of autoinducer synthesis and demolition of the auto-inducer by enzymatic degradation and cleavage (Brooks and Brooks, 2014).

1.1.2 Mechanisms of gene transfer

There are three major mechanisms for transferring genes: transformation, conjugation and transduction (Lerminiaux and Cameron, 2019).

1.1.2.1 Transformation

Transformation **(Figure 1.2)** can be defined as a process in which bacteria obtain free DNA from their environment by direct transmission between neighboring bacterial cells (Hall *et al.*, 2017). In this process, antibiotic resistance is achieved through target protein modification by the production of mosaic genes (Blair *et al.*, 2015). For example, *S. pneumoniae* is resistant to penicillin by forming mosaic penicillin-binding protein genes (PBP). Additionally, in MRSA, *S. aureus* resists methicillin by obtaining the staphylococcal cassette chromosome *mec* (SCC*mec*) gene (Blair *et al.*, 2015).

1.1.2.2 Transduction

A method by which the phage components are inserted into bacterial DNA instead of the phage (also known as bacteriophage) is called transduction **(Figure 1.2)** (Van-Hoek *et al.*, 2011). A genetic transfer can be done by utilizing a vector, which is usually a virus (phage) that is capable of infecting bacteria (Alanis, 2005). In this process, the virus adheres and injects its nucleic acids into the bacterial cell, which leads to the introduction of new genes into the bacterial genome (Roe and Pillai, 2003). Transduction can be generalized (any segment of bacterial DNA is transmitted to the phage head) or specialized (a specific set of bacterial DNA near to the insertion site of phage on the chromosome can be packaged) (Van-Hoek *et al.*, 2011). *E. coli*, *A. baumannii*, *P. aeruginosa*, *Vibrio vulnificus*, *K. pneumoniae*, *Salmonella* spp., *Enterococcus faecium* and *S. aureus* are examples of bacteria that depend on bacteriophages (Brooks and Brooks, 2014). Transduction plays a significant role in the exchange of resistant genes with other microbes, particularly in freshwater (Finley *et al.*, 2013).
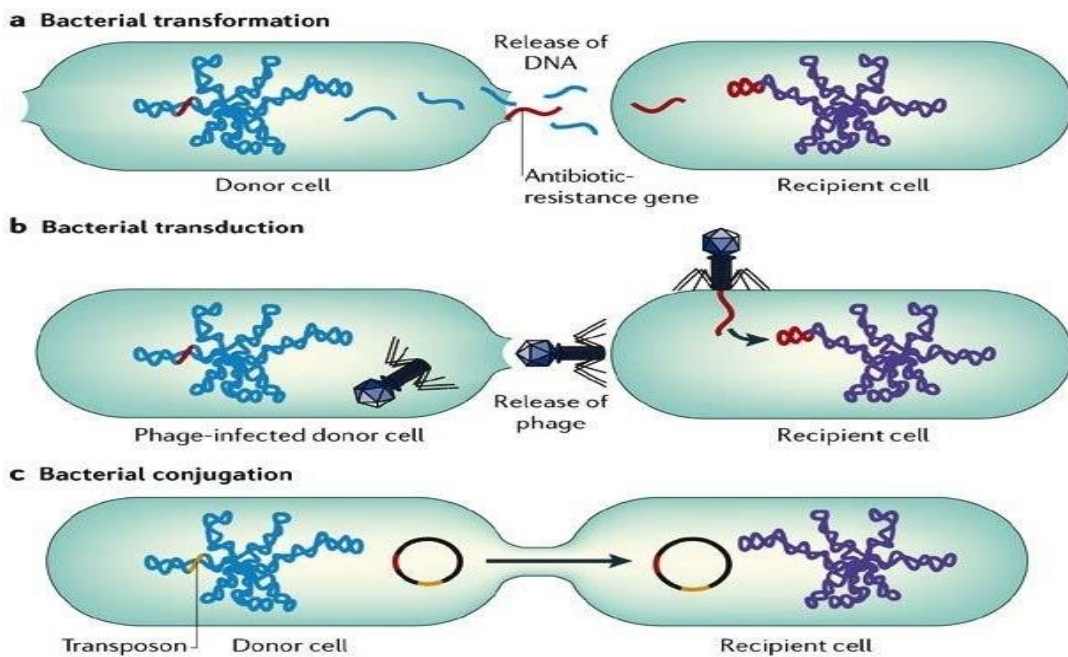
Figure 1.2: Mechanisms of gene transfer. From (Acharya, 2013).

1.1.2.3 Conjugation

Conjugation **(Figure 1.2)** is a procedure in which the bacterial cells physically contact to each other in order to exchange genetic materials between recipient and donor cells (Cabezón *et al.*, 2015). In this mechanism, the plasmids can be transferred to other bacteria via a pilus, which is temporarily formed between bacteria next to each other in order to pass DNA fragments (Alanis, 2005). An example of this kind is the dissemination of genes encoding ESBL and carbapenemases (Hwang and Gums, 2016). Furthermore, a plasmid-mediated resistance gene (mcr-1) to colistin has emerged in people and pigs in China (Robinson *et al.*, 2016).

1.1.3 Mechanisms of bacterial resistance

The microbe has the ability to develop resistance to antibiotics via several mechanisms (Reygaert, 2018). These mechanisms can be divided into three groups: reducing the intracellular concentrations of antibiotics by impermeability and efflux pumps, target alteration by genetic mutation and inactivation of antimicrobial drugs through modification or hydrolysis (Blair *et al.*, 2015).

1.1.3.1 Impermeability

The cytoplasmic membrane of bacteria can be acted as a barrier to antimicrobial compounds through the lack of porins, loss of non-essential transporters or mutations, which in order lead to decrease the influx of antibiotics (Bockstael and Aerschot, 2009). The access to intercellular targets in bacteria is essential for antibacterial agents to increase their bactericidal and bacteriostatic activities (Poole, 2002). Therefore, any problem in the permeability of antibiotics may lead to a decrease in antibiotics' availability and make them ineffective. For example, several Gram-negative bacteria are intrinsically

resistant to macrolides due to the restricted penetrability of macrolides (Meerwein *et al.*, 2020). Moreover, Gram-negative bacteria are resistant to vancomycin because their outer membrane is impermeable to this drug. (Skandalis *et al.*, 2021).

In addition, the resistance to imipenem in *Pseudomonas aeruginosa* is attributed to the loss of a transporter OprD2 (Martinez, 2014). The impermeability **(Figure 1.3)** can be accomplished by substituting porins with more selective channels or downregulation of porins (Blair *et al.*, 2015). As an example, *Enterobacteriaceae* is resistant to β-lactams due to the loss of porins channels (MacGowan and Macnaughton, 2017). Porins can be defined as protein channels that are responsible for the transportation of nutrients into the cell (Ramalingam, 2015). Furthermore, biofilms can work as a physical barrier to antibiotics which leads to reduce their activities on bacterial cells (Kumar *et al.*, 2017).

1.1.3.2 Efflux pumps

The resistance of *E. coli* to tetracycline by using an efflux pump was deemed to be the first efflux pump discovered by Stuart Levy and co-workers (Kumar and Varela, 2013). Efflux pumps **(Figure 1.3)** are transporter proteins that are involved in expelling toxic compounds or drugs from the intracellular environment to the external environment (Khameneh *et al.*, 2016). One protein is able to implement efflux alone; some of these proteins utilize ATP to obtain energy such as the *Lmr* protein in *Lactobacillus* (Levy, 2002). In general, there are two main types of efflux pumps: a primary active transport (also known as for ATP-binding cassette or P-glycoprotein transporters) that depends on hydrolysis of ATP to actively expel drugs from cells, while the second kind is a secondary active transport that utilizes an ion gradient for exporting drugs from cells (Kumar and Varela, 2013). Specific groups of efflux pumps expel many toxins from bacterial cells such as poisonous compounds and heavy metals (Allen *et al.*, 2010). Efflux pumps may include

narrow substrates such as the Tet pumps or broad substrates such as MDR pumps (Blair *et al.*, 2015). According to primary sequence homologies and mechanisms of efflux pumps, there are five families: the ATP-binding cassette superfamily (ABC), the resistance-nodulation-division family (RND), the multidrug and toxic compounds extrusion (MATE), the major facilitator superfamily (MFS) and finally the small multidrug resistance family (SMR) (Bockstael and Aerschot, 2009). The last four families are secondary transporters that use either sodium ion motive force or proton motive force (PMF) in order to efflux antibiotics from cells (Bockstael and Aerschot, 2009). Overall, the RND family is responsible for intrinsic resistance in Gram-negative bacteria (Cox and Wright, 2013). In order to be efficient, the efflux mechanism must be more effective than the influx mechanism (Alanis, 2005).

1.1.3.3 Target alteration

Antimicrobial agents bind to specific targets in order to confer their activities; any structural change in these targets makes these drugs ineffective and leads to resistance (Blair *et al.*, 2015). Target alteration **(Figure 1.3)** may be achieved by target mutation, enzymatic modification of the target, target protection and target replacement (Martinez, 2014). The mutation is a natural change in the DNA sequence within the gene, which contributes in an amendment in the feature that codes for it (Abebe *et al.*, 2016). For instance, quinolone resistance results from mutations in bacterial topoisomerases (Martinez, 2014). The decreased expression or lack of the OprD porin of *Pseudomonas aeruginosa* make it resistant to carbapenems (Shaikh *et al.*, 2015). Resistance in macrolide is attributed to nucleotides base replacements in the 23S rRNA genes (Van-Hoek *et al.*, 2011). This mutation can be done through encoding three types of genes:

genes of regulators that restrain the expression of transporters, genes of the targets of the antibiotic and genes of their transporters (Martinez, 2014).

Moreover, the target site of macrolides on ribosomes is modified by methylation of an adenine residue in domain V of the 23S rRNA (Andersson and Hughes, 2010). Another example is the target ribosome of aminoglycosides, which is also modified by methylation (Blair *et al.*, 2015). These are examples of enzymatic modification of the target. The acquisition of a new PBP in *Staphylococcus aureus* that leads to resistance to β-lactams is regarded as an example of target replacement (Kumar and Varela, 2013). For a further example of the target protection mechanism, methylates A2503 in the 23S rRNA by chloramphenicol–florfenicol resistance (*cfr*) methyltransferase confers resistance to several antibiotics such as phenicols, streptogramins, oxazolidonones, lincosamides and pleuromutilins (Blair *et al.*, 2015). Furthermore, the QnrA protein protects bacterial topoisomerases from the antimicrobial action of quinolones (Martinez, 2014).

1.1.3.4 Inactivation of drugs

Inactivation of drugs **(Figure 1.3)** can be carried out by hydrolysis or modification such as transfer of chemical groups and redox mechanisms (Abebe *et al.*, 2016). For hydrolysis of drugs, bacterial enzymes target some specific chemical bonds such as amide and ester bonds and therefore inactivate antibiotics; these bonds are available in most antimicrobial drugs such as β-lactams and aminoglycosides (Ramalingam, 2015). For instance, β-lactams (such as penicillin) can be inactivated by β-lactamase, an enzyme that hydrolyzes the β-lactam ring of the compound (Andersson and Hughes, 2010). Another hydrolytic enzyme is esterase, which is responsible for macrolide resistance (Dinos, 2017). In addition, bacterial enzymes are able to add a chemical group such as

phosphate, ribitol, nucleotidyl and acyl groups to susceptible sites on drugs in order to deactivate the action of antibiotics (Blair *et al.*, 2015). For instance, adding an acetyl group to chloramphenicol via acetyltransferases makes it inactive (Andersson and Hughes, 2010). Flavin-dependent monoxygenase enzyme (TetX) transfers one hydroxyl group to tetracycline at location 11 which results in decreasing the ability of tetracycline to link to its bacterial target and thus becomes ineffective (Kumar and Varela, 2013). This oxidation process is an example of redox mechanisms. Furthermore, *Streptomyces virginiae* produces an antibiotic called virginiamycin M1; this compound is subjected to reduction by reducing a ketone group to alcohol at location 16 in order to protect itself from its own antibiotic (Shaikh *et al.*, 2015).
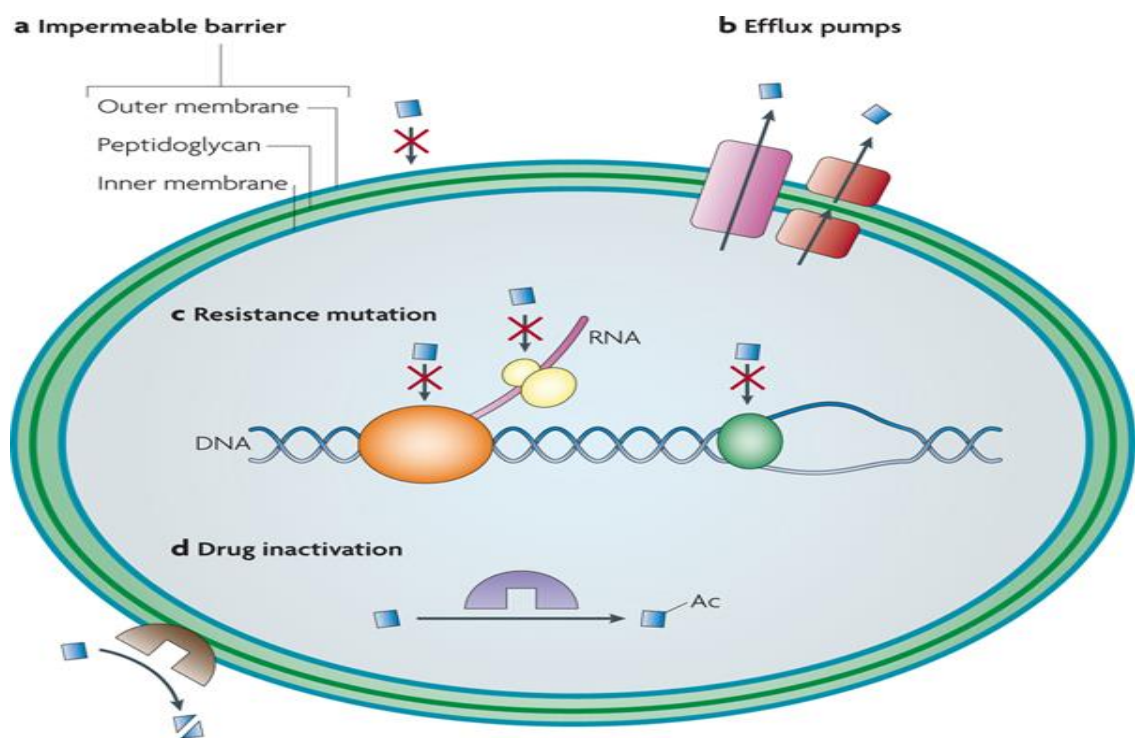
Figure 1.3: Mechanisms of bacterial resistance. From (Allen *et al.*, 2010).

Table 1.3 shows brief information concerning natural antibiotic classes and their mechanisms of resistance.

Table 1.3: Some popular antibiotics and their resistance mechanisms.

Mechanism of Action	Antibiotics Class	Drug	Mechanism of Resistance	Reference
Cell Wall Synthesis Inhibition	β-lactams	Penicillin	Alteration of the porin channels. Efflux pumps. β -lactam-hydrolyzing enzymes.	Chellat *et al.*, 2016
	Glycopeptides	Vancomycin	Production of modified peptidoglycan precursors.	Van-Hoek *et al.*, 2011
Protein Synthesis Inhibition	Tetracyclines	Chlortetracycline	Efflux pumps. Ribosomal protection proteins. Mutations. Enzymatic-alteration mechanism.	Alanis, 2005 Chellat *et al.*, 2016
	Aminoglycosides	Streptomycin	Ribosomal mutations and modification. Cell membrane modification. Efflux pumps. Inactivation of the drugs by Aminoglycoside-modifying enzymes.	Garneau-Tsodikova and Labby, 2016 Van-Hoek *et al.*, 2011
	Chloramphenicol	Chloramphenicol	Enzymatic inactivation by acetylation.	Van-Hoek *et al.*, 2011
	Macrolides	Erythromycin	Efflux pumps. Ribosomal target alterations. Substrate inactivating enzymes.	Alanis, 2005 Chellat *et al.*, 2016
	Streptothricins	Streptothricin	Enzymatic inactivation by acetylation.	Van-Hoek *et al.*, 2011

1.2 Hot springs

Springs can be defined as places where the groundwater flows at the Earth's surface (Davis *et al*., 2017). As Fensham *et al.* (2016) demonstrated, there are two fundamental types of springs: outcrop (gravity) springs (where groundwater infiltrates through the aquifer sediments and is transferred to the surface either above the steeped area of the aquifer or percolates through fractures at the ground surface), and the second is discharge (artesian) springs, which originate under artesian pressure from a restricted aquifer in which the artesian groundwater moving upward through the aquifer sediments.

Hot springs are springs where their temperatures are higher than the air temperature of the neighboring area according to the definition of the Encyclopaedia Britannica (Mahajan and Balachandran, 2017). Terrestrial hot springs have been found since the early evolution of Earth and are distributed worldwide in the modern era (Klales *et al*., 2012). Thermal spring structures usually contain extreme environmental conditions that can differ individually across spring properties; these variable conditions can be pH, temperature and salinity (Oliverio *et al*., 2018). As an example, hot springs located near to volcanic habitats are usually acidic; in contrast, the pH of springs adjacent to limestone areas is neutral or slightly alkaline (Urbieta *et al*., 2015). Furthermore, thermal springs close to volcanic zones may obtain heat from magma; however, some hot springs can have elevated temperature due to connective circulation in which groundwater goes deeply down to the Earth's crust, where the temperature is around 30°C (Mahajan and Balachandran, 2017).

Hot springs have been used for spas as well as for treating dermatological infections (Hussein and Loni, 2011). Moreover, some tourists visit thermal springs for the purpose of balneotherapy (Shakhatreh *et al*., 2017). For example, some people in Tunisia

traditionally used hot springs for recreation and health (Trabelsi *et al.*, 2016). Furthermore, thermal springs in Turkey are called Hammam and are utilized as a prophylactic and therapeutic factor against several kinds of disease and toxicity (Trabelsi *et al.*, 2016). It was suggested that the Ma'in hot springs (Jordan) might be utilized to cure illnesses such as arthritis ankylosis, influenza, respiratory system troubles, muscle contractions, central circulation troubles, rheumatism and skin diseases (Shakhatreh *et al.*, 2017). Some people take baths in order to perform some spiritual activities (Poddar and Das, 2018). In addition, some people used hot springs as a cooking resource, especially in rural communities (Khole, 2020). In general, people can do this by bathing in these springs or drinking its water, or inhaling its vapors (Trabelsi *et al.*, 2016).

Bacteria are diverse in both physiology and morphology. Moreover, they can be found in the marine and terrestrial environments around the world. One of the most important habitats is geothermal springs. It is believed that the characterization of thermophilic bacteria that were able to produce aerobic spores as well as to grow at 70°C was the first research in this field, and it was conducted by Miquel in 1888 (Adiguzel *et al.*, 2009). Thomas Brock is considered to be one of the pioneers who found out that microbes are able to survive in the boiling thermal springs of Yellowstone National Park in 1966 (Mahajan and Balachandran, 2017). Microorganisms that live in this habitat are either thermophilic or hyperthermophilic. A thermophile is defined as an organism that has the ability to live at or near the highest temperatures for the taxonomic class of which it is a portion (Satyanarayana *et al.*, 2005). Generally, the optimum growth temperature for hyperthermophiles is roughly above 80°C, whereas that for thermophiles is approximately between 55 and 80°C (Aanniz *et al.*, 2015). There are only two bacterial families that are considered as hyperthermophiles: *Thermotogaceae* and *Aquificaceae* (Urbieta *et al.*, 2015).

In order to thrive or adapt in extreme environments, thermophilic organisms have different systems from other microorganisms. These microorganisms can adapt some mechanisms like changes in their sequences of amino acids in their proteins, which leads to the conference of structural flexibility, variations, charge and hydrophobicity of enzymes (Mahajan and Balachandran, 2017). For instance, thermophilic organisms have more thermo-stable enzymes and protein synthesis systems that function effectively at high temperatures; these proteins are stable due to more hydrogen bonds and other non-covalent bonds that bolster the structure as well as they have a higher molecular weight and a more highly organized hydrophobic interior. Furthermore, thermophilic proteins possess shorter amino acid lengths in comparison to non-thermophilic microbes (Urbieta *et al.*, 2015). Moreover, the existence of a large amount of saturated fatty acids, reverse DNA gyrase and significantly stabilizing bonds like disulfide bridges assist thermophilic microbes to live in a harsh habitat (Mahajan and Balachandran, 2017). The stability of bacterial DNA is attributed to the presence of unique histone-like proteins (Wang *et al.*, 2015). Furthermore, membrane lipids tend to be more saturated and branched as well as the presence of proline **(Figure 1.4)** in a small quantity and glycine **(Figure 1.4)** in a large amount makes the polypeptide chain more flexible (Fields, 2001).

Figure 1.4: Structures of proline and glycine.
A: Proline, **B:** Glycine.

Because of their harsh environment, it is believed that thermophilic bacteria are considered as a reservoir for the production of secondary metabolites (Alrumman *et al*,

2018). It has also been illustrated that thermophilic bacteria are able to produce numerous valuable products such as antibiotics, thermostable enzymes and anticancer compounds (Shakhatreh *et al.*, 2017). Additionally, thermophiles can be used in removing heavy metals such as mercury from waste, leaching processes, producing significant enzymes and producing renewable energy, whether directly or indirectly (Urbieta *et al.*, 2015). A Firmicutes *Thermincola* spp. strain JR is regarded as an example of thermophiles that produce electrical energy using acetate as an electron donor (Wrighton *et al.*, 2008). Due to their ability to produce thermostable enzymes which have industrial and pharmaceutical applications, they have gained importance and research interest globally (Salem *et al.*, 2016).

1.3 Hot spring bacteria

It is believed that microorganisms occurred on the Earth more than 3.8 billion years ago (Toma and Deyno, 2015). Based on a cellular structure, microorganisms can be classified into two groups: Eukaryotes and Prokaryotes. Eukaryotes are usually composed of many cells. However, prokaryotes are consisting of one cell but the main difference between them is that eukaryotes have a nuclear envelope (membrane-bound nucleus) and prokaryotes do not (Hao and Starr, 2019). Prokaryotes are categorized into two types: Bacteria and Archaea. The term prokaryote is composed of two parts: *pro,* which means before, and *Karyon* that is a Greek term for kernel or nut that means nucleus (Boyle, 2017). Biologically, a prokaryotic cell is usually composed of a cell wall, a cytoplasmic-membrane (a plasma membrane), ribosomes, plasmids, a nucleoid, inclusion bodies and external components of the cell wall such as capsules, S-layer and flagella (Kolivand and Kolivand, 2017) **(Figure 1.5)**. Bacteria might be found as a single cell or clusters (Huber and Stetter, 2001)**.**

The cell wall may function as a protective layer and to maintain the cell integrity and shape as well as to inhibit large molecules from entering into the cell (Lobanovska and Pilla, 2017). The periplasm is a space between the cell wall and plasma membrane, which include a various number of proteins and ions that are required for abundant functions such as substrate hydrolysis, cellular transport and degradation and detoxification (Malanovic and Lohner, 2016).

The cytoplasmic membrane is composed of a phospholipid bilayer (Malanovic and Lohner, 2016). The cytoplasmic membrane (CM) can act as a barrier between the cytoplasm and the external environment (Cox and Wright, 2013). The nucleoid contains a single chromosome of DNA that is considered essential for reproduction. The majority

of prokaryotic cells can be reproduced by using binary fission. In this process, the cytoplasm splits into two approximately equal daughter cells (Donachie, 2002; Margolin, 2014). In terms of morphology, the prokaryotic cell shape and size tend to be not more varied, and so that a large number of species can be described as coccoid or rod shape with a length between 1 to 5 µm (Oren, 2009) and a diameter between 1 to 2 µm (Huber and Stetter, 2001).
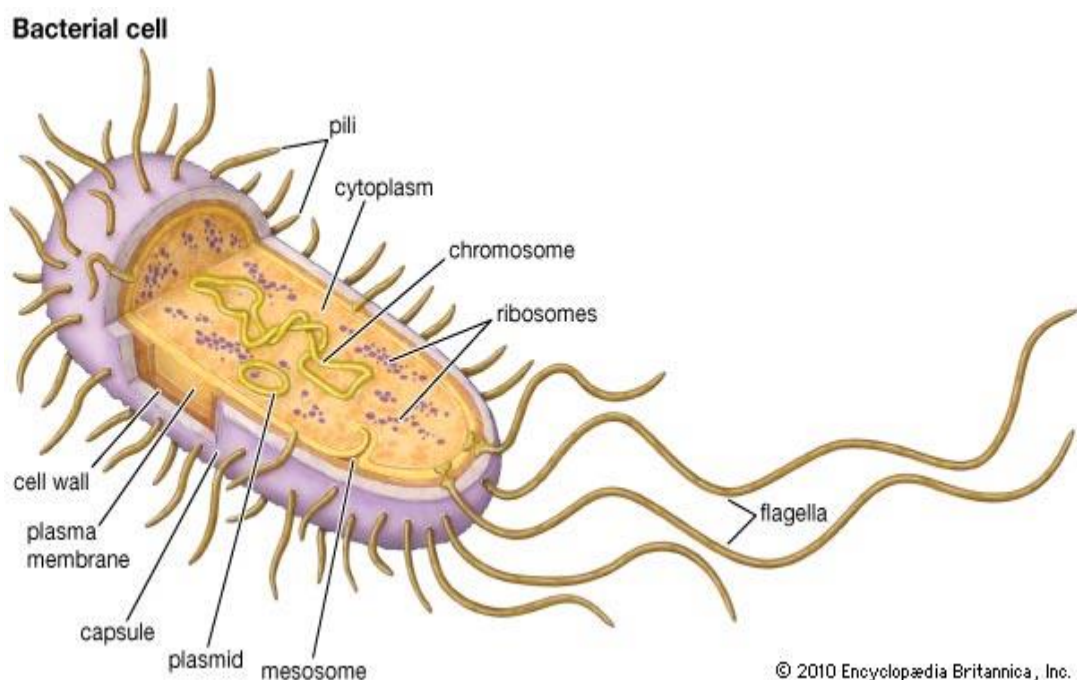
Figure 1.5: The components of the bacterial cell. From (Rogers and Kadner, 2017).

Additionally, prokaryotic cells may include extra chromosomes that are regarded as not fundamental for growth, but they can confer some advantages to the prokaryotic cells such as toxin production and the production of pili. These extra chromosomes are called plasmids. Moreover, plasmids are able to confer antibiotic resistance and autonomous replication (Carattoli, 2013). Plasmids are capable of transferring from one cell to another cell via a process called conjugation **(Section 1.1.2.3)** in order to exchange

the additional genes between bacteria (Beveridge, 2001). Plasmids can be conjugative or mobilizable; conjugative plasmids contain conjugation genes, whereas mobilizable plasmids solely include an origin of transfer (oriT) but they can utilize of the conjugation functions of conjugative plasmids to move to a new host (Van-Hoek *et al.*, 2011). Conjugative plasmids have a significant role in the development of pathogenic organisms as a result of their ability to be easily spread by horizontal transfer between and within species (SCENIHR, 2009). There are various types of plasmids that can be found in prokaryotic cells. For example, the F factor, col plasmids, metabolic plasmids, virulence and R plasmids. Each one of these plasmids has a different function. As an example, R plasmids are responsible for antibiotic resistance whilst virulence plasmids have the ability to make hosts more pathogenic.

In comparison to eukaryotic cells, bacterial ribosomes are small and are about 70S unit, which is composed of two subunits attached to each other: a small 30S subunit and a large 50S subunit (Dezfully and Heidari, 2016). The small subunit (30S) consists of the 16S rRNA chain and 20 proteins; however, the large subunit (50S) includes the 23S and 5S rRNA chains and 34 proteins (McCoy *et al.*, 2011). The large 50S subunit connects to aminoacyl tRNA (aa-tRNA) in order to stimulate peptidyl transfer and regulate the elongation process, while the small 30S subunit binds to mRNA, which leads to initiate protein synthesis (Chellat *et al.*, 2016)

One of the most important components of prokaryotic cells is inclusion bodies. Generally, these inclusions can act as storage or reservoir of some elements for energy (Shively *et al.*, 2011). For instance, the purple sulfur bacteria have the ability to use sulfur granules to oxidize sulfur compounds. Moreover, some bacteria use glycogen to obtain energy in a short period (Beveridge, 2001). On the other hand, some inclusion bodies

may directly take part in the metabolic reactions of a cell as well as in the cell's stability in order to deal with changing environmental conditions (Shively *et al.*, 2011).

Gas vesicles are essential for some bacteria that live in an aquatic habitat such as phototrophic bacteria. These vesicles are responsible for the float level of the bacterial cells in water due to the presence of gases (Beveridge, 2001). Shively *et al.* (2011) pointed out that gas vesicles can regulate the buoyancy of cells from the deep areas to the water surface in order to be close to oxygen and light.

Bacteria utilize various modes to generate energy. For example, energy might be generated by oxidizing both organic and inorganic compounds (Oren, 2009). Additionally, Oren (2009) reported that carbon dioxide is regarded as the source of carbon in prokaryotic cells. This process is called chemolithotrophy. Moreover, the metabolic diversity of prokaryotes **(Figure 1.6)** may be divided into four groups: chemoorganotrophs (getting energy from organic sources), chemolithotrophs (getting energy from inorganic sources), phototrophs (getting energy based on photosynthesis) and lactic acid bacteria.
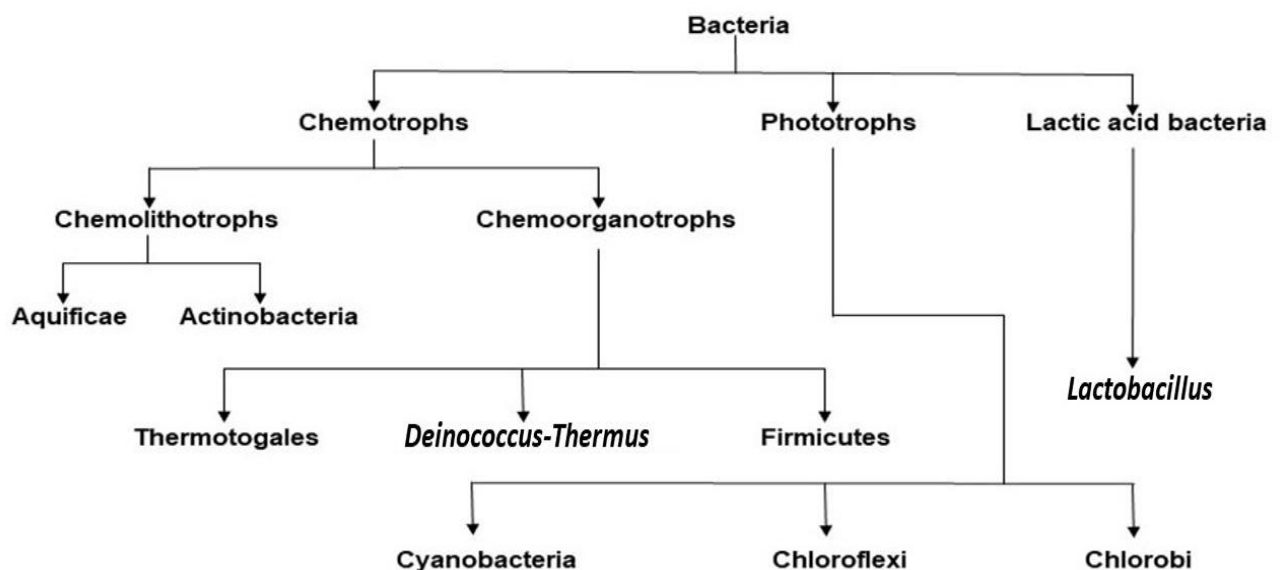
Figure 1.6: Metabolic diversity of some bacteria living in hot springs.

In general, bacteria might be classified based on the Gram-stain, a stain made by Christian Gram in 1884, into two groups: Gram-positive and Gram-negative bacteria (Li *et al.*, 2020). The composition of a cell wall of Gram-positive bacteria **(Figure 1.7)** is different from Gram-negative bacteria. For Gram-positive bacteria, the cell wall is thick and includes peptidoglycan as well as secondary polymers such as teichuronic acid and teichoic acid (Beveridge, 2001). Peptidoglycan (also known as murein) is a large macromolecule contains glycan chains (polysaccharides) that are considered as the backbone to peptidoglycan; these chains are connected to each other via short peptide bridges (Huber and Stetter, 2001). The thickness of peptidoglycan layer of Gram-positive bacteria is about 40 – 80 nm; however, it is around 7 – 8 nm in Gram-negative bacteria (Malanovic and Lohner, 2016).
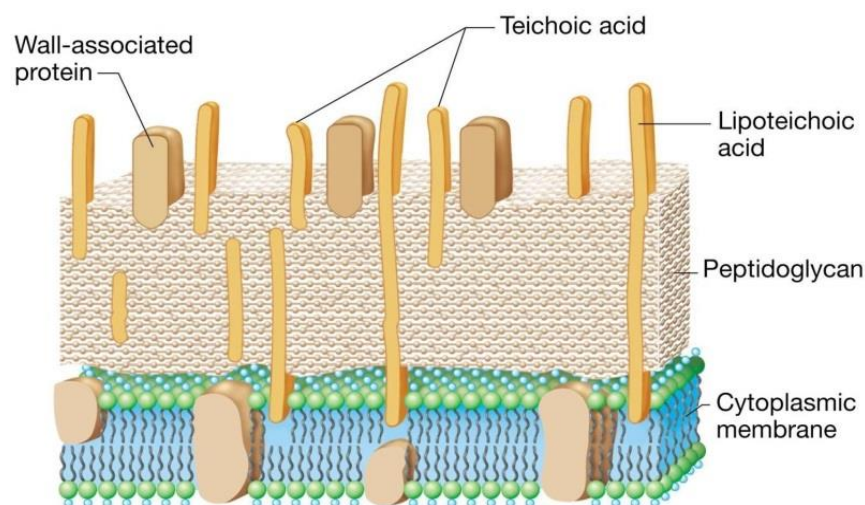
Figure 1.7: The cell wall of Gram-positive bacteria. From (Acharya, 2013).

Moreover, a lot of Gram-positive cells have lipoteichoic acid attached to the plasma membrane (Beveridge, 2001; Young, 2010). Teichoic acid is a very negatively charged molecule because of the phosphate group's presence; it is attached to *N*-acetylmuramic

acid (NAM) with a length of roughly 30 residues (Young, 2010). Therefore, it is thought that this compound is in charge of the negative charge of the cell wall. As Young (2011) mentioned, peptidoglycan consists of two repeating residues, NAM and *N*-acetylglucosamine (NAG) **(Figure 1.8)** that comprise a glycan chain (a carbohydrate polymer). In addition, a short chain of a peptide is linked to every NAM residue; this chain is composed of four or five L- and D- amino acids (Beveridge, 2001; Young, 2010). This combination of NAG–NAM disaccharide with its peptide side-chain is known as a muropeptide (Young, 2011). These amino acids are L- and D-Alanine, diaminopimelic acid (DAP) and D-glutamic acid **(Figure 1.8)**. As a result of the existence of peptidoglycan in the cell wall, the bacterial cells have a high internal osmotic pressure that enables these cells to be protected from disruption (Mayer, 2012).
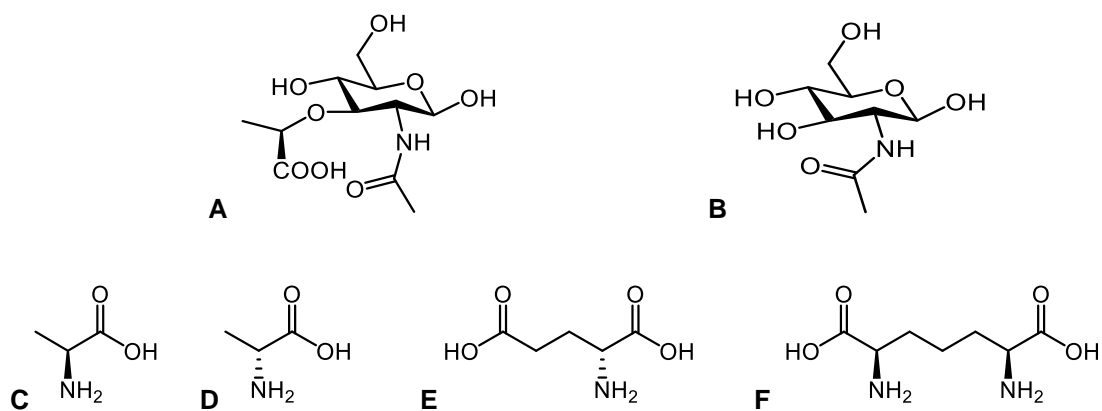
Figure 1.8: Chemical composition of peptidoglycan.
A: NAM, **B:** NAG, **C:** L- Alanine, **D:** D- Alanine, **E:** D-glutamic acid, **F:** DAP.

In comparison with the cell wall of Gram-positive bacterium, the cell wall of Gram-negative bacterium is complicated **(Figure 1.9)**. It is constituted of a thin layer of peptidoglycan and an outer membrane (Beveridge, 2001). The outer membrane is a

characteristic feature of Gram-negative bacteria located above the peptidoglycan layer; this membrane is a specific lipid bilayer (Young, 2010). Malanovic and Lohner (2016) indicated that the inner part of the outer membrane contains phospholipid; in contrast, the outer part includes lipopolysaccharide (LPS). Furthermore, LPS is known as the endotoxin of Gram-negative bacteria as a result of its toxic and biological traits (Liljestrand *et al.*, 2017). LPS can be classified into three parts: lipid A, a core oligosaccharide and O-antigen (Young, 2010). It is believed that the outer membrane is high permeable in compared with the cell membrane due to the existence of porins that permit small molecules (500 Da or less) to penetrate the OM (Epand *et al.*, 2016). The term porins refers to proteins that are responsible for forming nonspecific diffusion channels; these channels can be water-filled channels that work as general diffusion porins or specific porins include binding locations that contribute in bacterial growth (Cox and Wright, 2013). Porins can allow drugs to enter a bacterial cell by some mechanisms such as hydrophobicity, charge repulsion and size limitations (Cox and Wright, 2013).

Gram-Negative Envelope
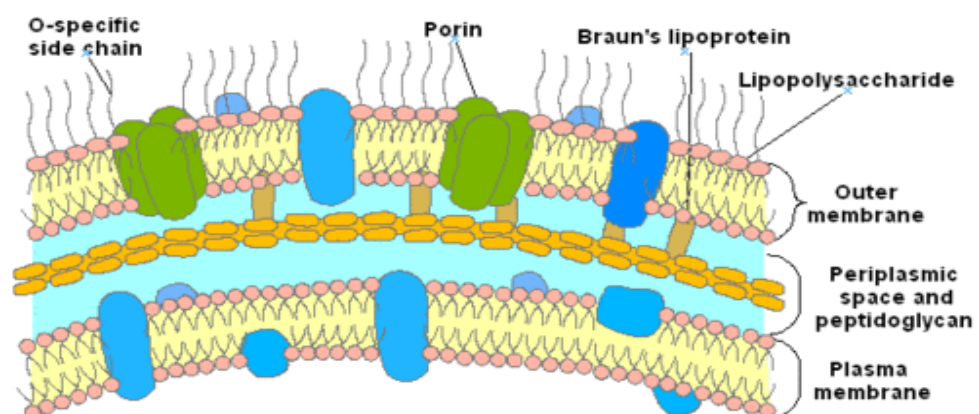
Figure 1.9: The cell wall of Gram-negative bacteria. From (Burns, 2010).

1.3.1 Types of hot spring bacteria

Classification of thermophilic bacteria depends on 16S ribosomal DNA sequences:

1.3.1.1 Aquificae

It is believed that this phylum is the oldest branch of the bacterial domain. It is composed of one class, one order, Aquificales and eight genera. The order Aquificales can be categorized into three families: *Desulfurobacteraceae*, *Hydrogenothermaceae* and *Aquificaceae* (Bonch-Osmolovskaya, 2008). The Aquificales are considered highly thermophilic, microaerophilic rods, non-spore-forming Gram-negative bacteria (Huber and Stetter, 2001). Moreover, they are chemolithoautotrophs, which obtain energy through oxidizing sulfur, hydrogen and thiosulfate (Huber and Stetter, 2001). *Aquifex* is able to thrive in a lack of oxygen through reducing nitrate (Stetter, 2006). Furthermore, a large number of Aquificales can be highly motile by using monopolar or bipolar flagellation (Bonch-Osmolovskaya, 2008).

Various members of the order Aquificales were discovered from different hot springs (Liu *et al.*, 2016). For example, the genus *Sulfurihydrogenibium* was isolated from thermal springs worldwide; from the Azores Islands and Japan to the Yellowstone National Park (Vullo *et al.*, 2013). Additionally, the genus *Aquifex* that has the ability to thrive at a high temperature 95°C was isolated from terrestrial thermal springs (Ferrera and Reysenbach, 2007). *H. thermophilus* was obtained from a geothermal spring in Japan, while *C. hydrogenophilum* was discovered from a thermal spring in Kamchatka (Russia) (Huber and Stetter, 2001). Furthermore, *H. halophilus* was isolated from a seaside saline hot spring in Izu Peninsula, Japan (Huber and Stetter, 2001).

Thermovibrio ammonificans was discovered from a deep-sea hydrothermal vent in the East Pacific Rise; ammonificin A and B **(Figure 1.10)** were isolated from this

bacterium (Murphy *et al.*, 2012). Later, ammonificins C and D **(Figure 1.10)** were discovered from the same organism (Andrianasolo *et al.*, 2012). Ammonificin B demonstrated antimicrobial activity toward *Bacillus cereus* (Andrianasolo *et al.*, 2012).

R = OH – Ammonificin A   **R = OH** – Ammonificin C
R = Br – Ammonificin B   **R = Br** – Ammonificin D
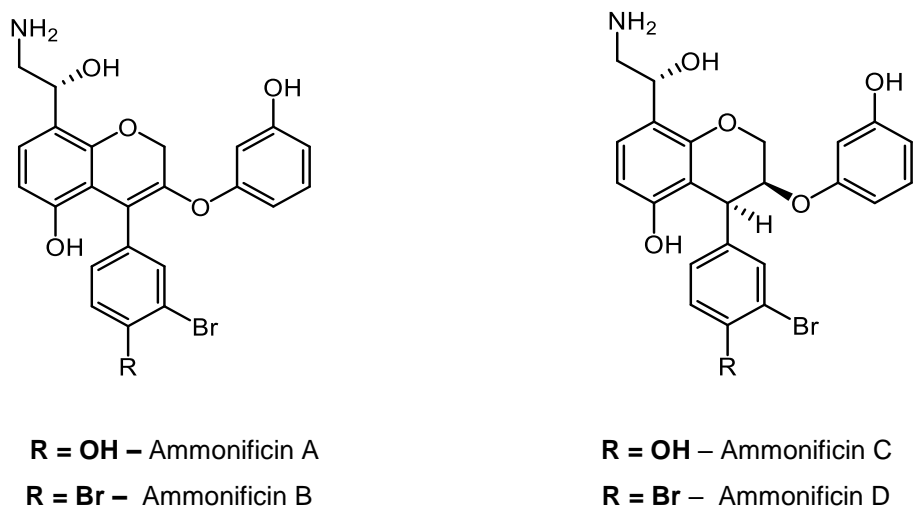
Figure 1.10: Structures of ammonificins.

1.3.1.2 Thermotogales

The phylum Thermotogales is regarded as the second oldest branch in the bacterial domain. *Thermotoga* are thermophilic, non-spore forming, rod-shaped, Gram-negative bacteria with an outer sheath-like membrane called a toga (Huber and Stetter, 2015). Although the *Thermotoga* are Gram-negative, diaminopimelic acid (DAP) is absent. Members of this phylum can be motile or non-motile (Huber and Stetter, 2001). Additionally, their core lipids consist of fatty acid methyl esters. Thermotogales are considered high organotrophs, which ferment preferentially complex organic matter as well as complex and simple carbohydrates such as glucose, xylose, starch, glycogen, cellulose and ribose (Huber and Stetter, 2001). As examples of this phylum, *Thermotoga*

neapolitana and *T. maritima* are hyperthermophilic that thrive at a maximum temperature of 90°C; and the optimal is 80°C (Bonch-Osmolovskaya, 2008). Endo-β-1,3-glucanases is a thermostable enzyme that isolated from *T. maritime* with antifungal activity against *Candida albicans* (Woo *et al.*, 2014).

1.3.1.3 *Deinococcus-Thermus*

The phylum includes a single class called Deinococci; this class is composed of two orders: Thermales and Deinococcales (Battista, 2016). The Thermales are thermophilic bacteria that grow at 60-80°C, whereas Deinococcales are known for their resistance to ultraviolet light and ionizing radiation (Battista, 2016). In 1969, the discovery of *Thermus aquaticus* by Brock and Freeze led to establish the genus *Thermus* (Dwivedi *et al.*, 2015). *Thermus* spp. are thermophilic Gram-negative bacteria and are considered one of the most ubiquitous genera of thermophilic bacteria (Cava *et al.*, 2009). *Thermus* spp. contain branched-chain fatty acids in the lipids like Gram-positive bacteria (Williams, 2021). Moreover, *Thermus* spp. use simple organic matter for obtaining energy as well as they reproduce faster under suitable conditions (Grogan, 2013). As Battista (2016) said, *Deinococcus* spp. are not thermophilic except for two species *D. murrayi* and *D. geothermalis,* which are able to thrive at 45-50°C; these species were isolated from thermal springs. *T. parvatiensis* was obtained from a hot spring in Manikaran, India (Dwivedi *et al.*, 2015). *T. kawarayensis* was observed in thermal springs in Japan (Kurosawa *et al.*, 2005). *T. aquaticus* was first discovered in an alkaline thermal spring in Yellowstone National Park (Ferrera and Reysenbach, 2007). *Meiothermus roseus* and *Meiothermus timidus* are thermophilic bacteria found in a thermal spring in Tengchong County, Yunnan province, south-western China (Ming *et al.*, 2015). These are examples of the diversity of the genus *Thermus* in hot springs worldwide. Ts2631 endolysin was

isolated from *Thermus scotoductus* bacteriophage which has bactericidal activity against the multidrug-resistant clinical strains of *Pseudomonas aeruginosa*, *Acinetobacter baumannii* and pathogens from the Enterobacteriaceae family (Plotka *et al.*, 2019).

1.3.1.4 Firmicutes (Endospore bacteria)

Firmicutes is a term that can be derived from the Latin terms *firmus* and *cutis*; *firmus* means strong, however, *cutis* means skin (Murphy *et al.*, 2012). Endospore bacteria are strictly resistant to radiation, poor nutrition, desiccation and harsh habitats such as high temperatures, harsh chemicals and extreme pH (Beveridge, 2001). The cell structure and chemical contents in bacterial spores tend to be clearly different from the vegetative cells (Marquis and Gerhardt, 2001). Bacterial endospores have no metabolic activity because they are dormant cells, which enable them to live for a long time without using energy (Mury and Popham, 2014). Dipicolinic acid (DPA) **(Figure 1.11)** is considered to be the unique chemical compound in bacterial spores (Marquis and Gerhardt, 2001).
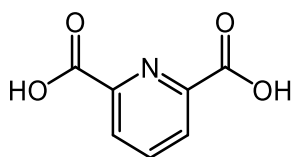
Figure 1.11: Structure of dipicolinic acid.

Bacillus and *Clostridium* spp. are the most important representatives of the endospore bacteria. *Bacillus* spp. are one of the permanent genera among the thermophilic bacteria widely studied (Lele and Deshmukh, 2016). The genus *Bacillus*

comprises of 377 species (latest update in January 2019) and can be found in aquatic environments, soil, food as well as gut microbiota of mammals and arthropods (Caulier *et al*, 2019). *Bacillus* spp. are classified as rod-shaped, Gram-positive bacteria (Sumi *et al.*, 2015). In addition, *Bacillus* can be found singly or in pairs, and in chains or as long filaments (Logan and Vos, 2015). The thermophilic *Bacilli* may survive better at temperatures between 45 to 70°C (Adiguzel *et al.*, 2009). The genus *Paenibacillus* was isolated from soil and springs of the Valley of Geysers in Russia (Andreeva *et al.*, 2010). Additionally, *Geobacillus gargensis* (a thermophilic nitrate reducing bacterium) was obtained from Garga springs (Lebedeva *et al.*, 2005). *Brevibacillus* spp. was also isolated from a thermal spring close to Konkan, Maharashtra, India (Panda *et al.*, 2014). In order to degrade sugars, *Clostridia* use butyrate fermentation (Dürre, 2015). Moreover, *Clostridia* are capable of fermenting amino acids to obtain energy through oxidizing one amino acid and utilizing another as an electron acceptor in a process called the Stickland reaction. *C. thermosulfurogenes* (a fermentative chemoorganotroph) was reported as the first bacterium that converts thiosulphate to sulfur (Jannasch, 2017).

Thermophilic *Bacillus* has the ability to produce a large number of extra cellular thermostable enzymes that have industrial importance like lipases, amylases, cellulases and proteases (Lele and Deshmukh, 2016). Furthermore, several *Bacillus* species are able to create various secondary metabolites which are diverse in function and structure (Athukorala *et al.*, 2009). For example, peptide antibiotics such as gramicidins, bacitracins and tyrocidines **(Figure 1.12)** are produced by *Bacillus* members (Esikova *et al.*, 2002).
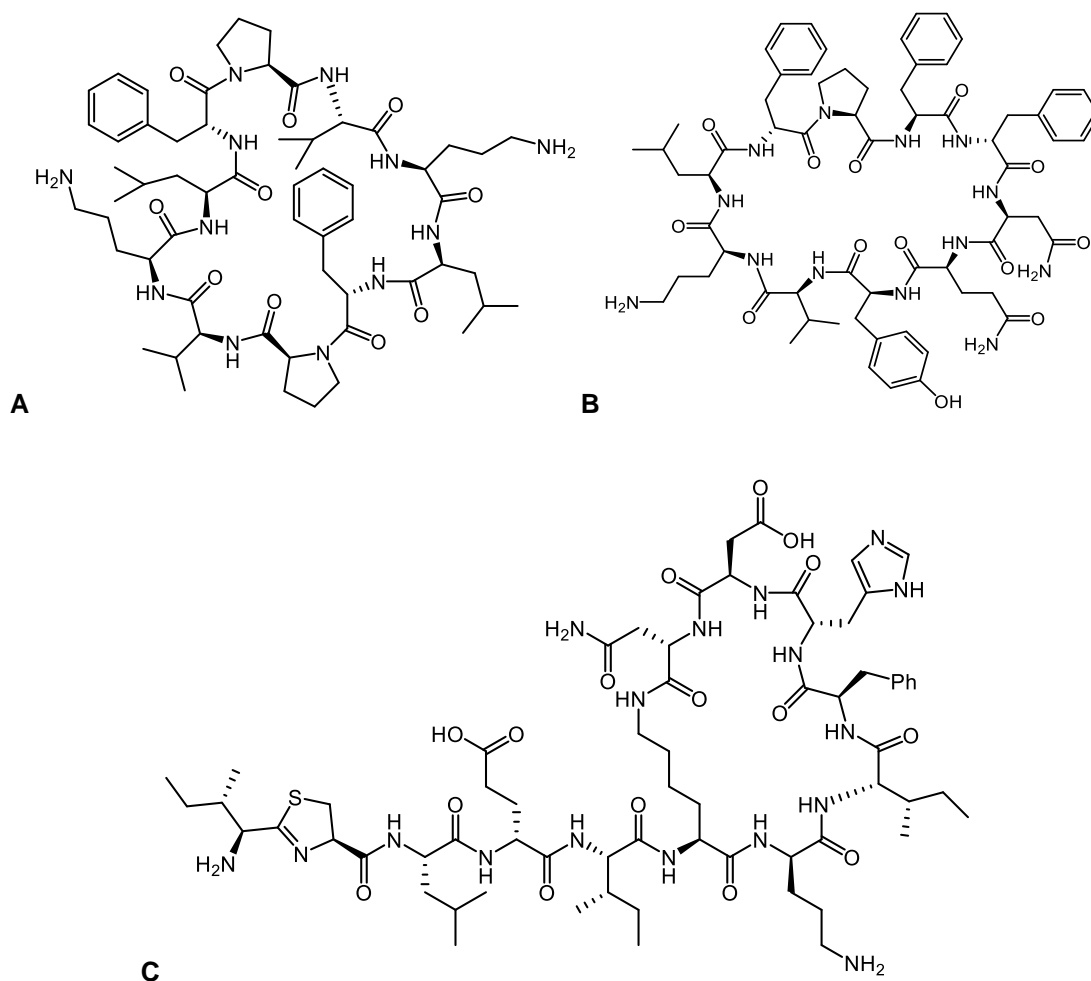
Figure 1.12: Some examples of antibiotics from *Bacillus* spp.
A: Gramicidin C, **B:** Tyrocidine A, **C:** Bacitracin.

Bacillus licheniformis is motile rods, Facultatively anaerobic, Gram-positive bacteria that form ellipsoidal to cylindrical spores which lie centrally, para-centrally and sub-terminally in unswollen sporangia (Logan and Vos, 2015). A *Bacillus licheniformis* strain was isolated from a hot spring in the Azores, Portugal, has shown strongly antibacterial activity against Gram-positive bacteria (Mendo *et al.*, 2004). A new fucose and fructose rich exopolysaccharide (EPS1-T14) was isolated from thermophilic *Bacillus licheniformis* T14, which isolated from shallow hydrothermal vent of Panarea Island, has illustrated activity on biofilm formation (Spanò *et al.*, 2016). Lichenysin **(Figure 1.13)** is an antibiotic peptide which was isolated from *B. licheniformis* (Sumi *et al.*, 2015). Another

example of active compounds from Bacillus licheniformis is fungicin M-4, it is a polypeptide that consists of 34 amino acid residues of seven kinds which has antifungal activity (Maldonado *et al.*, 2009). Bacteriocin-like compound was discovered from *B. licheniformis* demonstrated antagonistic activity toward several species of Gram-positive only (Sumi *et al.*, 2015). *B. licheniformis* isolated from an Antarctic geothermal lake was capable of thriving at 68°C (Logan and Vos, 2015). Furthermore, benzoic acid **(Figure 1.13)** is another compound that separated from *B. licheniformis* with antifungal activity against mycelial growth of *R. solaniand C. gloeosporides* with MIC of 128 µg/mL (Jeong *et al.*, 2017). Surfactin **(Figure 1.13)** is a lipopeptide antibiotic that obtained from *B. licheniformis* with fungicidal activity against *M. grisea* at a concentration of 1 µg/mL (Tendulkar *et al.*, 2007). Additionally, indole, 3-phenylpropionic acid and a dimer 4,4′-oxybis[3-phenylpropionic acid] **(Figure 1.13)** were isolated from *B. licheniformis;* these compounds showed different antimicrobial activities (Devi *et al.*, 2010). Indole illustrated significant activity against methicillin sensitive *S. aureus*, *Candida albicans* and *Salmonella typhi* with inhibition zone around 7-10 mm for each, 3-phenylpropionic acid has strong antifungal activities against *Rhodotorula* spp. and moderate one against both *Aspergillus niger* and *Candida albicans* and the last compound demonstrated significant antifungal activities against *Aspergillus fumigatus* and moderate activities against both *Vibrio cholerae* and *Salmonella typhi* (Devi *et al.*, 2010).
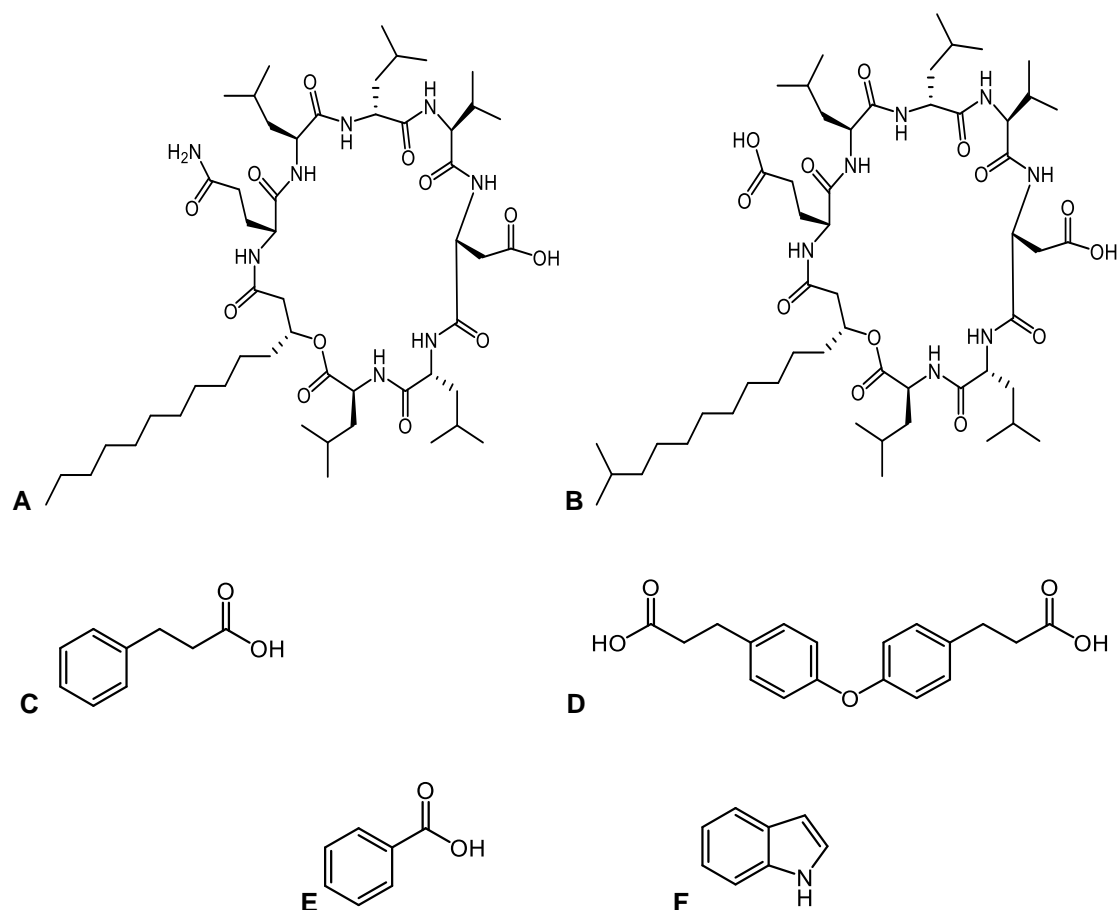
Figure 1.13: Some examples of antibiotics from *B. licheniformis*.
A: Lichenysin D, **B:** Surfactin, **C:** 3-phenylpropionic acid,
D: 4,4′-oxybis[3-phenylpropionic acid], **E:** Benzoic acid, **F:** Indole.

B. paralicheniformis is a facultative anaerobic, motile Gram-positive bacterium, which is closely related to *B. sonorensis* and *B. licheniformis* based on phylogenetic analysis (Du *et al.*, 2019). Fengycin **(Figure 1.14)** is a peptide antibiotic drug that has been discovered from *B. paralicheniformis* (Du *et al.*, 2019). Formicin **(Figure 1.14)** is a lantibiotic peptide that is produced by *B. paralicheniformis* (Collins *et al.*, 2016).

Both *B. licheniformis* and *B. paralicheniformis* have been utilized for years in the biotechnology sector in order to synthesize antibiotics, enzymes as well as consumer and biochemical products (Du *et al.*, 2019). Moreover, they both widely used commercially for

plant protection, as live organisms in feed applications and in aquaculture (Agersø *et al.*,

2019).
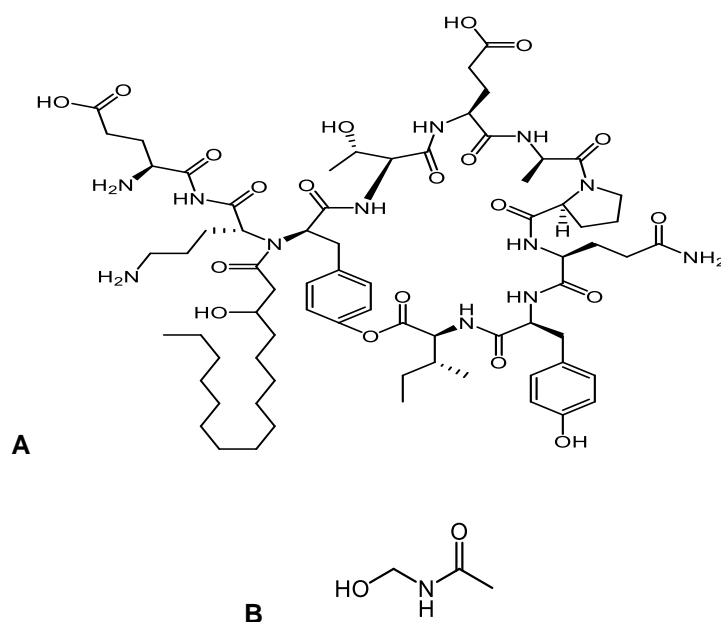
Figure 1.14: Some examples of antibiotics from *B. paralicheniformis.*
A: Fengycin, **B:** Formicin.

B. cereus is a Gram-positive bacterium which is capable of producing spores and

surviving in harsh environmental circumstances (Tusgul *et al.*, 2017). It exists universally

in soil, vegetables, marine environments, human skin and the intestinal tracts of

invertebrates (Ikeda *et al.*, 2015). Two *B. cereus* (MR1 and ALT17) illustrated antibiotic

activity were separated from sea water and hot spring moss in Thailand, respectively

(Manitchotpisit *et al.*, 2013). In Japan, YM-266183 **(Figure 1.15)** is a cyclic peptide which

consists of six thiazole rings, a pyridine ring and a number of unusual amino acids which

has antimicrobial activity against a number of Gram-positive drug-resistant bacteria, and

has been isolated from *B. cereus* (Murphy *et al.*, 2012). Moreover, homocereulide **(Figure**

1.15) is a cyclic peptide that was isolated from *B. cereus* from the sea snail *Littorina* spp.,

which displayed antibacterial activity (Murphy *et al.*, 2012). In addition, pyrrolo-(1,2-a)-

pyrazine-1,4-dione, hexahydro-3-(2-methylpropyl) **(Figure 1.15)** is an antibacterial

compound that showed activity against *Streptococcus aureus*, which was isolated from *B. cereus* (Kumar *et al.*, 2019). Kanosamine and zwittermycin A **(Figure 1.15)** also another antimicrobial drugs which isolated from this bacterium (Yan *et al.*, 2018).
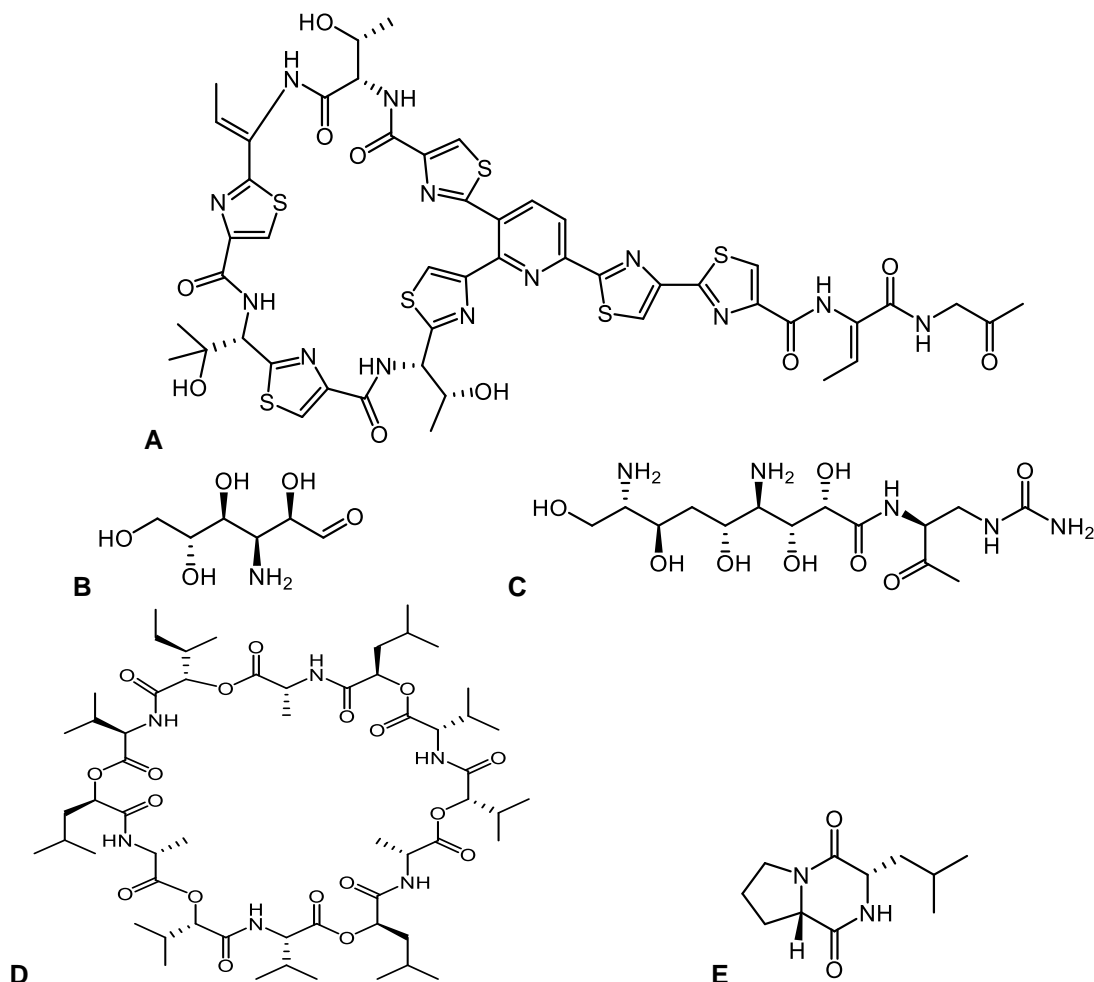
Figure 1.15: Some examples of antibiotics from *B. cereus.*
A: YM-266183, **B:** Kanosamine, **C:** Zwittermycin A, **D:** Homocereulide,
E: Pyrrolo-(1,2-a)-pyrazine-1,4-dione, hexahydro-3-(2-methylpropyl).

B. pumilus is a facultative aerobic or anaerobic, Gram-positive bacterium, which can yield spores; and it extensively spreads in soil, air, root system and plant surface (Chu *et al.*, 2019). Two novel cationic peptides P-1 and P-2 with antifungal activity against *T. roseum* were separated from *B. pumilus* (Yan *et al.*, 2018). *B. pumilus* S6-15 was isolated from a marine source found to be able to prevent the biofilm formation in both

Gram-positive and Gram-negative pathogens (Spano` *et al.*, 2016). Pumilacidin B and C

(Figure 1.16) were isolated from *B. pumilus* (Brack *et al.*, 2015). Bacillamidins A–D

(Figure 1.16) demonstrated antimicrobial activities against *P. aeruginosa* and *A.*

baumannii with MICs between 58 - 64 µg/mL (Zhou *et al.*, 2018). 3,4-dipentylhexane-2,5-

diol, 1,1′-(4,5-dibutylcyclohexane1,2-diyl)*bis*(ethan-1-ol) and 1,1′-(4,5-dibutyl-3,6-

dimethylcyclohexane-1,2-diyl)*bis*(ethan-1-one) **(Figure 1.16)** are compounds isolated

from *B. pumilus* (Chu *et al.*, 2019).
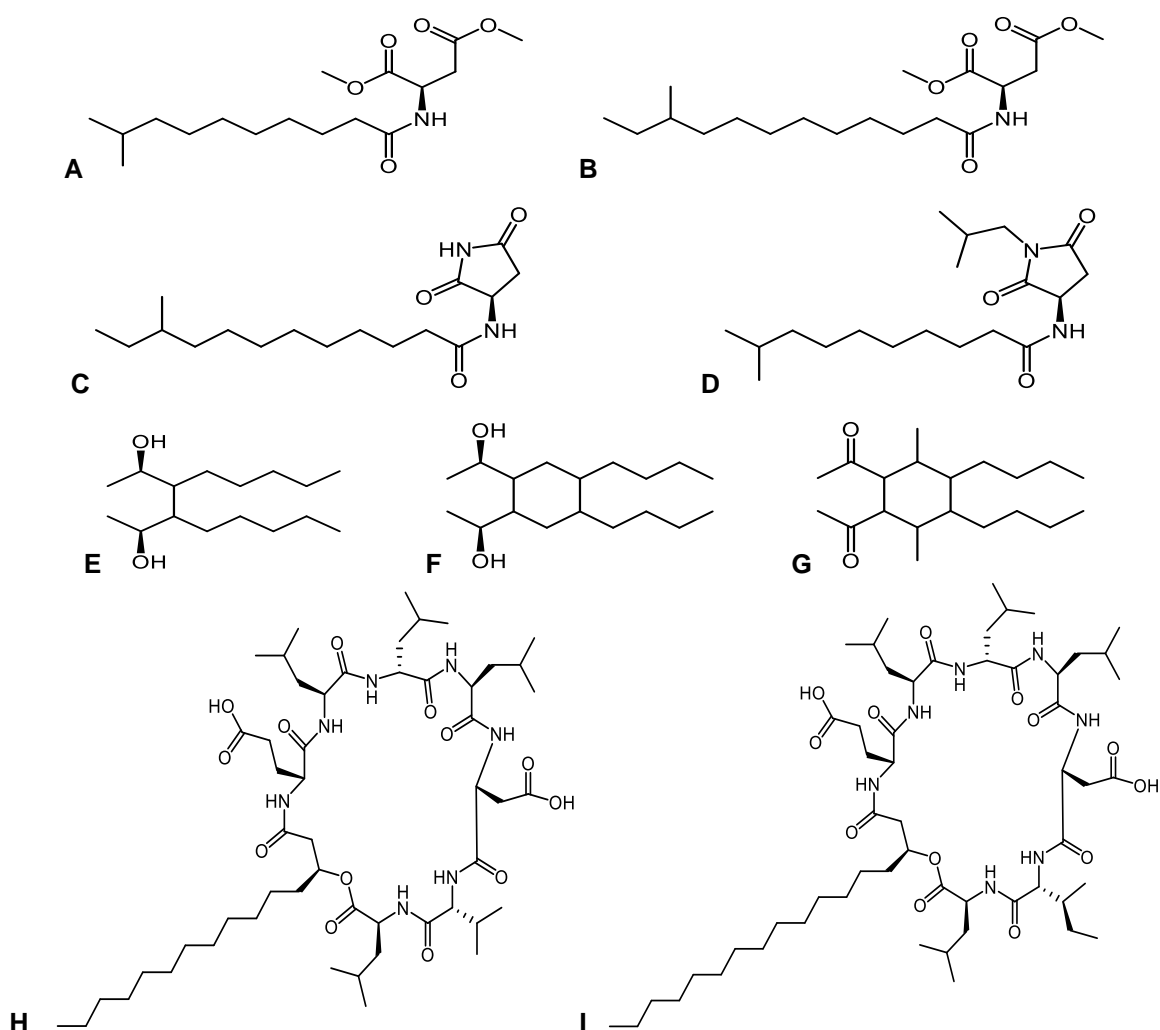
Figure 1.16: Some examples of antibiotics from *B. pumilus.*
A: Bacillamidin A, **B:** Bacillamidin B, **C:** Bacillamidin C, **D:** Bacillamidin D, **E:** 3,4-dipentylhexane-2,5-diol, **F:** 1,1′-(4,5-dibutylcyclohexane1,2-diyl) *bis*(ethan-1-ol), **G:** 1,1′-(4,5-dibutyl-3,6-dimethylcyclohexane-1,2-diyl)*bis*(ethan-1-one), **H:** Pumilacidin B, **I:** Pumilacidin C.

1.3.1.5 Cyanobacteria

Cyanobacteria (blue-green algae) are prokaryotic microbes that have the ability to achieve oxygenic photosynthesis (like plants and algae) by utilizing water and light during the reduction of carbon dioxide (Palinska, 2008). In the presence of light and the lack of oxygen, photosynthetic bacteria are able to oxidize H_2S to sulfate or sulfur (Giampaoli *et al.*, 2013). Like the red algae, cyanobacteria utilize phycobiliproteins as an accessory pigment. The permanent mode of growth in photoautotrophy is done by fixing CO_2 by the process called Calvin cycle (Herrero *et al.*, 2001). In addition, cyanobacteria are regarded as the biggest sub-group of Gram-negative bacteria (Sinha and Häder, 2008). Phycobilins and chlorophyll are available in the oxygenic phototrophic bacteria (Palinska, 2008). Like eukaryotes, cyanobacteria possess photosystems I and II in order to perform oxygenic photosynthesis.

Based on microscopic investigations, the diversity of cyanobacteria tends to be more available in thermal springs in comparison to the sediment surface and lake water (Dadheech *et al.*, 2013). Cyanobacteria are widespread in most hot springs where the temperature is below 72°C and the pH is more than 6 (Mohamed, 2008). For instance, the species *Synechococcus lividus* was found in the Octopus spring (Stal, 2012). Additionally, the genus *Synechococcus* was observed in the North American hot springs at a high temperature of 72°C as well as in the Yellowstone hot spring (Papke *et al.*, 2003). Mohamed (2008) stated that *S. lividus* is distributed in Jazan hot springs in Saudi Arabia. Another filamentous cyanobacterium (*Oscillatoria amphigranulata*) was obtained from geothermal springs in both Japan and New Zealand (Papke *et al.*, 2003).

Norharmane and 4,4-dihydroxybiphenyl **(Figure 1.17)** are antibiotic drugs that isolated from *Nodularia harveyana* and *Nostoc insulare*, respectively; these compounds

showed antibacterial and antifungal activities (Volk and Furkert, 2006). Moreover, α-dimorphecolic acid, coriolic acid and linolenic acid **(Figure 1.17)** are extracted from *Oscillatoria redekei syn. Limnothrix redekei,* which isolated from the Müggel see in Germany (a freshwater lake); these drugs are active against *B. subtilis*, *Micrococcus flavus* and *Staphylococcus aureus* (Mundt *et al.*, 2003).
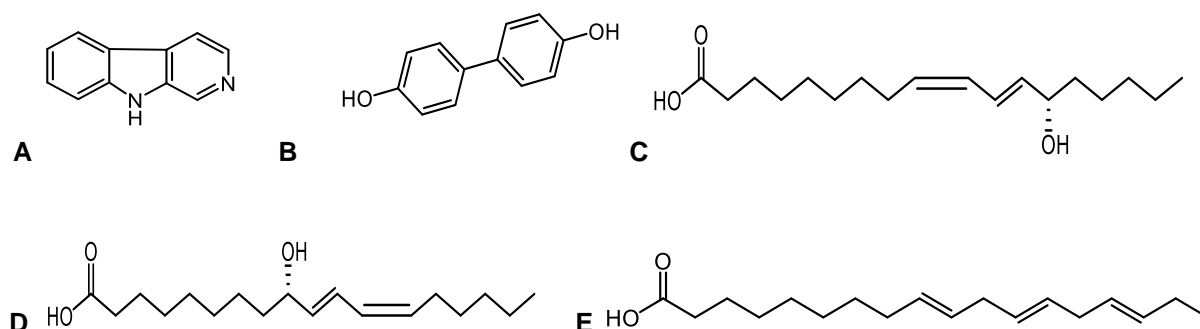
Figure 1.17: Some examples of antibiotics from cyanobacteria.
A: Norharmane, **B:** 4,4-dihydroxybiphenyl, **C:** Coriolic acid,
D: α-dimorphecolic acid, **E:** Linolenic acid**.**

1.3.1.6 Chloroflexi

The phylum Chloroflexi (known as green nonsulfur bacteria) contains both photosynthetic (*Chloroflexus*) and nonphotosynthetic members (*Herpetosiphon*). Moreover, it is regarded as the only bacteria that possess gliding motility (Murphy *et al.*, 2012). The genus *Chloroflexus* is considered a filamentous, anoxygenic phototrophic member, which was first discovered from a thermal spring in Japan (Ferrera and Reysenbach, 2007). The green nonsulfur bacteria are filamentous, Gram-negative bacteria except for *Oscillochloris chrysea*, which is a Gram-positive member (Overmann, 2008). The metabolism of *Chloroflexus* may be accomplished by anoxygenic photosynthesis in the presence of organic compounds as a carbon source. To clarify this

point, Overmann (2008) reported that Chloroflexi is a photoorganoheterotrophic bacterium in terms of the mode of growth, which means that these bacteria use organic molecules such as glycerol, acetate, pyruvate, glucose and glutamate as a carbon source as well as an electron donor. This genus includes both bacteriochlorophyll A and C and has the ability to use sulfide and organic matter as an electron donor (Ferrera and Reysenbach, 2007). Filamentous *Chloroflexus auranticus* was isolated from the Octopus spring (Imhoff, 2017). Moreover, *Caldilinea aerophila* was found in a sulfur turf of a hot spring in Japan (Overmann, 2008). *Heliothrix oregonensis* was obtained from a thermal spring in Oregon in the USA (Ferrera and Reysenbach, 2007). Siphonazole **(Figure 1.18)** is a new type of natural product containing both aromatic and oxazole moieties; this compound was isolated from a *Herpetosiphon* spp. (Murphy *et al.*, 2012).
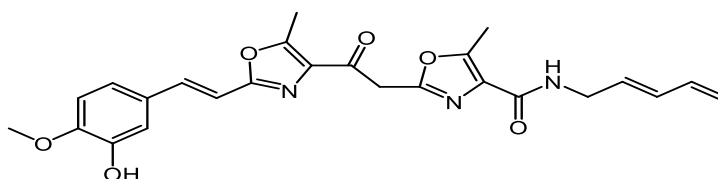
Figure 1.18: Structure of siphonazole.

1.3.1.7 Chlorobi

The phylum Chlorobi (known as green sulfur bacteria) is composed of two classes Ignavibacteria and Chlorobia (Iino *et al.*, 2010). The order Chlorobiales contains only one family called *Chlorobiaceae*. This phylum has a shared root with the phylum Bacteroidetes and is considered as Gram-negative bacteria (Iino *et al.*, 2010).

These bacteria are distributed in sulfur springs (Imhoff, 2014). The Chlorobi are obligate phototrophs that use reduced sulfur molecules as an electron donor as well as being able to grow under highly anoxic conditions (Overmann, 2007). These bacteria can utilize some simple organic carbon substrates in order to form biomass in the presence

of carbon dioxide (Overmann, 2007). As an example of this phylum, *Chlorobaculum tepidum* inhabits in the hot springs at an optimal temperature of 48°C and can tolerate up to 55°C (Imhoff, 2014).

1.3.1.8 Actinobacteria

The phylum Actinobacteria is a large complex phylum which consists of one class and six orders. All Actinobacteria are Gram-positive bacteria with more than 50% of the G + C content (guanine and cytosine) in their genome (Trujillo, 2016). Actinobacteria may be found as motile or non-motile, aerobes or anaerobes, spore or non-spore-forming bacteria (Shivlata and Satyanarayana, 2015). It was thought that the filamentous Actinobacteria (formerly called Actinomycetes) belong to the true fungi due to their ability to produce hyphae and mycelia. As a result, they were called ray fungi (Trujillo, 2016). Actinobacteria can reproduce either by an asexual mode such as conidia and spore formation or by a vegetative mode based on the fragmentation of mycelia (Shivlata and Satyanarayana, 2015). In order to get nutrients, a plethora of genera use hemicellulose, cellulose, fats and proteins to yield extracellular hydrolytic enzymes (Trujillo, 2016).

The Actinobacteria include some thermophilic bacteria. For example, a *Streptomyces*-like Actinomycete strain was observed in a sediment sample collected from a Hehua hot spring in Tengchong, Yunnan province, south-west China (Duan *et al.*, 2014). In addition, the genus *Rubrobacter* lives at a temperature of around 45 to 60°C and was obtained from thermal springs. Moreover, *Acidimicrobium ferrooxidans* thrives at a temperature of 45 to 50°C as well as *Thermoleophilum* is able to survive between 45 to 70°C (Trujillo, 2016). *Acidithiomicrobium* spp. are a chemolithoautotroph that grow in hot habitats and obtain energy by using sulfur (Shivlata and Satyanarayana, 2015). In

general, the theromphilic Actinobacteria are regarded as high aerobes and obligate chemoorganotrophs obtaining energy by using organic matter besides *Acidithiomicrobium* spp. and *Streptomyces thermoautotrophicus,* which gain energy by utilizing sulfur and $CO_2 + H_2$, respectively (Shivlata and Satyanarayana, 2015).

Actinobacteria are popular with producing a large number of secondary metabolites that have useful applications in medicine, agriculture and veterinary (Valverde *et al.*, 2012). Granaticin and granaticinic acid **(Figure 1.19)** were obtained from a thermophilic *Streptomyces* spp. XT-11989; granaticinic acid showed a mild antibiotic property in comparison with granaticin (Wilson and Brimble, 2009). A thermophilic *Thermomonospora* spp. T-SA-125 was discovered from Saudi Arabian desert soil; this bacterium yields a water-soluble antibiotic that has activity toward Gram-positive bacteria and moderate activity against Gram-negative bacteria (Mahajan and Balachandran, 2017).
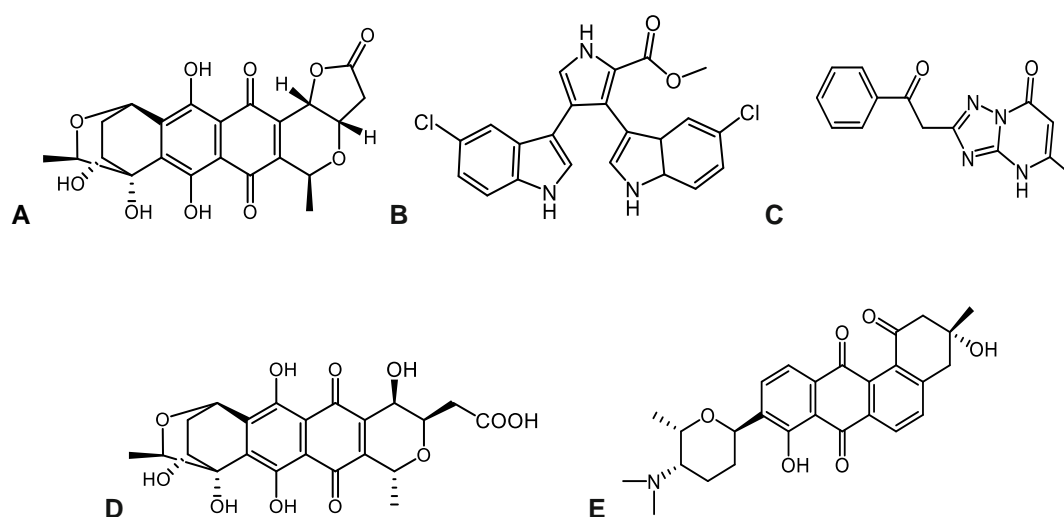
Figure 1.19: Some examples of antibiotics from Actinobacteria.
A: Granaticin, **B:** Lynamicin A, **C:** Essramycin, **D:** Granaticinic acid, **E:** Frigocyclinone.

Essramycin, shown in **(Figure 1.19),** is a new triazolopyrimidine antibiotic extracted from *Streptomyces* spp.; this drug illustrates broad-spectrum activity against

Gram-positive and Gram-negative bacteria with MIC of 2–8 μg/mL (Manivasagan *et al*., 2014). In addition, Lynamicins and Frigocyclinone **(Figure 1.19)** are antibacterial agents that isolated from *Marinispora* spp. and *Streptomyces griseus,* respectively; Lynamicins has broad-spectrum activity against both Gram-positive and Gram-negative organisms, particularly against MRSA and VRE, while Frigocyclinone demonstrates antibacterial activities only against Gram-positive bacteria (Manivasagan *et al*., 2014).

1.4 Microbial drug discovery

1.4.1 An overview

Historically, it is thought that the ancient Chinese first used antibiotics over 2,500 years ago through discovering mouldy soybean and utilizing it for treating carbuncles, furuncles and similar infections (Kourkouta *et al.*, 2018). Moreover, John Parkinson in his book Theatrum Botanicum, published in 1640, indicated that ancient China, Greece, Rome, Serbia and Egypt used mouldy bread topically due to its beneficial activities (Gould, 2016).

In 1890, Paul Vuillemin used the word antibiosis as an antonym to the term symbiosis for the first time in order to describe the antagonistic activity between different microbes (Nicolaou and Rigol, 2018). The origin of the term antibiosis comes from the Greek language (Dezfully and Heidari, 2016.). Literally, the term antibiotic means against life (Kolivand and Kolivand, 2017). In the current time, it can be defined as any substance that possesses a biological action against living microorganisms (Kümmerer, 2009). Antibiotics can be produced naturally or synthetically as well as they inhibit the growth of microbes or kill them (Ramalingam, 2015).

Mycophenolic acid and pyocyanin (pyocyanase) **(Figure 1.20)** are active agents that thought to be the first antibiotics that discovered in the modern era. In 1893, mycophenolic acid was isolated from *Penicillium glaucum* (*P. brevicompactum*) by the Italian scientist Bartolomeo Gosio; this compound is believed to be the first antibiotic (Nicolaou and Rigol, 2018). Furthermore, Oscar Löw and Rudolph Emmerich (German researchers) isolated pyocyanase from *Pseudomonas aeruginosa* in the late 1890s (Kourkouta *et al.*, 2018). In the 20th century, the discovery of antibiotics is deemed to be one of the greatest scientific discoveries (Carvalho and Santos, 2016). Furthermore,

Antibiotics (as secondary metabolites) are considered one of the most important types of natural bioactive substances with a low molecular weight around (MW 3,000); they can be obtained from different organisms by fermentation such as (fungi, bacteria, lichens, algae, green plants, etc.), which are able to terminate or inhibit all metabolic cell activities (Dezfully and Heidari, 2016).
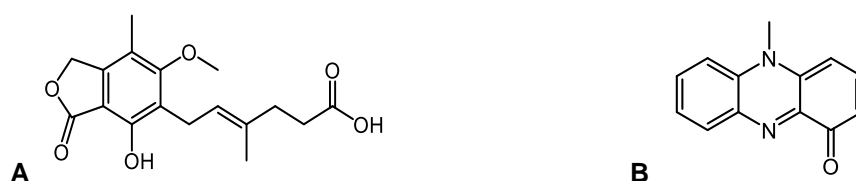
Figure 1.20: Structures of the first antibiotics.
A: Mycophenolic acid, **B:** Pyocyanin.

Based on the antibacterial activity of antibiotics, they can be classified into two types: bactericidal antibiotics, which destroy the bacterial cell directly, or bacteriostatic antibiotics that hinder the growth of bacteria by stopping the production of folic acids and vitamins (Kolivand and Kolivand, 2017).

Antibiotics are used for treating lethal infections, wounds, infected cuts and various bacterial diseases like cholera and syphilis (Abebe *et al.*, 2016). Moreover, antibiotics can be utilized for curing bacterial infectious diseases, cancer, prophylactic treatment and supporting surgical interventions (Le Page *et al.*, 2017). Furthermore, they also can be used widely in domestic animal and livestock, veterinary and as growth promoters in aquaculture (Le Page *et al.*, 2017). Additionally, it is noticed in some common infectious diseases such as syphilis, pneumonia, tuberculosis, gonorrhea and communicable diseases of childhood that the level of morbidity and mortality was significantly decreased using antibiotics (Carvalho and Santos, 2016).

Some microorganisms are able to produce secondary metabolites for protection. Bacteria, as an example, have the ability to produce antibiotics **(Figure 1.21)**. For example, Actinobacteria are one of the most prolific antibiotic producers, specifically the genus *Streptomyces* (Trujillo, 2016). The genus *Streptomyces* is known as an effective source for producing antibiotics; more than 50% of antibiotics are produced by *Streptomyces* spp. (Shivlata and Satyanarayana, 2015). Mesophilic and thermophilic *Streptomyces* are beneficial as a source for yielding enzymes, antibiotics and other bioactive metabolites due to their rapid autolysis of mycelia (Abussaud *et al.*, 2013). For instance, the ethyl acetate extract of a thermophilic *Streptomyces* spp*.* from the Tharban hot spring in Saudi Arabia exhibited the ability to inhibit the growth of bacteria and fungi (Al-Dhabi *et al.*, 2016).
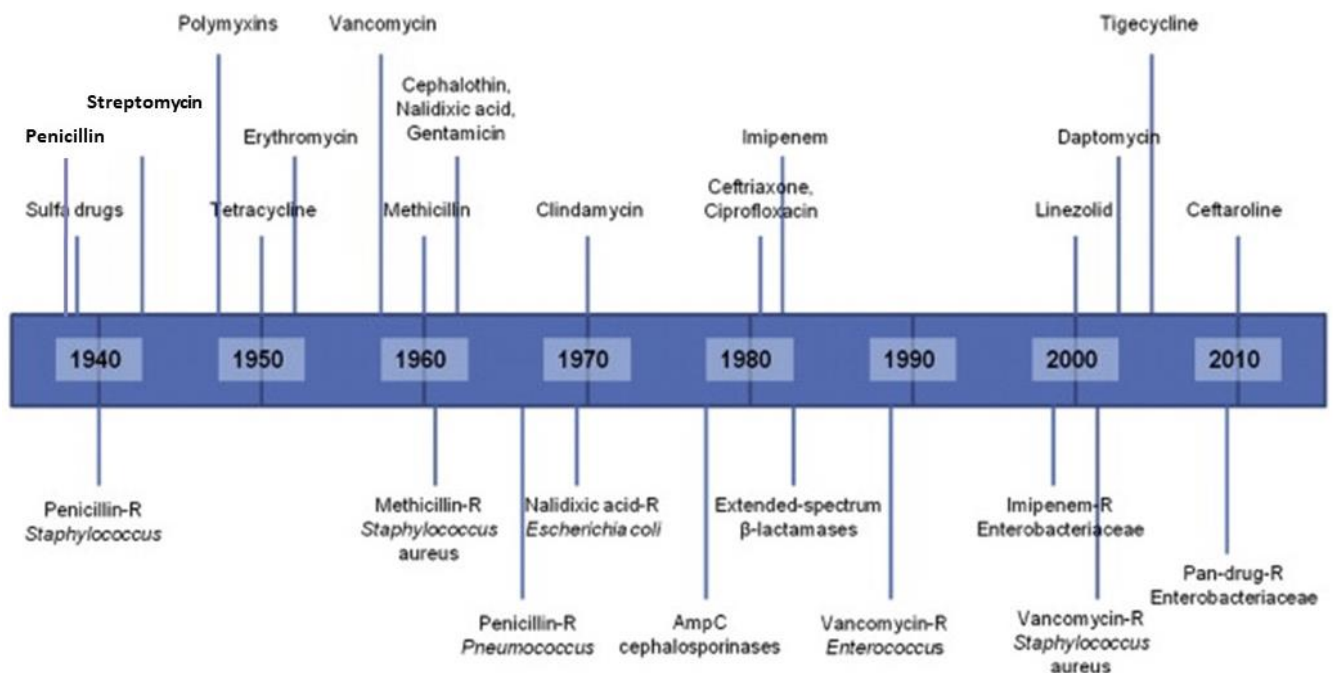
Figure 1.21: Timeline of antibiotic discovery versus the development of antibiotic resistance. From (Tang *et al.*, 2014).

Additionally, hot spring water has been reported to have antifungal and bactericidal activities on dermatological diseases by several authors (Giampaoli *et al.*,

2013). For instance, various compounds were isolated from cyanobacteria that show inhibitory activities on cancer cells, viruses, enzymes such as protease, fungal and bacterial growth (Singh *et al.*, 2011). Antibacterial diterpenoids were isolated from *Nostoc commune* and antifungal peptides in *Tolypotrix byssoidea* are examples of secondary metabolites from cyanobacteria (Volk and Furkert, 2006). The polar extract of cyanobacteria from the Nakhl hot spring showed significant antibacterial activity against *K. pneumoniae* (Dobretsov *et al.*, 2011). Furthermore, strains from thermophilic *Bacillus* discovered from the hot spring of the Kamchatka Peninsula produced very stable peptide antibiotics against Gram-positive bacteria (Běhal, 2003). *B. licheniformis* was isolated from a thermal spring in the Azores, Portugal; this strain has antibacterial activity against Gram-positive bacteria (Mendo *et al.*, 2004). Overall, *Actinomycetes* (especially the genus *Streptomyces*), cyanobacteria, myxobacteria, *Pseudomonas* species and *Bacillus* spp. are regarded as the most prevalent bacterial sources for producing antibiotics. (Pidot *et al.*, 2014).

1.4.2 Types of natural antibiotics

Natural antibiotics can be classified according to their mode of actions into four groups: inhibition of cell wall synthesis, plasma membrane inhibition, inhibition of nucleic acid synthesis and inhibition of protein synthesis.

1.4.2.1 Inhibition of cell wall synthesis

β-lactams and glycopeptides are the most well-known members of this group that are able to prevent bacteria from synthesizing their cell wall through stopping the synthesis of peptidoglycan (Dezfully and Heidari, 2016). β-Lactam antibiotics can be classified as bactericidal agents (Bush and Bradford, 2016). β-lactams are the most

popular used antibiotics in the globe (Meletis, 2016). Moreover, β-lactams are divided into four classes: penicillins, cephalosporins, carbapenems and monobactams. All β-lactam antibiotics consist of a bicyclic-fused ring system, including a β-lactam ring except for monobactams, which contain one ring (Mahajan and Balachandran, 2017). They inhibit bacterial growth by binding to a group of enzymes such as penicillin-binding proteins (PBPs), which leads to synthesize and remodel peptidoglycan (Singh *et al.*, 2017). As a consequence of this binding, the terminal transpeptidation step in the bacterial cell wall is blocked, which finally leads to cytolysis or death of a cell because of osmotic pressure (Van-Hoek *et al.*, 2011).

By accident, penicillin was first isolated from *Penicillium notatum* by Alexander Fleming in 1928 when he found out that a culture of *Staphylococcus aureus* on a plate was cleared by *Penicillium notatum* colonies (Lewis, 2017). Chemically, penicillins are composed of a β-lactam ring, thiazolidine nucleus and a side chain at position 6 (Ramalingam, 2015). Penicillin can be derived from three amino acids; valine, cysteine as proteinogenic and α-aminoadipate **(Figure 1.22)** that is an intermediate in lysine metabolism (Clardy *et al.*, 2009). Due to purification, instability and low yield of penicillin, it was not used clinically until the 1940s when it was developed for treating wounded soldiers from the USA and its allies during World War Two (Aminov, 2017). As an example of this group, benzylpenicillin (penicillin G) **(Figure 1.23)** was the first β-lactams used clinically, especially against streptococcal infections due to its high activity at that time (Bush and Bradford, 2016). In addition, it is considered the first β-lactam antibiotic which naturally discovered in 1928 but was not introduced clinically until 1938 (Fair and Tor, 2014).
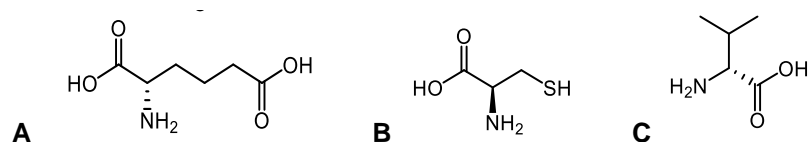
Figure 1.22: Chemical composition of penicillin.
A: α-aminoadipate, **B:** Cysteine, **C:** Valine.

Cephalosporin was obtained from the fungus *Cephalosporium acremonium* in 1945, and it was active against typhoid fever, brucellosis and streptococcal infections (Yılmaz and Özcengiz, 2017). Moreover, *Cephalosporium acremonium* was discovered by Giuseppe Brotzu from sewer water in Cagliari in Sardinia, Italy (Zaffiri *et al.*, 2012). Cephalosporins are composed of a β-lactam ring, a dihydrothiazine nucleus and sulphur atom at position 1 (Ramalingam, 2015). Cephalosporin C **(Figure 1.23)** is regarded as the first cephalosporin, which was discovered in 1945 (Fair and Tor, 2014).

Carbapenems consist of a thiazolidine ring and a β-lactam ring fused together by tetrahedral carbon atoms and nitrogen (Ramalingam, 2015). In terms of activity, they have a broad antimicrobial spectrum which are efficacious against Gram-positive, Gram-negative, anaerobic bacterial infections as well as nosocomial infections and sepsis caused by MDR pathogens (Ramalingam, 2015). Thienamycin **(Figure 1.23)** is regarded as the first carbapenem that was isolated from *Streptomyces cattleya*; it was inappropriate for therapeutic use because it was not stable at a pH greater than 8 (Ramalingam, 2015).

The first monocyclic β-lactam antibiotic was isolated from *Chromobacterium violaceum* (Ramalingam, 2015). In addition, sulfazecin **(Figure 1.23)** is a monobactam drug isolated from *Pseudomonas acidophila*, which has antibacterial activities against Gram-negative bacteria and weak activity against most of Gram-positive bacteria (Decuyper *et al.*, 2018).
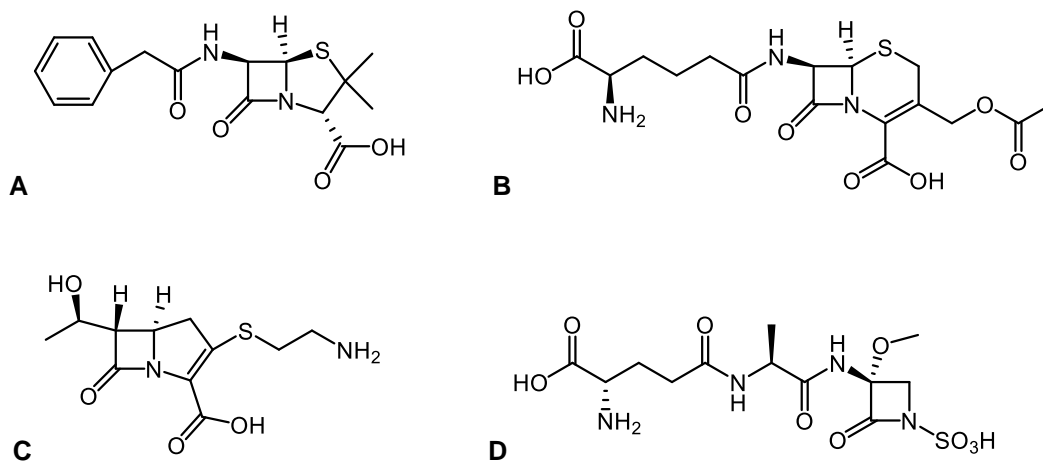
Figure 1.23: Some examples of β-lactams.
A: Penicillin G, **B:** Cephalosporin C, **C:** Thienamycin, **D:** Sulfazecin.

There are four mechanisms of resistance to β-lactams: modification of the porin channels, efflux pumps, production of β-lactam hydrolyzing enzymes (β-Lactamases) and the existence of an exogenous β-lactam-resistant PBP called PBP2a like MRSA; the first two methods are rare and occur in Gram-negative bacteria (Chellat *et al.*, 2016).

Glycopeptides antibiotics consist of polycyclic or glycosylated cyclic peptides, which are produced non-ribosomally (Aminov, 2017). They are tricyclic or tetracyclic molecules attached to heptapeptide (a core made up of seven amino acids) in which two sugar moieties are connected (Henson *et al.*, 2015). In 1953, Edmund Kornfeld and the team at Eli Lilly isolated vancomycin **(Figure 1.24)** from *Amycolatopsis orientalis* (formerly *Nocardia orientalis* and *Streptomyces orientalis*) (Aminov, 2017). The mode of action of vancomycin is to attach to the terminal dipeptide, D-alanine-D-alanine, of Lipid II (a precursor of the peptidoglycan), which leads to inhibit cell wall synthesis (Singh *et al.*, 2017). As a result, the essential reactions for cell wall biosynthesis such as transglycosylation and transpeptidation are inhibited (Binda *et al.*, 2014).

Glycopeptides are usually utilized in preventing and curing infections caused by Gram-positive bacteria (Zaffiri *et al.*, 2013). For instance, vancomycin is used for treating the gut anaerobe *Clostridium difficile* infections and MRSA (Butler *et al.*, 2014). Teicoplanins (teichomycins) **(Figure 1.24)** is another natural glycopeptides that isolated from *Actinoplanes teichomyceticus* in 1978 but was not used clinically until 1988 in Europe and 1998 in Japan (Binda *et al.*, 2014).
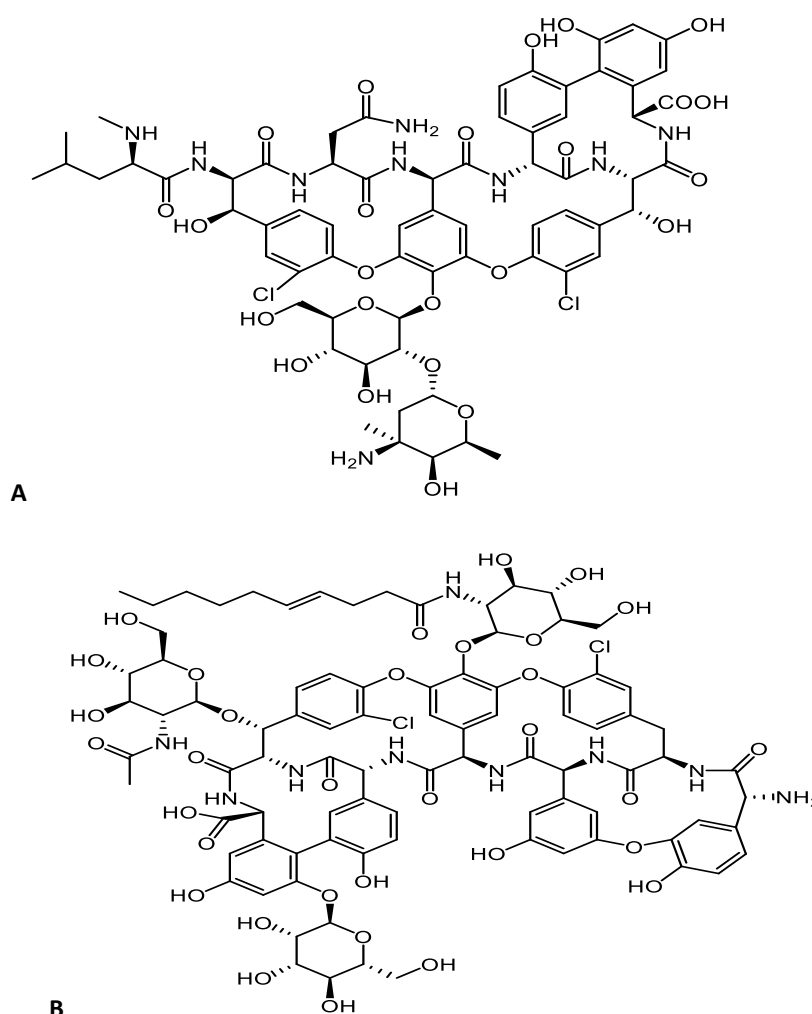
Figure 1.24: Some examples of glycopeptides.
A: Vancomycin, **B:** Teicoplanin A$_2$-1.

The first glycopeptides resistance was stated in 1987 and 1988 with the recognition of VanA enterococci, while resistance to vancomycin is very unusual among streptococci

(Woodford, 2005). Moreover, the mutation is a common mechanism of resistance toward glycopeptides, specifically in enterococci (Butler *et al.*, 2014).

1.4.2.2 Plasma membrane inhibition

There are two groups of peptide antibiotics that are able to inhibit cell membrane biosynthesis: polypeptides and lipopeptides. The chemical structure of lipopeptides is composed of a cyclic peptide with a hydrophobic tail (Aminov, 2017). For example, daptomycin and colistin **(Figure 1.25)**. Daptomycin was isolated in the early 1980s from *Streptomyces roseosporus* by Eli Lilly and Company; however, it was not used clinically until 2003 (Aminov, 2017). The antimicrobial activity of daptomycin is only against Gram-positive bacteria (Zaffiri *et al.*, 2013). It is highly active for curing nosocomial Gram-positive infections such as VRE and MRSA strains as an intravenous antibiotic (Singh *et al.*, 2017).

Daptomycin kills bacterial cells via mislocalization of important cell division proteins, which results in defects in the cell membrane, and this leads to cell death (Aminov, 2017). In contrast, Eli Lilly and Company abandoned daptomycin because of its toxicity and side effects such as myopathy (Wencewicz, 2016).

Another lipopeptide antimicrobial is colistin (also known as polymyxin E). It was isolated from *Paenibacillus polymyxa* (formerly *Bacillus polymyxa var. colistinus*) in Japan in 1947 (Aminov, 2017). In addition, polymyxins are cyclic peptides connected to peptidyl side chains, which are linked to a fatty acid tail (Fair and Tor, 2014). Polymyxins are categorized as narrow-spectrum antibiotics that work against common Gram-negative bacteria (Poirel *et al.*, 2017). They work through binding to phospholipids of the cell membrane, preventing them from functioning as osmotic barriers (Dezfully and Heidari,

2016). To clarify, they connect to anionic LPS molecules in the outer membrane of Gram-negative organisms and replace calcium and magnesium, which resulting in a disruption in the outer membrane that leads to cell death (Aminov, 2017).
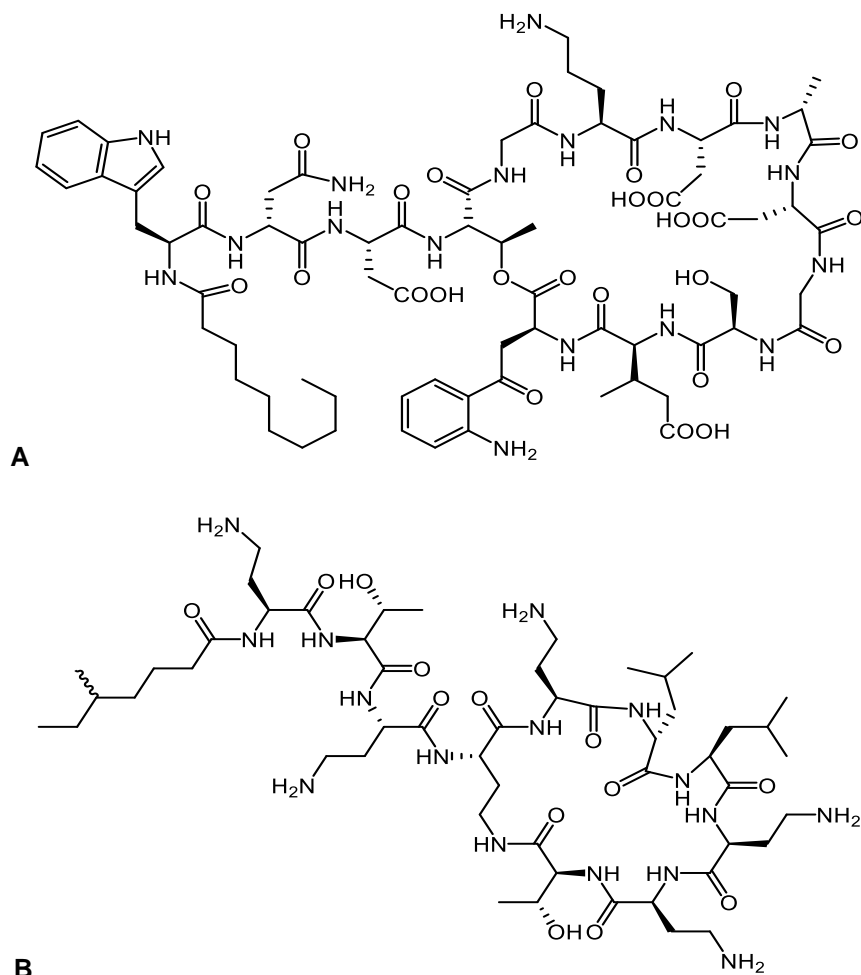
Figure 1.25: Some examples of lipopeptide antibiotics.
A: Daptomycin, **B:** Colistin.

Colistin has been used currently in the treatment of MDR Gram-negative bacterial infections, particularly *Klebsiella*, *Pseudomonas* and *Acinetobacter* strains, specifically containing NDM-1 producers (Fair and Tor, 2014). It is believed that the *N*-terminal fatty acyl segment is responsible for the antimicrobial activity of polymyxins (Poirel *et al.*, 2017).

At the end of the 1930s, tyrothricin **(Figure 1.26)** (a polypeptide antibiotic) was discovered from *Brevibacillus brevis* (formerly *Bacillus brevis*) by René Dubos (Aminov, 2017). Tyrothricin consists of a mixture of linear and cyclic polypeptides that possess antibacterial activity (Aminov, 2017). It works by forming channels in the cell membrane, which leads to an increase in permeability and destroying the ion gradient between the extracellular environment and the cytoplasm (Aminov, 2017).
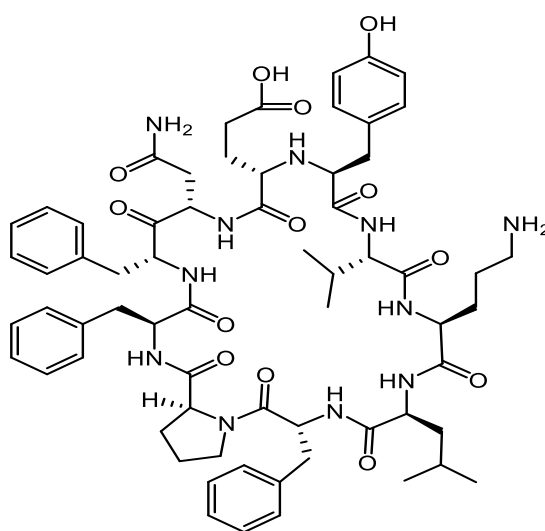
Figure 1.26: Structure of tyrothricin.

1.4.2.3 Inhibition of nucleic acid synthesis

Rifamycin, an ansamycin antibiotic, has a macrocyclic structure linked to an aromatic moiety (Fair and Tor, 2014). Rifamycin (it is a mixture of rifamycins A, B, C, D, and E) **(Figure 1.27)** is the active compound that targets bacterial DNA-dependent RNA polymerase and consequently inhibits bacterial growth (Aminov, 2017). Moreover, rifamycin binds to DNA gyrase (topoisomerase), stopping the supercoiling of DNA, and therefore inhibiting DNA synthesis (Dezfully and Heidari, 2016). It was discovered in Milan in 1957 by Maria Teresa Timbal, Piero Sensi and Pinhas Margalith when working at

Gruppo Lepetit SpA (Aminov, 2017). Rifamycin was isolated from *Amycolatopsis rifamycinica* (formally *Streptomyces mediterranei*, *Nocardia mediterranei* and *Amycolatopsis mediterranei*) (Aminov, 2017).

Chromosomal mutations in *rpo*B, which encrypts the β-subunit of RNA polymerase, resulting in resistance to rifampicin (Woodford, 2005). Additionally, change of cell permeability, enzymatic modifications of rifamycin and duplication of the target are other mechanisms of resistance to this agent (Aminov, 2017).

Mupirocin (pseudomonic acid) **(Figure 1.27)** is a polyketide-fatty acid mixture that was discovered from *Pseudomonas fluorescens* in 1971; it functions as Ile-tRNA synthetase inhibitors (Wencewicz, 2016). It is highly active against MDR pathogens like MRSA and for this reason, it was approved by the FDA in 1987 as a nasal spray and topical ointment for curing skin infections (Wencewicz, 2016).

Macrolactone polyketides consist of unsaturated lactone cores attached to deoxysugars and aromatic parts (Fair and Tor, 2014). Fidaxomicin (lipiarmycin) **(Figure 1.27)**, as an example, is regarded as an 18-membered macrolactone polyketide which was naturally obtained from *Actinoplanes deccanensis* in 1976 (Wencewicz, 2016). Furthermore, it was introduced for clinical use in 2011, and its mode of action is via inhibiting RNA polymerase in Gram-positive and some Gram-negative bacteria (Fair and Tor, 2014).
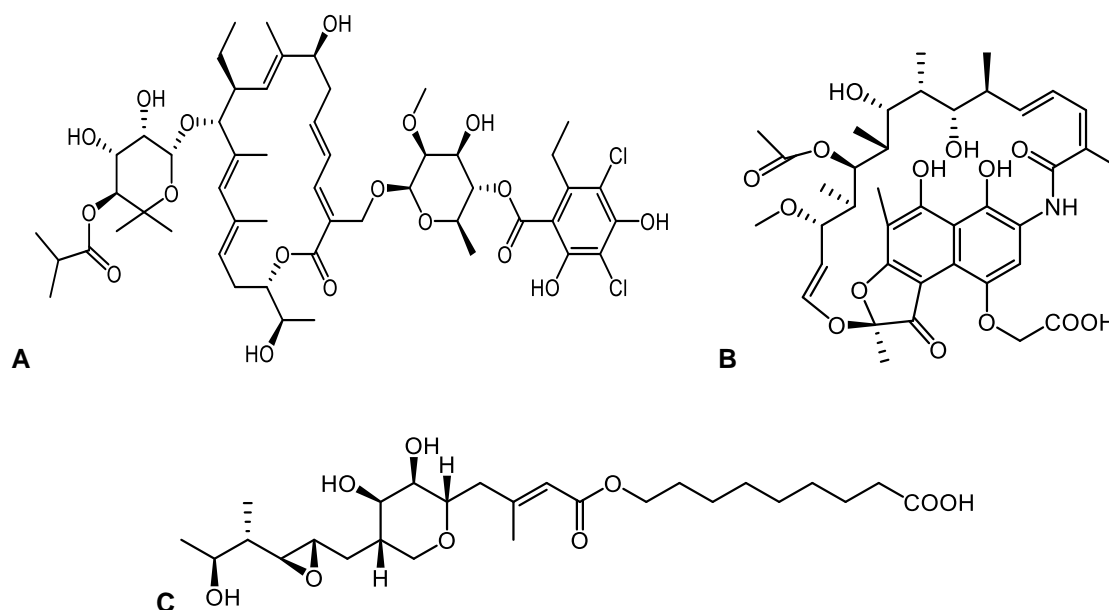
Figure 1.27: Some examples of nucleic acid synthesis inhibitors.
A: Fidaxomicin, **B:** Rifamycin B, **C:** Mupirocin.

1.4.2.4 Inhibition of protein synthesis

There are several natural antibiotics that hinder protein synthesis in the bacterial cell. For example, aminoglycosides, macrolides and tetracyclines. Aminoglycosides are natural antibiotics that are derived from *Actinomycetes*. They are composed of amino sugars attached to a dibasic aminocyclitol by glycosidic linkages (Krause *et al.*, 2016). Streptomycin **(Figure 1.28)** was discovered in 1943 and is regarded as the first aminoglycoside antibiotic (Fernandes and Martens, 2017). Furthermore, it was isolated from strains of *Streptomyces griseus* by Albert Schatz at Rutgers University (Aminov, 2017). Streptomycin is deemed the first antimicrobial drug used for treating tuberculosis (Yılmaz and Özcengiz,2017).

In Addition, gentamicin **(Figure 1.28)** was isolated in the 1960s; and used for treating *P. aeruginosa* infections (Dodds, 2017). Aminoglycosides act through the inhibition of protein synthesis by binding to the 16S rRNA subunit of the 30S ribosome

(Singh *et al.*, 2017). Mechanism of resistance to aminoglycoside can be done in several ways: alterations at the ribosomal binding sites, production of aminoglycoside modifying enzymes, decreasing cell permeability and active efflux (Van-Hoek *et al.*, 2011).
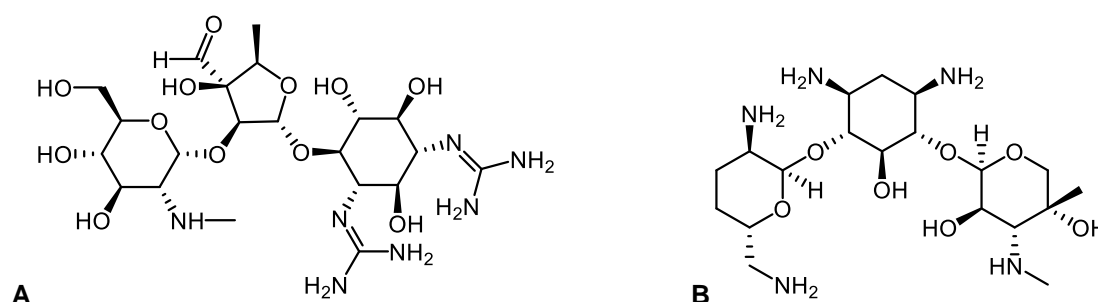
Figure 1.28: Some examples of aminoglycoside antibiotics.
A: Streptomycin, **B:** Gentamicin.

Tetracyclines possess a fused linear tetracyclic structure that is able to make chelation complexes with divalent cations (Dodds, 2017). The first antibiotic of tetracyclines is chlortetracycline **(Figure 1.29)**, which was separated from *Streptomyces aureofaciens* by Benjamin Minge Duggar in 1945 at Lederle Laboratory of Division of American Cyanamid Company (Aminov, 2017). Moreover, oxytetracycline (terramycin) **(Figure 1.29)** was isolated from *Streptomyces rimosus* from the Terra Haute, Indiana in the USA by Alexander Finlay from Pfizer in the early 1950s (Nguyen *et al.*, 2014). The mode of action of tetracyclines can be done through inhibiting acyl-tRNA transfer on the 30S ribosome, which leads to protein synthesis inhibition (Fernandes and Martens, 2017).

Tetracycline antibiotics have a broad spectrum of activity; they are active against Gram-positive and Gram-negative bacteria, spirochetes and protozoan parasites (Grossman, 2016) as well as rickettsiae, chlamydia and mycoplasma (Daghrir and Drogui, 2013). In addition, tetracycline can be used for human therapy, for veterinary purposes and as feed additive in the agriculture sector (Daghrir and Drogui, 2013).

Bacteria can resist the activity of tetracyclines by various methods: efflux pump and blocking the tetracycline-binding site on the ribosome via small proteins (Singh *et al.*, 2017) as well as enzymatic inactivation of tetracycline and mutations near a binding site (Chellat *et al.*, 2016).
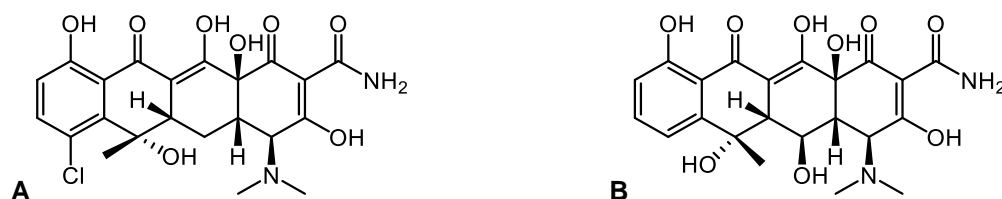
Figure 1.29: Some examples of tetracyclines antibiotics.
A: Chlortetracycline, **B:** Oxytetracycline.

Structurally, macrolides are composed of a large macrocyclic lactone ring that contains 14-, 15- or 16-membered and deoxy sugars may connected to the lactone ring (Aminov, 2017). Macrolides have strong anti-inflammatory properties and are usually used for respiratory tract infections (Fernandes and Martens, 2017). Pikromycin **(Figure 1.30)** was the first compound of this class and was isolated from *Streptomyces venezuelae* in 1950 by Brockmann and Henkel (Aminov, 2017). Later, erythromycin, the first commercially successful macrolide **(Figure 1.30)**, was isolated from *Saccharopolyspora erythraea* (formerly *Streptomyces erythraeus*) by the team of scientists led by J. M. McGuire at Eli Lilly (Aminov, 2017). Macrolides are considered the second most prescribed antibacterial drugs after the β-lactams (Aminov, 2017).
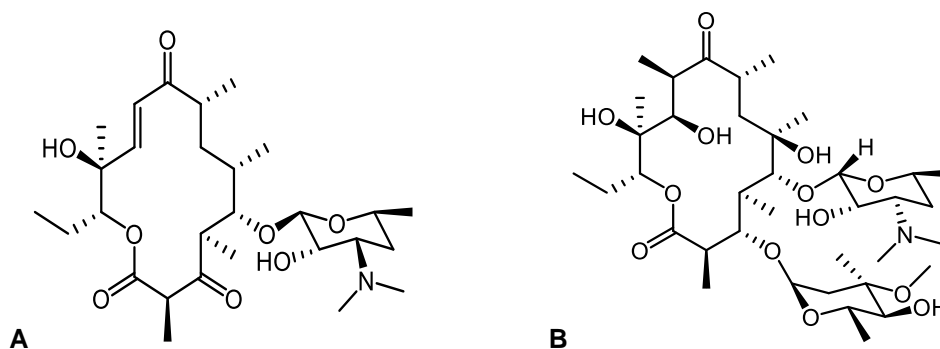
Figure 1.30: Some examples of macrolide antibiotics.
A: Pikromycin, **B:** Erythromycin.

In terms of activity, macrolides are broad-spectrum that work against aerobic and anaerobic Gram-positive and some Gram-negative bacteria (Fair and Tor, 2014). Macrolide antibiotics are safe and active for treating human infectious diseases such as gonorrhoea and community-acquired bacterial pneumonia (Seiple *et al.*, 2016). Macrolides act through the inhibition of protein synthesis by attaching to the 23S rRNA of the 50S ribosomal subunit (Singh *et al.*, 2017). Macrolide resistance can be conducted by efflux proteins and methylases at the binding site on the 23S RNA (Dodds, 2017) as well as inactivating enzymes like esterases (Chellat *et al.*, 2016).

Another example of protein synthesis inhibitors is chloramphenicol **(Figure 1.31)**. Chloramphenicol belongs to the amphenicols class which are a group of phenylpropanoid antibiotics (Fair and Tor, 2014). It was discovered from *Streptomyces venezuelae* by David Gottlieb in 1947 (Aminov, 2017). Chloramphenicol has a high affinity to attach to the peptidyl transferase of the 50S ribosomal subunit of 70S ribosomes, which leads to inhibition of peptide chain elongation (Van-Hoek *et al.*, 2011). Chloramphenicol is considered the drug of choice for treating bacterial meningitis caused by *Streptococcus*

pneumoniae, *Neisseria meningitides* and *Haemophilus influenza*e due to its ability to cross the haematoencephalic barrier (Aminov, 2017).

The most frequent mechanism of resistance to chloramphenicol is inactivation by acetyltransferases (Roberts and Schwarz, 2017). Furthermore, mutations of the target site, inactivation by phosphotransferases, efflux pumps and permeability barriers are also examples of mechanisms of resistance but less frequent (Van-Hoek *et al.*, 2011).
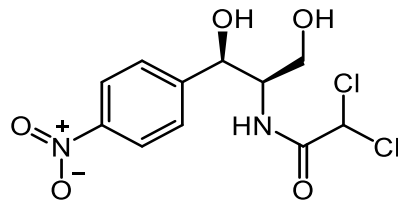
Figure 1.31: Structure of chloramphenicol.

1.5 Hot springs selected for this study

The Kingdom of Saudi Arabia (KSA) is considered the largest country of the Arabian Plate, which occupies around 80% of its area (Rehman and Shash, 2005). Geologically, Saudi Arabia is composed of several different types of rocks which can be divided into two main parts; the Arabian Shield and Arabian Platform (Rehman and Shash, 2005). The Arabian Shield generally consists of complicated assemblages of crystallophylline (phylline means leaf-like shape) and crystalline (crystallized minerals) rocks of Precambrian-Cambrian age with a volcanic stream of Tertiary-Quaternary age, which covers the western part of the Arabian Plate (Bazuhair *et al.*, 1990). In contrast, the Arabian Platform (also known as the Arabian Shelf) is constituted of a sedimentary sequence that spreads unevenly on the top of the base rocks of the Arabian Shield and downgrades toward the Arabian Gulf, which represents the eastern area of the Arabian Plate (Bazuhair *et al.*, 1990).

Most geothermal activities are concentrated along the western and south-western coast of Saudi Arabia because of the volcanic heating connected with the opening of the Red Sea/Gulf of the Suez Rift, which leads to constitute hydrothermal resources and hot, dry rocks (Harrats) in this area (Lashin *et al.*, 2015). The volcanic centers constitute roughly 45% of the Arabian Shield and they are responsible for producing geothermal springs in this region, particularly in Al-Laith and Jazan regions, whereas 55% is occupied by the post-orogenic granites (Lashin *et al.*, 2015).

Many springs have been known for hundreds of years for their use for both domestic and irrigation purposes in the KSA; most of which are located in the western part of Saudi Arabia (Alsaleh, 2017). Six hot springs from different locations of the Arabian Shield were selected for this study. These springs are popular among domestic people

for their activities in healing eye and skin infections. All six springs are located in the western part in three areas: Al-Laith, Aseer and Jazan **(Figure 1.32).**
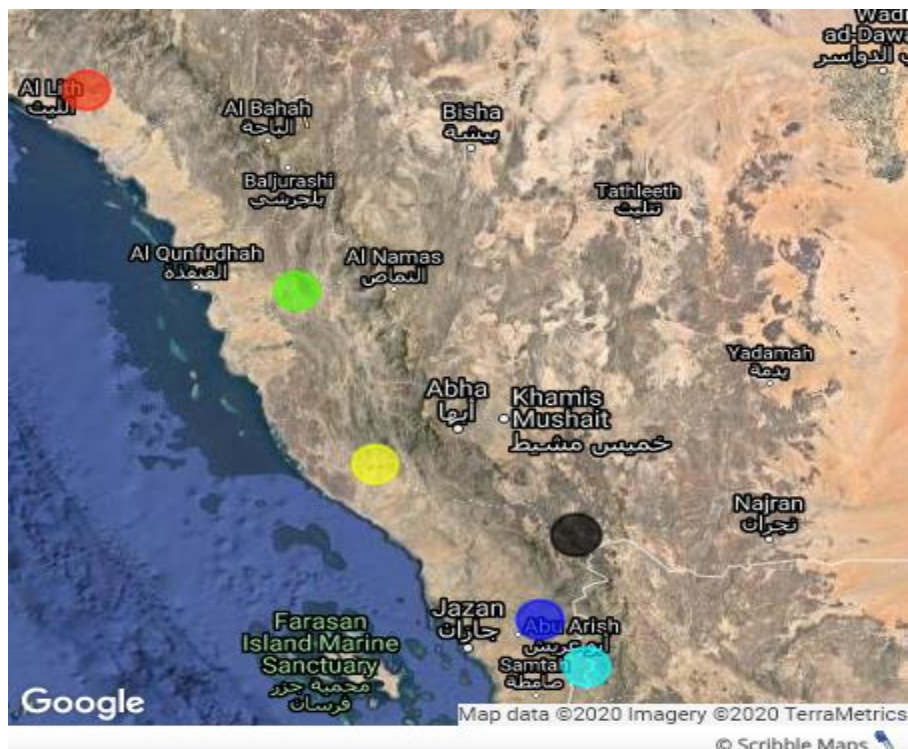
Figure 1.32: Locations of the selected hot springs on map of Saudi Arabia.
● Ghomygah spring   ● Tharban Spring   ● Al-Haridhah Spring.
● Al-Aridhah Spring   ● Al-Khobh Spring   ● Thebah Spring.

1.5.1 Ghomygah spring (GH) (Al-Harra)

Ghomygah spring (40°28**E**- 20°29**N**) **(Figure 1.33)** is a hot fracture spring that possesses a temperature of approximately 85.6°C (Bazuhair and Hussein, 1990). It is positioned near to a granite boundary along a cataclastic zone (Rehman and Shash, 2005). It is located 180 Km south of Makkah (Orfali and Perveen, 2019) as well as 205 Km southeast of Jeddah city in the Al-Laith area. It is composed of 48% surface water (Al-Dayel, 1988). According to Salem *et al.* (2016), 11 strains of *B. licheniformis* and 15 strains of *B. subtilis* were isolated from this spring. All strains were Gram-positive with rod-shaped bacteria (Salem *et al.*, 2016). *B. thermoamylovorans* also was found in this spring (Khiyami *et al.*, 2012).

One study showed that five compounds were isolated from *Penicillium* spp. from this spring. Two of these compounds are novel compounds; 3-(furan 12-carboxylic acid)-6-(methoxycarbonyl)-4-hydroxy-4-methyl-4 and 5-dihydro-2H-pyran as well as 3α-methyl-7-hydroxy-5-carboxylic acid methyl ester-1-indanone **(Figure 1.34)**, while the others are known compounds such as emodin, austinol and 2-methyl-penicinoline **(Figure 1.34)** (Orfali and Perveen, 2019). All compounds illustrated activities against *B. licheniformis*, *S. aureus*, *Escherichia fergusonii*, *Enterobacter xiangfangensis* and *Pseudomonas aeruginosa* (Orfali and Perveen, 2019).

Figure 1.33: Ghomygah spring.
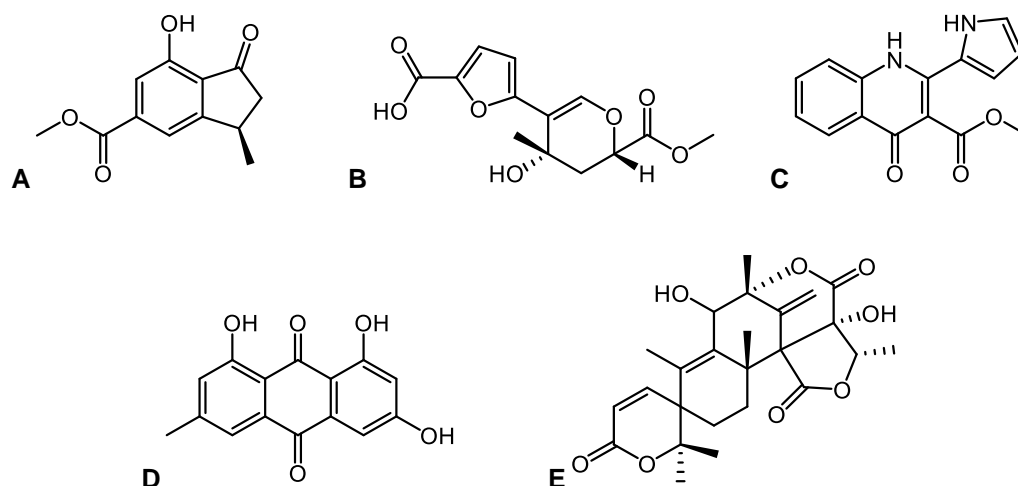
Figure 1.34: Some antibiotics isolated from Ghomygah spring.
A: 3α-methyl-7-hydroxy-5-carboxylic acid methyl ester-1-indanone, **B:** 3-(furan 12-carboxylic acid)-6-(methoxycarbonyl)-4-hydroxy-4-methyl-4 and 5-dihydro-2H-pyran,
C: 2-methyl-penicinoline, **D:** Emodin, **E:** Austinol.

1.5.2 Tharban spring (TH)

Tharban **(Figure 1.35)** (41°67**E**-19°03**N**) is a hot spring that is located in Aseer region in the southwest part of Saudi Arabia. The spring is located 183 km northwest of Abha city. The temperature of this spring reaches around 70°C. Al-Dhabi-1, a thermophilic *Streptomyces* spp., was isolated from this spring and showed antibacterial activity (Al-Dhabi *et al.*, 2016). From this species, pyrrolo-(1,2-a)-pyrazine-1,4-dione, hexahydro-3-(2-methylpropyl) (see above **Figure 1.15**) and benzene acetic acid **(Figure 1.36)** have been isolated; the latter has antifungal and antibacterial activities (Al-Dhabi *et al.*, 2019).

Figure 1.35: Tharban spring.

1-Dotriacontanol, tabtoxinine-β-lactam, citrinin, diethyl-2-pyrrolidinone and (3-aminopropyl) dibutylborane **(Figure 1.36)** are compounds that obtained from *Brevibacillus parabrevis* from this spring (Alrumman *et al.*, 2019). These compounds have different antimicrobial activities; for example, tabtoxinine-β-lactam has activity against multi-drug-resistant gram-negative bacteria (Alrumman *et al.*, 2019).
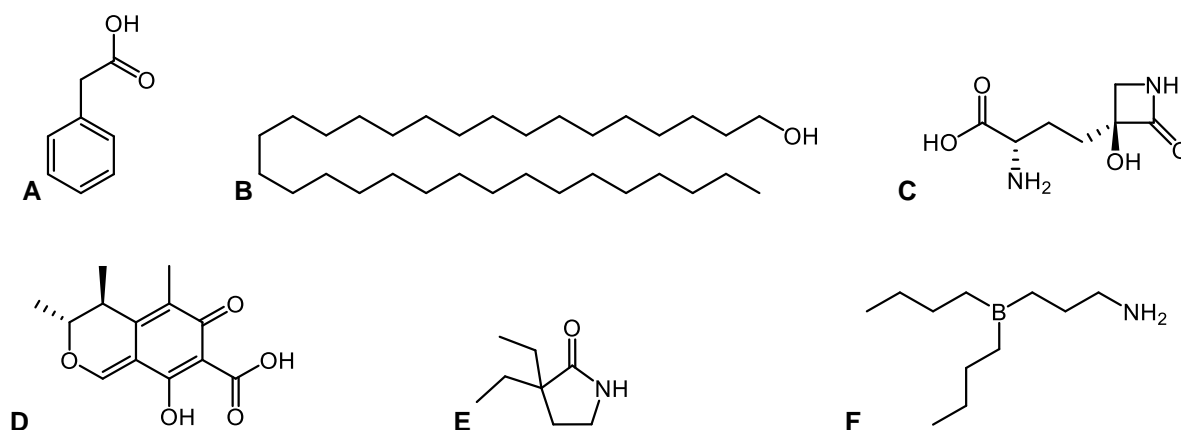
Figure 1.36: Some antibiotics isolated from Tharban spring.
A: Benzene acetic acid, **B:** 1-dotriacontanol, **C:** Tabtoxinine-β-lactam,
D: Citrinin, **E:** Diethyl-2-pyrrolidinone, **F:** (3- aminopropyl) dibutylborane.

1.5.3 Al-Aridhah spring (AR) (AL-Wagrah)

Al-Aridhah **(Figure 1.37)** (42°97**E**- 17°03**N**) is a hot spring that is 1 m in depth and 1.5 m wide and is located approximately 53 Km northeast of Jazan city (Basahy, 1994). It is composed of seven wells with a surface temperature between 43 and 61°C (Lashin and Al Arifi, 2012). These springs illustrate two fractions of a mixture of shallow water aquifer and thermal water (Rehman and Shash, 2005). *Deinococus geothermals* has been isolated from this spring (Khalil, 2011). Furthermore, *Synechococcus lividus* is a cyanobacterium that separated from this spring (Mohamed, 2008).

Cyclohexyl acrylate, imiloxan **(Figure 1.38)**, 1-dotriacontanol (see above **Figure 1.36**) and (3- aminopropyl) dibutylborane (see above **Figure 1.36**) are compounds that were isolated from *B. thermocopriae* from this spring (Alrumman *et al.*, 2019). These compounds have different antimicrobial activities; for example, cyclohexyl acrylate has an antibacterial property through binding to bacteria's phenyl moiety due to its acryl species (Alrumman *et al.*, 2019). Moreover, imiloxan has antimicrobial activity because of the imidazole component (Alrumman *et al.*, 2019).

Figure 1.37: Al-Aridhah spring.

Figure 1.38: Some antibiotics isolated from Al-Aridhah spring.
A: Cyclohexyl acrylate, **B:** Imiloxan.

1.5.4 Al-Khobh spring (KH)

Al-Khobh **(Figure 1.39)** (43°07**E**- 16°45**N**) is a hot spring that is 1 m deep and 5 m wide and is located approximately 55 Km southeast of Jazan city (Basahy, 1994). Two wells of this spring are accumulated at the volcanic water area with a high level of sulphate (Lashin and Al Arifi, 2012). The surface temperature for this spring is around 75.5°C (Rehman and Shash, 2005). *Bacillus* spp. and *Brevibacillus borstelenesis* have been isolated from this spring (Khalil, 2011). *B. thermoamylovorans* was also found in this spring (Khiyami *et al.*, 2012). *Synechococcus lividus* has also been isolated from this spring (Mohamed, 2008). Moreover, K10 strain was isolated from this spring, which was identified as *Bacillus subtilis* (El-Gayar *et al.*, 2017).

Figure 1.39: Al-Khobh spring.

Mephenesin (known as a muscle relaxant), lauric acid **(Figure 1.40)**, diethyl-2-pyrrolidinone (see above **Figure 1.36**), (3- aminopropyl) dibutylborane (see above **Figure 1.36**), culmorin **(Figure 1.40)** and 1-dotriacontanol (see above **Figure 1.36**) are antibiotic drugs that were isolated from *B. sonorensis* from this spring (Alrumman *et al.*, 2019). These compounds have different antimicrobial activities; for example, mephenesin demonstrated antibacterial activity against *Mycobacterium abscessus* and *Mycobacterium chelonae* (Alrumman *et al.*, 2019). Furthermore, lauric acid illustrated inhibitory activity against Gram-positive bacteria and fungi (Alrumman *et al.*, 2019).

Additionally, (3-Aminopropyl) dibutylborane, 1-dotriacontanol and cyclohexyl acrylate (see above **Figure 1.36**) are antibacterial molecules that were obtained from *Brevibacillus borstelenesis* from this spring (Alrumman *et al.*, 2019). These drugs have different antimicrobial activities; for example, etomidate showed antibiotic potency against *S. aureus*, *E. coli* and *P. aeruginosa* (Alrumman *et al.*, 2019).
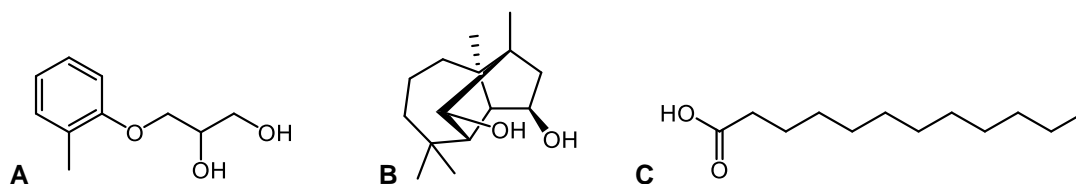
Figure 1.40: Some antibiotics isolated from Al-Khobh spring.
A: Mephenesin, **B:** Culmorin, **C:** Lauric acid.

1.5.5 Al-Haridhah spring (AH)

Al-Haridhah **Figure 1.41** (42°05**E**- 18°01**N**) is a thermal spring located near the Red Sea coast. It is located approximately 132 Km west of Abha city and 156 Km north of Jazan City. The temperature of Al-Haridhah spring is roughly 44°C.

Figure 1.41: Al-Haridhah spring.

1.5.6 Thebah spring (TB)

Thebah spring **Figure 1.42** (43°15**E**- 17°62**N**) is a hot spring that is composed of two hot springs with a temperature around 47°C. It is located approximately 158 Km southeast of Abha city near the border of Yemen and 170 Km west of Najran city. It is famous for its therapeutic activities against eye and skin infections.

Figure 1.42: Thebah spring.

1.6 Rationale of this study

The rationale of this study is as follows:

- Secondary metabolites from microbes are an important source of lead compounds such as antibiotics.

- Hot springs are one of the global hotspots for microorganisms diversity. This diversity is a harbor for various active compounds with pharmacological potential.

- It is expected that less than 5 % of the hot springs from Saudi Arabia have been screened pharmacologically.

1.7 Aims

There are two aims for this project:

- To screen hot spring water in order to find antibiotic-producing bacteria.

- To discover antibiotics that are able to fight bacterial resistance.

1.8 Objectives

The objectives of the study were as follows:

- To screen water samples from six different hot springs collected from different locations from Saudi Arabia for antimicrobial activities.

- To identify the bacterial strains that are responsible for producing antibiotics using cross-streak assay.

- To distinguish between Gram-positive and Gram-negative bacteria by utilizing Gram-stain method.

- To fermentate antibiotic-producing bacteria in a large scale using solid-phase fermentation in order to isolate the active compounds.

- To identify and characterize the genus and species of bacteria using PCR and whole-genome sequencing (WGS).

- To isolate the bioactive compounds from the extracts of the active fermentations using bioassay-guided isolation.

- To elucidate the structures of the bioactive compounds using various spectroscopic techniques such as NMR, MS and IR.

- To evaluate the antibacterial properties of extracts and isolated compounds using disc diffusion and MIC assays.

2 Materials and Methods

All chemicals were supplied by Sigma-Aldrich Company Ltd. (Dorset, UK) unless otherwise stated.

All selected methods were chosen based on the protocol used in the lab. Moreover, popularity, accuracy, quality, cost and time were taken into consideration during choosing the methods. For examples, PCR, DNA extraction and 16S rRNA gene sequence are the optimal and common methods for identifying the genus and species of bacteria. NMR, MS and IR were utilized because they are the popular techniques in the elucidation of chemical structures. MIC assay was used because it gives the accurate concentration of the active compounds or extracts; however, disc diffusion assay is the best for screening the antimicrobial activity.

2.1 Spring selection

The hot springs studied in this project are all used traditionally in the treatment of eye and infectious skin diseases as well as some other diseases such as rheumatism. They were selected based on their traditional uses by local people. Moreover, the popularity, location and temperature were taken into consideration in selecting these thermal springs.

2.2 Sample collection

All water samples were collected in June 2016 from six different hot springs in Saudi Arabia. Each sample was collected in a 20 mL sterile tube. Fifteen samples were collected from the Jazan area, thirteen from the Aseer area and the last four samples were from the Al-Laith area. All samples were transported to the School of Pharmacy at

UCL for further work and stored at 4°C until analysis. All samples are shown in (see above

Table 2.1).

Table 2.1: A list of collected samples.

Hot spring	Sample	Source	Temperature
Ghomygah (GH)	GH-A	From the origin of hot spring	>50°C
	GH-B	From the origin of hot spring	>50°C
	GH-C	From the stream of hot spring	<25°C
	GH-D	From the stream of hot spring	<25°C
Tharban (TH)	TH-A	From the origin of hot spring	>50°C
	TH-B	From the origin of hot spring	>50°C
	TH-C	From the stream of hot spring	<25°C
	TH-D	From the stream of hot spring	<25°C
Al-Haridhah (AH)	AH-A	From the origin of hot spring	25-50°C
	AH-B	From the stream of hot spring	<25°C
	AH-C	From the origin of hot spring	25-50°C
	AH-D	From the origin of hot spring	25-50°C
	AH-E	From the origin of hot spring	25-50°C
Al-Aridhah (AR)	AR-A	From the origin of hot spring	>50°C
	AR-B	From the origin of hot spring	>50°C
	AR-C	From the origin of hot spring	>50°C
	AR-D	From the origin of hot spring	>50°C
	AR-E	From the origin of hot spring	>50°C
	AR-F	From the origin of hot spring	>50°C
	AR-G	From the origin of hot spring	>50°C
	AR-H	From the origin of hot spring	>50°C
	AR-I	From the origin of hot spring	>50°C
	AR-J	From the origin of hot spring	>50°C
	AR-K	From the stream of hot spring	<25°C
Al-Khobh (KH)	KH-A	From the origin of hot spring	>50°C
	KH-B	From the origin of hot spring	>50°C
	KH-C	From the stream of hot spring	25-50°C
	KH-D	From the origin of hot spring	>50°C
Thebah (TB)	TB-A	From the origin of hot spring	25-50°C
	TB-B	From the origin of hot spring	25-50°C
	TB-C	From the origin of hot spring	25-50°C
	TB-D	From the origin of hot spring	25-50°C

2.3 Microbiological analysis

2.3.1 Bacterial strains

The extracts, fractions and isolated compounds were all tested against some susceptible- and resistant-strains for antibacterial activity. Five Gram-positive and three Gram-negative bacteria were used in this project. **Table 2.2** gives a brief overview of these strains.

Table 2.2: A list of resistant- and susceptible-bacterial strains.

Strains	Source	Note
S. aureus (25923)	ATCC	*Staphylococcus aureus* (susceptible strain)
SA 1199B	G. Kaatz (Kaatz *et al.*, 1993)	Multidrug-resistant *Staphylococcus aureus* strain
EMRSA-15	NCTC	Epidemic methicillin-resistant *Staphylococcus aureus* strain
XU212	E. Udo (Gibbons and Udo, 2000)	Tetracycline-resistant *Staphylococcus aureus* strain
B. subtilis	NCTC	*Bacillus subtilis* (susceptible strain)
E. coli (10418)	NCTC	*Escherichia coli* (NCTC 10418) (susceptible strain)
P. aeruginosa (10662)	NCTC	*Pseudomonas aeruginosa* (susceptible strain)
K. pneumoniae	NCTC	*Klebsiella pneumoniae* (susceptible strain)

ATCC: American type culture collection, **NCTC:** National collection of type cultures

2.3.2 Growth and isolation of bacteria

150 µL of each water sample was transferred onto a blood agar plate (Oxoid) and spread using a disposable cotton swab. Subsequently, plates were incubated at 37°C for 72h (Genlab). After incubation, each colony with a different colour or morphology **(Figure 2.1)** was collected with a disposable sterilized loop and streaked onto a new blood agar plate, and stored at 4°C until analysis.
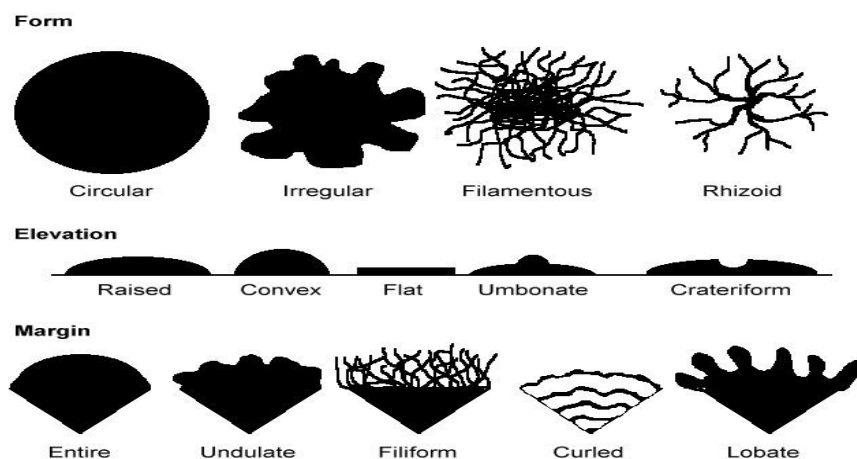
Figure 2.1: Morphology of bacterial colonies. From (Acharya, 2013).

2.3.3 Bacterial culture

The streak-plate method **(Figure 2.2)** is designed to isolate pure cultures of bacteria or colonies from varied populations by easy mechanical separation (Sanders, 2012). Each isolated bacterium was transferred onto a blood agar plate and streaked in different directions in order to ensure of its purity and to make a bacterial culture, which was used as a stock culture.
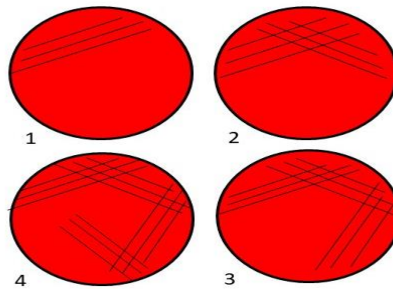
Figure 2.2: Streak-plate method.

2.3.4 Solid-state fermentation

Solid-state fermentation (SSF) can be defined as a fermentation procedure in which microbes are able to grow on solid materials without the existence of free liquid (Krishna, 2005). SSF can be used for the production of secondary metabolites such as antibiotics (Bhargav *et al*., 2008). The SSF method has the potential to yield preferred microbial products more efficiently than submerged fermentation (SMF) (Kumar and Ray, 2014).

One single colony was inoculated onto one blood agar plate and distributed in the form of the circle near to the edge of the agar in order to be cultured. The plate was then incubated at 37°C for 24h. After incubation, a large number of colonies were transferred into a reagent bottle containing 30 mL of PBS as a stock solution. The PBS was prepared

according to the manufacture's protocol and then autoclaved (Dixons) at 121°C for 15 min. Then, 1 mL of stock solution was transferred into a vial containing 20 mL of PBS. After that, 1 mL was inoculated onto one blood agar plate and then incubated for one week at 37°C. 600 plates **(Figure 2.3)** were used as a large-scale fermentation for each bacterium. The large-scale fermentation was used for only six bacteria and 20 plates were utilized as a small scale fermentation for the others.

Figure 2.3: Solid-state fermentation of AR-G2.

2.3.5   Extraction

After seven days of incubation, the agar was cut into small cubes (approximately 1 cm in length of each side) and then scraped away and transferred into a conical flask (500 mL). (3 X 300 mL) of chloroform was first utilized to kill bacteria as well as to extract compounds from the agar. Next, (3 X 300 mL) of methanol and (3 X 300 mL) of water were used to extract active compounds, respectively. All extractions were performed by incubation (Stuart) on a rotatory shaker (IKA) at 160 rpm/min. at 37°C for 24h **(Figure 2.4).** Subsequently, all extracts were sonicated (Grant) at 40°C for 30 min and then filtered into a round-bottom flask. Chloroform and methanol extracts **(Figure 2.4)** were evaporated using a rotatory evaporator (Buchi). However, the water extract was

evaporated via freeze-drying (Savant). All extracts were weighed and kept at 4°C until analysis.

Figure 2.4: Solvent Extraction of KH-A1.
A: Extraction, **B:** Methanol extract.

2.3.6 Gram-stain technique

The Gram-stain was discovered in the late 1800s by Hans Christian Gram, a Danish clinician, and utilized as a diagnostic tool for clinical microbiology (Beveridge, 2001). The Gram-stain still plays an essential role in the identification and classification of bacteria (Smith and Hussey, 2005). It is a rapid and economical tool that is used for distinguishing between Gram-positive and Gram-negative bacteria.

5 µL of distilled water was pipetted onto the middle of a glass slide. A single colony was taken from a culture of bacteria by a sterile loop and added to the distilled water and then spread on the surface of the slide in the form of a circle. After that, the slide was exposed to a Bunsen burner's flame for two seconds and repeated three times in order to fix the bacterial cells onto the surface of the slide and to remove excess water. Crystal violet reagent (Pro-Lab Diagnostics) was added to the slide and left for one minute and washed off with distilled water. Next, Gram's iodine (Pro-Lab Diagnostics) was poured

onto the smear and allowed to stay for 60 seconds and then rinsed with distilled water. Decolorizer (50% ethanol and 50% acetone) was used for 5 seconds to decolorize the sample and this was then rinsed with distilled water. Safranin was added to the smear for 45 seconds and then washed off with water. The slide **(Figure 2.5)** was observed under a light microscope with a 100X lens (Nikon). The violet colour indicated Gram-positive bacteria and the pink colour Gram-negative bacteria.
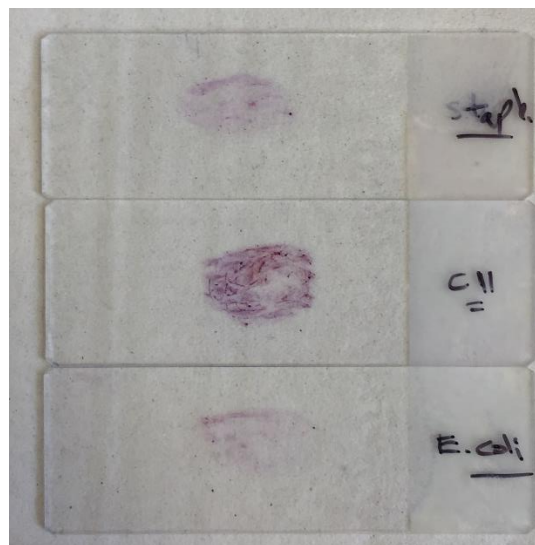
Figure 2.5: Gram-stains of _S. aureus, E. coli_ and GH-C11.

2.3.7 Extraction of genomic DNA from isolated bacteria

Fourteen bacterial strains were cultured on a blood agar plate (each strain in one plate) and then incubated at 37°C for 18h in order to be ready for DNA extraction. The DNeasy® UltraClean® Microbial Kit (Qiagen, Germany) was used for extraction. According to the manufacturer's protocol, a majority of bacterial colonies were resuspended in 300 µL of PowerBead Solution and then 50 µL of Solution CB1 was added to them and then gently vortexed to mix. Next, they were incubated at 70°C for 10 min (Fisher Scientific) and transferred into a PowerBead tube and vortexed for 10 min at 13,000 rpm. The tubes were centrifuged at 13,000 rpm for 1 min at room temperature

and the supernatants transferred to collection tubes. After that, 100 µL of Solution IRS was added to the supernatant and incubated at 5°C for 5 min. After centrifuging for 1 min, 900 µL of Solution SB was added to the supernatant and loaded onto an MB spin column in order to centrifuge at the maximum speed for 1 min to get rid of the flow-through liquid. 300 µL of Solution CB was added to the column and then centrifuged for 1 min. Finally, 50 µL of Solution EB was added to the center of the white filter membrane in order to collect the isolated DNA and then analyzed on the gel electrophoresis and Nanodrop (Thermo) and stored at 4°C for further analysis.

2.3.8 PCR amplification of isolated DNA

It is believed that PCR was discovered by Kary Mullis at the Cetus Corporation in California in 1983 (Bartlett and Stirling, 2003). PCR is considered a simple enzymatic assay that allows amplification of a specific DNA fragment from a complicated pool of DNA, and it is widely used to diagnose diseases, clone and sequence genes (Garibyan and Avashia, 2013).

Fourteen isolated DNA samples from different bacterial strains were subjected to the PCR technique in order to amplify them for 16S rRNA gene sequencing. PCR amplification was performed according to the conditions recommended by the manufacturer for the Phusion High-Fidelity DNA Polymerase (New England Biolabs – Massachusetts, USA). Each bacterial colony was suspended in 1 mL of distilled water to be ready for analysis. The reaction mixture for each sample (50 µL) contained: 1 µL of the isolated DNA, 10 µL of a 5X Phusion buffer, 1 µL of dNTPs (10mM), 0.5 µL of each primer (FD1 + RP1) (10 µM) **(Table 2.3)**, 0.5 µL of Phusion polymerase and 36.5 µL of microbiological H_2O. Reaction conditions for amplification were 94°C for 5 min, 35 cycles

[94°C for 30 secs, 62°C for 30 secs, 72°C for 30 secs] and 72°C for 5 min (Bio Rad). The PCR products were purified using a QIAquick PCR Purification Kit (Qiagen, Germany) according to the manufacturer's protocol. All tubes were then analyzed by gel electrophoresis and Nanodrop and stored at 4°C for further analysis.

Table 2.3: Primers used in this work.

Primer	Sequence
Forward PCR Primer (FD1)	5'-AGAGTTTGATCCTGGCTCAG-3' (Epicenter Technologies – Wisconsin, USA)
Reversed PCR Primer (RP1)	5'-ACGGTTACCTTGTTACGACTT-3' (Epicenter Technologies – Wisconsin, USA)

2.3.9 Gel electrophoresis

Electrophoresis is defined as the migration of solutes or ions under the influence of an electric field (Sekhon, 2011) or charged particles are subjected to an externally applied electric field in order to migrate toward the electrode of opposite sign for electrophoretic separation (Li and Wu, 2000). Agarose gel electrophoresis is a simple way of separating, purifying and identifying DNA fragments of varying sizes ranging from 0.5 bp to 25 kb (Voytas, 2000).

PCR reaction products were run on a 1% agarose gel containing 0.5% GelRed™ (Biotium Inc., USA) in TAE buffer (40 mM Tris, 20mM acetic acid and 1 mM EDTA) for 90 mins at 65 V **(Figure 2.6)**. Before loading, each sample was mixed with Purple Gel Loading Dye (New England BioLabs Inc., USA) according to the manufacturer's protocol. A 100 bp ladder (New England BioLabs Inc., USA) was utilized as a molecular size marker based on the manufacturer's procedures and gel bands were visualized via a UV transilluminator (Syngene). For extracted DNA, the same steps of PCR products were

performed except the molecular size marker, which was 1 kb ladder (New England BioLabs Inc., USA).
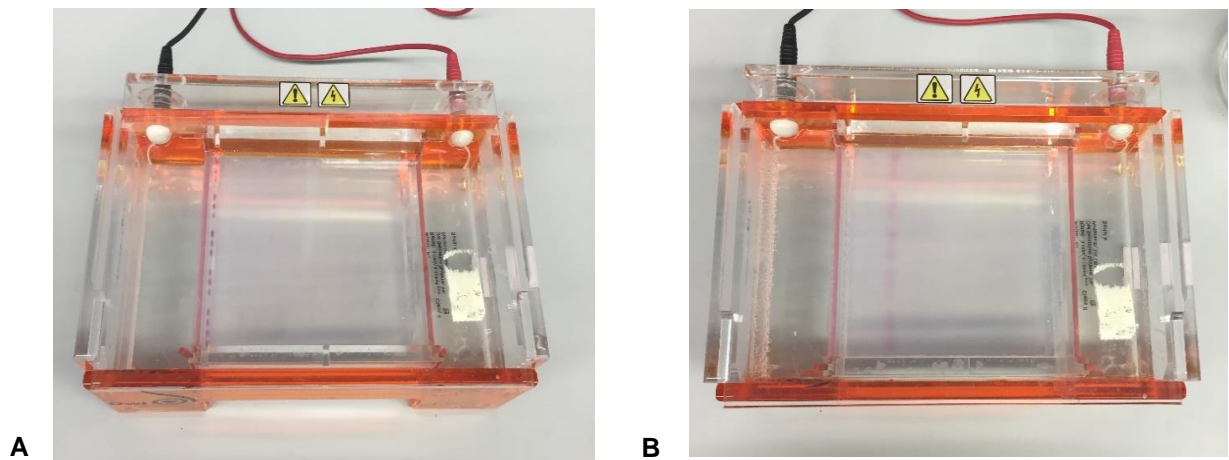
Figure 2.6: Gel electrophoresis of isolated DNA.
A: At the beginning, **B:** After 30 min.

2.3.10 Nanodrop analysis

Nanodrop is a UV/Vis spectrophotometric instrument that analytically used for nucleic acids analysis as well as has wide applications for protein assays (O'Neill *et al.*, 2011). Moreover, this technique enables the assessment of nucleic acid concentrations, which range from 1 pg/µL to 15,000 ng/µL with minimal consumption of sample (Desjardins and Conklin, 2010).

1 µL from each PCR products and extracted DNA samples were added to the upper and lower optical surfaces of the microvolume spectrophotometer in order to obtain the concentration of DNA in ng/µL. The solution EB was used as a blank before adding the samples.

2.3.11 16S rRNA gene sequence

16S rRNA gene sequence has been utilized as a vital tool for phylogenetic analysis and classification of bacteria since the 1980s (Cai *et al.*, 2003).

30 ng/µL from each single DNA was prepared in EB solution in order to be ready for sequencing. All extracted DNA samples were sealed and barcoded and transported to MicrobesNG (BBSRC & The University of Birmingham) by courier to obtain the whole genome sequence. Sequencing was performed on the Illumina MiSeq and HiSeq 2500 platforms. The reads were trimmed using Trimmomatic and the quality was assessed using in-house scripts combined with the following software: Samtools, BedTools and BWA-mem (http://bio-bwa.sourceforge.net). Paired-end reads were analyzed using Kraken to determine the closest available reference genome. For PCR products, they were sent to a UCL Sequencing Facility for 16S rRNA gene sequencing. The chromatograms of obtained nucleotide sequences of PCR products were manually assessed for quality using SnapGene Viewer 3.0.1. (GSL Biotech LLC, USA). Quality was assessed using Bioedit 7.2.5. (Ibis Biosciences, USA). The sequence data was saved as a FASTA file and then converted to a translated sequence and compared for homology using BLASTx (http://blast.ncbi.nlm.nih.gov, National Center for Biotechnology Information, USA).

2.3.12 Phylogenetic tree

The word "phylogeny" depicts the relationships between entities such as genes, genomes or species in such a way in order to reflect their evolutionary histories (De Bruyn *et al.*, 2014). This term was invented by Haeckel in 1866, which was derived from the concept of genealogy (De Bruyn *et al.*, 2014). Phylogenetic tree analysis is regarded as an integral portion of bioinformatics because it determines the evolutionary relationship between organisms or molecules (Narayanan *et al.*, 2017). The key aim of drawing trees is to envisage the phylogenetic relationships of the organisms and to let the reader identify these relationships at a glance (Ludwig and Klenk, 2005).

The phylogenetic tree was constructed using molecular evolutionary genetic analysis (MEGA) software version 7.0.21 with the 16S rRNA sequences. The 16S rRNA nucleotide sequences were analyzed by using BLAST (blastn) search and the sequences were compared with other available bacterial 16S rRNA sequences in the GenBank database (https://www.ncbi.nlm.nih.gov/genbank/). Then, using MEGA software, the selected sequences were aligned under ClustalW. The aligned sequences were then used to construct the phylogenetic tree. The Neighbor-Joining tree option in MEGA software was used to construct the phylogenetic tree.

2.4 Chromatographic methods

The chromatography term was obtained from Greek, 'chroma' meaning colour and 'graphein' meaning writing, so the word chromatography means 'colour writing' (Parasuraman *et al.*, 2014). Chromatography is defined as a physicochemical process for the separation of complex mixtures and was discovered in 1903 by Russian–Italian botanist Mikhail Tswett (Luxminarayan *et al.*, 2017). Chromatographic techniques are used to separate components of an analyte between two phases: mobile and stationary phases. The separation in both normal and reverse phases can be accomplished by adsorption and partition. In this study, several chromatographic methods were carried out in order to isolate the active compounds such as partitioning chromatography, gravity column chromatography, vacuum liquid column, solid-phase extraction, Liquid Chromatography-Mass Spectrometry (LC-MS) and thin layer chromatography.

2.4.1 Partitioning chromatography

Partition chromatography can be defined as the separation of compounds depending on the partition of a solute between two solvents; a liquid stationary phase,

which is immiscible with the mobile phase, is adsorbed to the surface of the solid adsorbent (Parasuraman *et al.*, 2014).

The crude methanolic extract was dissolved in 200 mL of water: methanol – (95:5) and then partitioned with *n*-hexane (3 X 200 mL). The resulting *n*-hexane fractions were combined together and evaporated using a rotatory evaporator. The aqueous-methanolic layer was then partitioned with chloroform (3 X 200 mL). The chloroform layer was collected and dried. Next, the aqueous-methanolic layer was extracted with ethyl acetate (3 X 200 mL) and then collected in the same way as the hexane and chloroform partitions. After that, *n*-butanol (3 X 200 mL) was used for partitioing with the aqueous-methanolic layer. Thus, the crude methanolic extract was split into five sub-extracts **(Figure 2.7)**: *n*-hexane, chloroform, ethyl acetate, *n*-butanol and water. All sub-extracts were dried using a rotatory evaporator except for the water sub-extract which was freeze-dried. This method was used with the methanolic extracts of **TB-A3**, **TH-C4**, **AR-G2** and **AH-E1** isolates.
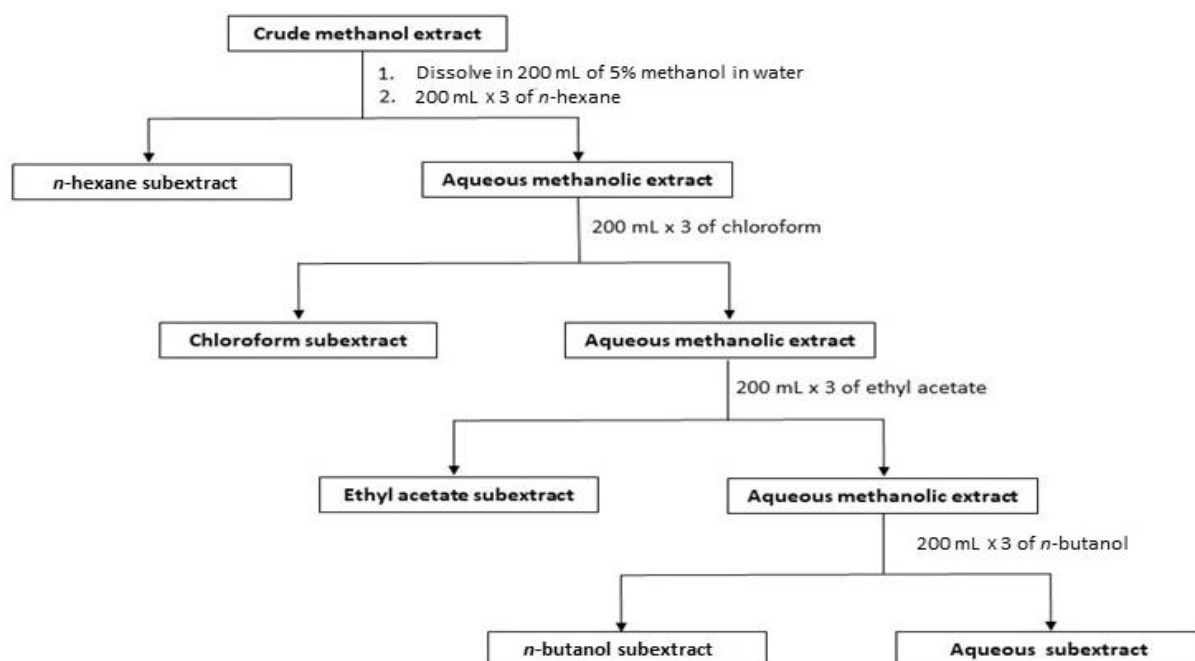
Figure 2.7: Scheme of liquid-liquid partitioning.

2.4.2 Gravity column chromatography

The gravity column chromatography is a separation technique that is utilized for the isolation and purification of compounds from extracts or fractions. The column (35/20 100mL reservoir, 10.5 x 300mm) was clamped vertically and half-filled with 50 g of silica gel 60 (Merck) **(Figure 2.8)**. The mobile phase was slowly poured onto the column in order to avoid any changes in the surface level of the silica. The stopcock was opened to allow any excess solvent to drain and to support silica gel packing. The mobile phase drained until just above the level of silica and then the methanolic extract (1.2 g) was introduced onto the column gradually to keep the surface even. The solvent elution was performed under the influence of gravity. The mobile phase used for this method was 100% *n*-hexane to 100% ethyl acetate with 10% increment, and 100% methanol was used as a final wash. 50 mL of the mobile phase was utilized for every fraction. All fractions were collected in a 100 mL beaker and then dried by a rotatory evaporator and assessed for their antibacterial activities against *S. aureus* by utilizing the disc diffusion assay **(Section 2.6.2)**. This method was used only for the **GH-C8** extract.
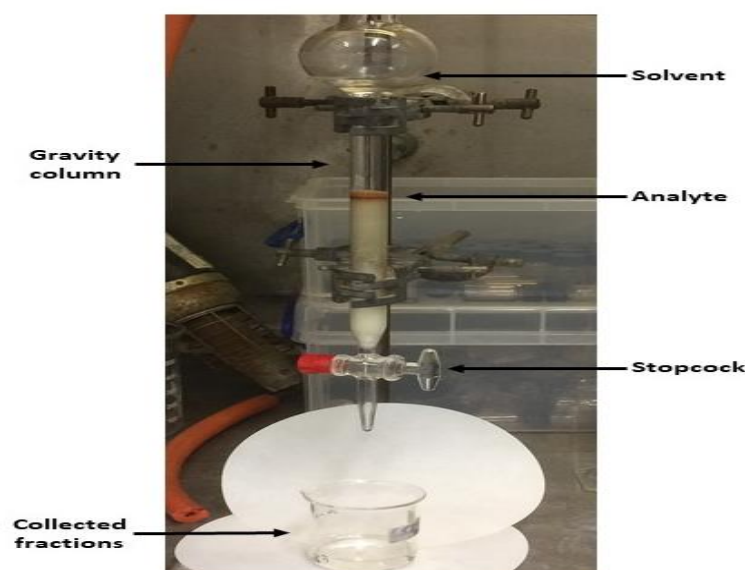
Figure 2.8: Gravity column of GH-C8.

2.4.3 Vacuum liquid column chromatography

Vacuum liquid column (also known as flash dry column chromatography) is a separation method that is accelerated and conducted under the influence of a vacuum. It is usually used for the fractionation of a large amount of crude extracts. 150 g of normal phase silica gel (Merck) was firmly packed into a glass column (70 x 170 mm, 70 x 510 mm). The column was then vibrated to get rid of any air bubbles and a vacuum was applied to tighten the packing **(Figure 2.9)**. The column was conditioned with the first eluent (*n*-hexane). Next, the methanolic extract (3.6 g) was dissolved in a small amount of methanol and then slowly loaded into the column. Aliquots of the mobile phase were added to the column to elute the fractions in a gradient from 100% *n*-hexane to 100% ethyl acetate in 5% increments of ethyl acetate. 100 mL of the solvent was used for each fraction. The round bottom flasks (250 mL) were used to collect the fractions. The collected fractions were dried using a rotatory evaporator and then tested for their activity against *S. aureus* by utilizing a disc diffusion assay **(Section 2.6.2)**. This method was used only for the **KH-A1** extract.
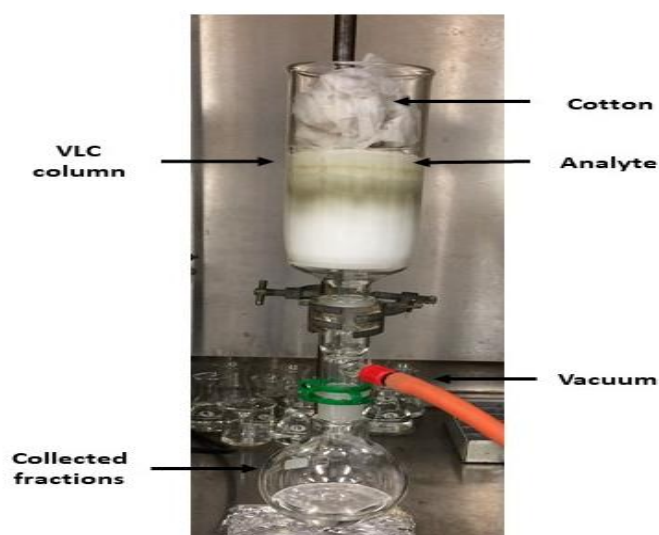
Figure 2.9: VLC chromatography of KH-A1.

2.4.4 Solid-phase extraction

Solid-phase extraction (SPE) is considered to be one of the most effective extraction techniques because of its versatility as well as its ability to efficiently purify and enrich analytes from their liquid sample matrices (Fontanals *et al.*, 2010).

The SPE cartridge was first connected to the vacuum manifold **(Figure 2.10)**. 50 mL of *n*-hexane was used to condition the column in the case of the normal phase SPE, while 50 mL of acetonitrile was utilized for RP-SPE. All sub-extracts (not more than 5% of the silica weight) were dissolved in an appropriate solvent and then transferred into the column under vacuum. For normal phase separations, the Strata SI-1 silica (55 µm, 70A) 70g/150 mL Giga tubes (Phenomenex) were used. Strata C18-E (55 µm, 70A) 10g/60 mL Giga tubes (Phenomenex) were utilized for RP-SPE. 50 mL of increasingly polar (10% gradient) mobile phase (100% *n*-hexane – 100% ethyl acetate) was used for the normal phase. 100% of methanol was utilized as a final wash. For reversed-phase, 100% acetonitrile to 100% methanol in 10% increments was used to elute fractions and then 100% of chloroform was used as a final step. All fractions were dried using a rotatory evaporator besides the aqueous fraction was freeze-drying. The collected fractions were subjected to the disc diffusion assay in order to determine the active antibacterial fraction. SPE was applied for the fractionation of extracts and purification of compounds.
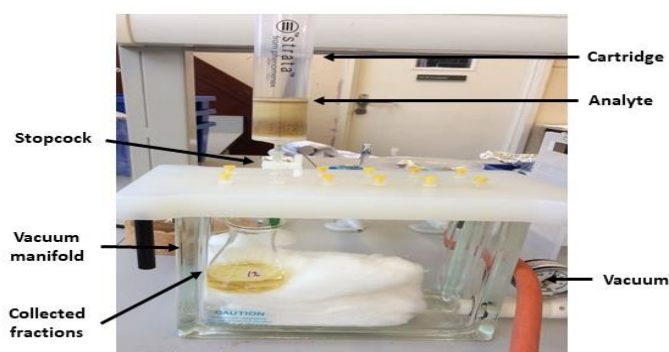
Figure 2.10: SPE of TB-A3.

2.4.5 Liquid Chromatography-Mass Spectrometry

The combination of high-performance liquid chromatography and mass spectrometry (LC/MS) has had an important impact on drug development during the last decades (Beccaria and Cabooter, 2020). LC-MS is regarded as a powerful technique for mixture analysis and has been extensively utilized for the identification of drug metabolites, the studies of organic reactions, the identification of impurities and degradants in pharmaceutical formulations (Wu, 2000). The sample can be separated by LC and then sprayed into an atmospheric pressure ion source in order to produce ions in the gas phase (Parasuraman *et al.*, 2014). The mass analyzer is then used to determine ions based on their mass-to-charge ratio (Parasuraman *et al.*, 2014).

1 mg/mL from each **OM3** and **OM6** was prepared by dissolving in methanol and then transferred into a HPLC vial in order to be ready for LC-MS analysis. a Shimadzu LCMS-2020, which is a single quadrupole mass spectrometer with a mass range from 50 Da to 2000 Da, was used in this experiment. The samples were put in the sample loader and a program was created to run the mobile phase in a gradient way with regular periods of washing in between two different solvent systems. 20 µL of each sample was injected into the instrument and an analytical column (XBridge, 3.0 X 50mm, 2.5µm) was utilized at a wavelength of 254 nm with a flow rate of 1 mL/min. The gradient system is summarized in **(Table 2.4)**.

Table 2.4: Gradient system used in LC-MS analysis.

Time (minutes)	Solvent A 0.1% formic acid	Solvent B 0.1%formic acid in acetonitrile
1.00	90%	10%
4.00	5%	95%
5.00	5%	95%
5.20	90%	10%
7.00	**Stop**	

2.4.6 Thin-layer chromatography

Thin-layer chromatography is an excellent method for the fast and simple profiling of plant extracts, reference methods in pharmacopoeial monographs for the quality control of medicinal herbs and it is cheap, easy to perform and generally utilized for the analysis and isolation of natural products (preparative-TLC) (Favre-Godal *et al.*, 2013). TLC can be performed on a sheet of plastic, glass, or aluminum foil, which is covered with a thin layer of adsorbent material, usually silica gel, cellulose, or aluminum oxide (Bele and Khale, 2011). In addition, TLC is considered a fast method in terms of identifying or detecting molecules (Rathee *et al.*, 2011). The principle of this technique depends on the affinity of a molecule between two phases: a stationary phase and mobile phase. The stationary phase is an adsorbent material such as silica gel that is coated onto an aluminum or glass plate. However, the mobile phase can be a mixture of solvents that has different polarities. Based on capillary properties, the mobile phase migrates the extract's constituents up to the top of the silica gel plate and the separation of compounds depends on their adsorption to the stationary phase. TLC is useful in the separation of mixtures and the identification of drugs or impurities (Luxminarayan *et al.*, 2017). The R_f value is used to determine the distance of travelling compounds on the stationary phase.

The R_f value can be calculated using the following equation:

$$R_f = DC / DS$$

DC is the distance that travelled by a compound up the plate while DS is the distance that travelled by the solvent front.

TLC can be divided into two types: analytical and preparative TLC. The analytical TLC was utilized for evaluating the purity and polarity of compounds in each fraction, whereas the preparative TLC was used for the isolation of the active compound.

2.4.6.1   Preparative TLC

Preparative TLC **(Figure 2.11)** was used for the further purification of the active compounds. Preparative TLC was performed on all of the active fractions according to the results of the bioautography assay **(Section 2.6.3)**. A normal phase silica gel plate 60 F$_{254}$ and a reverse-phase silica gel plate C-18 (10 x20 cm) were used in order to isolate the active molecule (Merck KGaA). Each fraction was dissolved in 1 mL of an appropriate solvent (methanol or chloroform) and then sonicated for 15 min at 40ºC and loaded onto the plate in a band around 1 cm from the base of TLC plate via a capillary tube. The solvent system that was used for each fraction was the same system as in the bioautography assay. Next, the TLC plate was put into a twin trough glass chamber saturated with the appropriate solvent for 30 min. The mobile phase was allowed to migrate 8 cm up the TLC plate and subsequently the plate was removed from the chamber and dried inside a sterile cabinet for 30 min. Vanillin-sulfuric acid was used as a general indicator.

The plate was then visualized under UV$_{254}$ and UV$_{366}$ nm by using a TLC visualizer (Camag) and the active antibacterial band was determined with a pencil in order to scratch it off. After scratching, all bands were resuspended in a suitable solvent and then filtered off to obtain the active compound and remove the silica; this process was repeated three times. The filtrate was then dried under a vacuum and the dried compounds were weighed and stored at 4°C.

Figure 2.11: RP-TLC (prep) of a compound OM7 under UV$_{254}$.

2.5 Spectroscopic methods

Spectroscopic methods are regarded as a helpful tool that provides structural information about a compound. Several spectroscopic techniques were used in this project for the identification of compounds: Nuclear Magnetic Resonance (NMR), Mass Spectrometry (MS) and Infrared Spectroscopy (IR).

2.5.1 Nuclear magnetic resonance (NMR)

The first historic NMR was discovered in 1946 by Purcell and Bloch (Sem and Pellecchia, 2001). NMR deals with the interaction between the magnetic fields and the magnetic moments of atomic nuclei, which is related to their nuclear spin (Kim *et al.*, 2013). This can be conducted by measuring the absorbance of radio frequency (RF) radiation that occurs when specific types of atomic nuclei like ^{1}H, ^{13}C and ^{15}N are put under strong magnetic fields (Wishart, 2005).

NMR spectroscopy is considered a powerful tool for the study of dynamics, interactions and structures of biomolecules (Schirra and Craik, 2008) and for the structural elucidation of unknown natural and synthetic compounds (Simmler *et al.*, 2014), as well as its applications in pharmaceutical analysis for identifying a drug and its accompanying impurities (Holzgrabe *et al.*, 2005).

NMR experiments can vary from simple one-dimensional to more complicated multidimensional experiments that identify spin-spin interactions and bond connectivities (Simpson *et al.*, 2018). The method that was used for 1D NMR spectra is the Fourier transform technique, which was introduced by Anderson and Ernst (Sem and Pellecchia, 2001). 2D NMR experiments such as COSY, HMQC and HMBC techniques are frequently used for structural elucidation because they decreased the obstacle of spectral crowding (Fotakis *et al.*, 2013).

In 1963, ^{1}H NMR was first introduced as an analytical tool for quantitative analysis by Jungnickel and Forbes (Bharti and Roy, 2012). It is regarded as a simple, fast and accurate method of analysis (Izunobi and Higginbotham, 2011). ^{1}H nuclei may lead to diverse NMR signals in the case of hydrogens as they are in different chemical environments (Alexandri *et al.*, 2017). The areas under the peaks in the spectra of ^{1}H NMR are proportional to the relative concentrations of the species that is being examined (Izunobi and Higginbotham, 2011). ^{1}H NMR provides information about hydrogen numbers within a compound as well as their chemical environments, which are known as a chemical shift (δ). The chemical shift of ^{1}H NMR ranges from 0 to 15 ppm. The hydrogen signals may be affected by shielding and deshielding neighboring electron-donating or withdrawing groups, respectively. Deshielding occurs as a result of conjugated systems, electron-withdrawing groups such as carbonyl groups and heteroatoms like nitrogen, oxygen and halide groups. Integration and multiplicity can be obtained from a ^{1}H NMR spectrum.

^{13}C NMR spectra are proton-decoupled spectra that have a large chemical shift (δ) range from 0 to 220 ppm (Izunobi and Higginbotham, 2011). Shielded carbons can be found at the lower chemical shift values while deshielded carbons at the higher ppm.

The distortionless enhancement by polarization transfer (DEPT-135) gives information about the type of carbon when compared to the broadband decoupled ^{13}C NMR spectrum. Methine (-CH) and methyl (-CH$_3$) carbons appear on a one side (positive), whereas the methylene (-CH$_2$) carbons are shown on the other (negative). The quaternary carbons are absent when compared to the ^{13}C NMR spectrum. Moreover, DEPT-90 provides information about the presence of methine (-CH) carbons only.

COrrelation SpectroscopY (COSY) has relatively short acquisition time due to its ability to record couplings between hydrogen nuclei with high natural abundance (Mahrous and Farag, 2015). It can demonstrate coupling between protons over two to three bonds distant, and four bonds distant in some cases. Moreover, five bonds distant can be seen in rare situations. A ^{1}H NMR spectrum can be plotted on both sides of the axes, which shows two kinds of peaks: cross and diagonal peaks. The cross-peaks show coupling between pairs of hydrogens; however, the diagonal peaks illustrate the hydrogen signals in the ^{1}H NMR spectrum.

The Heteronuclear Multiple-Quantum Correlation (HMQC) experiment demonstrates direct bonding between carbon and proton nuclei. The spectrum can be presented with a ^{1}H NMR spectrum displayed on the top axis and a ^{13}C NMR spectrum on the left axis. HMQC spectra show correlation peaks between hydrogens that are directly attached to carbon atoms. Quaternary carbons and any carbon not attached to hydrogen do not show correlation peaks.

Heteronuclear Multiple-Bond Correlation (HMBC) spectra illustrate long-range correlations between hydrogen and carbon nuclei. The HMBC method is deemed to be the single most significant technique for the structural elucidation of organic molecules because it is capable of providing correlation signals for carbon-hydrogen spin pairs, which points out to connectivities over two and three bonds and can thus be used to shape a molecular skeleton (Wagner and Berger, 1998). The spectrum can be presented with a ^{1}H NMR spectrum displayed on the top axis and a ^{13}C NMR spectrum on the left axis.

Nuclear Overhauser Effect SpectroscopY (NOESY) displays couplings between hydrogens through space, and it is significant in the determination of stereochemistry.

The spectrum format of NOESY is similar to that of COSY, and therefore the comparison between them is important in order to determine through space coupling signals from scalar through a bond coupling. The cross peak signals are not symmetrical in comparison to COSY.

1 mg of isolated compounds was dissolved in 700 µL of deuterated solvents based on their polarities and then centrifuged for 1 min at 13000 rpm in order to get rid of any solid material. Next, the supernatant was transferred into a NMR tube for the NMR experiment. In addition, deuterated solvents were used as an internal reference for the calibration of respective spectra **(Table 2.5)**. The NMR data were then processed by using Bruker Topspin software (integration, calibration, coupling constant and multiplicity) in order to start the structure elucidation process. Other spectroscopic methods such as MS, LC-MS and IR were utilized to confirm the structure.

Table 2.5: Chemical shifts of deuterated solvents used in the project (Cambridge isotope laboratories, 2020).

Deuterated solvents	Chemical formula	^{1}H-NMR (ppm)	^{13}C-NMR (ppm)	Residual H_2O
Chloroform-d	$CDCL_3$	7.26 (1)	77.2 (3)	1.50
Methanol-d_4	CD_3OD	3.31 (5), 4.87 (1)	49.1 (7)	4.90
Acetone- d_6	CD_3COCD_3	2.05 (5)	29.9 (7), 206.7 (13)	2.80
Benzene- d_6	C_6D_6	7.16 (1)	128.4 (3)	0.40

Full NMR spectra (^{1}H, ^{13}C, DEPT-90, DEPT-135, HMQC, HMBC, COSY, NOESY) were obtained for the structural elucidation on a Bruker Avance 500 MHz spectrometer. Chemical shifts were reported in parts per million (ppm) and calibration was accomplished by reference to the solvent peaks. Coupling constants (*J* values) were given in Hertz (Hz).

Table 2.6: Number of spins for each NMR method.

NMR application	Number of scans
^{1}H-proton	128
^{13}C-carbon	1024
DEPT-135	512
DEPT-90	512
HMQC	16
HMBC	16
COSY	8
NOESY	8

2.5.2 Mass spectrometry

Mass spectrometry is a popular analytical tool used to measure the molecular weight of a sample or to distinguish molecules by their mass-to-charge ratios (Feng *et al.*, 2008). It is operated by transforming the analyte molecules to a charged state (ionized) in which the ions and any fragment ions that are created during the ionisation process are analyzed depending on their mass to charge ratio (*m/z*) (Pitt, 2009).

In the 1980s, the team of John Fenn introduced electrospray ionization (ESI) which has become the first choice for coupling liquid chromatography with mass spectrometers (Urban, 2016). MS is one of the most important tools to obtain information about unknown compound structures, their molecular composition and the concentration of analytes in complex matrices during manufacturing chemical processes (Llamas *et al.*, 2007), as well as its use in both academia and industry for different purposes such as diagnostics, bio-analyses and drug discovery (Feng *et al.*, 2008).

There are two methods used to obtain mass spectra of isolated compounds: low-resolution and high-resolution methods. The low-resolution method was done by electrospray ionisation mass spectrometry (ESI-MS), utilizing both positive and negative modes on a LCQ Duo Ion-Trap spectrometer. All samples were run in either 0.1% formic

acid and 50% acetonitrile (positive mode) or methanol for the negative mode. The spectra were recorded on a ThermoQuest Navigator instrument.

High-resolution mass spectrometry (HRMS) was used for accurate mass determination and was performed on a Waters Q-TOF premier Tandem mass spectrometer. The mass spectrometric spectra were determined by the Research Service Unit at the School of Pharmacy at UCL.

The mass spectra were plotted as the abundance of the ions in % (x-axis) against the ratio of mass-to-charge (*m/z*) value (y-axis). The highest peak represented the most abundant ion being the most stable ion created during the ionisation process. 1-5 mg/mL of isolated compounds were dissolved in a suitable solvent and then transferred to a glass vial in order to submit for analysis.

2.5.3 Infrared spectroscopy

The infrared spectrum results from the absorption of electromagnetic radiation at frequencies that correspond to the vibration of specific groups of chemical bonds within a compound (Coates, 2006). IR radiation covers a part of the electromagnetic spectrum, which has wavenumbers ranging from 13,000 to 10 cm^{-1} (Bellisola and Sorio, 2012). IR has been used commercially since the 1940s (Stuart, 2000). IR spectroscopy is considered an essential and widespread tool for compound identification and structural elucidation (Szymanska-Chargot and Zdunek, 2013). Fourier transform spectroscopy relies on a mathematical process to extract data from the interference of radiation between two beams that leads to the production of an interferogram, which is a signal formed as result of the change of path length between the two beams (Stuart, 2000).

IR was utilized to obtain information on the functional groups that are found in compounds. A Perkin Elmer 100 FT-IR spectrometer was used to obtain FT-IR spectra of the isolated compounds. The frequencies were recorded in wavenumbers (cm^{-1}).

1 mg/mL of each of the isolated compounds was dissolved in a suitable solvent (methanol or chloroform) according to the polarity of each compound, and then transferred into a glass vial and then one drop was added to the thin films to obtain IR data.

2.6 Biological evaluation

2.6.1 Cross-streak assay

The cross-streaking assay is regarded as a simple and fast method for screening cultures in order to find new antibiotics (Velho-Pereia and Kamat, 2011).

One colony of each bacterium was streaked onto a blood agar plate and incubated at 37°C for three days. Next, one colony from each resistant- and susceptible-bacterial test strains was streaked as a single line perpendicular to the edge of the isolated bacteria **(Figure 2.12)** and then incubated at 37°C for 24h. Following incubation, a ruler was used to measure the zone of inhibition in mm.
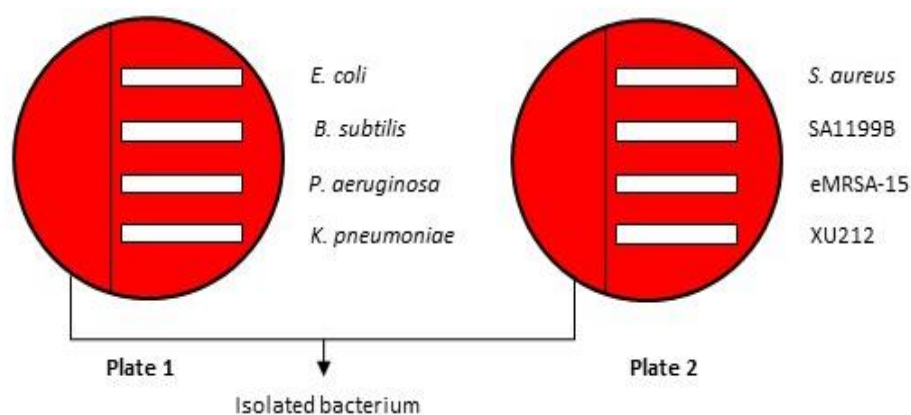
Figure 2.12: Diagram of the cross-streak assay.

2.6.2 Disc diffusion assay

Disc diffusion **(Figure 2.13)** is defined as the diffusion of an antimicrobial substance that has a specific concentration from discs into the agar medium that has already been inoculated with the pure microbial culture (Tomar *et al.*, 2015). It was developed in 1940 and was considered the official technique for testing antimicrobial susceptibility in several clinical microbiology laboratories (Balouiri *et al.*, 2016). This method depends on the relation of microbial sensitivity to the antimicrobial agents through the determination of an inhibition zone (Tomar *et al.*, 2015). It is a simple and cheap technique that has several uses in the antimicrobial screening of essential oils, plant extracts and other drugs (Balouiri *et al.*, 2016).

A small amount of resistant- and susceptible-strains from a fresh culture was taken with a sterile loop and suspended into 2 mL of a sterile PBS solution. The absorbance of this solution was then measured at OD_{600} nm using a UV spectrophotometer (Thermo Scientific Helios α). The solution was adjusted until the reading was 0.1 A, which was approximately equivalent to an inoculum of 1×10^8 CFU mL^{-1}. This process is based on the Beer-Lambert law. The bacterial suspension was then diluted to the final density of 5×10^5 CFU mL^{-1}. 1 mL of which was poured and spread over a blood agar plate and then left for 30 min inside a sterile cabinet to dry.
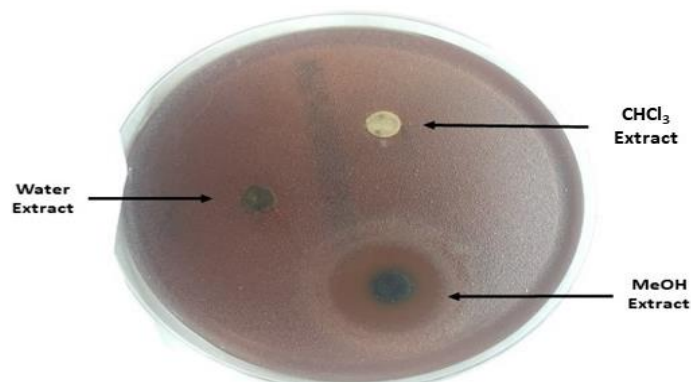
Figure 2.13: Disc diffusion result of TH-C4 extraction.

10.24 mg from each extract was dissolved in 1 mL of a solvent (water and methanol extracts in methanol, a chloroform extract in chloroform). 50 µL from each extract (which was equivalent to 512 µg/mL) was applied to a sterile blank paper disk (Oxoid) and directly placed into a sterile cabinet for drying for one hour before transferring to a blood agar plate and then incubated for 18h at 37°C. After incubation, 500 µL of (3-[4,5-dimethylthiazol-2-yl]-2,5-diphenyltetrazolium bromide) MTT (Lancaster Synthesis) was added to the plate and incubated for 30 min. The clear zone indicated to the zone of inhibition while the purple colour showed the living organism. Norfloxacin (10 µg/mL) was used a positive control. For screening of antibacterial activity, *S. aureus* was used only to detect the active fraction.

2.6.3   Overlay assay (Bioautography)

Paper chromatography-based bioautography **(Figure 2.14)** was introduced for the first time in 1946 by Goodall and Levi in order to evaluate the purity of penicillins (Balouiri *et al.*, 2016). Later, TLC-based bioautography was introduced by Fisher and Lautner in 1961 (Dewanjee *et al.*, 2015). Bioautographic methods are generally divided into three kinds: direct bioautography, agar diffusion or contact bioautography and immersion or agar overlay bioautography (Tomar *et al.*, 2015). The method used in this study was overlay bioautography. Agar overlay is regarded as a combination of direct and contact bioautography (Dewanjee *et al.*, 2015).

Bioautographic methods are commonly used for screening several samples for antimicrobial activity; this can be made by absorbing chemical agents onto the surface of TLC plates and then putting them directly in contact with a medium which is already inoculated with fungal or bacterial cultures (Wedge and Nagle, 2000). TLC–bioautography is an easy, effective and low-cost technique for the isolation of a complex

mixture and for the determination of the active compounds on the TLC plate (Balouiri *et al.*, 2016).
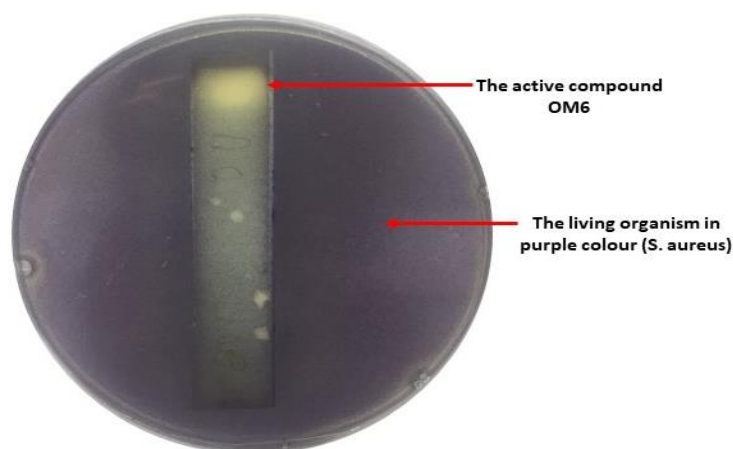
Figure 2.14: Bioautography assay of OM6.

Active fractions from bacterial extracts were applied on a normal or reverse phase TLC plate (5 x 10 cm) in order to separate the active compound. Three solvent systems were used for this method: the first (*n*-hexane: ethyl acetate: methanol) (80:20:1) was used for the fractions of **AH-E1** and **AR-G2**. For the fractions of **TH-C4, TB-A3** and **KH-A1**, (chloroform: methanol) (90:10) was used. The last system (*n*-hexane: ethyl acetate) (90:10) was used for a fraction of **GH-C8**. 50 mg from each fraction was dissolved in 1 mL of a suitable solvent (methanol or chloroform) and then 5 drops from each were spotted onto the TLC plate at least 1 cm from its bottom edge. Next, the TLC plate was developed in a twin trough glass chamber saturated with the mobile phase solvents for 30 min up to the distance of 80 mm. After solvent development, the plate was visualized under UV TLC visualizer at UV_{254} nm and UV_{366} nm to ensure that the separation was of sufficient quality. The TLC plate was then directly placed into a sterile cabinet for drying for at least one hour, and then transferred into a sterile petri dish. A bacterial inoculum of *S. aureus* with a density of 5 x 10^{5} CFU/mL^{-1} was prepared in a similar way to the protocol

described in **(section 2.6.2)** and added to 20 mL of molten nutrient agar. After gentle shaking (to avoid air bubbles), the molten agar was poured over the TLC plate and incubated for 18 hours at 37°C. After incubation, the plate was treated with a 1 mg/mL solution of MTT in methanol and incubated for 30 min at 37°C in order to reveal the inhibition zones. Living bacteria were seen as a purple colour, whereas the yellow zone indicated an active compound that was able to inhibit the bacteria.

2.6.4 Minimum inhibition concentration assay (MIC)

The MIC method is the lowest concentration of an antimicrobial compound that totally prevents the growth of the organism in micro-dilution wells or tubes (Balouiri *et al.*, 2016). The determination of the lowest concentration of antimicrobials in this method is simple and rapid (Tomar *et al.*, 2015). The inhibition of growth can be detected by the unaided eye or by adding MTT (Balouiri *et al.*, 2016).

2.2 g of MH broth powder (Fluka Analytical) was weighed and transferred to a 150 mL Duran bottle. 100 mL of distilled water was added to the bottle and gently shaken until the powder was completely dissolved. Next, the broth was autoclaved at 121°C for 15 min and then cooled before use.

One colony of each resistant- and susceptible-strains was prepared in a similar way to the protocol described in **(section 2.6.2)** in order to reach the final density of 5 x 10^5 CFU/mL^{-1}.

51.2 g mg of each extract was added to a reaction tube (1.5 mL) and then 1 mL of dimethylsulphoxide (DMSO) was added to make a stock solution. Next, the stock solution was sonicated (Grant) for 15 min at room temperature and centrifuged at 13,000 rpm for 5 min. The supernatant was filtered using a 0.22 µm syringe filter (microfiltration)

into a new reaction tube and kept at 4°C. 10 µL was transferred to 500 µL of the broth

in order to obtain 512 µg/mL of the extract as the final concentration in the first well.
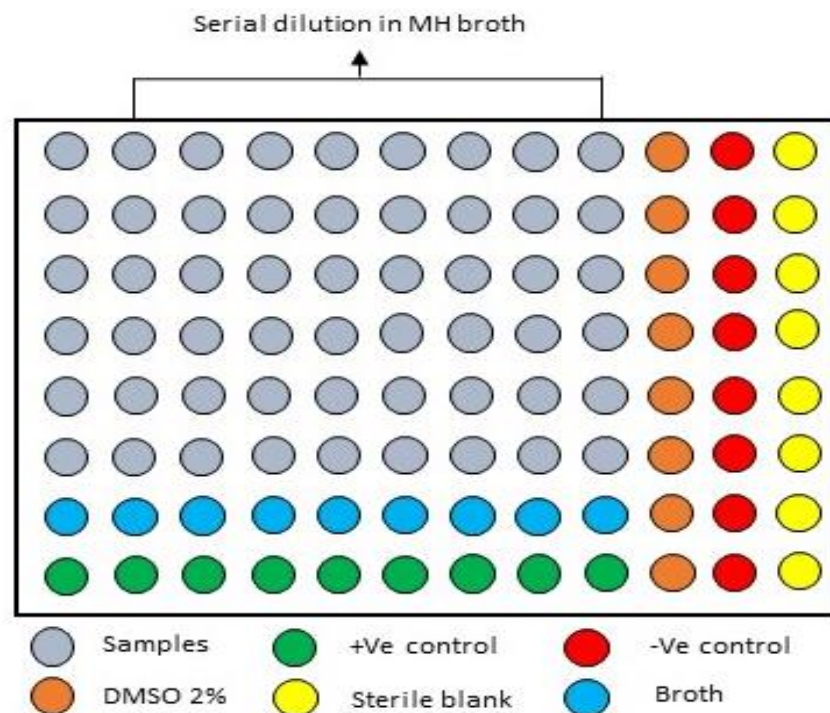
Figure 2.15: Diagram of MIC assay.

A 96-well plate (Thermo Scientific) was used to perform this experiment **(Figure 2.15)**. 200 µL of each sample was transferred to the first column. 100 µL of MH broth was pipetted into the wells from column 2 to column 9 in order to be used for serial dilution. 100 µL from each well in the first column was then transferred to the second column and mixed well. This step was repeated until column 9. After that, the excess amount was transferred to column 12 as a sterile control for each sample. 100 µL of a tested organism was added to the column 11 to be used as a negative control. Norfloxacin (2.5 mg/mL in distilled water) (Fluka BioChemika) was used as a positive control in row 8 with all tested strains except for tetracycline (2.5 mg/mL), which was used with SA 1199B strain. 2% of DMSO was added to column 10 to ensure it had no positive

effect on inhibition of bacterial growth. MHB was added to row 7 as a blank. 100 of the tested strain was added to each well and then the plate was incubated at 37°C for 18h. After the incubation, 20 µL of MTT was added to each well to obtain the final result. The blue colour indicated growth and the yellow colour indicated a lack of growth. MIC values were recorded as the lowest concentration at which no colour change was observed. The MIC experiment was done in duplicate per plate and repeated in at least three independent experiments.

3   Results

The isolates were named according to the spring source that they were isolated from. **(Figure 3.1)** illustrates the way that was used to name the isolates.

The spring name (Ghomygah spring)   Sample name i.e.: A, B, C etc.   The number of a bacterial colony

GH – D 4
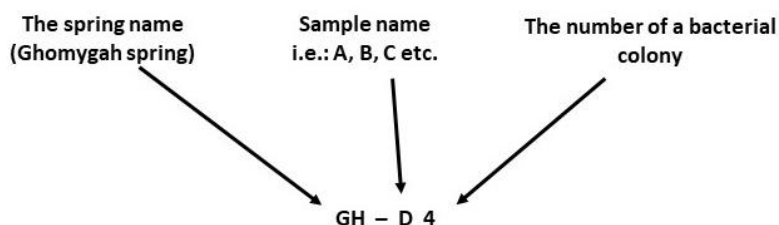
Figure 3.1: The naming method of bacterial isolates.

Three different methods were used for extraction: gravity column chromatography, vacuum liquid column chromatography and solid-phase extraction. The gravity column chromatography was used only once with the **GH-C8** isolate and never used again because it was very slow. Instead of that, solid-phase extraction was utilized with the others because it was faster, easier and more accurate. The vacuum liquid column chromatography was also used once with the **KH-A1** isolate because the amount of the methanol extract was high and not suitable to be used with the SPE technique.

3.1   Microbiological results

3.1.1   Bacterial growth

Thirty-two water samples from six different hot springs from Saudi Arabia were streaked on blood agar plates. Blood agar was used because it gave the optimal results in terms of the growth of bacteria in comparison with other agars such as nutrient agar. The plates were then incubated for three days at 37°C. Colonies with a different colour and morphology were taken out and streaked on a new blood agar plate. 125 bacterial isolates were obtained as below in **(Table 3.1)**.

Table 3.1: Bacterial isolates from water samples of hot springs.

Sample \ Spring	A	B	C	D	E	F	G	H	I	J	K
Ghomygah Spring (GH)	1	5	13	4							
Tharban Spring (TH)	4	1	8	4							
Al-Aridhah Spring (AR)	2	5	3	5	5	7	2	2	6	3	7
Al-Khobh Spring (KH)	3	1	2	2							
Al-Haridhah Spring (AH)	2	3	2	4	6						
Thebah Spring (TB)	2	2	6	3							
Total	125										

In general, 125 bacterial isolates were isolated from these thermal springs. 47 bacterial isolates were isolated only from the **AR** spring, which showed the highest number of isolates, while the **KH** spring was the lowest with eight isolates. These isolates were subjected to a cross-streak assay in order to determine which bacterial isolates had the ability to produce antibiotics. *S. aureus* was used only for this assay because it is a susceptible Gram-positive organism, which means that antibacterial agents are able to inhibit its growth easier than that of Gram-negative bacteria. The outcomes of this assay are shown in **(Table 3.2)**.

Table 3.2: Number of isolates that produce antibiotics.

Spring	Antibiotics-Producing Bacteria
Ghomygah Spring (GH)	16
Tharban Spring (TH)	6
Al-Aridhah Spring (AR)	7
Al-Khobh Spring (KH)	5
Al-Haridhah Spring (AH)	4
Thebah Spring (TB)	5
Total	43

Only 43 bacterial isolates from 125 showed antibacterial activity against *S. aureus*. Although the **AR** spring produced 47 isolates, only seven isolates demonstrated

antimicrobial activities. However, 23 bacterial isolates were isolated from the **GH** spring, 16 of which had antimicrobial activity. In general, 14 bacterial isolates were chosen for further work. Antimicrobial activity, morphology and type of the hot spring were taken into consideration during the choice of bacterial isolates for further investigation. These antibiotic-producing bacteria are presented in **(Table 3.3)**.

Table 3.3: Bacterial isolates chosen for further work.

Spring	Antibiotics-Producing Bacteria
Ghomygah Spring (GH)	GH-C1, GH-C8, GH-C11, GH-D4, GH-D6
Tharban Spring (TH)	TH-C4, TH-C8
Al-Aridhah Spring (AR)	AR-F7, AR-G2
Al-Khobh Spring (KH)	KH-A1, KH-B2
Al-Haridhah Spring (AH)	AH-D1, AH-E1
Thebah Spring (TB)	TB-A3

3.1.2 Bacterial culture

All 14 isolates **(Figure 3.2)** were transferred onto a new blood agar plate for each isolate in order to culture them using the streak plate method. The purpose of this step was to ensure that all isolates were not contaminated as well as to use them as a culture, which was then stored at 4°C until further analysis.

Figure 3.2: Cultures of chosen isolates on blood agar.

3.1.3 Gram-stain

All selected isolates were subjected to a Gram-stain assay in order to find out if they were Gram-positive or -negative organisms. The findings of this method **(Figure 3.3)** illustrated that all tested isolates were rods in terms of the shape and had a violet colour, indicating that all were Gram-positive. *S. aureus* and *E. coli* were utilized as a control. (**Table 3.4)** summarizes the results of this technique.

Table 3.4: The results of the Gram-stain assay.

Sample	Shape	Colour	Type
AH-D1	Rod	Violet	Gram-positive
AH-E1	Rod	Violet	Gram-positive
AR-F7	Rod	Violet	Gram-positive
AR-G2	Rod	Violet	Gram-positive
GH-C1	Rod	Violet	Gram-positive
GH-C8	Rod	Violet	Gram-positive
GH-C11	Rod	Violet	Gram-positive
GH-D4	Rod	Violet	Gram-positive
GH-D6	Rod	Violet	Gram-positive
KH-A1	Rod	Violet	Gram-positive
KH-B2	Rod	Violet	Gram-positive
TH-C4	Rod	Violet	Gram-positive
TH-C8	Rod	Violet	Gram-positive
TB-A3	Rod	Violet	Gram-positive

S. aureus

E. coli

GH-C1

GH-C8

GH-C11

GH-D4

GH-D6

AH-E1

AH-D1

KH-A1

KH-B2

AR-F7

AR-G2

TH-C4

TH-C8

TB-A3
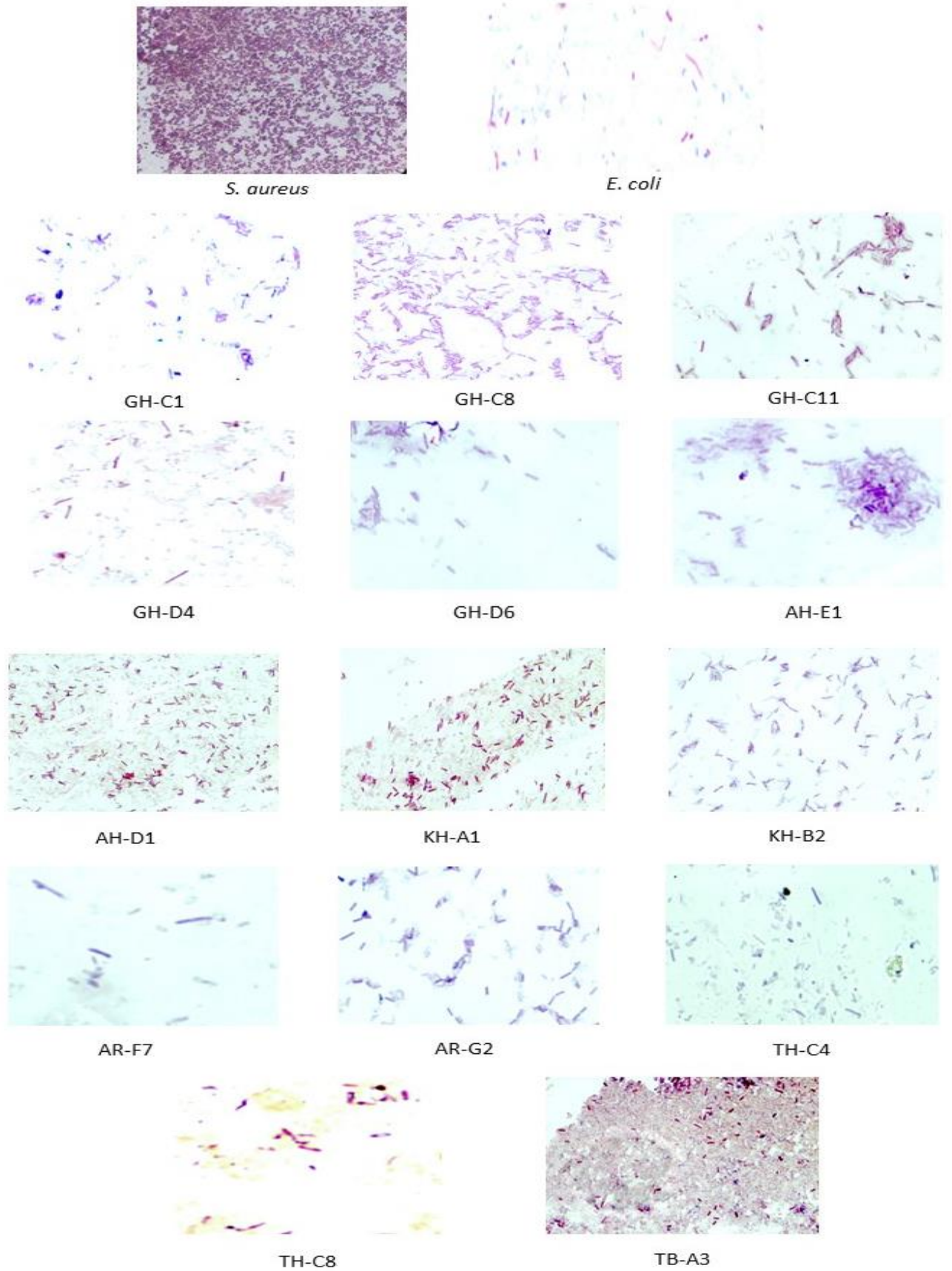
Figure 3.3: Gram-stain results of selected isolates.

3.1.4 Gel electrophoresis

1% agarose gel electrophoresis was used to assess the purity of both extracted DNA samples and PCR products. The 14 DNA extractions and PCR products were analysed on an agarose gel to assess the size of DNA fragments obtained. The reason to use PCR was to amplify the extracted DNA sequence in order to identify the genus and species of bacterial isolates. All extracted DNA samples **(Figure 3.4)** showed a distinct band that had migrated just above the 10 kb band of the molecular marker except for five extracted DNA samples that gave faint bands. These five isolates were **TB-A3**, **GH-C8**, **TH-C8**, **GH-C11** and **AH-E1**. All bands were almost at the same level in the agar, which suggested that the isolates may have the same size. There was also a faint band in four isolates (**TB-A3**, **TH-C4**, **GH-D4** and **AR-F7**) beneath the distinct band. These bands were approximately at the same level of around 8 kb, which implied that these isolates might have the same DNA size. These bands could also be for the plasmids. The smearing seen in **KH-A1**, **GH-D4** and **GH-D6** isolates could be due to a degradation of the DNA, an overloading of the sample into the agarose gel or an artefact caused by the presence of contaminants in the DNA samples that absorb UV.
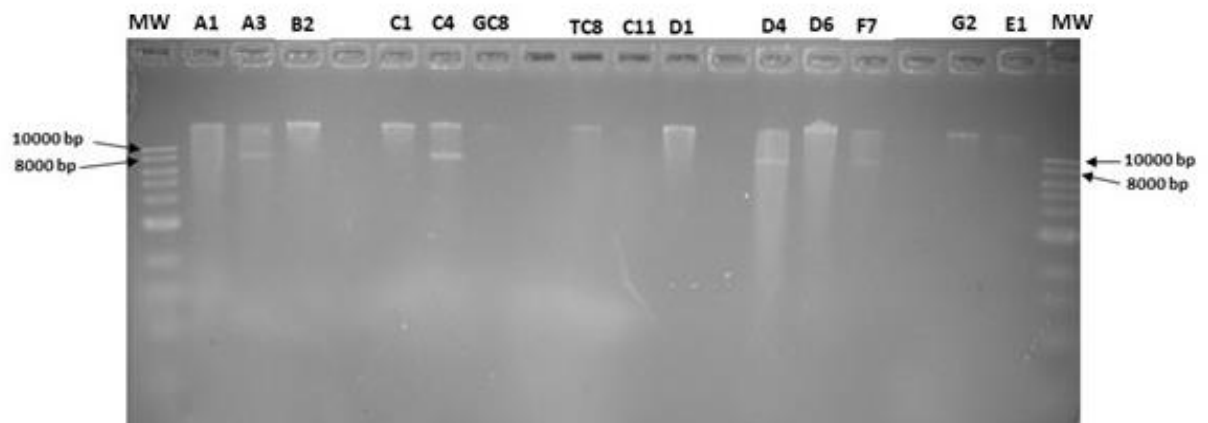
Figure 3.4: Gel electrophoresis of extracted DNA.

All PCR products **(Figure 3.5)** exhibited a distinct band that had migrated just above the 1517 bp band of the molecular marker. There was no band seen in the control, which means that there was no contamination in the PCR samples. All bands were almost at the same level in the agar, which suggested that all isolates may have the same DNA size. By looking at the size of band for each sample in both extracted DNA samples and PCR products, the size of bands is different. For example, the band of the extracted DNA of **TB-A3** is above 10 kb; in contrast, the band in PCR it is above 1517 bp and this because the PCR technique is able to amplify a small segment of DNA, not the whole DNA (Liu *et al.*, 2019).
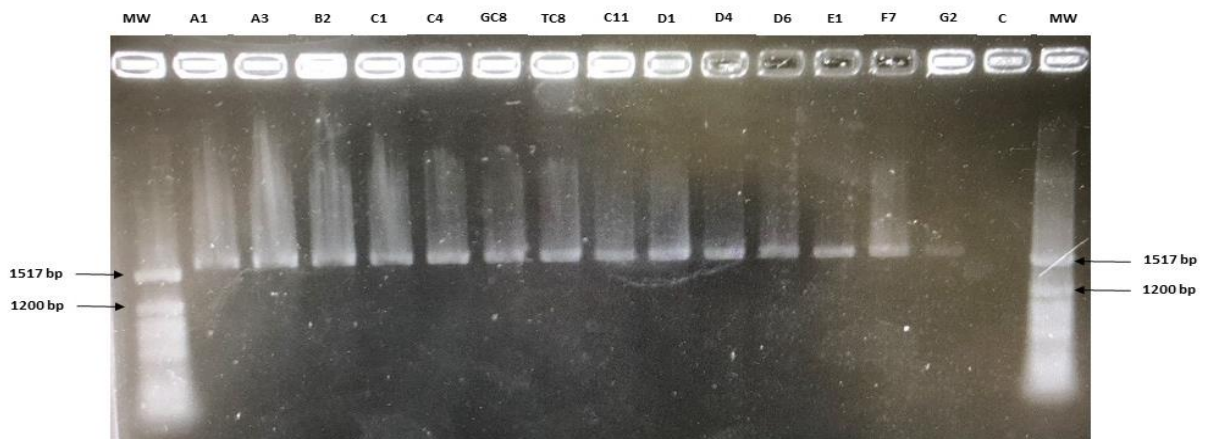
Figure 3.5: Gel electrophoresis of PCR products.

3.1.5 Nanodrop results

All extracted DNA samples and PCR products were analysed by a nanodrop technique in order to obtain the concentration of samples and also to check the purity of DNA. This step was essential in order to prepare the optimal concentration for each sample before doing the 16S rRNA gene sequencing. **(Table 3.5)** shows the results of the extracted DNA samples with information about the purity. There are two ratio measurements of DNA quality which were recorded: $A_{260/280}$ and $A_{260/230}$. Nucleic acids

can strongly absorb UV light at 260 nm, while proteins absorb strongly at 280 nm; this is due to the presence of tyrosine and tryptophan side chains in proteins, but not in nucleic acids (O'Neill *et al.*, 2011). In general, a perfect quality DNA sample should have an $A_{260/230}$ absorbance ratio of greater than 1.5 and an $A_{260/280}$ absorbance ratio of 1.7-2.0 (O'Neill *et al.*, 2011). Moreover, pure nucleic acids typically give an $A_{260/280}$ ratio of ~1.8 and an $A_{260/230}$ ratio of 1.8-2.2 (Desjardins and Conklin, 2010). Any different purity ratios may point to the existence of phenol, protein or other contaminants that absorb strongly at or near 280 nm (Desjardins and Conklin, 2010).

Table 3.5: Nanodrop analysis of each DNA extraction of bacterial isolates.

Sample (volume in µL)	Concentration (ng/µL)	Absorbance ratios	
		260/280	260/230
GH-C1 (50)	124.7	1.87	2.04
GH-C8 (50)	66.9	1.88	1.89
GH-C11 (50)	26.0	1.87	1.95
GH-D4 (50)	166.4	1.83	1.97
GH-D6 (50)	334.3	1.87	2.20
KH-A1 (50)	153.3	1.85	2.01
KH-B2 (50)	119.2	1.84	2.09
TH-C4 (50)	182.2	1.83	1.87
TH-C8 (50)	81.0	1.85	1.93
AR-F7 (50)	125.5	1.81	1.98
AR-G2 (50)	138.3	1.85	1.99
AH-D1 (50)	177.2	1.84	2.15
AH-E1 (50)	92.4	1.86	2.02
TB-A3 (50)	163.8	1.85	2.11

For the extracted DNA samples, an estimation of the concentration of each sample shows that a total of ~97.56 µg of DNA had been extracted from the 2.1 mL of water samples. Moreover, the mean $A_{260/280}$ ratio of the DNA extractions was approximately 1.85 and the $A_{260/230}$ ratio was 2.02, indicating that all extracted DNA samples were "pure".

For PCR products, the outcomes of a nanodrop technique are presented in **(Table 3.6)**. As discussed above in terms of DNA quality, the same standards of absorbance ratios ($A_{260/280}$ and $A_{260/230}$) were applied. The estimation of the concentration of each sample shows that a total of ~28.46 µg of DNA had been extracted from the 2.1 mL of

water samples. Furthermore, the mean $A_{260/280}$ ratio of the DNA extractions was approximately 1.80 and the $A_{260/230}$ ratio mean was 2.07, which indicated that all PCR products were considered to be "pure".

Table 3.6: Nanodrop analysis of PCR products of extracted DNA.

Sample (volume in µL)	Concentration (ng/µL)	Absorbance ratios	
		260/280	260/230
GH-C1 (50)	42.4	1.83	2.13
GH-C8 (50)	33.6	1.79	1.98
GH-C11 (50)	28.6	1.81	2.11
GH-D4 (50)	58.3	1.82	2.21
GH-D6 (50)	34.7	1.77	2.22
KH-A1 (50)	48.2	1.83	2.13
KH-B2 (50)	46.6	1.74	1.98
TH-C4 (50)	49.0	1.78	1.89
TH-C8 (50)	38.4	1.78	2.06
AR-F7 (50)	48.9	1.79	2.12
AR-G2 (50)	31.1	1.84	2.11
AH-D1 (50)	35.7	1.84	2.02
AH-E1 (50)	25.4	1.87	2.16
TB-A3 (50)	48.3	1.75	1.86

3.1.6 16S rRNA gene sequence and illumine sequence analysis

All selected bacterial isolates were sent to MicrobesNG in order to identify the bacteria at the genus level. **(Table 3.7)** illustrates the outcomes of illumine sequencing for all samples. Based on the illumine sequence analysis, it is obvious that all 14 isolates detected appeared to be close to the bacterial family *Bacillaceae*, specifically the genus *Bacillus*. Four different *Bacillus* species were found **(Figure 3.6)**: *Bacillus cereus, Bacillus licheniformis, Bacillus pumilus* and *Bacillus paralicheniformis.* These species were isolated from six different thermal springs in Saudi Arabia.
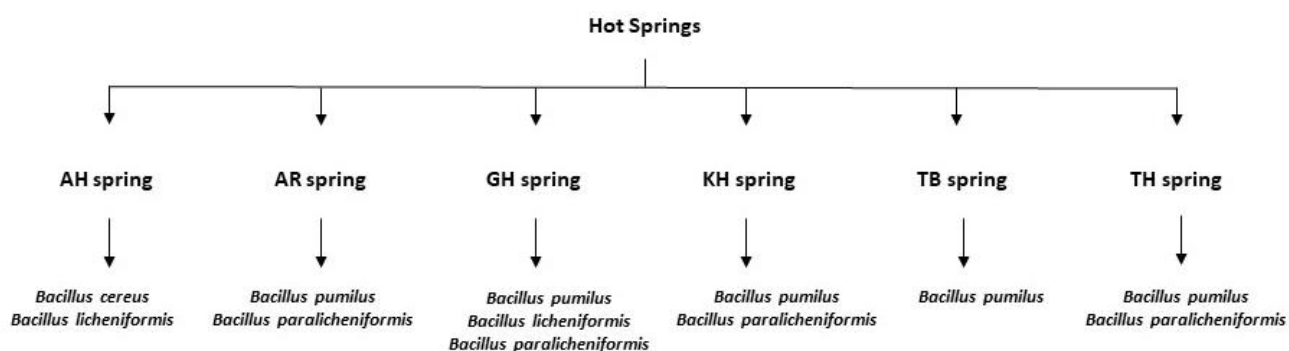
Figure 3.6: An overview of the types of isolates in each spring.

B. paralicheniformis was the most abundant isolate, accounting for six isolates. In contrast, *B. cereus* was the least common-organism with only one isolate detected; found in the **AH** spring. *B. pumilus* was the second most abundant with five isolates, *B. licheniformis* accounted for two isolates, obtained from the **AH** and **GH** springs. Generally, the sequence identity (%) of all tested organisms were acceptable (between 58 and 91%) except for two samples: **AH-E1** and **GH-C11**, which demonstrated very low percent around 8.87% and 7.72%, respectively.

Table 3.7: Illumine sequencing of bacterial isolates.

Sample	Illumine sequencing	Sequence Identity (%)
AH-D1	*Bacillus cereus*	62.23
AH-E1	*Bacillus licheniformis*	8.87
AR-F7	*Bacillus pumilus*	60.34
AR-G2	*Bacillus paralicheniformis*	90.73
GH-C1	*Bacillus paralicheniformis*	91.84
GH-C8	*Bacillus paralicheniformis*	89.16
GH-C11	*Bacillus paralicheniformis*	7.72
GH-D4	*Bacillus pumilus*	65.73
GH-D6	*Bacillus licheniformis*	91.35
KH-A1	*Bacillus pumilus*	58.08
KH-B2	*Bacillus paralicheniformis*	91.30
TH-C4	*Bacillus pumilus*	59.20
TH-C8	*Bacillus paralicheniformis*	90.21
TB-A3	*Bacillus pumilus*	66.56

For this reason, all samples were subjected to the PCR technique and later 16S rRNA sequencing by the UCL Sequencing Facility in order to confirm the results of

illumine sequencing. **(Table 3.8)** provides information about the genus and species of tested samples. The BLAST program in (NCBI) was utilized to align the 16S rRNA gene sequence of the new isolates with previously published sequences in the public database. 16S rRNA sequence analysis for all samples illustrated that there was a strong similarity between the isolates and representative strains of the genus *Bacillus* in GeneBank. The results of the 16S rRNA sequence were identical with the results of the illumine sequencing. 16S rRNA sequences were recorded twice (forward and reverse readings) for each sample in order to obtain the exact identity. The identical percentage for all samples was high (>90%), which may give credibility concerning the identification of bacterial isolates.

Table 3.8: 16S rRNA gene sequence of bacterial isolates.

Sample		Length (bp)	Sequence	Sequence Identity (%)	Accession
AH-D1	FD	649	*Bacillus cereus*	95.71	CP042874.1
	RP	699	*Bacillus cereus*	98.31	CP045606.2
AH-E1	FD	734	*Bacillus licheniformis*	96.83	MG818961.1
	RP	676	*Bacillus licheniformis*	97.02	KU056999.1
AR-F7	FD	877	*Bacillus pumilus*	98.12	KC692196.1
	RP	567	*Bacillus pumilus*	97.77	KP202723.1
AR-G2	FD	612	*Bacillus paralicheniformis*	96.91	MN746205.1
	RP	923	*Bacillus paralicheniformis*	97.07	MK802111.1
GH-C1	FD	798	*Bacillus paralicheniformis*	96.76	MK168631.1
	RP	766	*Bacillus paralicheniformis*	97.53	MN396257.1
GH-C8	FD	589	*Bacillus paralicheniformis*	97.12	MK070086.1
	RP	601	*Bacillus paralicheniformis*	97.70	MN179961.1
GH-C11	FD	683	*Bacillus paralicheniformis*	97.21	MT039446.1
	RP	641	*Bacillus paralicheniformis*	96.64	MK063845.1
GH-D4	FD	593	*Bacillus pumilus*	97.97	MN704531.1
	RP	771	*Bacillus pumilus*	97.64	EU239356.1
GH-D6	FD	704	*Bacillus licheniformis*	97.98	LC092832.1
	RP	698	*Bacillus licheniformis*	97.69	MH373542.1
KH-A1	FD	809	*Bacillus pumilus*	94.07	KX904728.1
	RP	723	*Bacillus pumilus*	97.79	EU594558.1
KH-B2	FD	668	*Bacillus paralicheniformis*	96.07	KY828474.1
	RP	631	*Bacillus paralicheniformis*	97.78	MK063857.1
TH-C4	FD	687	*Bacillus pumilus*	97.14	JQ308586.1
	RP	658	*Bacillus pumilus*	97.48	KP400535.1
TH-C8	FD	718	*Bacillus paralicheniformis*	91.50	MG757557.1
	RP	671	*Bacillus paralicheniformis*	96.38	MH542289.1
TB-A3	FD	607	*Bacillus pumilus*	97.17	KX426046.1
	RP	587	*Bacillus pumilus*	97.35	KT003271.1

FD = Forward reading, **RP** = Reverse reading

Isolates of **AR-G2, GH-C1, GH-C8, GH-C11, KH-B2** and **TH-C8** demonstrated comparatively high 16S rRNA sequence similarity with the closely-related type strain *B. paralicheniformis* 97.07%, 97.53%, 97.70%, 97.21%, 97.78% and 96.38%, respectively. Moreover, sequence data showed that isolates **AR-F7** (98.12%), **GH-D4** (97.97%)**, KH-A1** (97.79%)**, TH-C4** (97.48%) and **TB-A3** (97.35%) had the highest homology with *B. pumilus*, whereas **AH-E1** and **GH-D6** isolates showed 97.02 % and 97.98 % similarities with *B. licheniformis*, respectively. Isolate **AH-D1** demonstrated 98.31% similarity with *B. cereus.*

In comparison with the literature, all selected springs have been studied before apart from two new springs: the **AH** and **TB** springs, which were studied for the first time in this project. Numerous reports on the isolation of thermophilic bacteria from thermal springs in Saudi Arabia have been published. For instance, 15 thermophilic bacteria such as *B. cereus*, *B. licheniformis* and *B. thermoamylovorans* were isolated from the Al-Lith and Jazan hot springs (Khiyami *et al.*, 2012). Furthermore, *B. licheniformis* and *B. subtilis* have been found in the Jazan thermal spring (Sarhan and Alamrri, 2014).

For the **AH** and **TB** springs, it is believed that *B. licheniformis, B. cereus* and *B. pumilus* have been isolated from these springs for the first time because there has been no data reported about these springs. For the other springs, there are several studies on the isolation of *Bacillus* spp. from them. As an example, *B. licheniformis* (KKU-MS4), and *B. sonorensis* (KKU-MS14) have been isolated from the **TH** spring (Alrumman *et al.*, 2018). Additionally, *B. thermocopriae* (Alrumman *et al.*, 2019), *B. cereus*, *B. subtilis*, *B. schlegelii*, *B. licheniformis* and *B. vallismortis* have previously been found in the **AR** spring (Yasir *et al.*, 2019). According to Salem *et al.* (2016), 11 strains of *B. licheniformis* and 15 strains of *B. subtilis* were isolated from the **GH** spring. *B. cereus*, *B. subtilis*, *B. schlegelii*,

B. thermotolerans, *B. nealsonii* and *B. licheniformis* have also been reported from the **GH** spring (Yasir *et al.*, 2019). Furthermore, *B. thermoamylovorans* (Khiyami *et al.*, 2012), *B. subtilis* (El-Gayar *et al.*, 2017), *B. sonorensis*, (Alrumman *et al.*, 2019), *B. aerius* (KKU-KS5) (Alrumman *et al.*, 2019), *B. cereus*, *B. schlegelii*, *B. pumilus*, *B. licheniformis*, *B. paralicheniformis* and *B. zhangzhouensis* have been isolated from the **KH** spring (Yasir *et al.*, 2019).

3.1.7 Phylogenetic tree analysis

A phylogenetic tree generated through the MEGAS software was produced. Analysis of microbial communities of Saudi hot springs showed the presence of four different species of *Bacillus*. **(Figure 3.7)** shows the phylogenetic tree representing the evolutionary relationship between the various species such as *B. cerues*, *B. pumilus*, *B. lichinformis* and *B. paralichinformis*. The constructed phylogenetic tree clearly resolved the relationships among the 14 isolates and their relationships to the closest sequences based on the BLAST search.

The tested sequences were classified into 13 nodes, and data represented the relationship of the most isolates and it was a high percentage of bootstrap. For example, **AR-G2**, **GH-C1**, **GH-C8**, **GH-C11** and **KH-B2** isolates represented 84% similarity to *B. paralicheniformis* while the **TH-C8** isolate showed 72%. Additionally, **AR-F7**, **GH-D4**, **KH-A1**, **TH-C4** and **TB-A3** isolates exhibited 91% similarity to *B. pumilus*. Moreover, the **AH-D1** isolate showed 96% similarity to *B. cerues*, and **AH-E1** and **GH-D6** isolates showed 69% and 67% similarity to *B. lichenformis*, respectively. Bootstrapping of 1000 replications was calculated to find out confidence values for the edges of the maximum likelihood tree.

Figure 3.7: Phylogenetic tree based on 16S rRNA gene sequence of bacterial isolates from six hot springs of Saudi Arabia.

3.2   Chemical results

3.2.1   Compound OM1

Compound **OM1** was isolated as a pale yellow powder from the **KH-A1** isolate from the **KH** spring. The methanol extract (3.6 g) of the **KH-A1** isolate was subjected to VLC in order to identify the fractions with antimicrobial activity **(Figure 3.8)**. 22 fractions were collected and the fractions (11,12 and 13) (423.4 mg / 11.76% of the extract) showed antibacterial activities. These fractions were bulked and applied to (preparative-NP-TLC) with a solvent system (chloroform: methanol/ 90:10). A fourth TLC band with an R_f of 0.65 demonstrated activity in the *S. aureus* overlay assay. After purification, compound **OM1** (62.9 mg / 14.85% of the fraction) and **OM2** (43.6 mg / 10.29% of the fraction) were separated. The structure of the **OM1** is shown in **(Figure 3.9).**
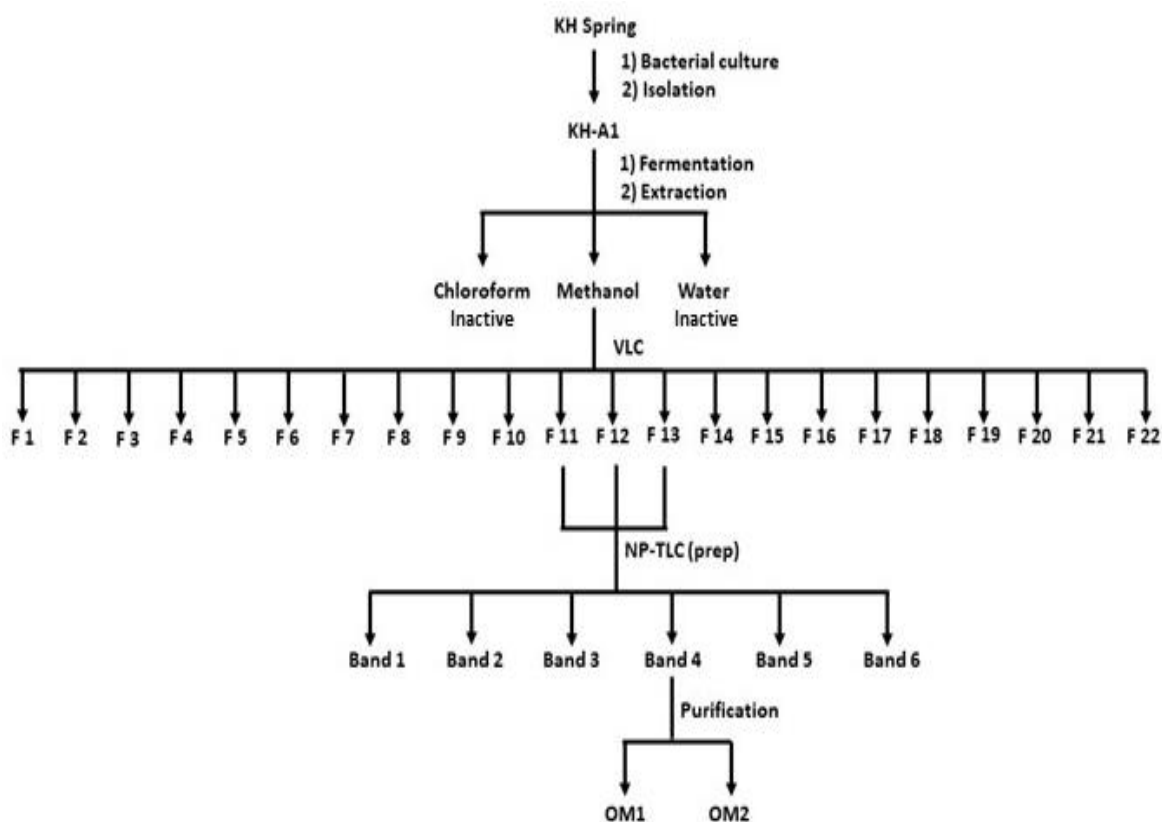
Figure 3.8: Scheme of isolation for compounds OM1 and OM2.

The molecular formula of **OM1** was determined as $C_{12}H_{14}N_2O$ and the molecular weight of the compound was calculated as 202, which corresponded to the ESI-MS *m/z* 225.13 [M+Na]$^+$ **(Figure 3.20)**.
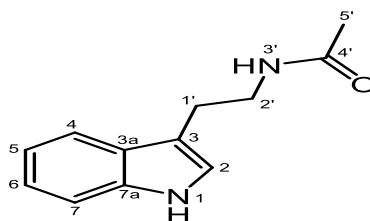
Figure 3.9: The structure of compound OM1.

The ^{1}H NMR spectrum **(Figure 3.10)** displayed five deshielded resonances; two broad doublets at δ_H 7.43 (*J*= 7.9 Hz, H-4) and δ_H 7.21 (*J*= 8.1 Hz, H-7), and two double triplets at δ_H 6.87 (*J*= 7.9 and 7.0 Hz, H-5) and δ_H 6.97 (*J*= 7.0 Hz, H-6) and a singlet at δ_H 6.95 (H-2). The doublet (H-4) had a splitting (*J*= 7.9 Hz), indicative of an *ortho* coupling to the double triplet (H-5) whose *J* value (7.9, 7.0 Hz) also indicated that it was *ortho* to the double triplet (H-6, *J*= 7.0 Hz). The *meta* coupling of H-4 to H-6 must be small and indicated by the broadness of H-4. Moreover, there were two slightly deshielded triplets at δ_H 3.34 (H$_2$-2'), which coupled to the nitrogen atom, and δ_H 2.81 (H$_2$-1'), which coupled to the indole ring. A peak appearing at lower ppm in the ^{1}H NMR spectrum integrating for 3 hydrogens (δ_H 1.80, H$_3$-5') could be attributed to a methyl group, which was present in this compound. Moreover, the peaks of the hydrogens H-2 and H-6 were overlapping with each other in the ^{1}H NMR spectrum.

The ^{13}C NMR spectrum **(Figure 3.11)** showed 12 carbon signals in total from which four were quaternary carbons at δ_C 113.2 (C-3), δ_C 128.8 (C-3a), δ_C 138.1 (C-7a) and δ_C 173.2 (C-4'). The DEPT-135 **(Figure 3.12)** showed two methylenes at δ_C 41.5 and δ_C 26.2. The remaining carbons were assigned to five methines at δ_C 123.3 (C-2), δ_C 119.2

(C-4), δ_C 119.5 (C-5), δ_C 122.3 (C-6) and δ_C 112.2 (C-7) in the indole ring and one methyl carbon at δ_C 22.6 (C-5').

In the HMBC spectrum **(Figures 3.16, 17** and **18)**, the position of the carbonyl at C-4' was confirmed by a ^2J correlation with the hydrogens H_3-5' and a ^3J correlation with the hydrogens of H_2-2'. In addition, the HMBC spectrum showed a ^3J correlation between H-2 and the carbon of C-1', confirming the position of the N-acetyl-ethylamine moiety at C-3. This was also confirmed by a long-range coupling in the COSY spectrum between H-2 and H_2-1' **(Figure 3.19)**. In the HMBC spectrum, the placement of the side chain was also supported by a ^3J correlation between H_2-2' and C-3 as well as H_2-1' and C-3a.

Further confirmation on the structure of the compound was obtained using FT-IR spectroscopy **(Appendix 2)**. The FT-IR spectrum was taken by dissolving the compound in methanol and the spectrum exhibited a C=O stretching absorption at 1665 cm^{-1}. There were also a broadband for N-H at 3443 cm^{-1}, alkyl C-H stretching at 2913 cm^{-1} and 2996 cm^{-1}, C-H bending at 1407 cm^{-1} and 1436 cm^{-1} as well as C-N stretching at 1042 cm^{-1}.

Compound **OM1** was therefore identified as *N*-(2-(1*H*-indol-3-yl)ethyl)acetamide, which is commonly known as *N*-acetyltryptamine. The ^{1}H and^{13}C NMR data of this compound are in good agreement with published literature for *N*-acetyltryptamine from bacteria (Zhang *et al.*, 2013). Moreover, compound **OM1** was compared to a ^{1}H NMR spectrum of a reference sample *N*-acetyltryptamine and it was identical **(Figure 3.21)**.

Several studies have shown the isolation of *N*-acetyltryptamine from various microbes. For example, it has been isolated from different bacteria such as *Corallococcus corraloides* (Böhlendorf *et al.*, 1996), *Intrasporangium* strain N8 (Okudoh and Wallis, 2012), *Streptomyces* spp. (AC-2) (Lin *et al.*, 2008), *Streptomyces* spp. strain TN58 (Mehdi *et al.*, 2009), *Streptomyces djakartensis* (Zhang *et al.*, 2013) and *Streptomyces* spp.

MBT76 (Wu *et al*., 2016). Furthermore, it has also been found in some fungi, including *Penicillium vitale* (Vinokurova *et al*., 2000), *Penicillium solitum* (Antipova *et al*., 2018) and *Fusarium poae* (Nagia *et al*., 2012). It has also been isolated from a *Micromonospora* spp*.* strain from the sponge *Tethya aurantium* (Tuan *et al*., 2017) as well as from *Microbispora aerate* from Antarctica (Bratchkova and Ivanova, 2011).

Table 3.9: ^{1}H (500 MHz), ^{13}C NMR (125 MHz) and HMBC spectroscopic data of OM1 recorded in CD$_3$OD.

Position	^{1}H	^{13}C	HMBC		^{13}C (CDCl$_3$) Zhang *et al*., 2013
			^2J	^3J	
NH	--	--	--	--	--
C-2	6.95 (s)	123.3	C-3	C-3a, C-1'	123.3
C-3	--	113.2	--	--	113.3
C-3a	--	128.8	--	--	128.8
C-4	7.43 (d)	119.2	C-3a	C-3, C-6, C-7a	119.2
C-5	6.87 (dt)	119.5	--	C-3a, C-7	119.6
C-6	6.97 (dt)	122.3	--	C-4, C-7a	122.3
C-7	7.21 (d)	112.2	--	C-3a, C-5	112.2
C-7a	--	138.1	--	--	138.2
C-1'	2.81 (t)	26.2	C-3, C-2'	C-2, C-3a	22.6
C-2'	3.34 (t)	41.5	C-1'	C-3, C-4'	41.6
NH	--	--	--	--	--
C-4'	--	173.2	--	--	173.2
C-5'	1.80 (s)	22.6	C-4'	--	22.6
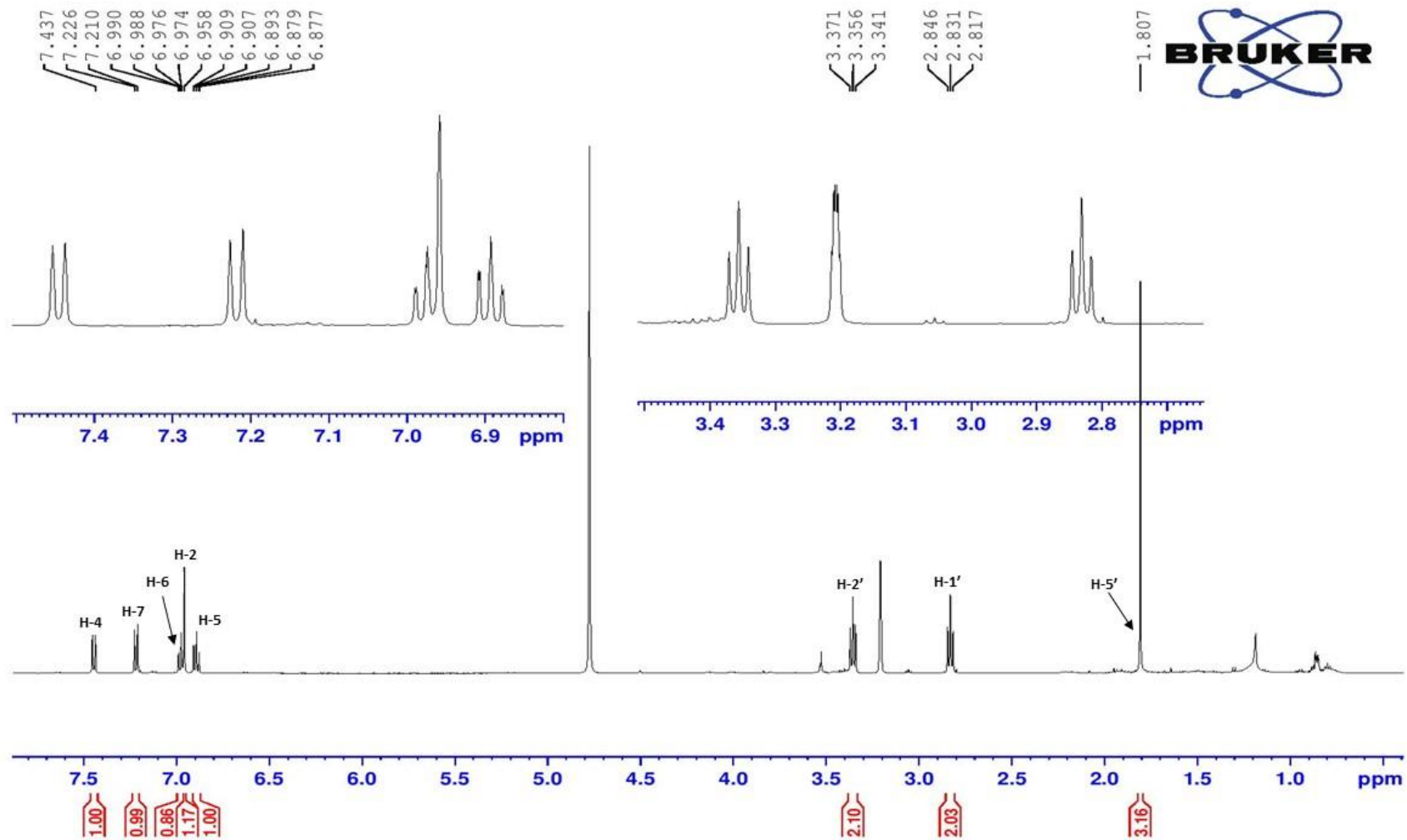
Figure 3.10: ¹H NMR spectrum of compound OM1 recorded in CD₃OD (500 MHz).
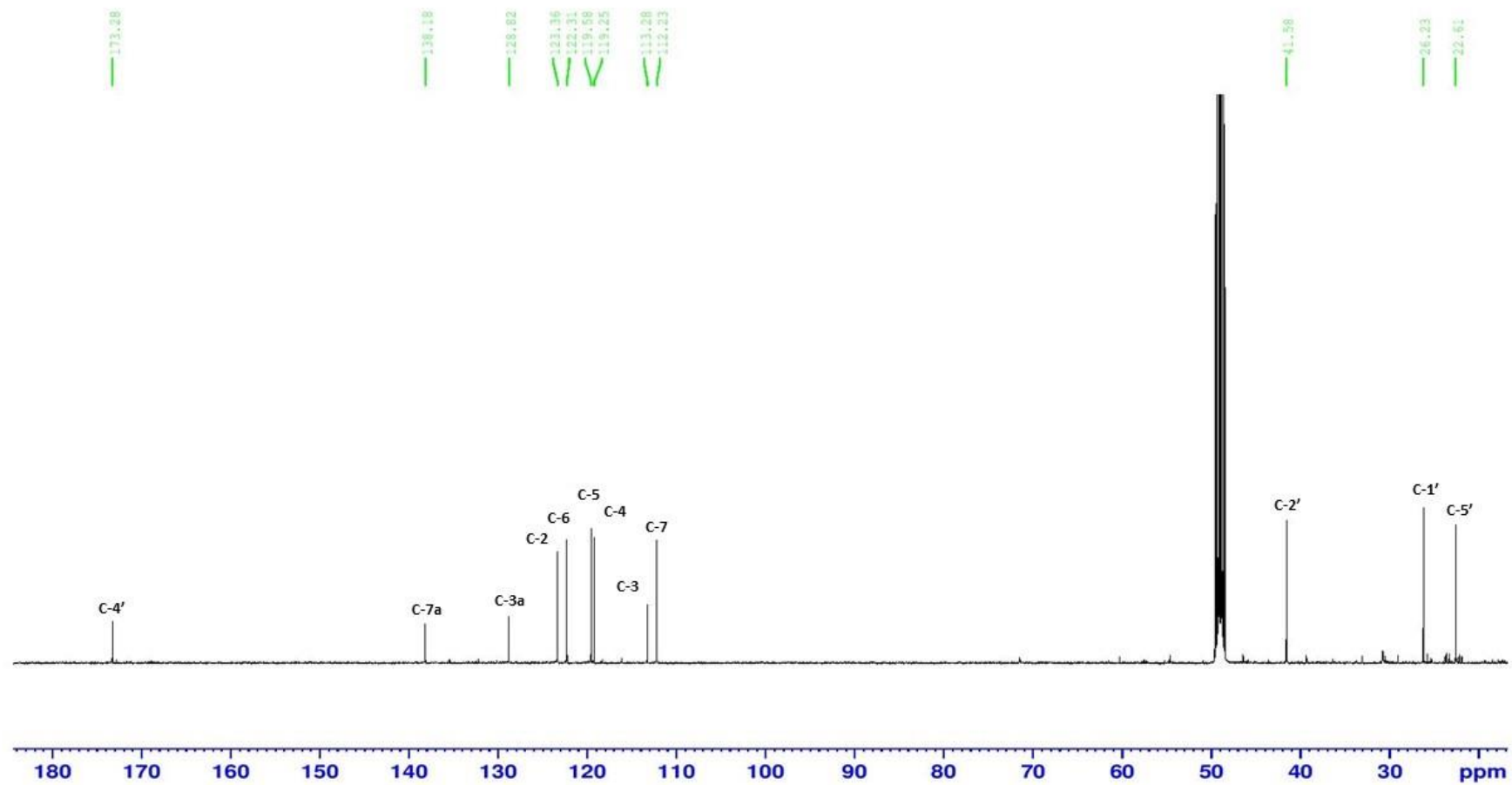
Figure 3.11: ^{13}C NMR spectrum of compound OM1 recorded in CD_3OD (125 MHz).
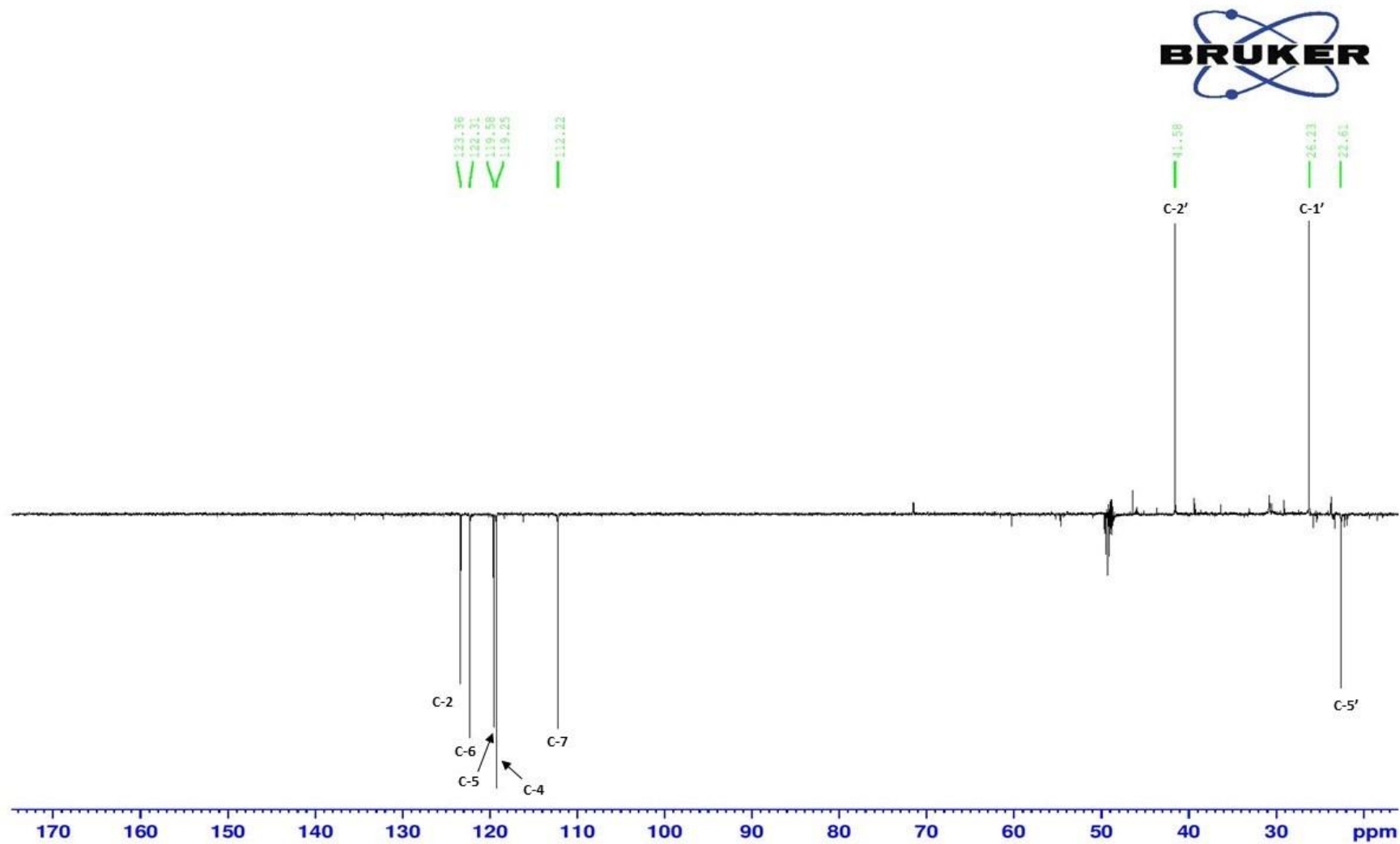
Figure 3.12: DEPT-135 spectrum of compound OM1 recorded in CD₃OD (125 MHz).
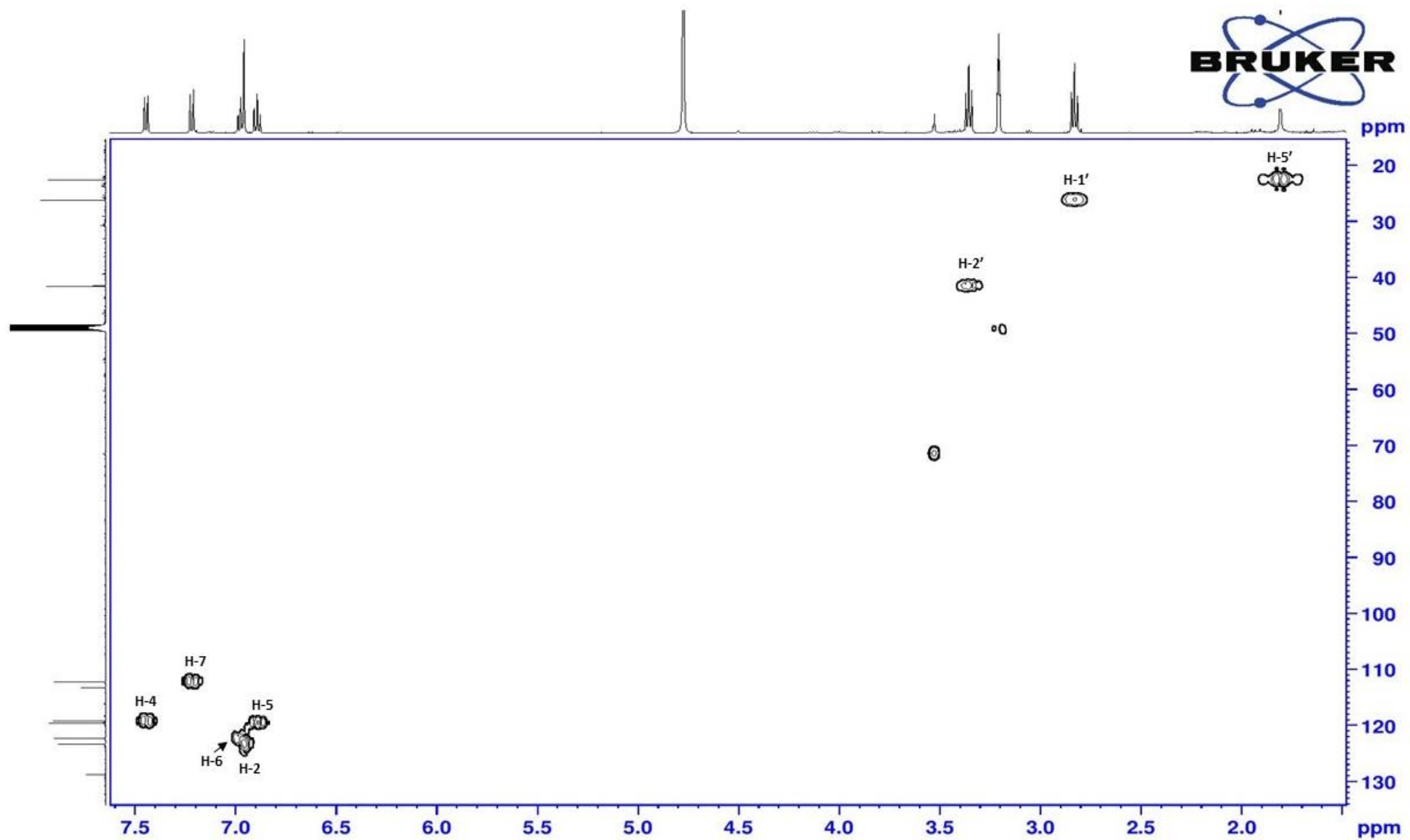
Figure 3.13: HMQC spectrum of compound OM1.
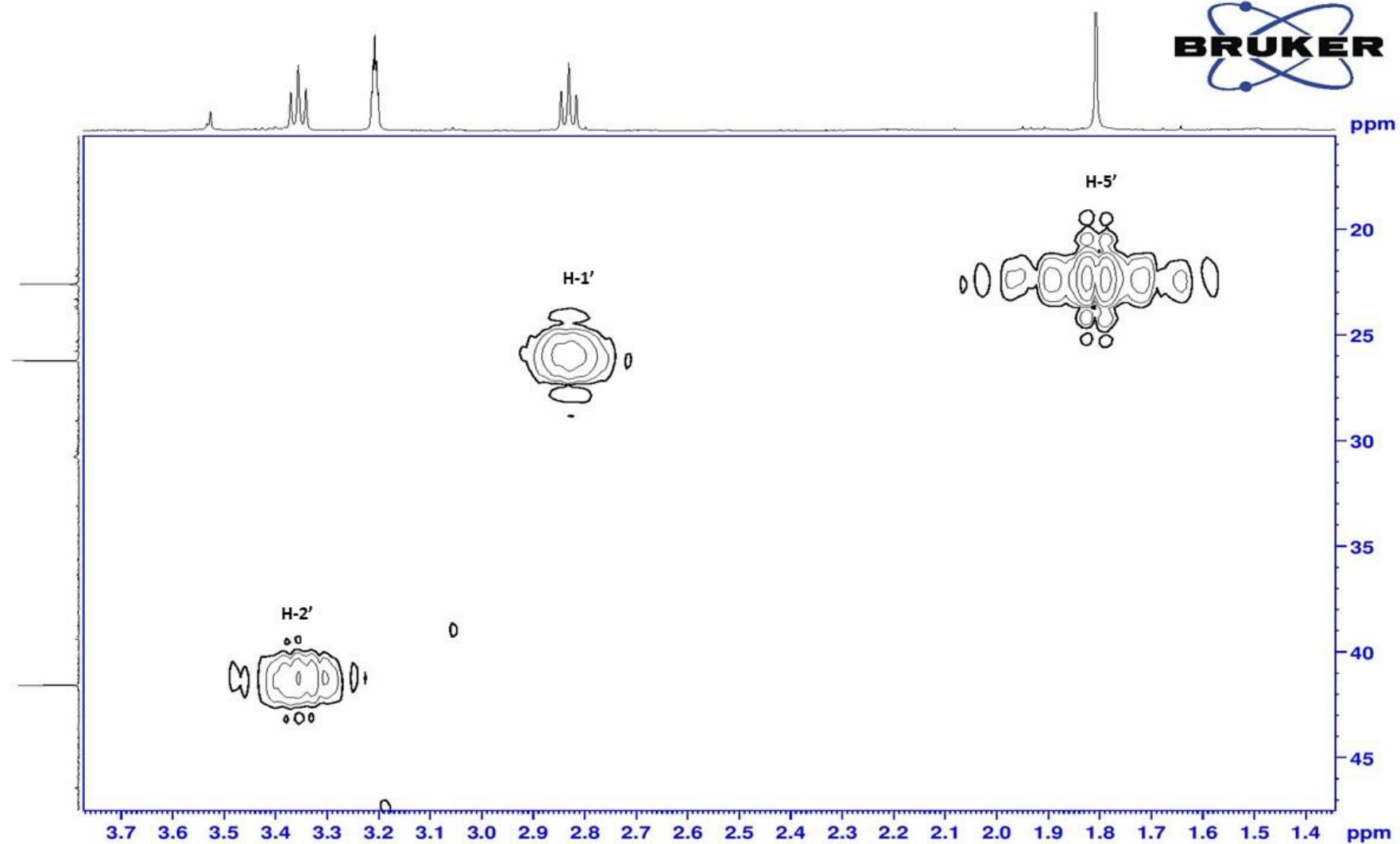
Figure 3.14: HMQC spectrum of compound OM1 (expanded).
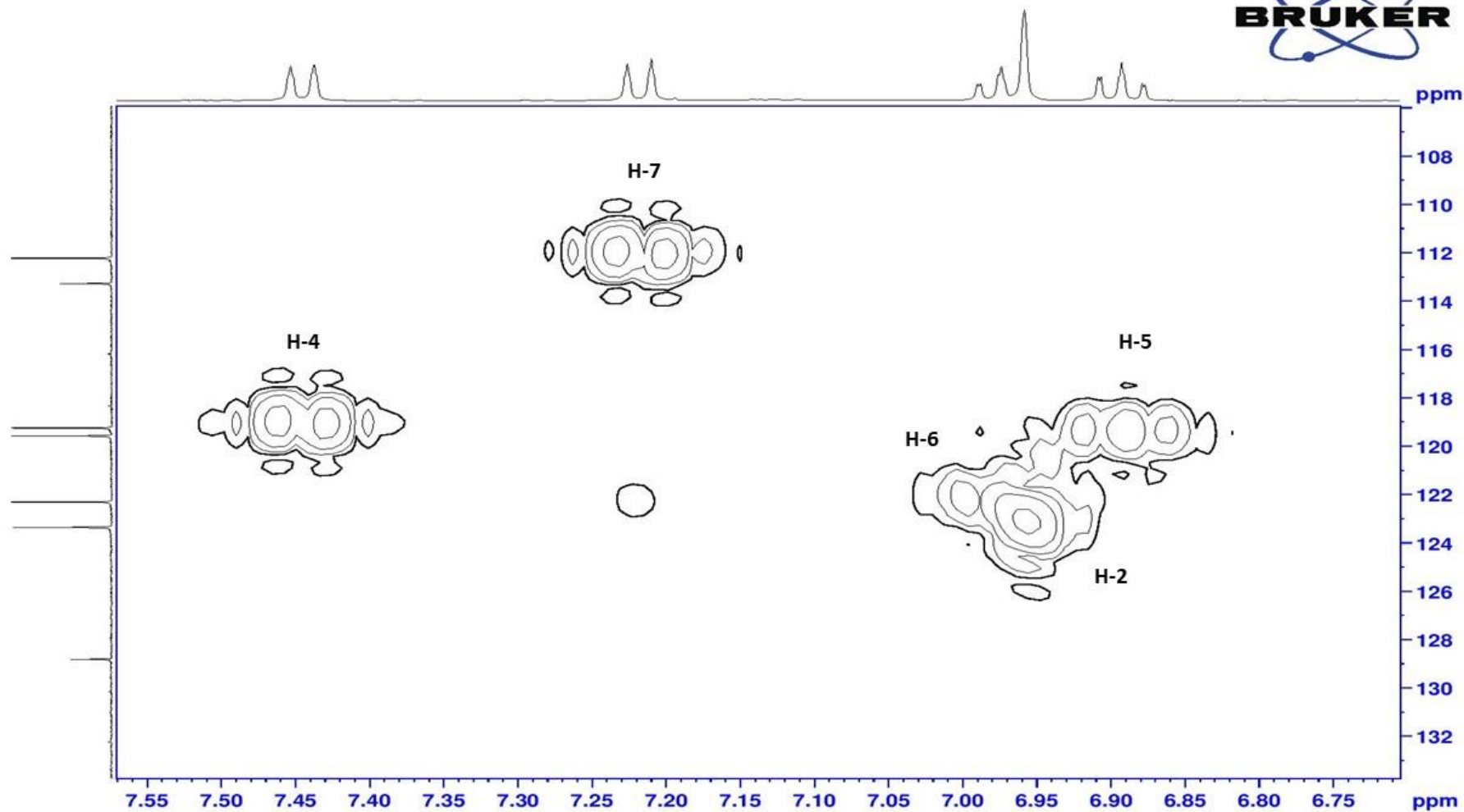
Figure 3.15: HMQC spectrum of compound OM1 (expanded).
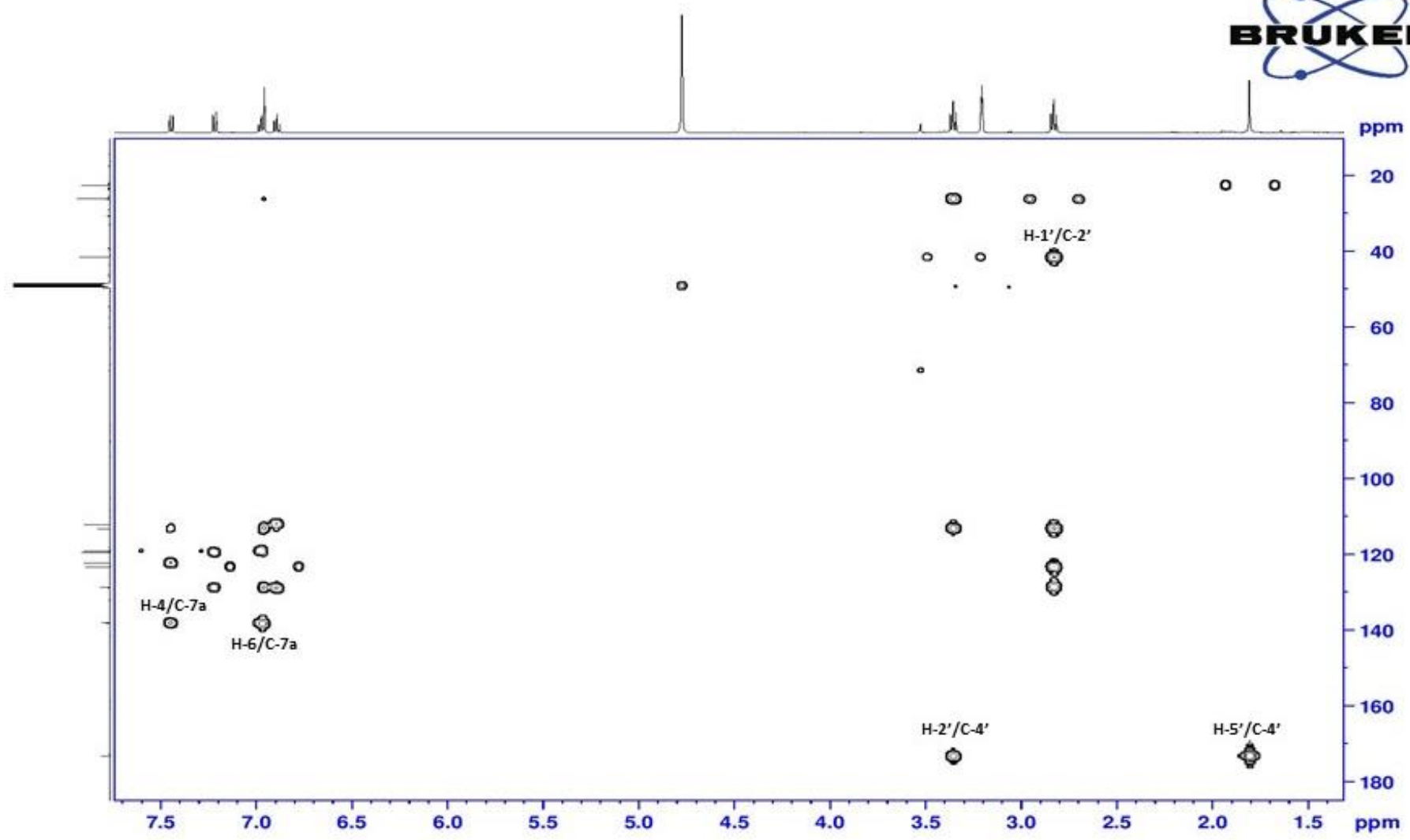
Figure 3.16: HMBC spectrum of compound OM1.
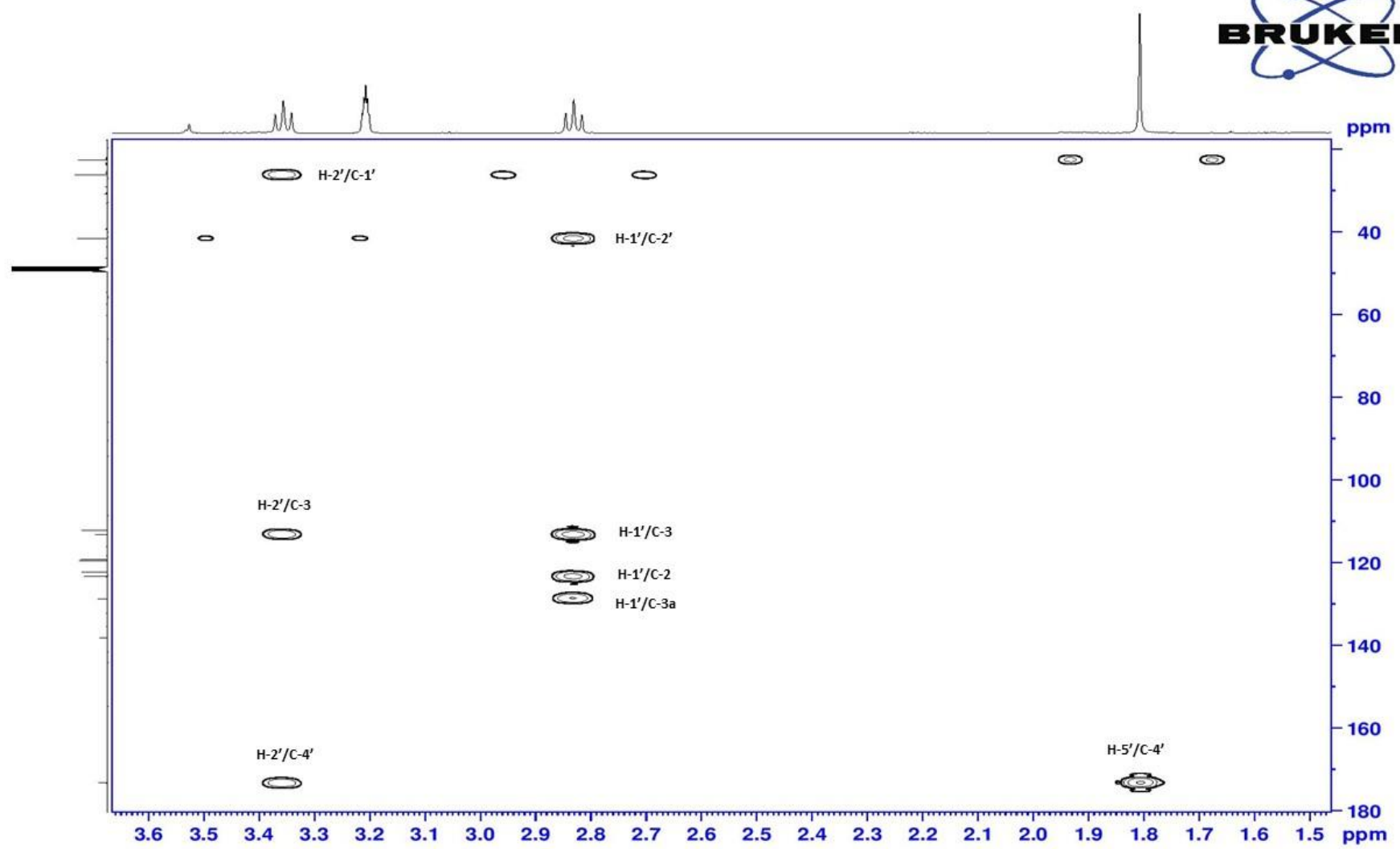
Figure 3.17: HMBC spectrum of compound OM1 (expanded).
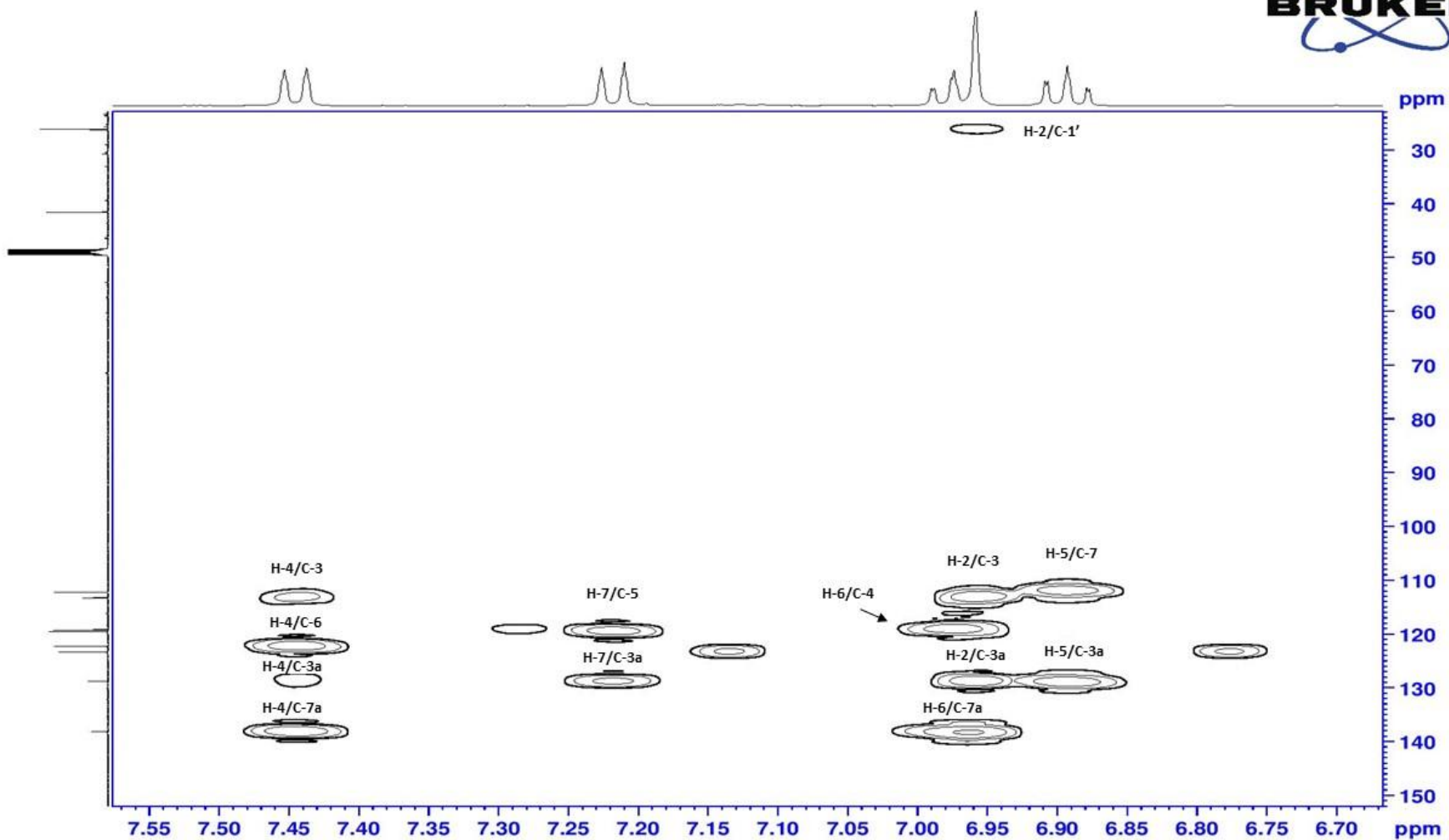
Figure 3.18: HMBC spectrum of compound OM1 (expanded).
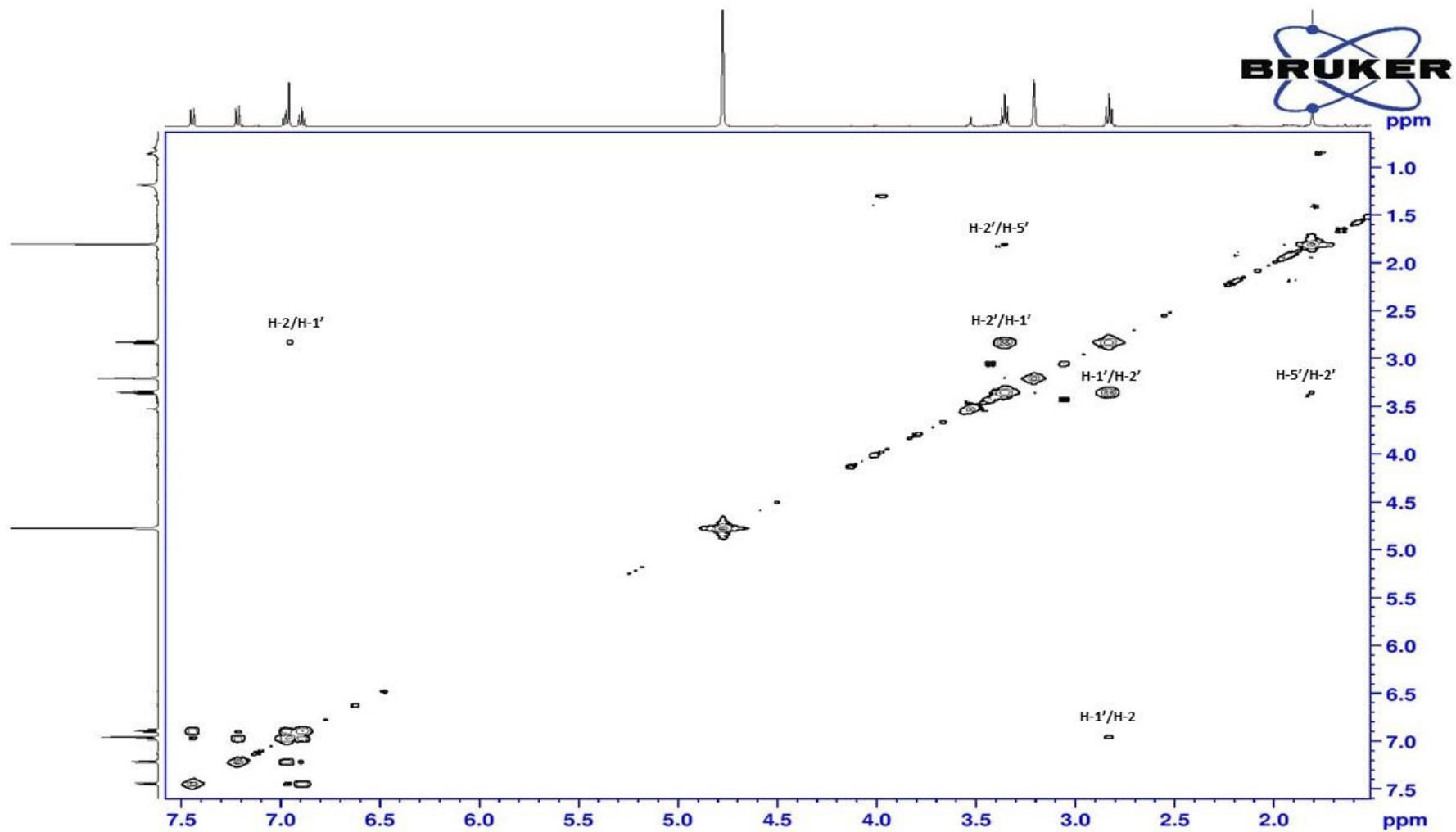
Figure 3.19: COSY spectrum of compound OM1.
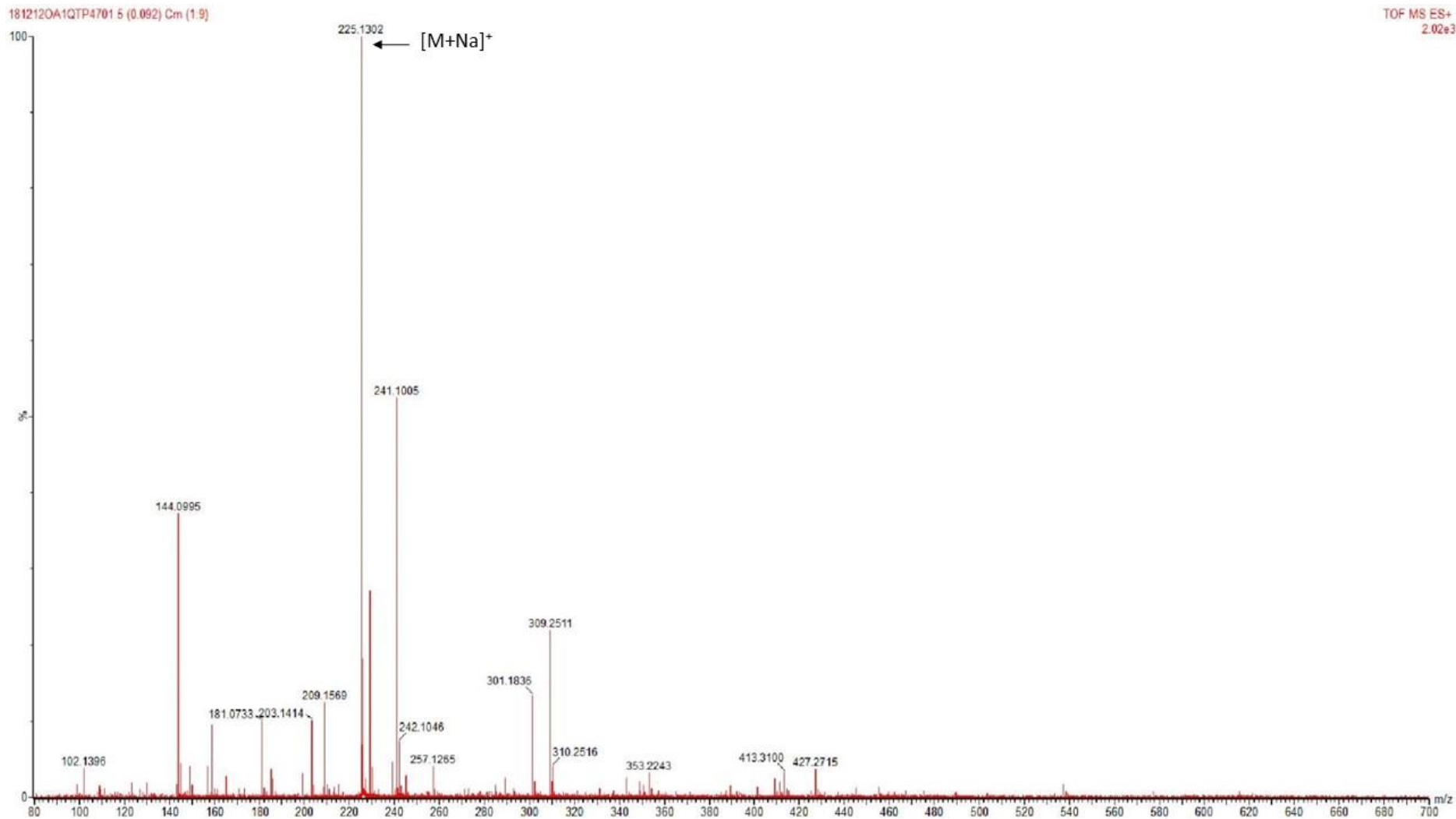
Figure 3.20: ESI-MS spectrum of compound OM1 showing peak ion at *m/z* 225.1302.
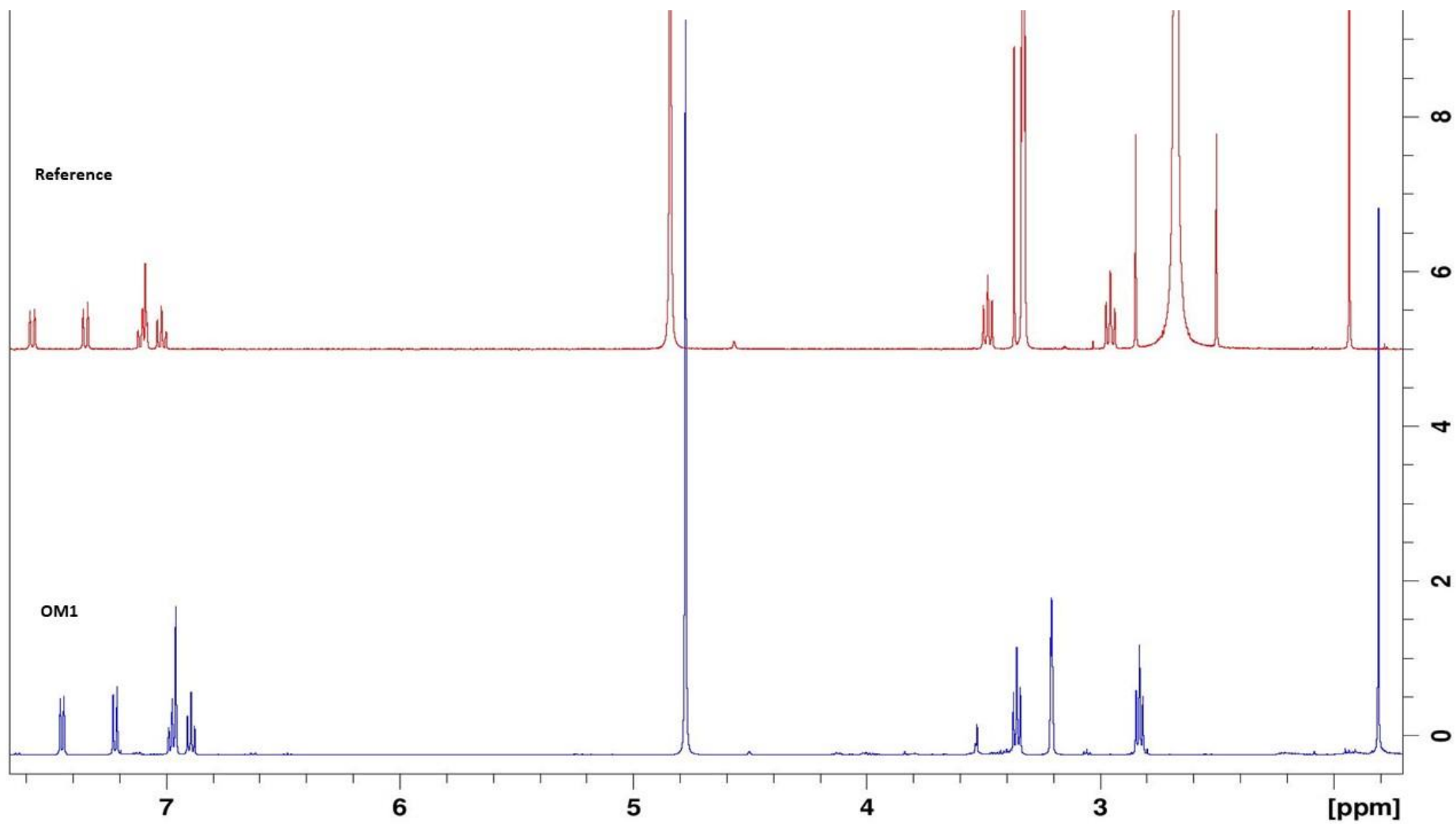
Figure 3.21: Comparison of ¹H NMR spectra of the reference (*N*-acetyltryptamine) and compound OM1.

3.2.2 Compound OM2

Compound **OM2** was isolated as a white powder from the **KH-A1** isolate from the **KH** spring. The steps for the isolation of this compound were discussed in **(Section 3.2.1) (Figure 3.8)**. The yield of **OM2** was approximately 43.6 mg (10.29 % of the fraction), and the structure of the **OM2** is shown in **(Figure 3.22).**
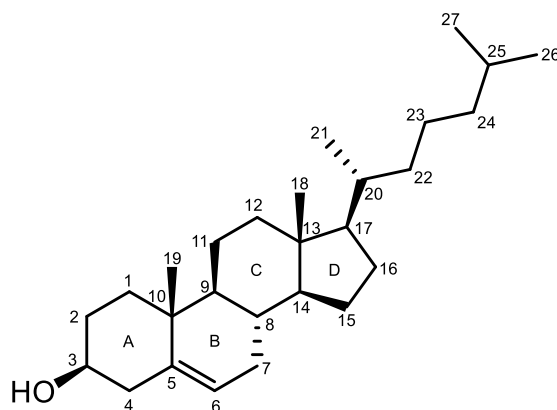
Figure 3.22: The structure of compound OM2.

The molecular formula of **OM2** was determined as $C_{27}H_{46}O$ and the molecular weight of the compound was calculated as 386, which corresponded to an ion peak in the ESI-MS at *m/z* 387.4 $[M+H]^+$ **(Appendix 1).**

The ^{1}H NMR spectrum **(Appendix 1)** showed a slightly deshielded methine proton at δ_H 5.37 (H-6), corresponding to olefinic hydrogen. The multiplicity of the peak should be a triplet due to the neighboring methylene group at C-7, but in the spectrum it appeared as a doublet with some fine splitting. This could be due to long-range coupling or due to some impurities in the compound. Additionally, there was further deshielded multiplet at δ_H 3.52, which could be attributed to an oxymethine hydrogen at C-3. The first four peaks which appeared at lower ppm in the spectrum corresponded to the five methyl groups that were present in the compound. Two of which were singlets that appeared at δ_H 0.70

(H$_3$-18) and δ$_H$ 1.03 (H$_3$-19), and the others were doublets found at δ$_H$ 0.88 (H$_3$-26 and H$_3$-27) and δ$_H$ 0.93 (H$_3$-21). The hydrogens H$_3$-26 and H$_3$-27 appeared as one peak in the same place in the spectrum. There were also around 10 shielded peaks ranging from δ$_H$ 1.10 to δ$_H$ 2.34; these peaks appeared as multiplets and some of which were overlapped. These peaks were composed of 11 methylene protons (nine of which were assigned to δ$_H$ 1.86 (H$_2$-1), 1.98 (H$_2$-2), 2.28 (H$_2$-4),1.52 (H$_2$-7), 2.04 (H$_2$-12), 1.10 (H$_2$-15), 1.15 (H$_2$-16), 1.65 (H$_2$-23) and 1.14 (H$_2$-24), respectively and six methine protons (three of which were assigned to δ$_H$ 1.88 (H-8), 1.05 (H-14) and 1.16 (H-17), respectively).

The ^{13}C NMR spectrum **(Appendix 1)** showed 27 carbon signals in total. Three of these signals were missing in the DEPT-135 spectrum **(Appendix 1)**, corresponding to the three quaternary carbons in the proposed structure as expected. The resonance peaks at δ$_C$ 140.7 and δ$_C$ 121.7 were attributed to the olefinic carbons in C-5 and C-6, respectively; whilst that at δ$_C$ 36.5 (C-10) and 42.3 (C-13) were attributable to the quaternary carbons. Moreover, the DEPT-135 recorded 11 methylene signals at δ$_C$ 37.2 (C-1), 31.6 (C-2), 42.3 (C-4), 31.9 (C-7), 21.0 (C-11), 39.7 (C-12), 24.7 (C-15), 28.2 (C-16), 36.2 (C-22), 23.8 (C-23) and 39.5 (C-24), respectively. Furthermore, the DEPT-90 **(Appendix 1)** suggested that there were eight methine signals at δ$_C$ 71.8 (C-3), 121.7 (C-5), 31.9 (C-8), 50.1 (C-9), 56.7 (C-14), 56.1 (C-17), 35.8 (C-20) and 28.0 (C-25). The remaining carbons were assigned for five methyl groups; two of which were on the ring system (δ$_C$ 11.8 and 19.4) and the others on the aliphatic side chain (δ$_C$ 18.7, 22.6 and 22.8).

In the HMBC spectrum **(Appendix 1)**, the position of the hydroxyl group at C-3 was confirmed by a ^2J correlation with the hydrogens of H$_2$-4 and a ^3J correlation with the hydrogens of H$_2$-1. In addition, the olefinic hydrogen, H-6, showed HMBC correlations to

the cyclic methylene carbon C-4, the cyclic methylene carbon C-7 and the quaternary carbon C-10; this confirmed its placement on ring B. Furthermore, the HMBC spectrum showed that a ^3J correlation between H-17 and H$_3$-21. This coupling confirmed the attachment of the aliphatic chain at C-17.

Further confirmation on the structure of the compound was obtained using FT-IR spectroscopy **(Appendix 2)**. The FT-IR spectrum was taken by dissolving the compound in chloroform and the spectrum exhibited an alkyl C-H stretching absorption at 2867 cm^{-1}, 2901 cm^{-1} and 2932 cm^{-1}, C-H bending at 1465 cm^{-1} and C-O stretching at 1056 cm^{-1}. Moreover, The IR bands at 3429 cm^{-1}, 1365 cm^{-1} and 1376 cm^{-1} confirmed the presence of a hydroxyl group, specifically alcohol. There was also an IR band at 957 cm^{-1}, which was attributable to C=C bending.

Compound **OM2** was therefore identified as 10,13-dimethyle-17-(6-methylheptan-2-yl)-2,3,4,7,8,9,10,11,12,13,14,15,16,17-tetradecahydro-*1H*-cyclopenta[a]phenanthren-3-ol. The above data were also in agreement with the published literature (Popjak *et al*.,1977) and are represented in **(Table 3.10)**, **OM2** was therefore assigned as the well-known natural product cholesterol. Moreover, compound **OM2** was compared to a ^{1}H NMR spectrum of reference cholesterol and it was identical **(Appendix 1)**.

It has been reported that cholesterol is produced by many bacteria such as *Streptomyces aureofaciens*, *Streptomyces griseus*, *B. megaterium*, *B. cereus*, *B. subtilis* and *Pseudomonas fluorescens* (Uwajima and Terada, 1976).

Table 3.10: ¹H (500 MHz), ¹³C NMR (125 MHz) and HMBC spectroscopic data of OM2 recorded in CDCl₃.

Position	¹H	¹³C	HMBC			¹³C(CDCl₃) Popjak *et al.*,1977
			²J	³J	⁴J	
C-1	1.86	37.2	--	C-3, C-5	C-4	37.6
C-2	1.98	31.6	--	--	--	32.0
C-3	3.52 (m)	71.8	--	--	--	72.1
C-4	2.28	42.3	C-3, C-5	C-2, C-6, C-10	--	42.6
C-5	--	140.7	--	--	--	141.1
C-6	5.37 (ds)	121.7	C-7	C-4, C-10	--	122.0
C-7	1.52	31.9	C-6, C-8	C-5	--	32.2
C-8	1.88	31.9	--	C-10	--	32.2
C-9	--	50.1	--	--	--	50.5
C-10	--	36.5	--	--	--	36.8
C-11	--	21.0	--	--	--	21.4
C-12	2.04	39.7	--	C-9, C-14	C-16	40.1
C-13	--	42.3	--	--	--	42.6
C-14	1.05	56.7	--	--	--	57.1
C-15	1.10	24.7	C-14	--	--	24.6
C-16	1.15	28.5	C-17	C-13	C-12	28.5
C-17	1.16	56.1	--	--	--	56.5
C-18	0.70 (s)	11.8	C-13	C-12, C-14	--	12.0
C-19	1.03 (s)	19.4	C-10	C-1, C-5, C-9	--	19.6
C-20	--	35.8	--	--	--	36.1
C-21	0.93 (d)	18.7	C-20	C-17	--	18.9
C-22	--	36.2	--	--	--	36.5
C-23	1.65	23.8	C-24	C-25	--	24.2
C-24	1.14	39.5	--	--	--	39.8
C-25	--	28.0	--	--	--	28.3
C-26	0.88 (d)	22.6	C-25	C-24, C-27	--	22.7
C-27	0.88 (d)	22.8	C-25	C-24	--	22.9

3.2.3 Compound OM3

Compound **OM3** was separated as a colourless powder from an extract of an isolate **(GH-C8)** from the **GH** spring. The methanol extract (1.2 g) of the **GH-C8** isolate was subjected to gravity column chromatography in order to fractionate the extract into 12 fractions **(Figure 3.23)**. Fractions 7 and 8 demonstrated antimicrobial activity. These fractions (93.7 mg / 7.80 % of the extract) were added to each other and then applied to (prep NP-TLC) with a solvent system of *n*-hexane: ethyl acetate / 90:10. A sixth TLC band with an R$_f$ of 0.78 demonstrated activity in the *S. aureus* overlay assay **(Figure 3.24).** This band represented compound **OM3** (14.8 mg / 15.79 % of the fraction), and its structure is shown in **(Figure 3.25).** Moreover, there was another active TLC band with an R$_f$ of 0.51, but the identification of the compound was difficult and is still under study. At R$_f$ 0.87, there was a resistant compound that conferred the *S. aureus* the ability to resist the therapeutic action of **OM3**. This was shown as a band of growth over the position on the TLC plate. This is very interesting as this band may inhibit the antibacterial action of **OM3**. The structural elucidation and mechanism of action of it have not been studied yet.
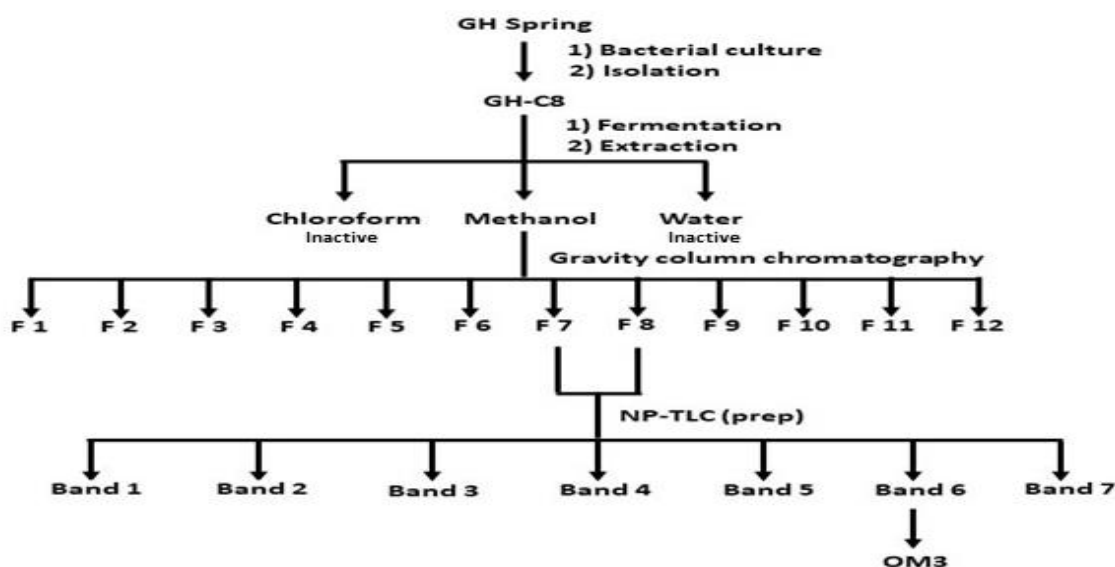
Figure 3.23: Scheme of isolation for compound OM3.

The molecular formula of **OM3** was determined as $C_{12}H_{16}N_4O_2$ and the molecular weight of the compound was calculated as 248.2804, which corresponded to an ion peak in the HRMS at *m/z* 249.1351 [M+H]$^+$ **(Figure 3.36).**

The ^{1}H NMR spectrum **(Figure 3.26)** revealed two aromatic signals; two doublets at δ_H 7.63 (*J*= 9.0 Hz, H-2/H-6) and δ_H 8.01 (*J*= 9.0 Hz, H-3/H-5). The hydrogens H-2 and H-6 were viewed as one peak as well as the hydrogens H-3 and H-5 because they were in the same environment. The resonances at δ_H 7.63 and δ_H 8.01 were roofed to each other and had coupling constants (*J*=9.0 Hz), indicative of an *ortho* coupling to each other. Furthermore, there were three slightly deshielded singlets at δ_H 3.04 (H$_3$-5'), 3.05 (H$_3$-6') and 3.18 (H$_3$-7'). They were deshielded due to their attachments to nitrogen atoms.
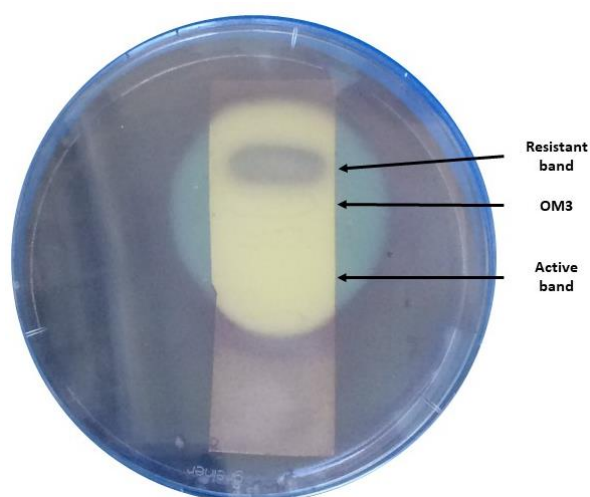
Figure 3.24: Bioautography assay of compound OM3

The ^{13}C NMR spectrum **(Figure 3.27)** revealed 10 resonances, which were consistent with the calculated molecular formula of the compound. The DEPT-135 spectrum **(Figure 3.29)** when compared to the broadband decoupled spectrum, revealed that three carbon signals at δ_C 126.4 (C-1), δ_C 126.9 (C-4) and δ_C 164.9 (C-7) were missing, which corresponded to the quaternary carbons. No methylene carbons were

found to be present. The DEPT-90 **(Figure 3.28)** showed two methines at δ_C 129.8 (C-3/C-5) and δ_C 133.5 (C-2/C-6). The two aromatic carbons at 2 and 6 positions of the compound were shown as one peak at δ_C 133.5. Similarly, carbons at 3 and 5 positions appeared as one peak at δ_C 129.8. Moreover, there were still two quaternary carbons at δ_C 149.3 (C-3') and δ_C 166.1 (C-1') did not evidently appear in ^{13}C NMR spectrum; however, they were present in the HMBC spectrum. The remaining carbon signals were assigned as methyl groups at δ_C 38.2 (C-7'), δ_C 38.2 (C-6') and δ_C 39.4 (C-5'), and they were slightly deshielded because they were attached to nitrogen atoms.
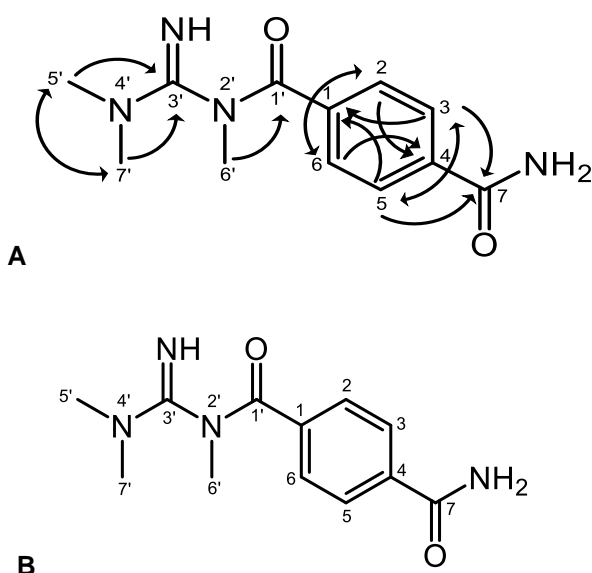
Figure 3.25: The structure of compound OM3.
A: HMBC correlations, **B: OM3** structure.

In the HMBC spectrum **(Figures 3.32, 33 and 34)**, the position of the carbonyl at C-7 was confirmed by a ^3J correlation with the hydrogens H-3 and H-5. In addition, the position of the carbonyl at C-1' was confirmed by a ^3J correlation with the hydrogens H3-6'. Furthermore, the placement of the C=NH was confirmed by the ^3J correlation with the hydrogens H3-5' and H3-7'.

Further confirmation on the structure of the compound was obtained using FT-IR spectroscopy **(Figure 3.37)**. The FT-IR spectrum was taken by dissolving the compound in methanol and the IR spectrum revealed an absorption at 1642 cm^{-1}, indicative of the presence of a C=NH functional group. There were also a band for C-N stretching at 1019 cm^{-1} and an alkyl C-H stretching at 2833 cm^{-1} and 2946 cm^{-1} present in the compound.

Additionally, the results of the LC-MS analysis showed that there was a peak at RT: 4.56 with A% = 64.8; this peak gave an ion peak at *m/z* 249.05 [M+H]$^+$ **(Figure 3.38)**, which confirmed the proposed structure.

According to the above data and SciFinder searches, compound **OM3** was novel and therefore identified as *N^1-*(*N, N*-dimethylcarbamimidoyl)-*N^1-*methylterephthalamide based on ChemDraw nomenclature. The compound has been given the trivial name Ghomygadine A, to reflect its spring source and the fact that it is a guanidine.

Table 3.11: ^{1}H (500 MHz), ^{13}C NMR (125 MHz) and HMBC spectroscopic data of OM3 recorded in CD$_3$OD

Position	^{1}H	^{13}C	HMBC	
			^2J	^3J
C-1	--	126.4	--	--
C-2	7.63 (d)	133.5	--	C-4, C-6
C-3	8.01 (d)	129.8	--	C-1, C-5, C-7
C-4	--	126.9	--	--
C-5	8.01 (d)	129.8	--	C-1, C-3, C-7
C-6	7.63 (d)	133.5	--	C-2, C-4
C-7	--	164.9	--	--
C-1'	--	166.1	--	--
N	--	--	--	--
C-3'	--	149.3	--	--
N	--	--	--	--
C-5'	3.04 (s)	39.4	--	C-3', C-7'
C-6'	3.05 (s)	38.2	--	C-1'
C-7'	3.18 (s)	38.2	--	C-3', C-5'
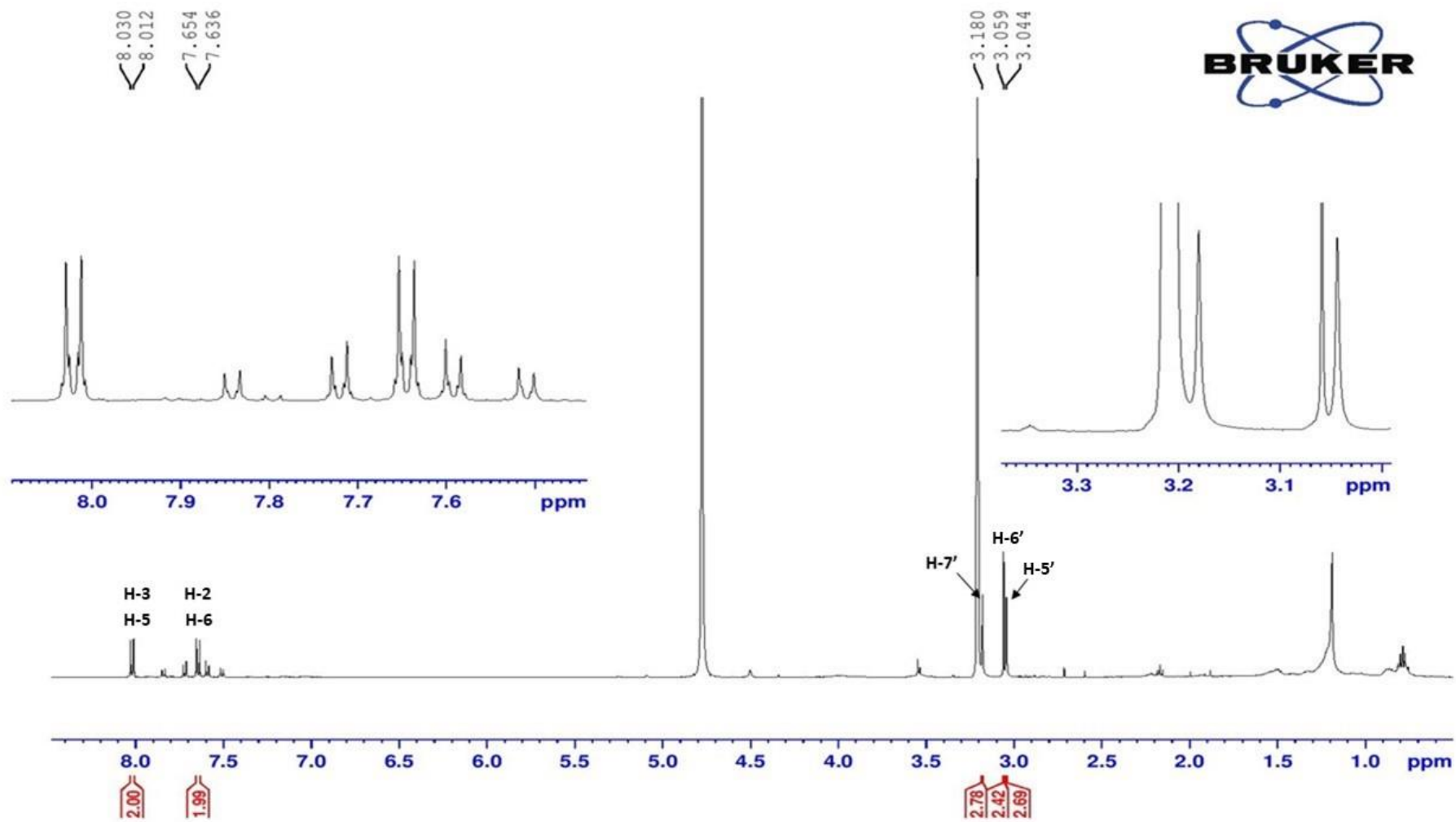
Figure 3.26: ^{1}H NMR spectrum of compound OM3 recorded in CD$_3$OD (500 MHz).
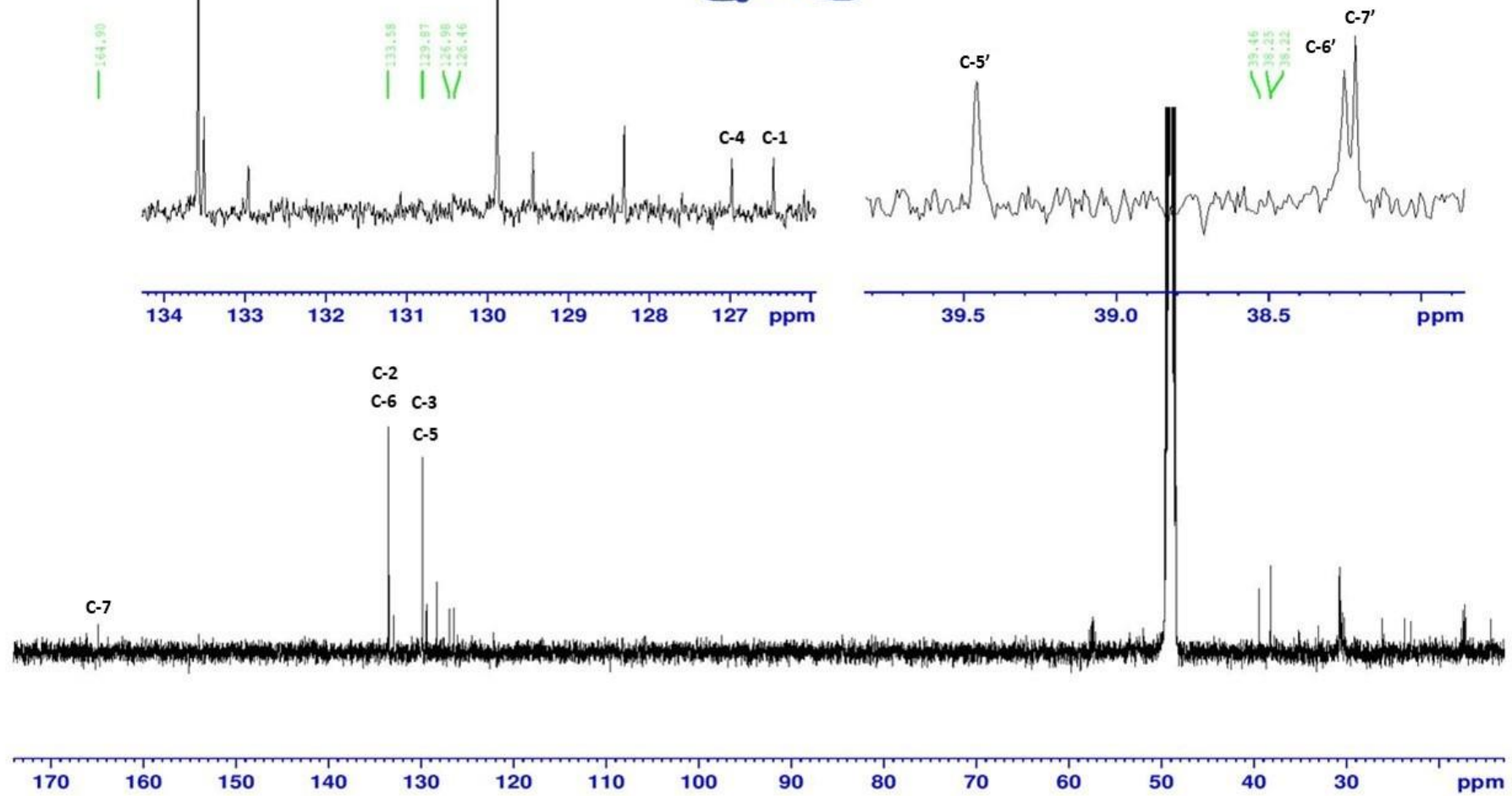
Figure 3.27: ^{13}C NMR spectrum of compound OM3 recorded in CD_3OD (125 MHz).
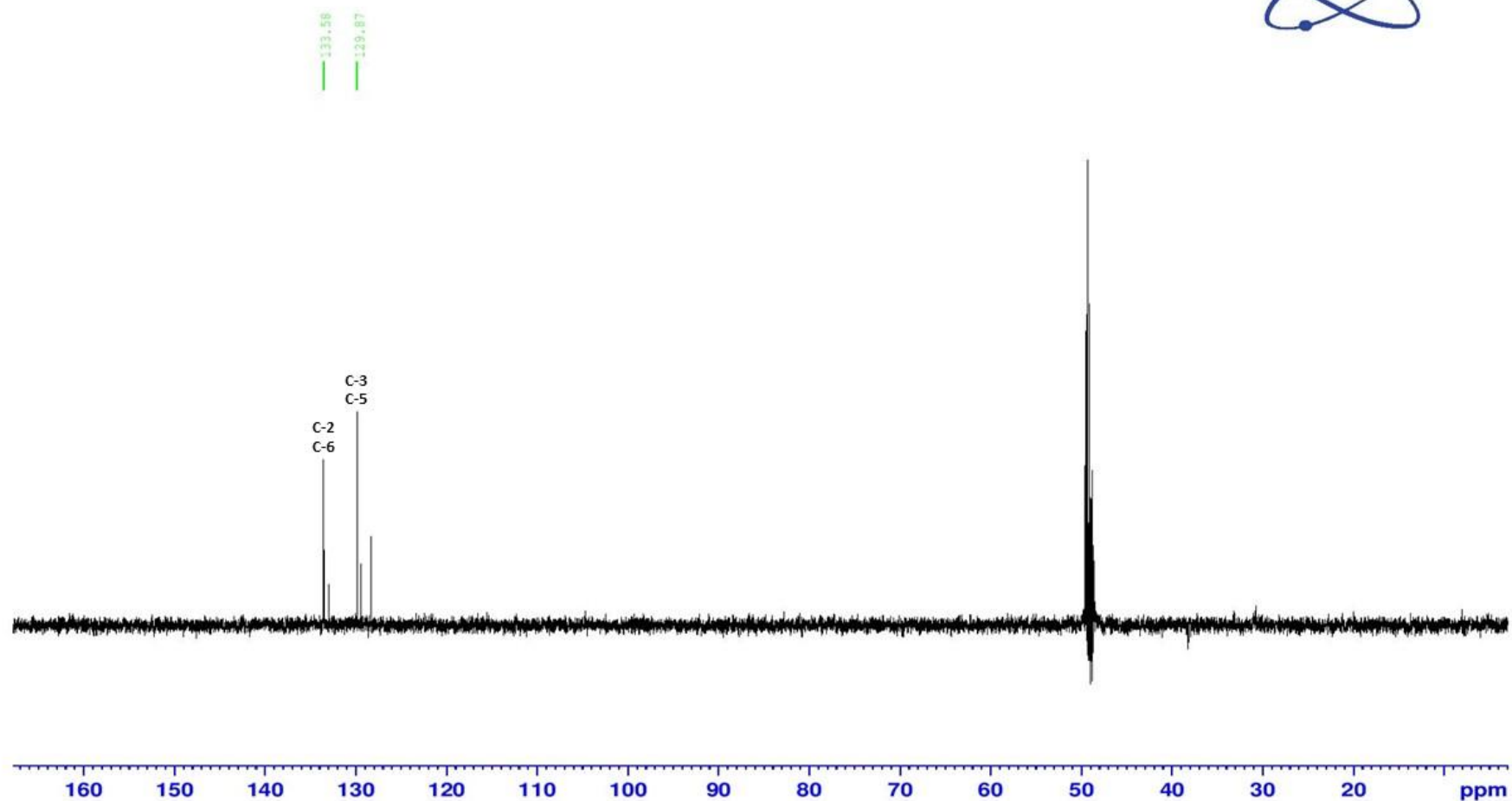
Figure 3.28: DEPT-90 spectrum of compound OM3 recorded in CD₃OD (125 MHz).
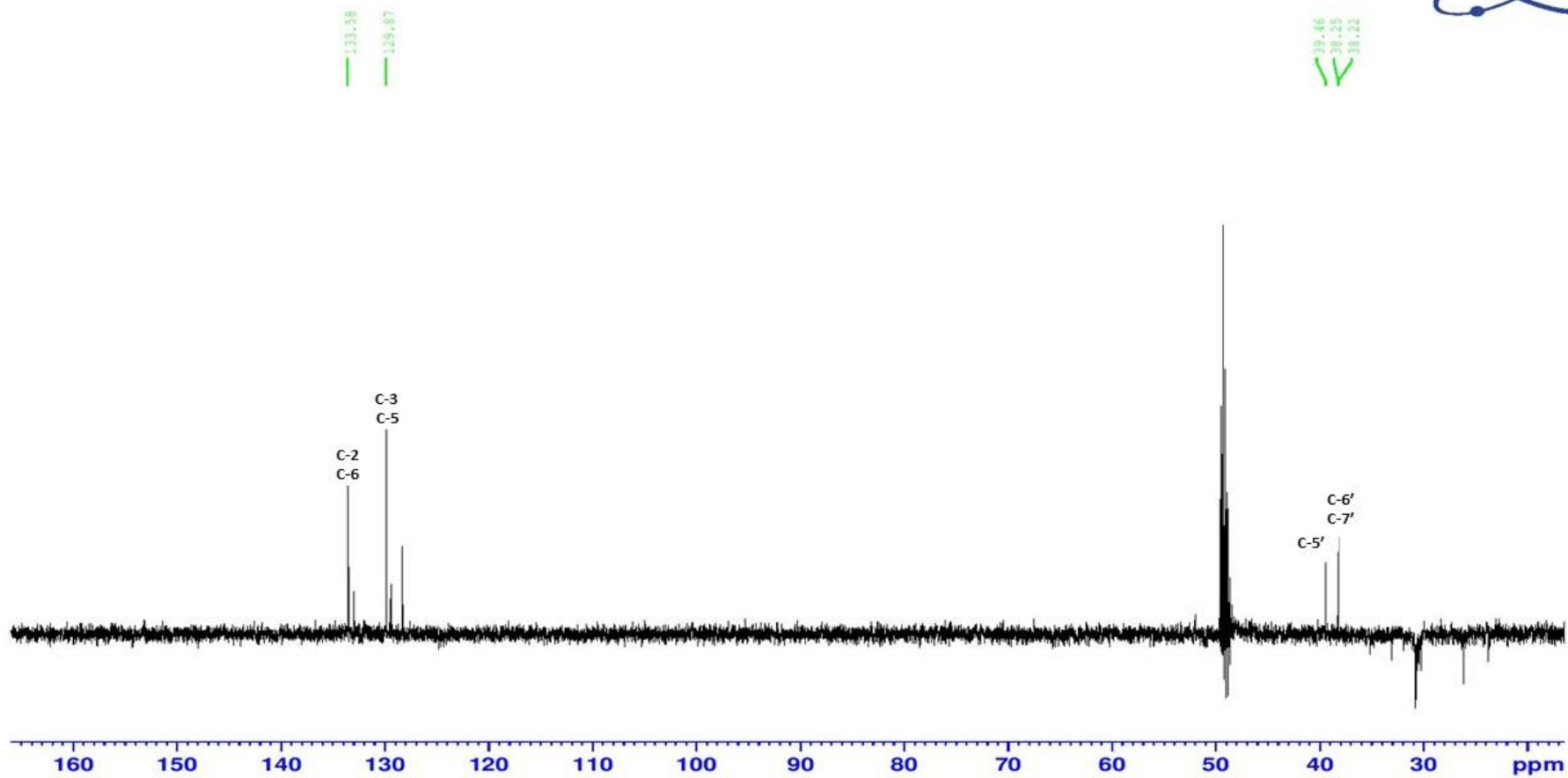
Figure 3.29: DEPT-135 spectrum of compound OM3 recorded in CD$_3$OD (125 MHz).
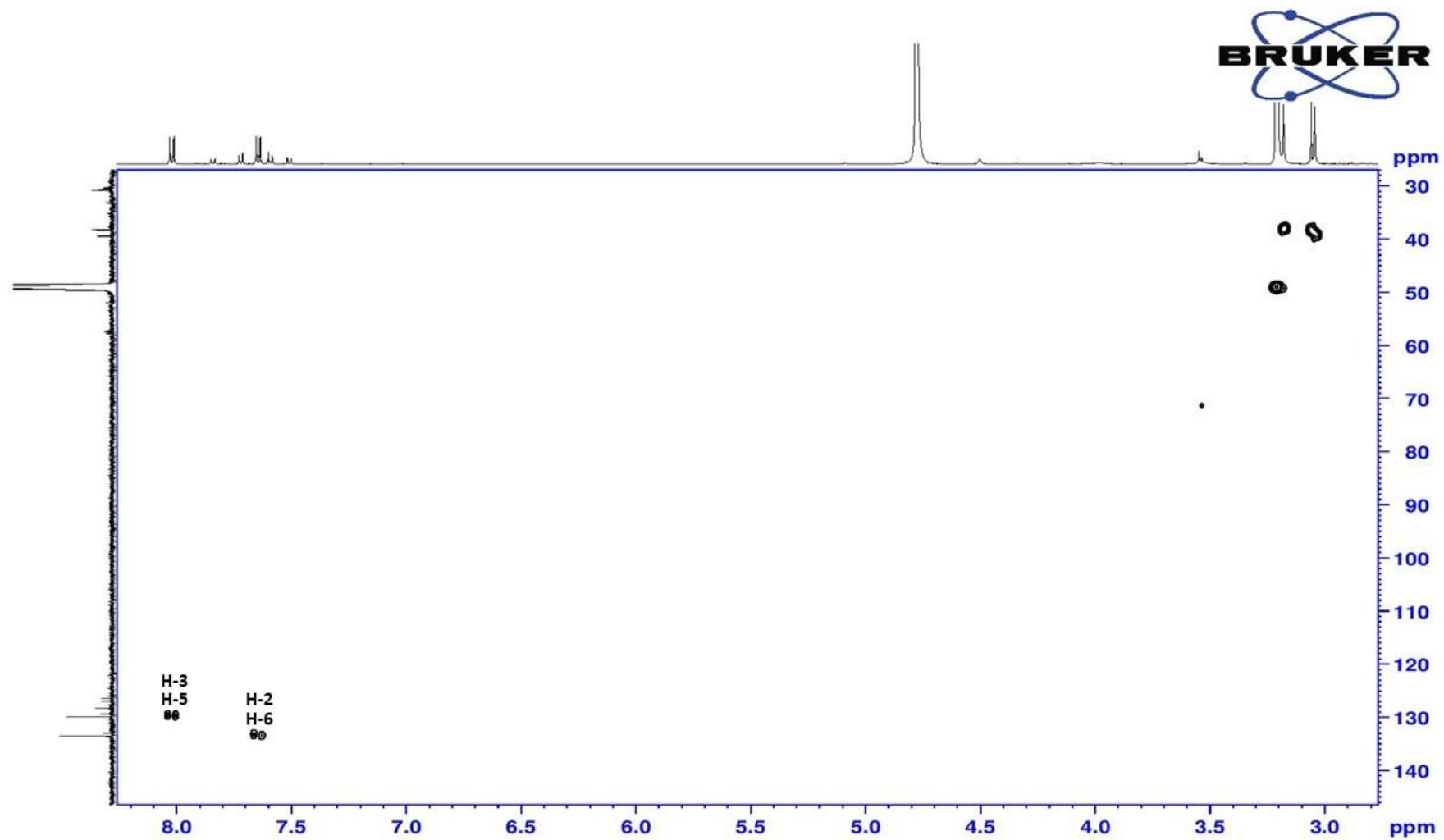
Figure 3.30: HMQC spectrum of compound OM3.
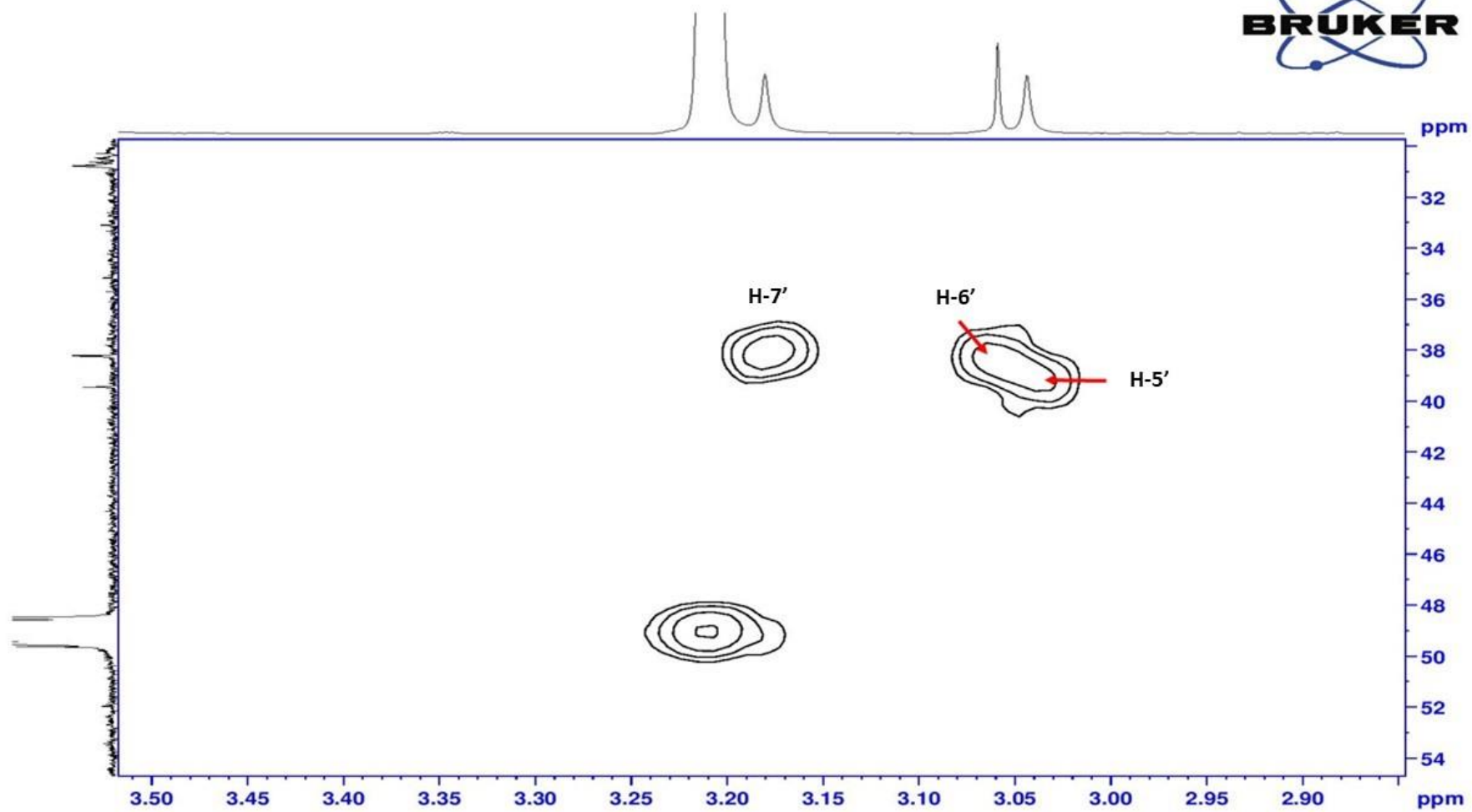
Figure 3.31: HMQC spectrum of compound OM3 (expanded).
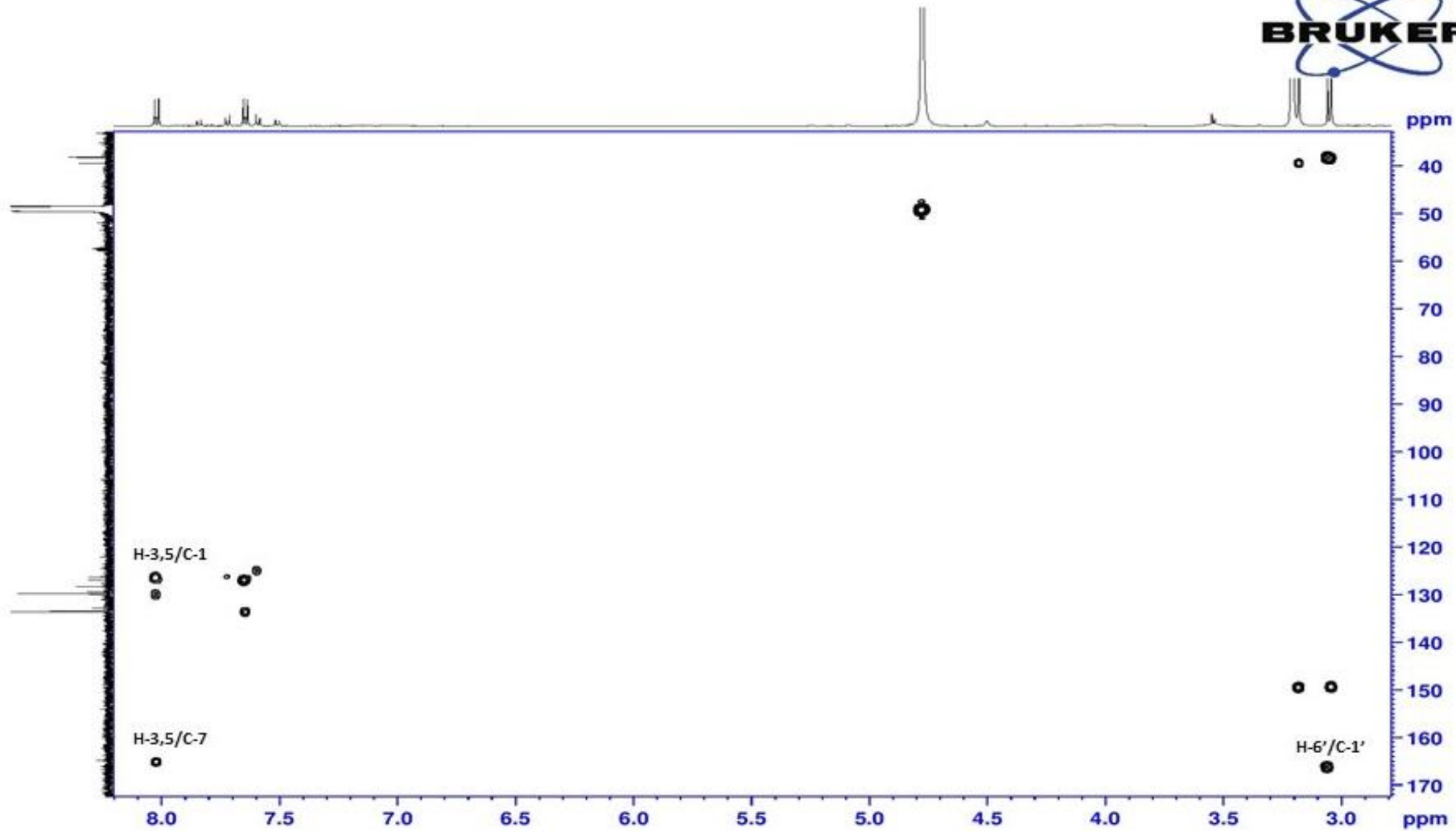
Figure 3.32: HMBC spectrum of compound OM3.
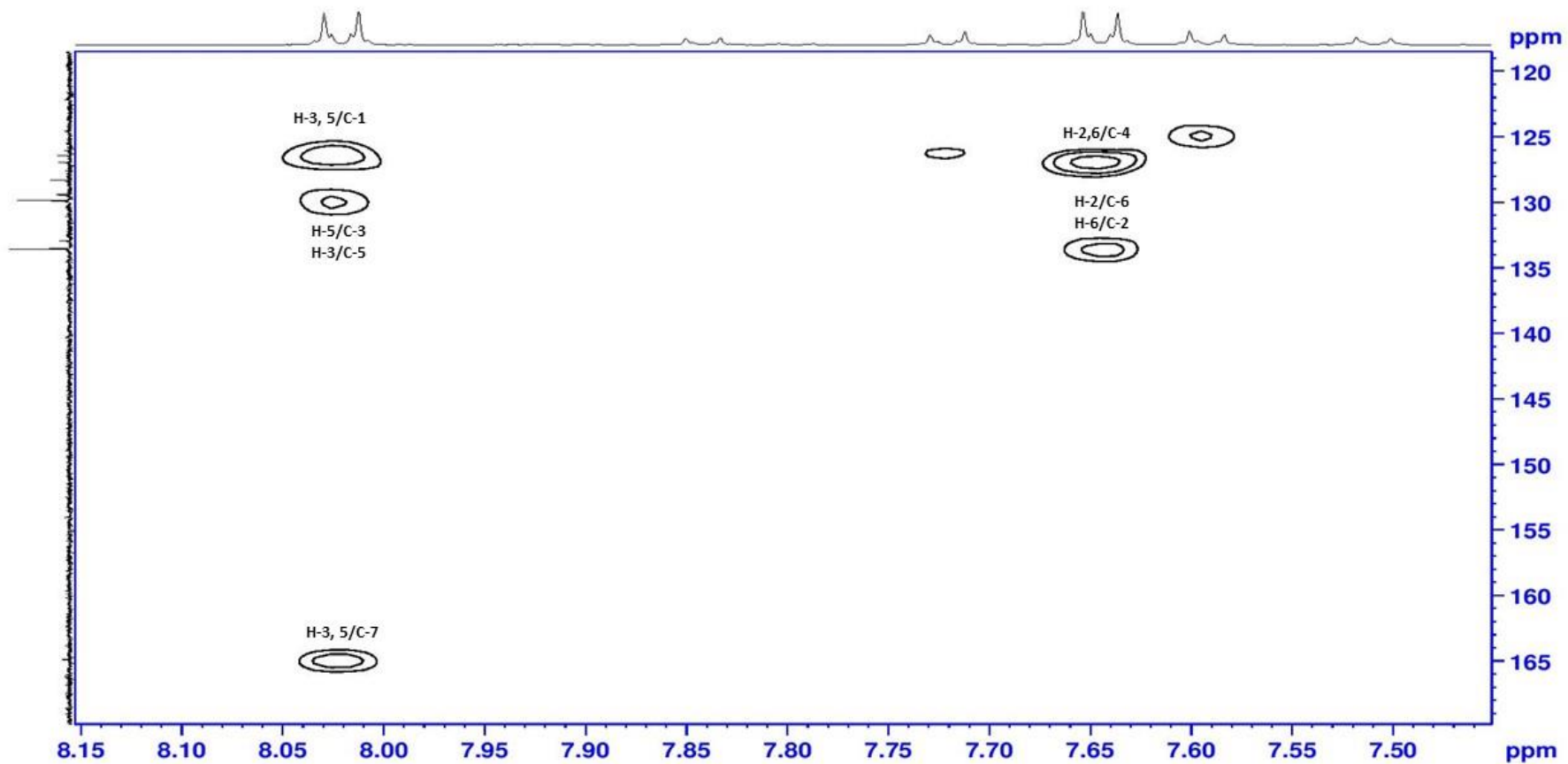
Figure 3.33: HMBC spectrum of compound OM3 (expanded).
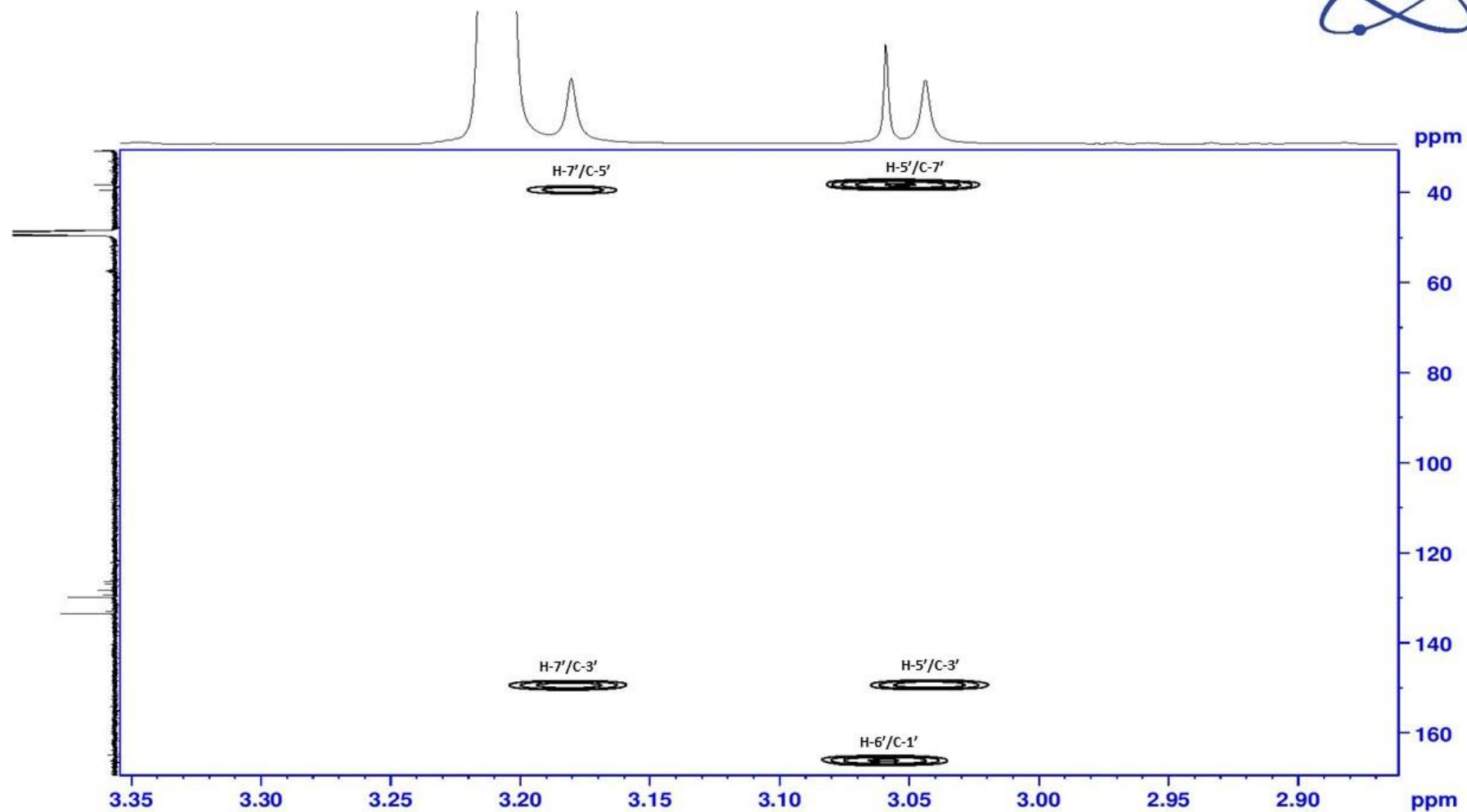
Figure 3.34: HMBC spectrum of compound OM3 (expanded).
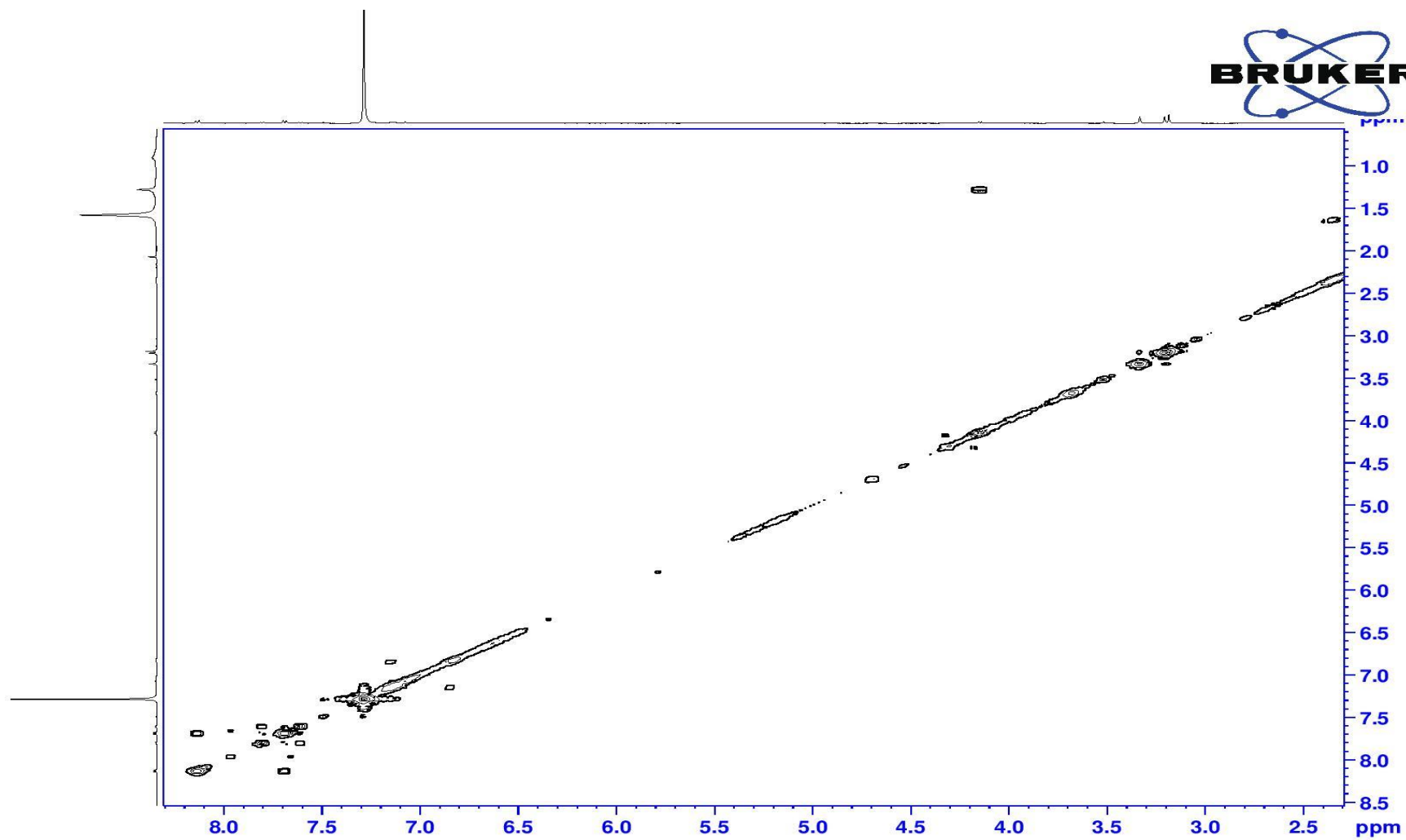
Figure 3.35: COSY spectrum of compound OM3.
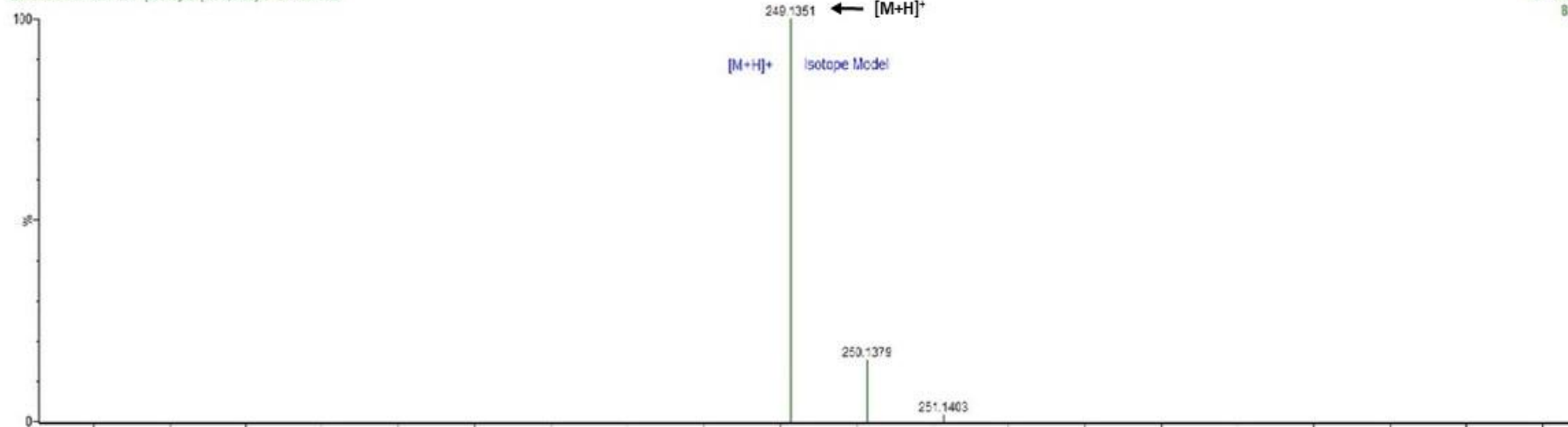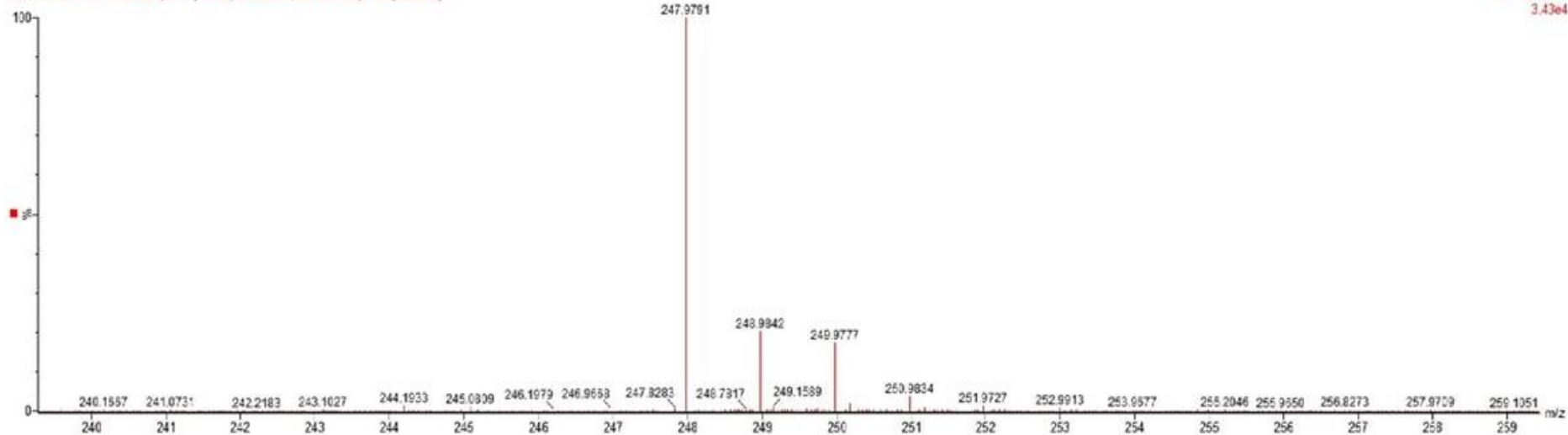
Figure 3.36: HRMS spectrum of compound OM3 showing peak ion at *m/z* 249.1351.
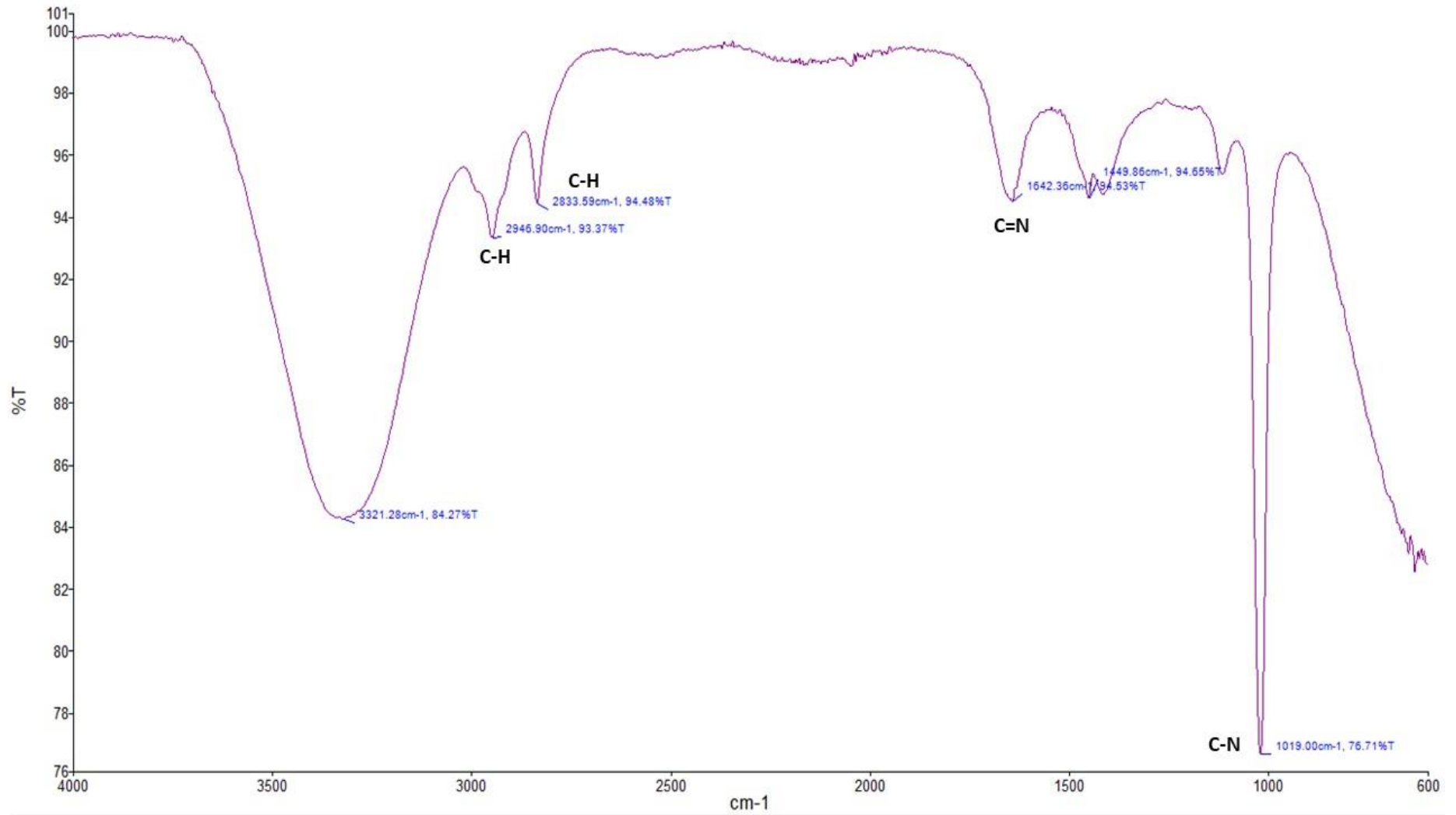
Figure 3.37: FT-IR spectrum of compound OM3.
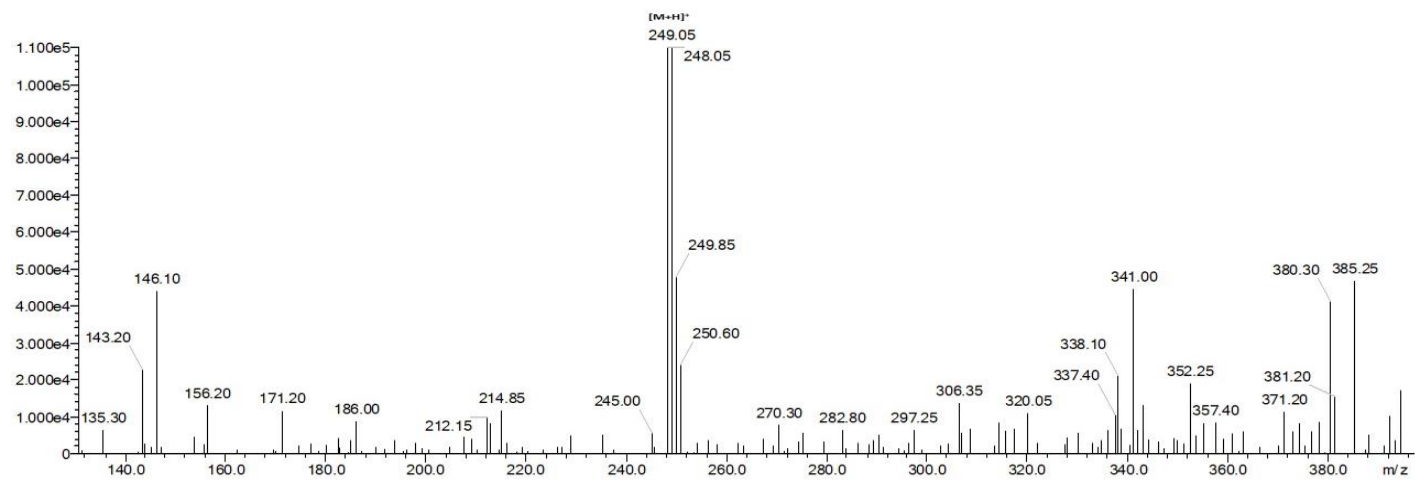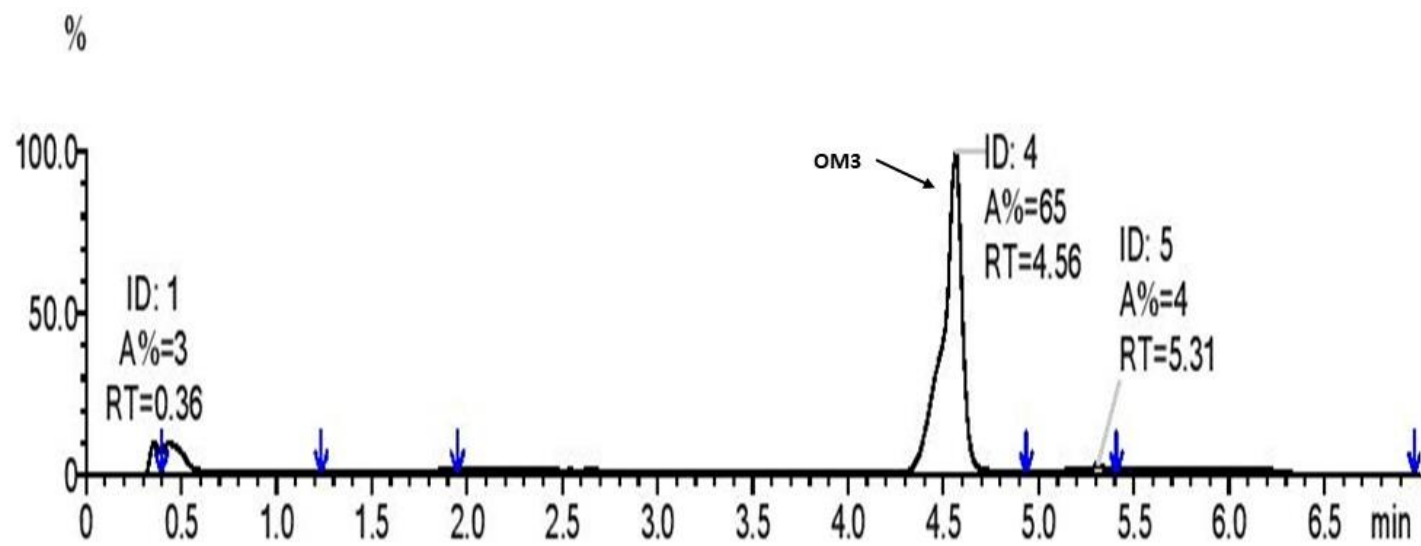
Figure 3.38: LC-MS spectrum of compound OM3 showing peak ion at *m/z* 249.05.

3.2.4 Compound OM4

Compound **OM4** was obtained as a colourless oil from the **TB-A3** isolate from the **TB** spring. The methanol extract (1.6 g) of the **TB-A3** isolate was subjected to partitioning chromatography in order to isolate the active compound **(Figure 3.39)**. Five sub-extracts were collected and the ethyl acetate sub-extract (433.8 mg / 27.11% of the extract) was active. The ethyl acetate sub-extract was, therefore, subjected to NP-SPE to identify the active fractions. Fractions (4, 5, 6, 7 and 8) demonstrated antimicrobial activity. These fractions (176.2 mg / 40.61% of the sub-extract) were combined and fractionated using RP-SPE into 12 fractions. Fractions (3, 4 and 5) (57.3 mg / 32.51% of the fraction) were active based on a disc diffusion assay and therefore applied to prep-NP-TLC with the solvent system chloroform: methanol (90:10). The first TLC band with an R_f of 0.28 demonstrated activity in the *S. aureus* overlay assay. This band afforded compound **OM4** (33.8 mg / 58.98 % of the fraction), and its structure is shown in **(Figure 3.40).**
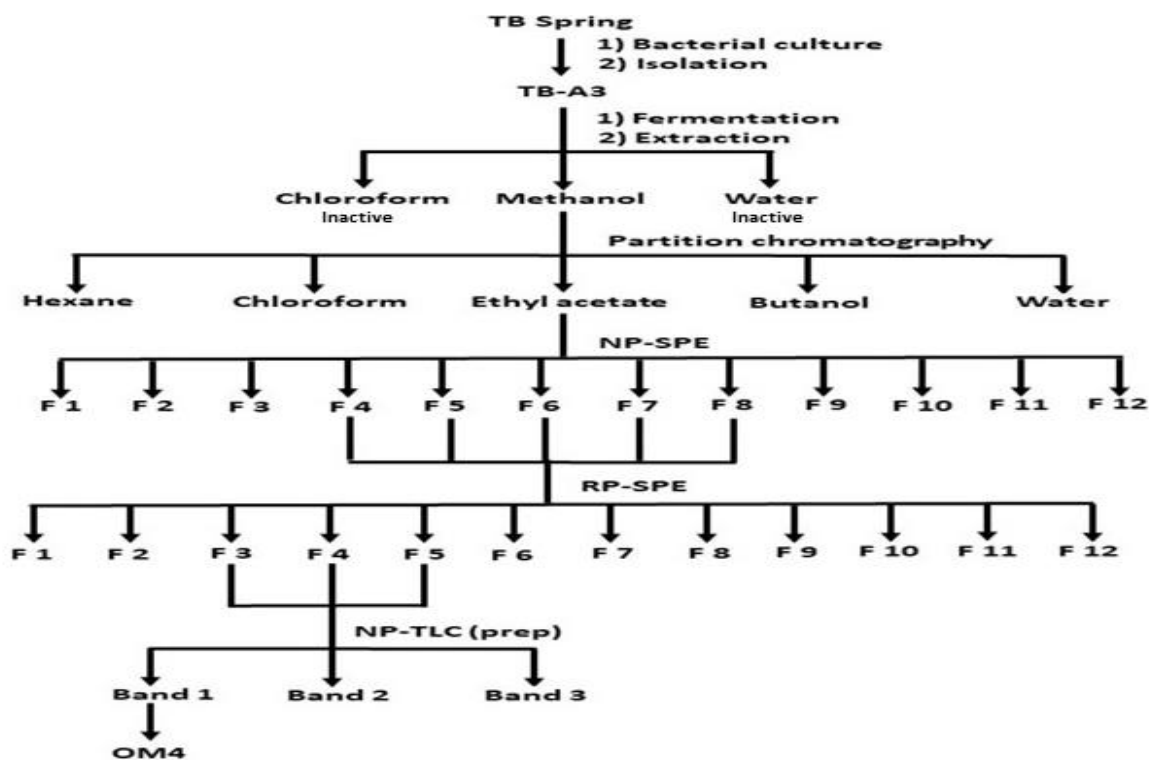
Figure 3.39: Scheme of isolation for compound OM4.

The molecular formula of **OM4** was determined as $C_5H_{10}O_2$ and the molecular weight of the compound was calculated as 102, which was deduced by the presence of an ion in the ESI-MS at *m/z* 101.0 [M-H]⁻ **(Figure 3.49)**.

The ¹H NMR spectrum **(Figure 3.41)** was very simple and exhibited only three shielded signals; two doublets at δ_H 2.16 (H$_2$-2) for methylene hydrogens and δ_H 0.91 (H$_3$-4/H$_3$-5) for 6 methyl hydrogens, and one multiplet at δ_H 1.99 (H-3) for a methine hydrogen. The hydrogens H$_3$-4 and H$_3$-5 were one peak because they were in the same chemical environment.
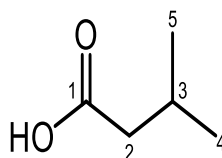
Figure 3.40: The structure of compound OM4.

The ¹³C NMR spectrum **(Figure 3.42)** revealed four carbon signals in total. The DEPT-135 **(Figure 3.43)** showed one methylene carbon at δ_C 43.1 (C-2) and one quaternary carbon at δ_C 179.4 (C-1), attributable to the carbonyl carbon of a carboxylic acid. The remaining carbons were allocated for one methine carbon at δ_C 25.4 (C-3) and two methyl carbons at δ_C 22.3 (C-4 and C-5). The two carbons of the methyl groups at positions 4 and 5 were shown as one peak at δ_C 22.3.

In the HMBC spectrum **(Figures 3.46** and **47)**, the position of the carbonyl at C-1 was confirmed by a ²*J* correlation with the hydrogens H$_2$-2 and a ³*J* correlation with the hydrogen H-3. In addition, the position of H-3 was confirmed by a ²*J* correlations with the hydrogens H$_2$-2, H$_3$-4 and H$_3$-5. The HMBC spectrum showed that there was a ³*J* correlation between H$_2$-2 and both H$_3$-4 and H$_3$-5.

Further confirmation on the structure of the compound was obtained using FT-IR spectroscopy **(Appendix 2)**. The FT-IR spectrum was taken by dissolving the compound in chloroform and gave a broad band between approximately 3500 cm^{-1} and 2500 cm^{-1}, which is indicative of the presence of a carboxylic group (O-H stretching). There were also a band for O-H bending at 1410 cm^{-1}, alkyl C-H stretching at 2876 cm^{-1} and 2961 cm^{-1} and C=O streching at 1703 cm^{-1}.

Compound **OM4** was therefore identified as 3-methylbutanoic acid, which is commonly known as isovaleric acid. The ^{1}H and ^{13}C NMR data of this compound are in close agreement with published literature for isovaleric acid (Bal *et al*., 2008). Furthermore, compound **OM4** was compared to a ^{1}H NMR spectrum of a reference sample of isovaleric acid and it was identical **(Figure 3.50)**.

Table 3.12: ^{1}H (500 MHz), ^{13}C NMR (125 MHz) and HMBC spectroscopic data of OM4 recorded in CDCl$_3$

Position	^{1}H	^{13}C	HMBC		^{13}C((CD$_3$)$_2$SO) Bal *et al*., 2008
			^2J	^3J	
C-1	--	179.4	--	--	181.5
C-2	2.16 (d)	43.1	C-1, C-3	C-4,C-5	45.9
C-3	1.99 (m)	25.4	C-2, C-4, C-5	C-1	28.0
C-4	0.91 (d)	22.3	C-3	C-2, C-5	24.2
C-5	0.91 (d)	22.3	C-3	C-2, C-4	24.2

Several studies have been described the isolation of isovaleric acid from microbes. As an example, it has been isolated from *Peptostreptococcus anaerobius* (Guerrant *et al*., 1982), *Pseudoalteromonas haloplanktis* strain (Hayashida-Soiza *et al*., 2008) and *Megasphaera hexanoica* spp. *Nov* (Jeon *et al*., 2017). Furthermore, it has also been isolated from *Bacillus* spp. For example, it has identified from *B. amyloliquefaciens* (Chen *et al*., 2017), *B. subtilis* (Hong *et al*., 2017), *B. velezensis* (Calvo *et al*., 2020), *B. subtilis*, *B. cereus* and *Paenibacillus polymyxa* (Mumtaz *et al*., 2019). In addition, isovaleric acid has also been found in some plants such as *Ferula vesceritensis* (Labed-Zouad *et al*.,

2015), *Achillea millefolium* (Mărghitaş *et al.*, 2011; Bobis *et al.*, 2015) and *Lantana camara* (Shriniwas and Subhash, 2017).
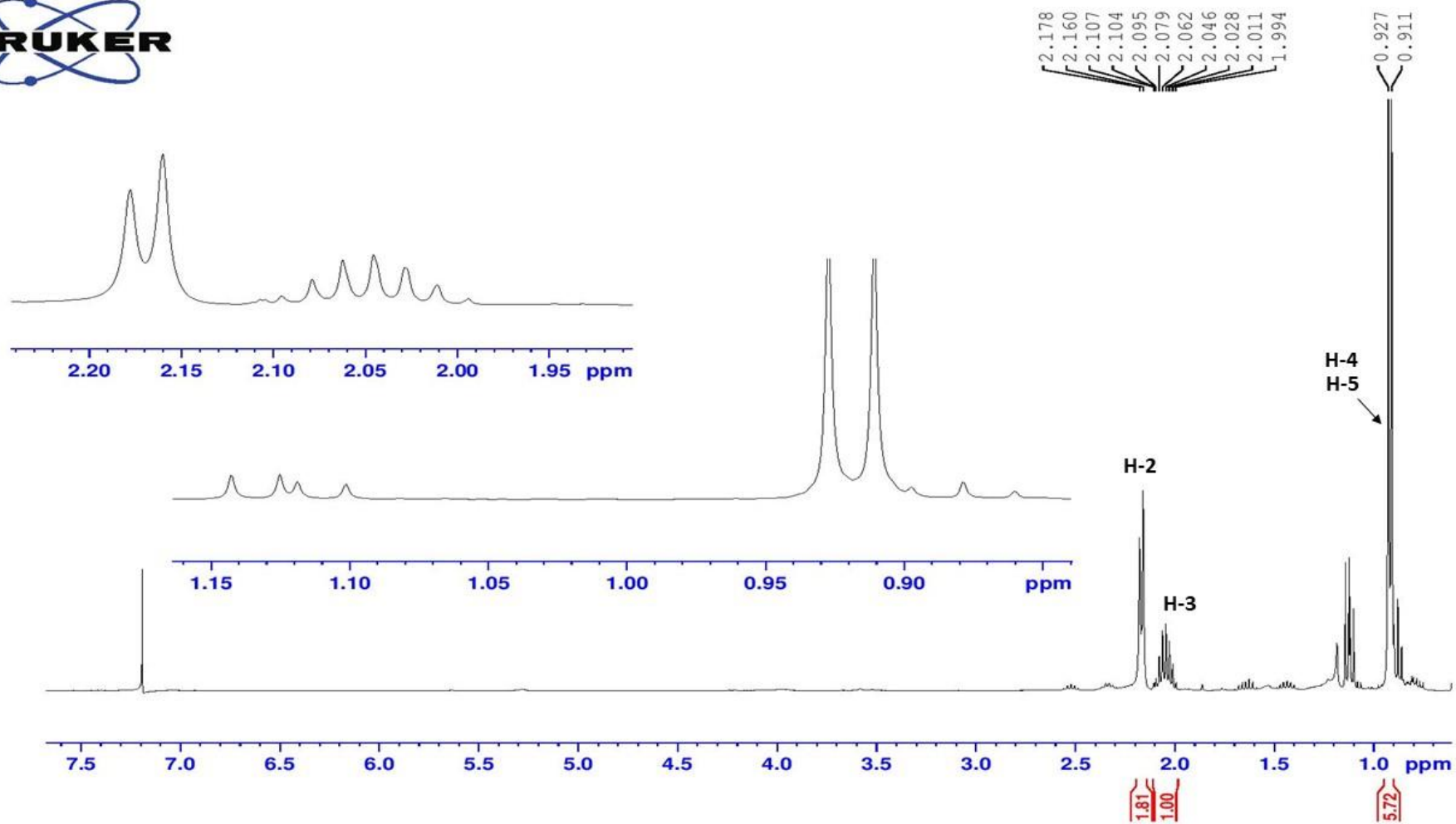
Figure 3.41: ^{1}H NMR spectrum of compound OM4 recorded in CDCl$_3$ (500 MHz).
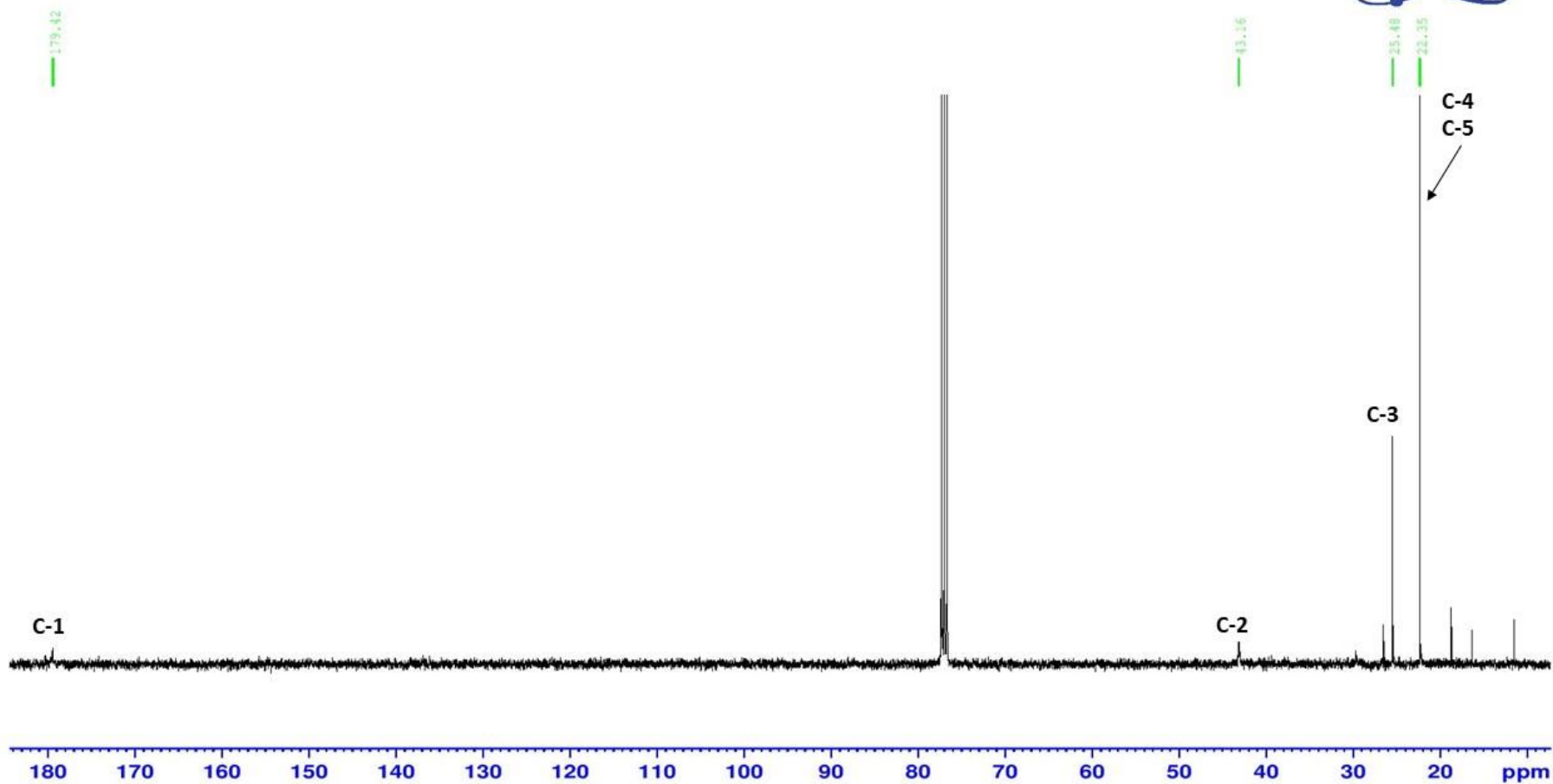
Figure 3.42: ^{13}C NMR spectrum of compound OM4 recorded in $CDCl_3$ (125 MHz).
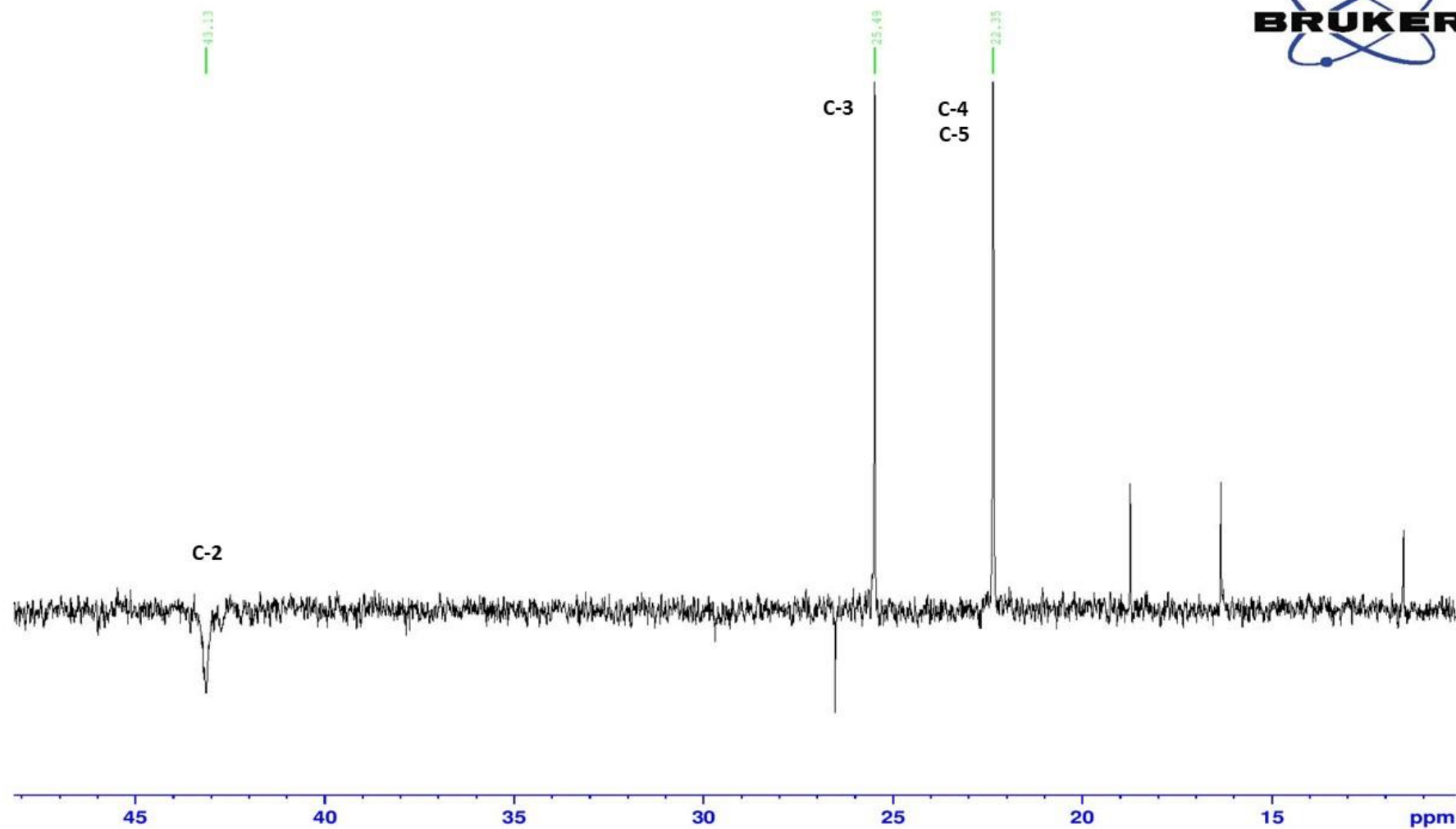
Figure 3.43: DEPT-135 spectrum of compound OM4 recorded in CDCl₃ (125 MHz).
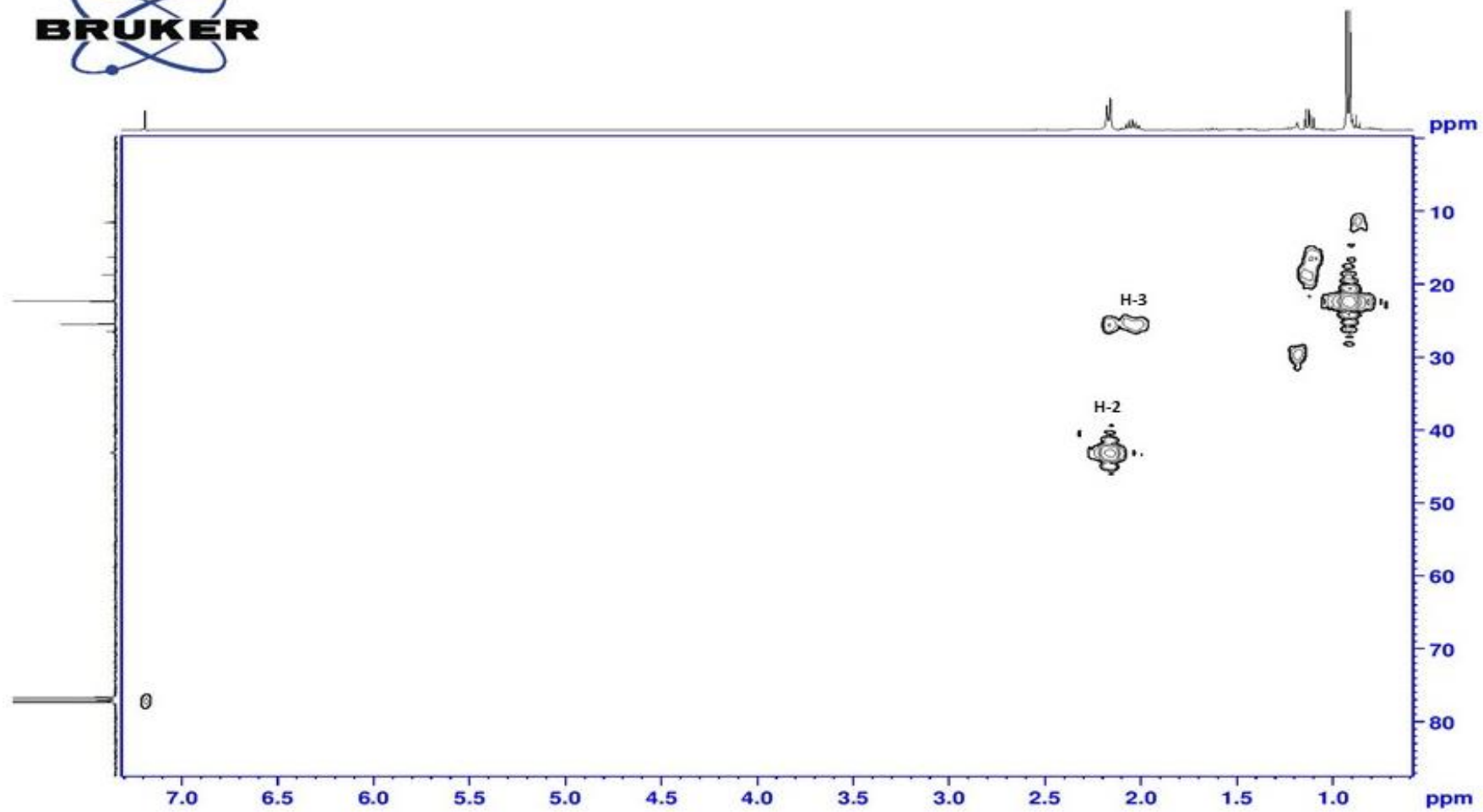
Figure 3.44: HMQC spectrum of compound OM4.
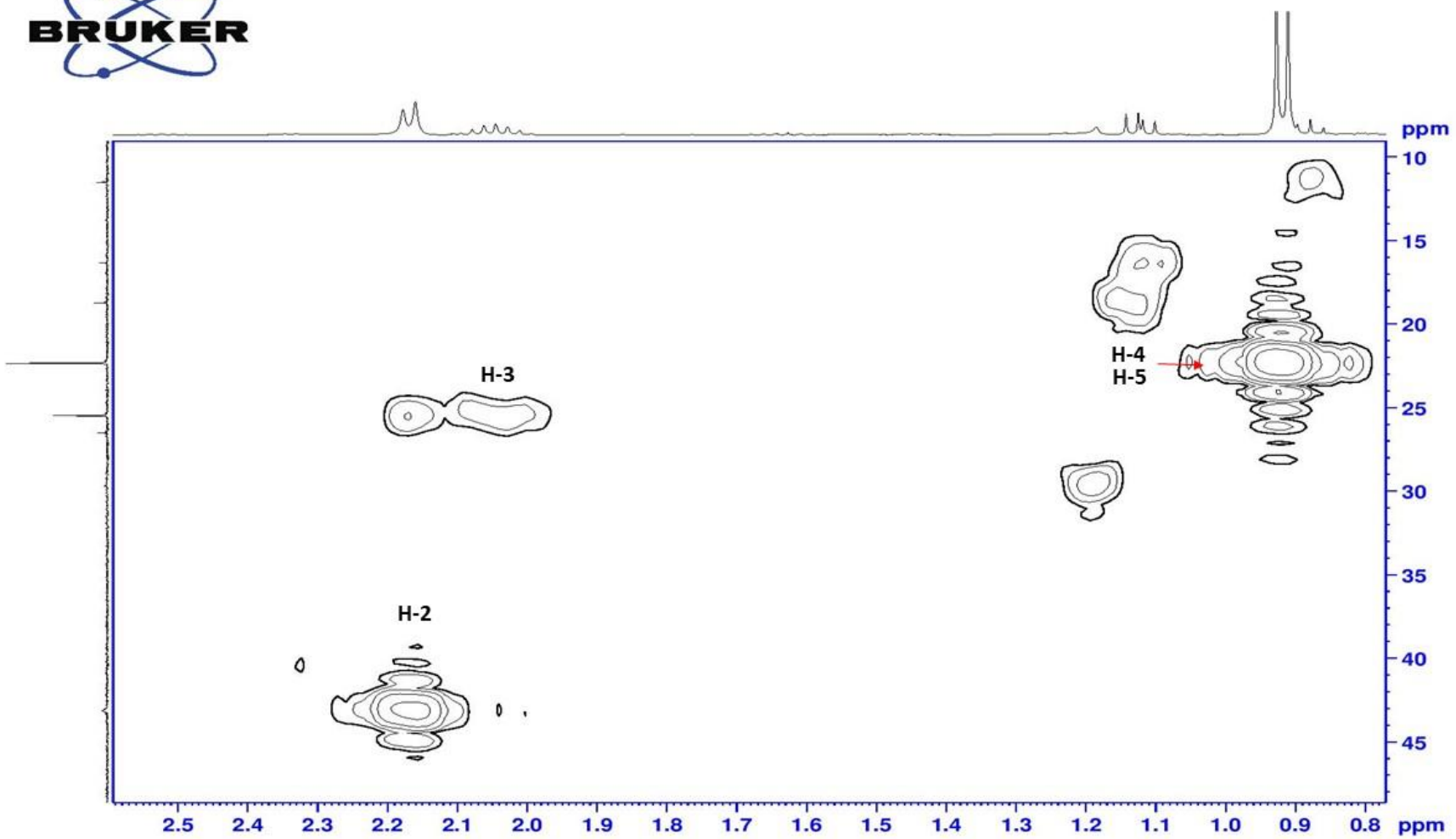
Figure 3.45: HMQC spectrum of compound OM4 (expanded).
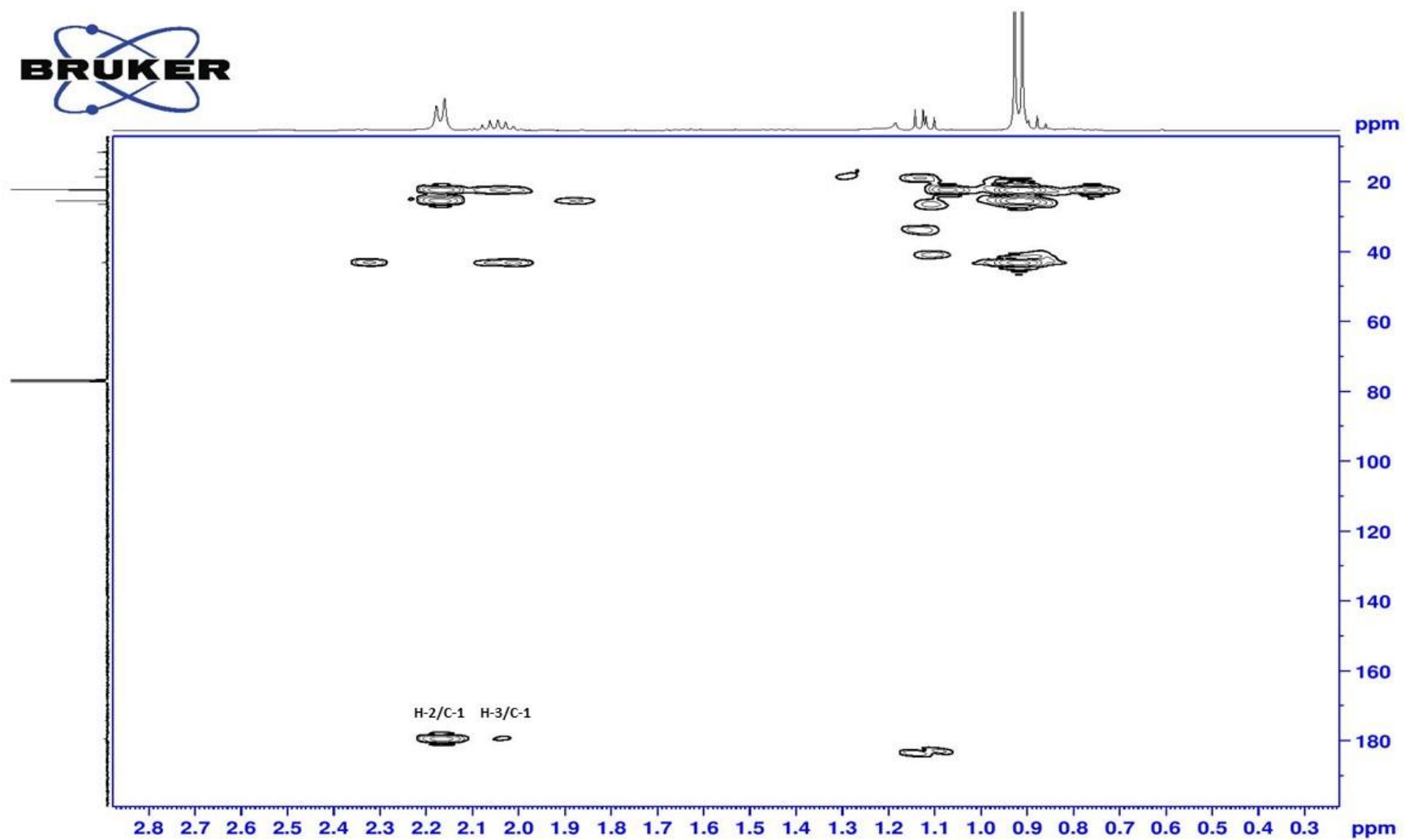
Figure 3.46: HMBC spectrum of compound OM4.
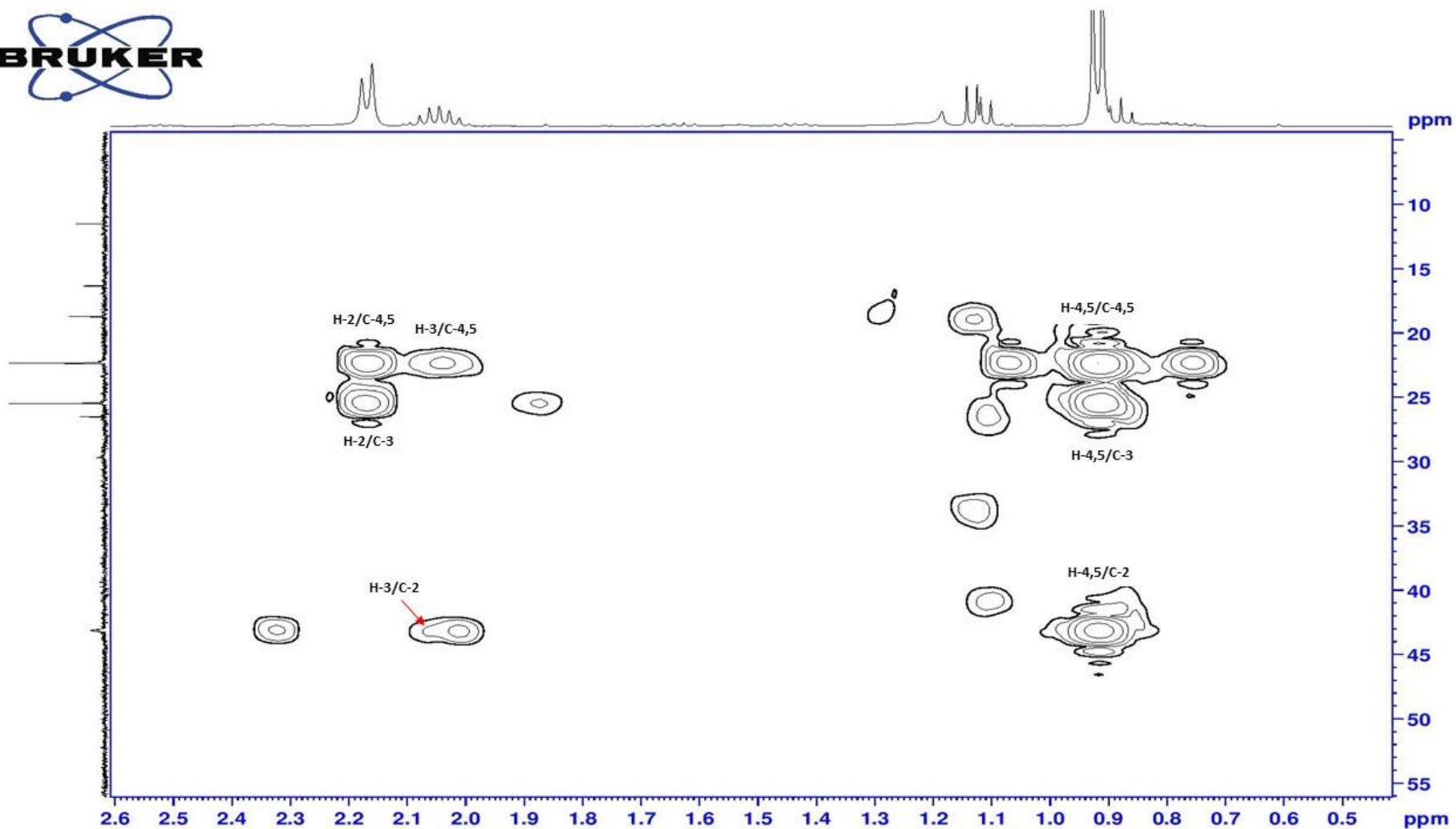
Figure 3.47: HMBC spectrum of compound OM4 (expanded).
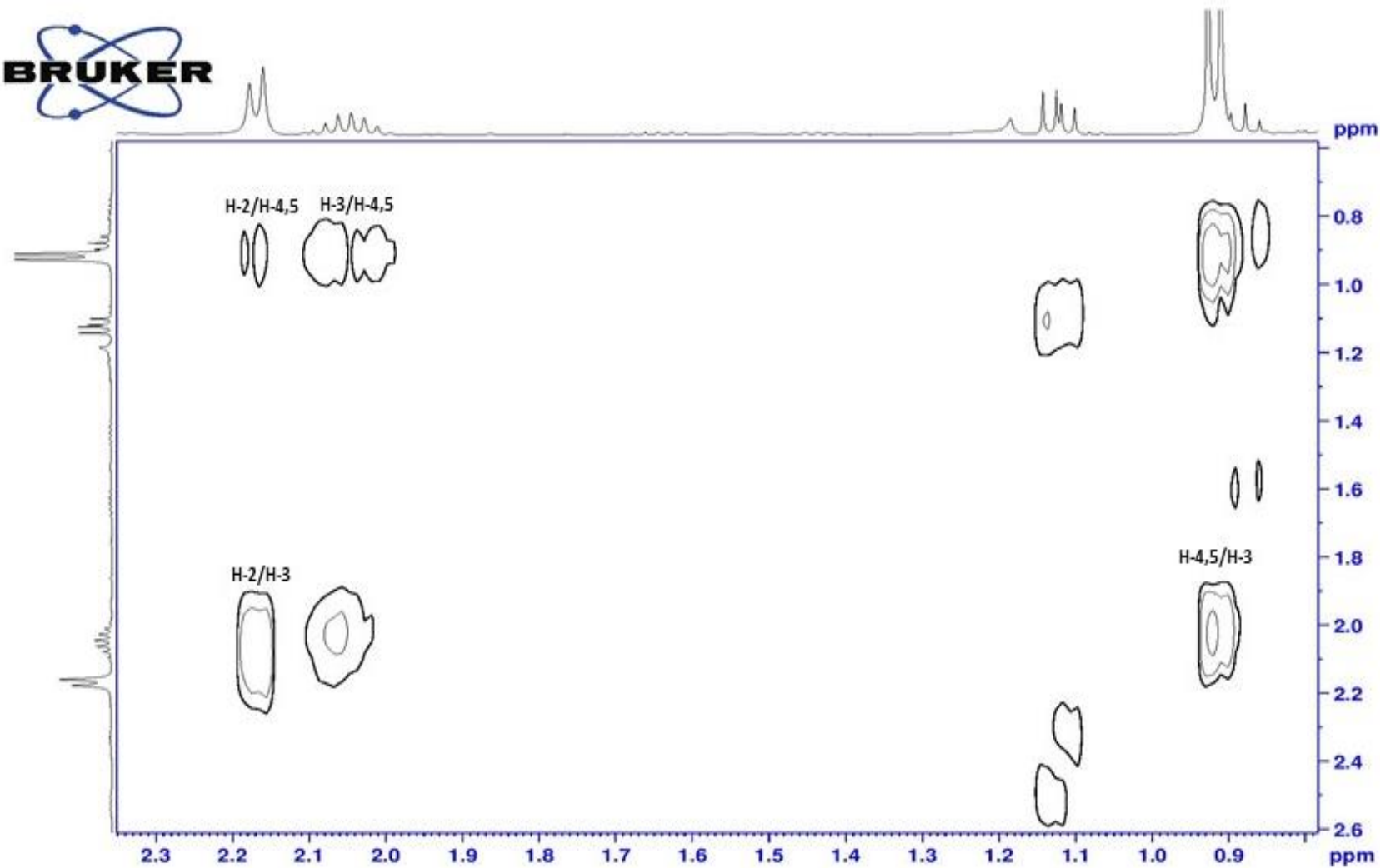
Figure 3.48: COSY spectrum of compound OM4.
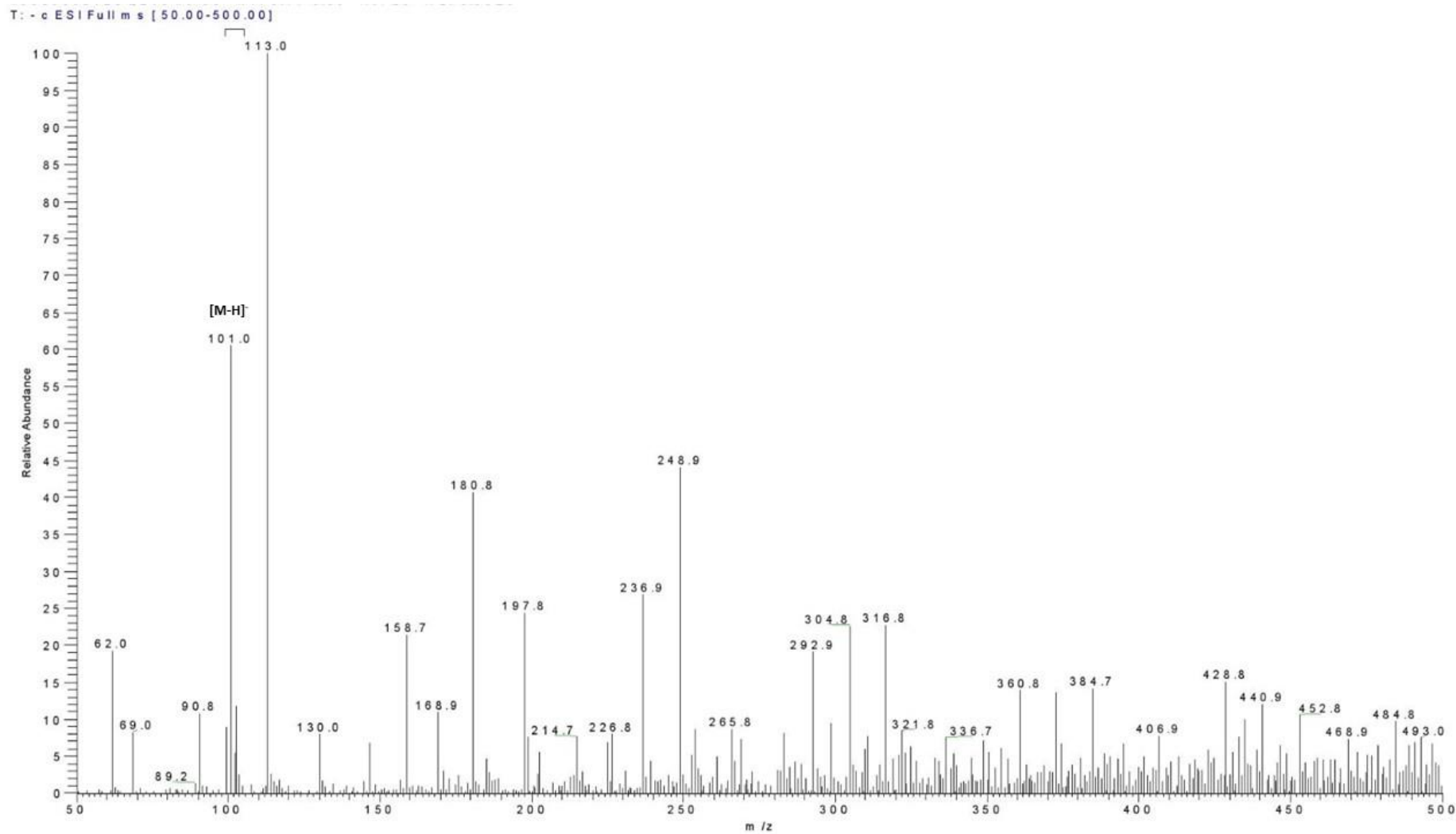
Figure 3.49: ESI-MS spectrum of compound OM4 showing peak ion at *m/z* 101.0.
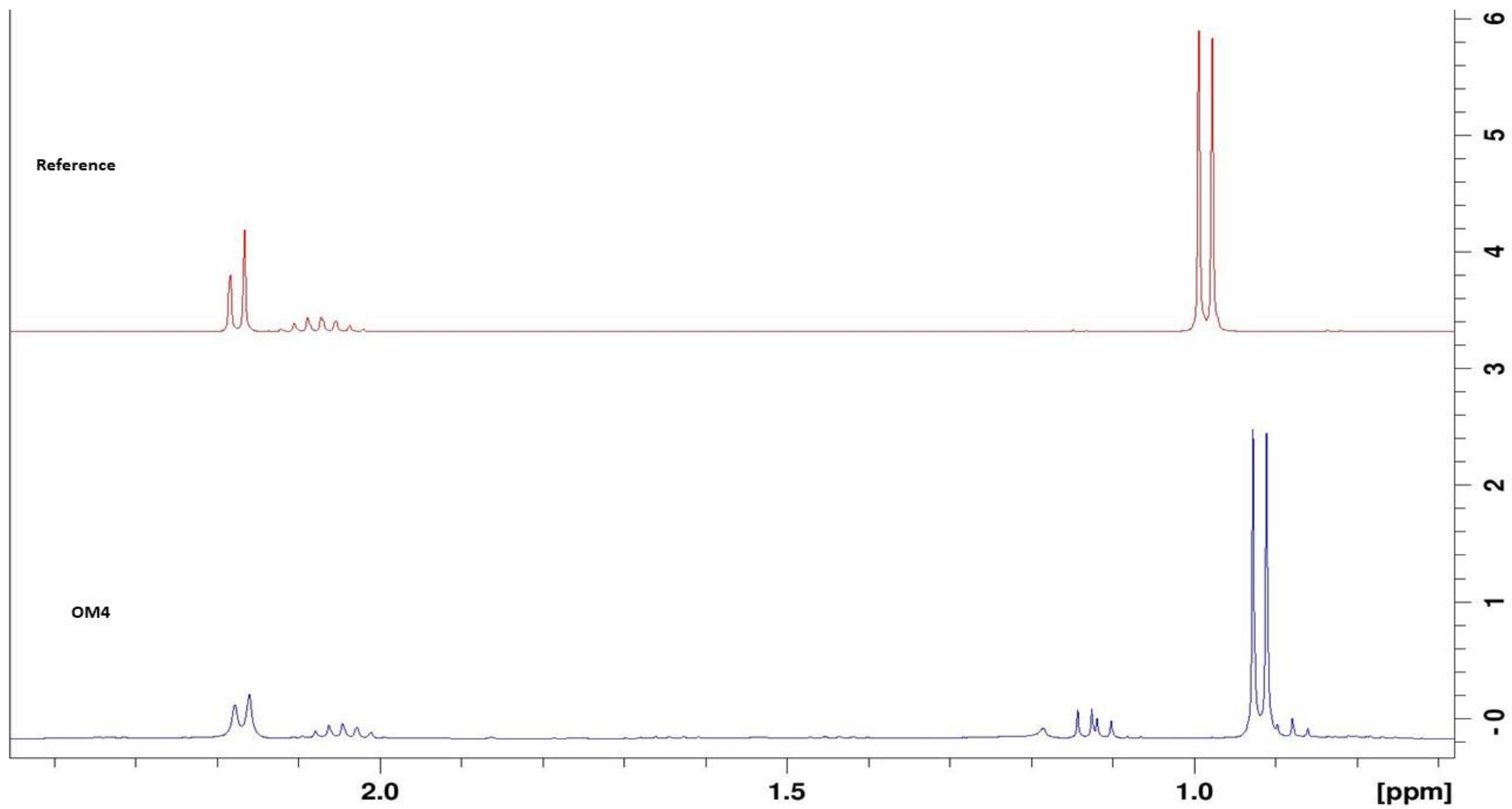
Figure 3.50: Comparison of ¹H NMR spectra of the reference (isovaleric acid) and compound OM4.

3.2.5   Compound OM5

Compound **OM5** was obtained as a colourless oil from the **AH-E1** isolate from the **AH** spring. The methanol extract (1.4 g) of the **AH-E1** isolate was subjected to partitioning chromatography in order to isolate the active compound **(Figure 3.51)**. Five sub-extracts were collected and the chloroform sub-extract (367 mg / 26.21% of the extract) was active. The chloroform sub-extract was, therefore, subjected to NP-SPE to identify the active fractions. Fractions (7, 8 and 9) showed antibacterial activity. These fractions (127.3 mg / 34.68% of the sub-extract) were bulked and then applied to prep-NP-TLC with the solvent system of *n*-hexane: ethyl acetate: methanol (80:20:1). A second TLC band with an R_f of 0.45 was purified by applying again on prep-NP-TLC with the same solvent system. A third TLC band with an R_f of 0.53 exhibited activity in the *S. aureus* overlay assay. This band gave compound **OM5** (39.8 mg / 31.26% of the fraction), and its structure is shown in **(Figure 3.52).**
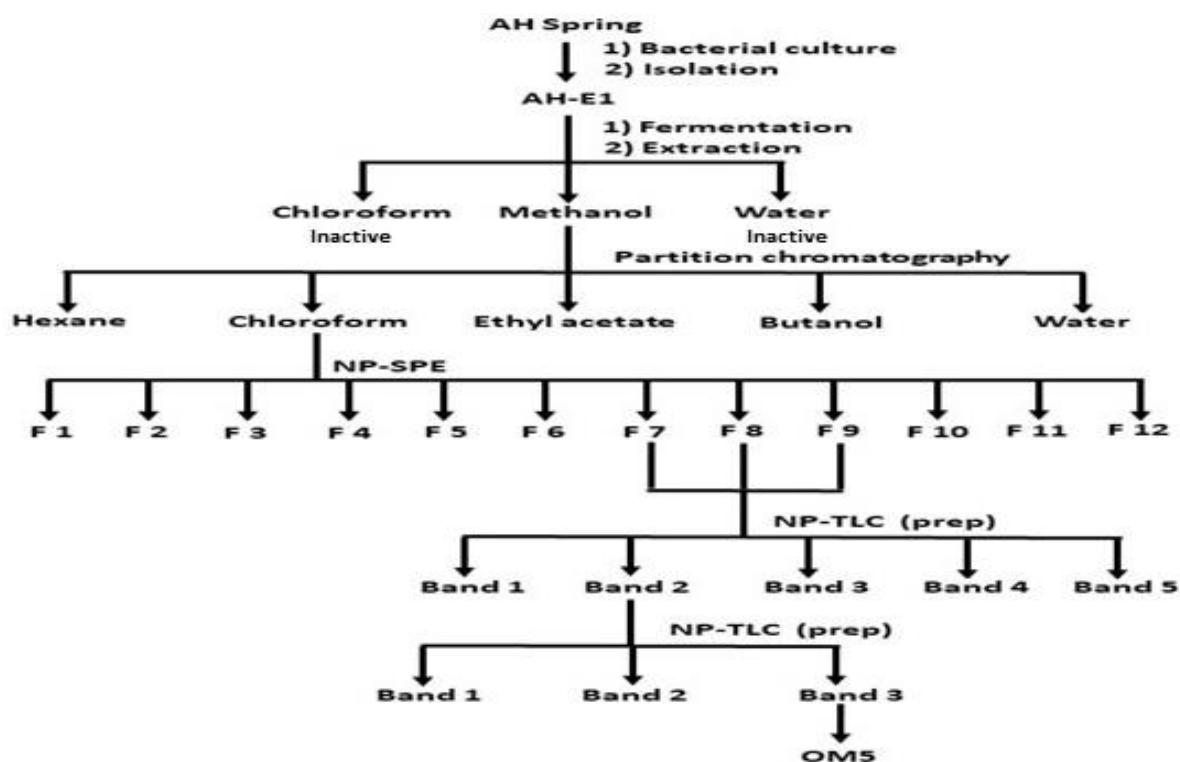
Figure 3.51: Scheme of isolation for compound OM5.

The molecular formula of **OM5** was determined as $C_{11}H_{14}O_3$ and the molecular weight of the compound was calculated as 194, which was supported by an ion in the ESI-MS at *m/z* 195.10 [M+H]$^+$ **(Figure 3.60)**.

The ^{1}H NMR spectrum **(Figure 3.53)** exhibited two deshielded signals; two doublets at δ_H 6.91 (*J*= 8.9 Hz, H-3/H-5) and δ_H 8.00 (*J*= 8.9 Hz, H-2/H-6). The hydrogens of H-2 and H-6 were observed as one peak as were those of H-3 and H-5 because they were in the same chemical environment. The resonances at δ_H 6.91 and δ_H 8.00 were roofed to each other and had coupling constants (*J*= 8.9 Hz), indicative of an *ortho* coupling to each other. This feature has been seen in **OM3** and is indicative of an AA'/BB' aromatic system resulting from an unsymmetrically 1,4-substituted aromatic ring. Furthermore, two slightly deshielded quartets (oxymethylene groups) were observed at δ_H 4.09 (H$_2$-12) and δ_H 4.34 (H$_2$-9). The downfield nature of these resonances supported that they were oxymethylene moieties. Additionally, two shielded triplets (methyl groups) were found at δ_H 1.39 (H$_3$-10) and δ_H 1.45 (H$_3$-13).
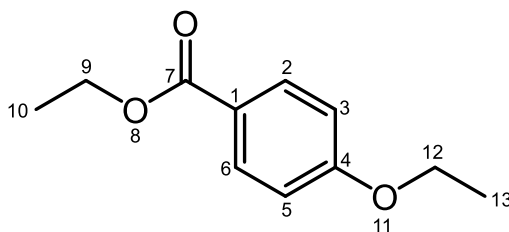
Figure 3.52: The structure of compound OM5.

The ^{13}C NMR spectrum **(Figure 3.54)** displayed 9 carbon signals. The DEPT-135 **(Figure 3.56)** supported the presence of two oxymethylene carbons at δ_C 60.6 (C-9) and δ_C 63.6 (C-12) as well as three quaternary carbons at δ_C 122.7 (C-1), δ_C 162.6 (C-4) and δ_C 166.4 (C-7). Furthermore, the DEPT-90 spectrum **(Figure 3.55)** showed two aromatic

methine signals at δ_C 131.5 and δ_C 113.9. The two aromatic carbons at 2 and 6 positions of the compound were viewed as one peak at δ_C 131.5. In the same way, carbons at 3 and 5 positions appeared as one peak at δ_C 113.9. The remaining carbons were assigned for two methyl carbons at δ_C 14.4 (C-10) and δ_C 14.7 (C-13).

In the HMBC spectrum **(Figure 3.58)**, the placement of the carbonyl at C-7 was confirmed by a ^3J correlation with the hydrogens H-2/6 and H_2-9. Moreover, the position of C-12 was supported by a ^3J correlation with C-4 and a ^2J correlation with the methyl hydrogens H_3-13.

Further confirmation on the structure of the compound was obtained using FT-IR spectroscopy **(Appendix 2)**. There were bands for alkyl C-H stretching at 2936 cm^{-1} and 2981 cm^{-1}, C=O stretching at 1707 cm^{-1}, C-O stretching at 1165 cm^{-1}, 1247 cm^{-1} and 1273 cm^{-1} and C=C stretching at 1606 cm^{-1} were present for the IR spectrum of the compound.

Compound **OM5** was therefore identified as ethyl-4-ethoxybenzoate. The ^{1}H and ^{13}C NMR data of this compound are in good agreement with published literature for ethyl-4-ethoxybenzoate (Siddique, 2019). Furthermore, compound **OM5** was compared to a ^{1}H NMR spectrum of a reference of ethyl-4-ethoxybenzoate and was identical **(Figure 3.61)**.

Ethyl-4-ethoxybenzoate has been isolated from both plants and microbes. For microbes, it has been isolated from the hexane extract of *B. licheniformis* (Sharma *et al.*, 2010) as well as from *Paenibacillus* spp. (Tahir *et al.*, 2019). From a plant source, it was isolated from an ethanol extract of the leaf of *Rhamnus prinoides* (Campbell *et al.*, 2019) and an ethanol extract of both *Sauropus thorelii* and *Sauropus androgynous* (Sawasdee *et al.*, 2019).

Table 3.13: ^{1}H (500 MHz), ^{13}C NMR (125 MHz) and HMBC spectroscopic data of OM5 recorded in CDCl$_3$.

Position	^{1}H	^{13}C	HMBC		^{13}C (CDCl$_3$) Siddique, 2019
			^2J	^3J	
C-1	--	122.7	--	--	122.8
C-2	8.00 (d)	131.5	--	C-4, C-6, C-7	131.6
C-3	6.91 (d)	113.9	C-4	C-1, C-5	114.2
C-4	--	162.6	--	--	162.8
C-5	6.91 (d)	113.9	C-4	C-1, C-3	114.2
C-6	8.00 (d)	131.5	--	C-2, C-4 C-7	131.6
C-7	--	166.4	--	--	166.5
O	--	--	--	--	--
C-9	4.34 (q)	60.6	C-10	C-7	60.9
C-10	1.39 (t)	14.4	C-9	--	14.5
O	--	--	--	--	--
C-12	4.09 (q)	63.6	C-13	C-4	63.7
C-13	1.45 (t)	14.7	C-12	--	14.9
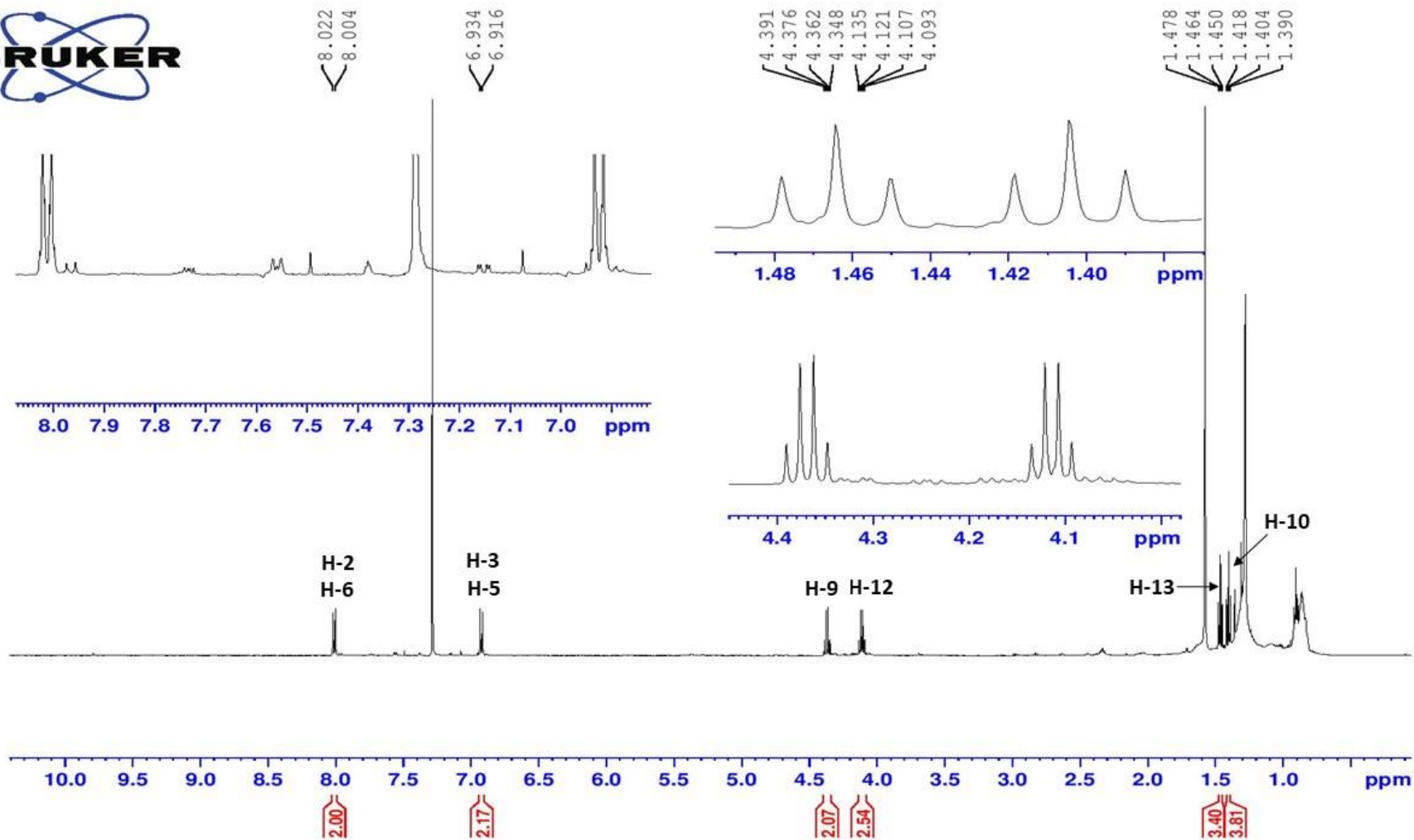
Figure 3.53: ^{1}H NMR spectrum of compound OM5 recorded in CDCl$_3$ (500 MHz).
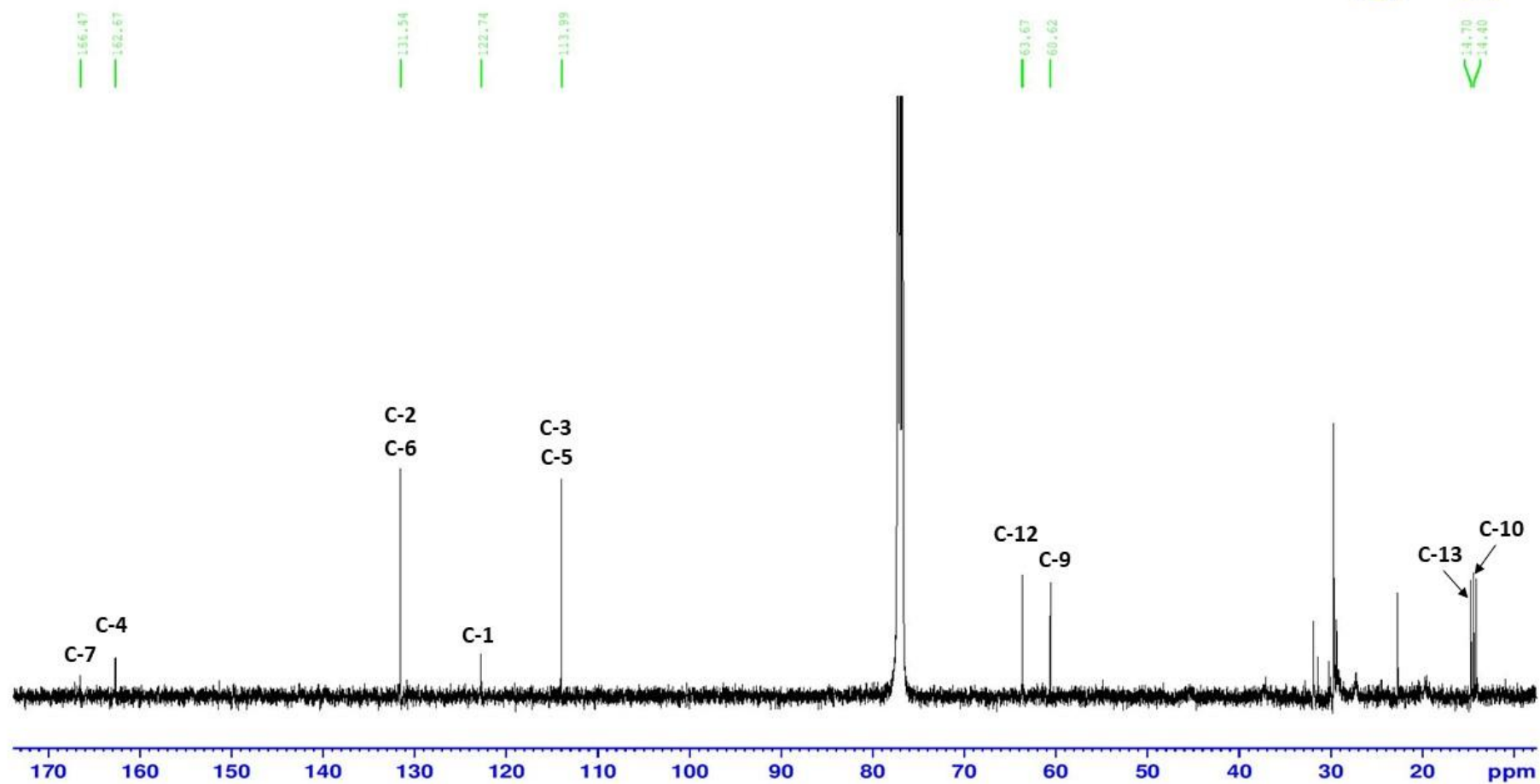
Figure 3.54: ^{13}C NMR spectrum of compound OM5 recorded in CDCl$_3$ (125 MHz).
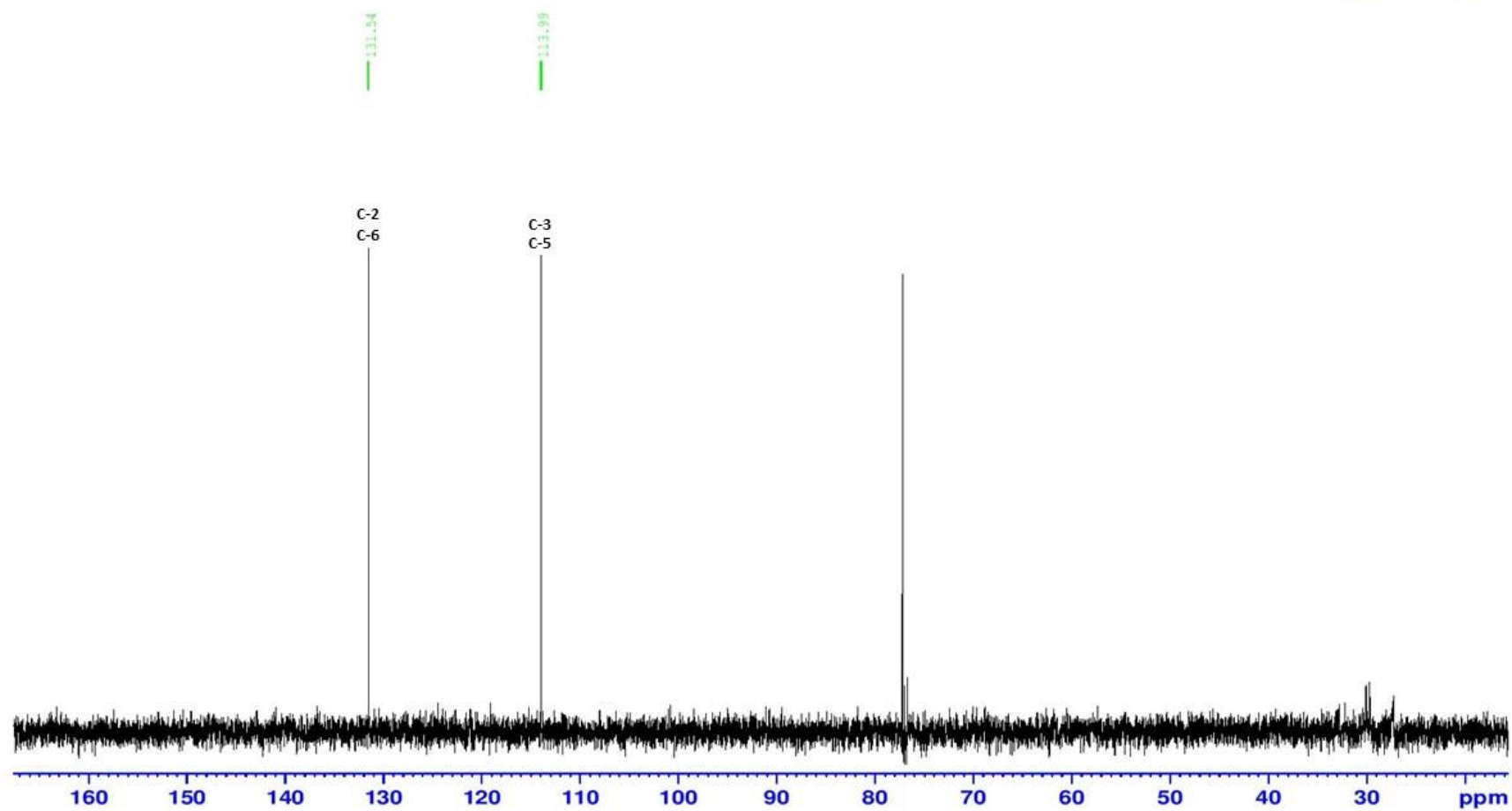
Figure 3.55: DEPT-90 spectrum of compound OM5 recorded in CDCl₃ (125 MHz).
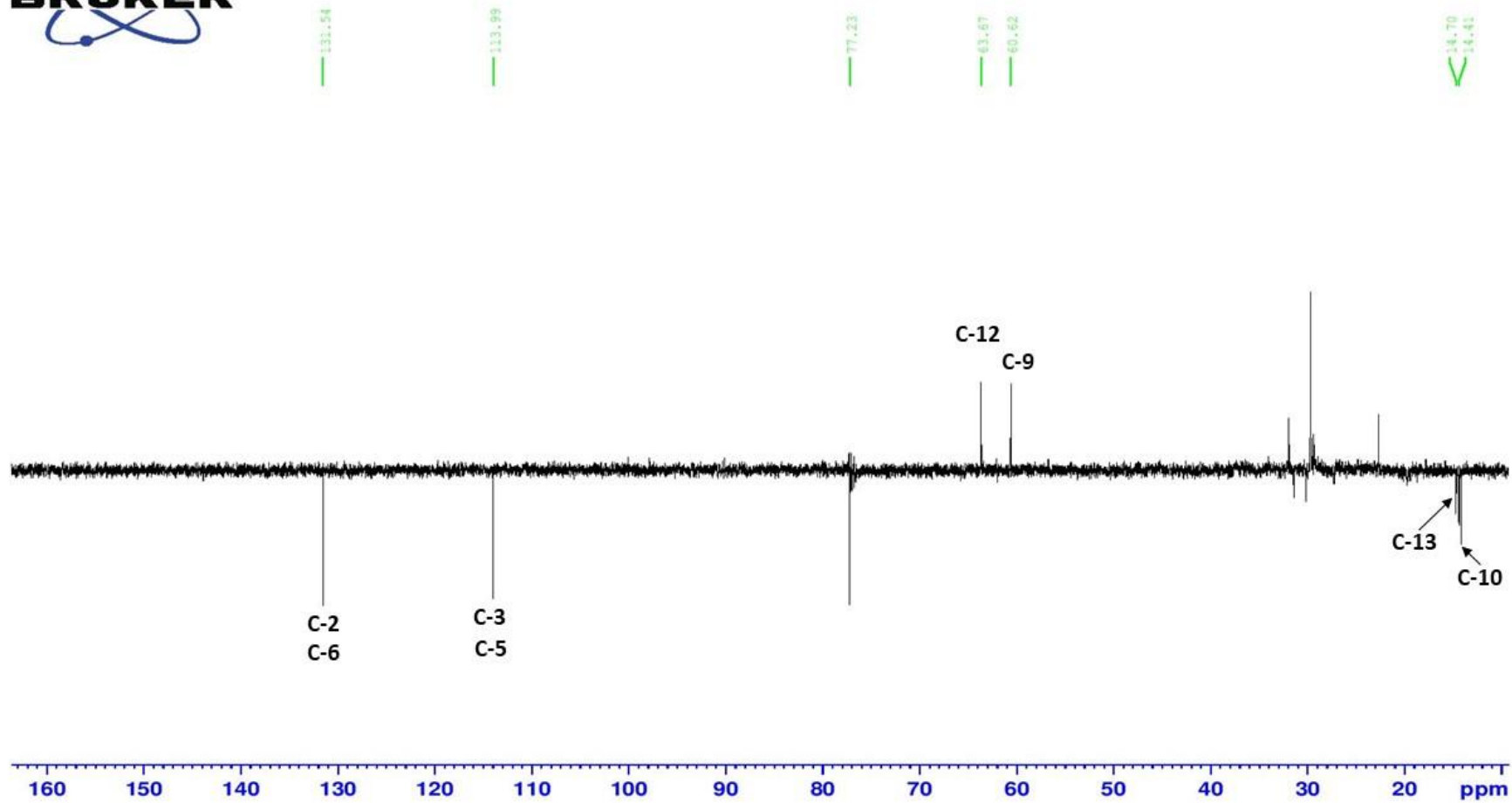
Figure 3.56: DEPT-135 spectrum of compound OM5 recorded in CDCl$_3$ (125 MHz).
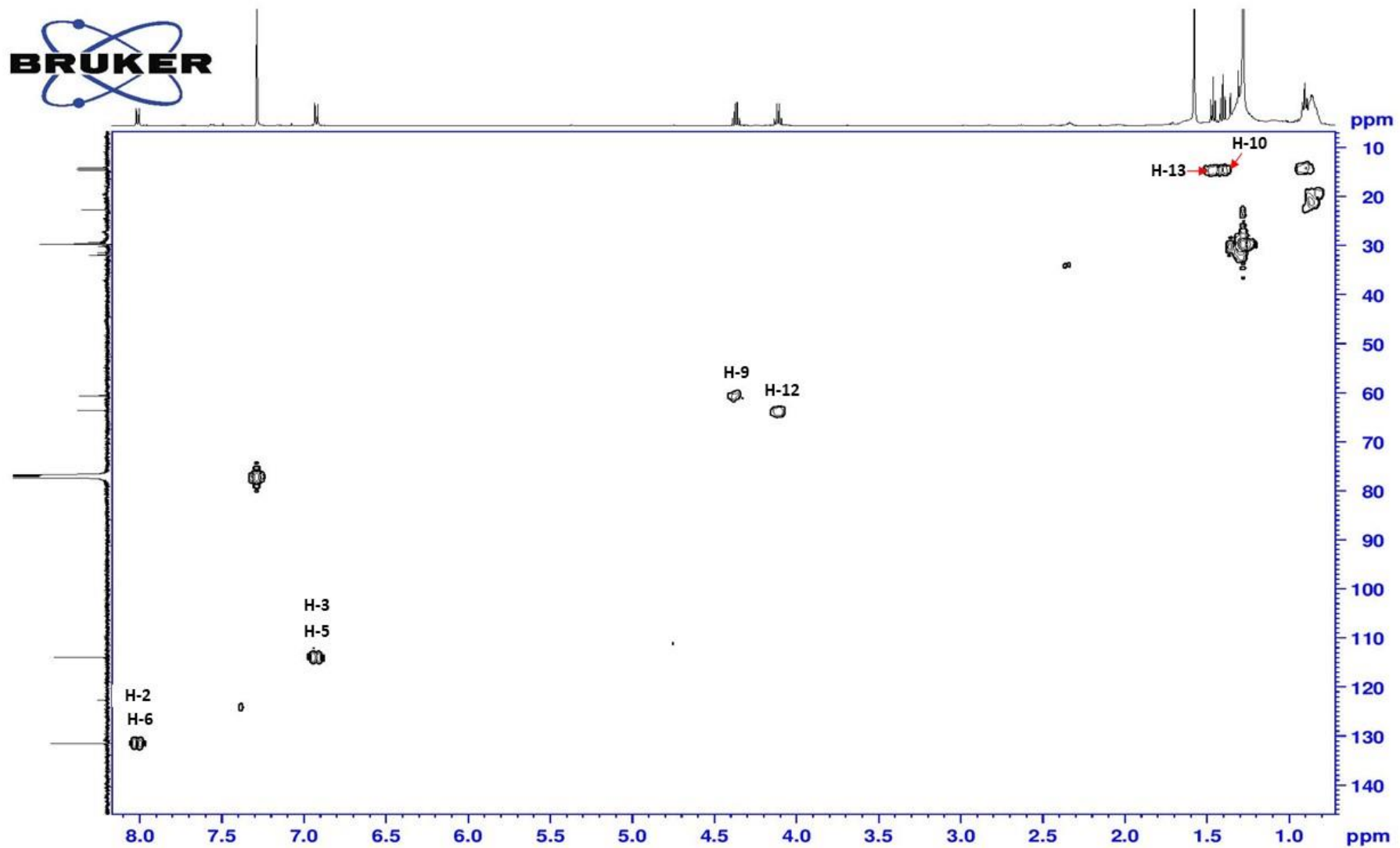
Figure 3.57: HMQC spectrum of compound OM5.
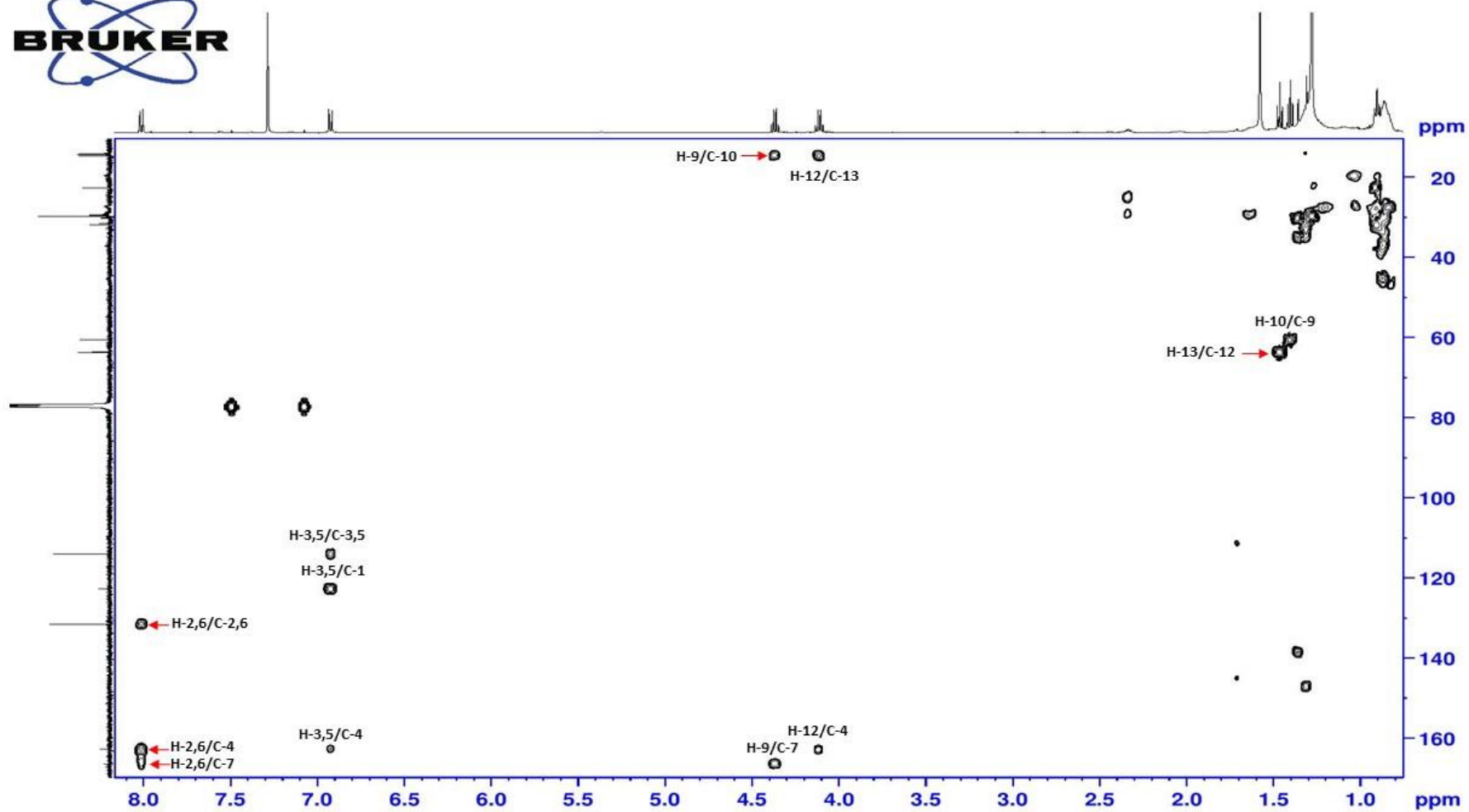
Figure 3.58: HMBC spectrum of compound OM5.
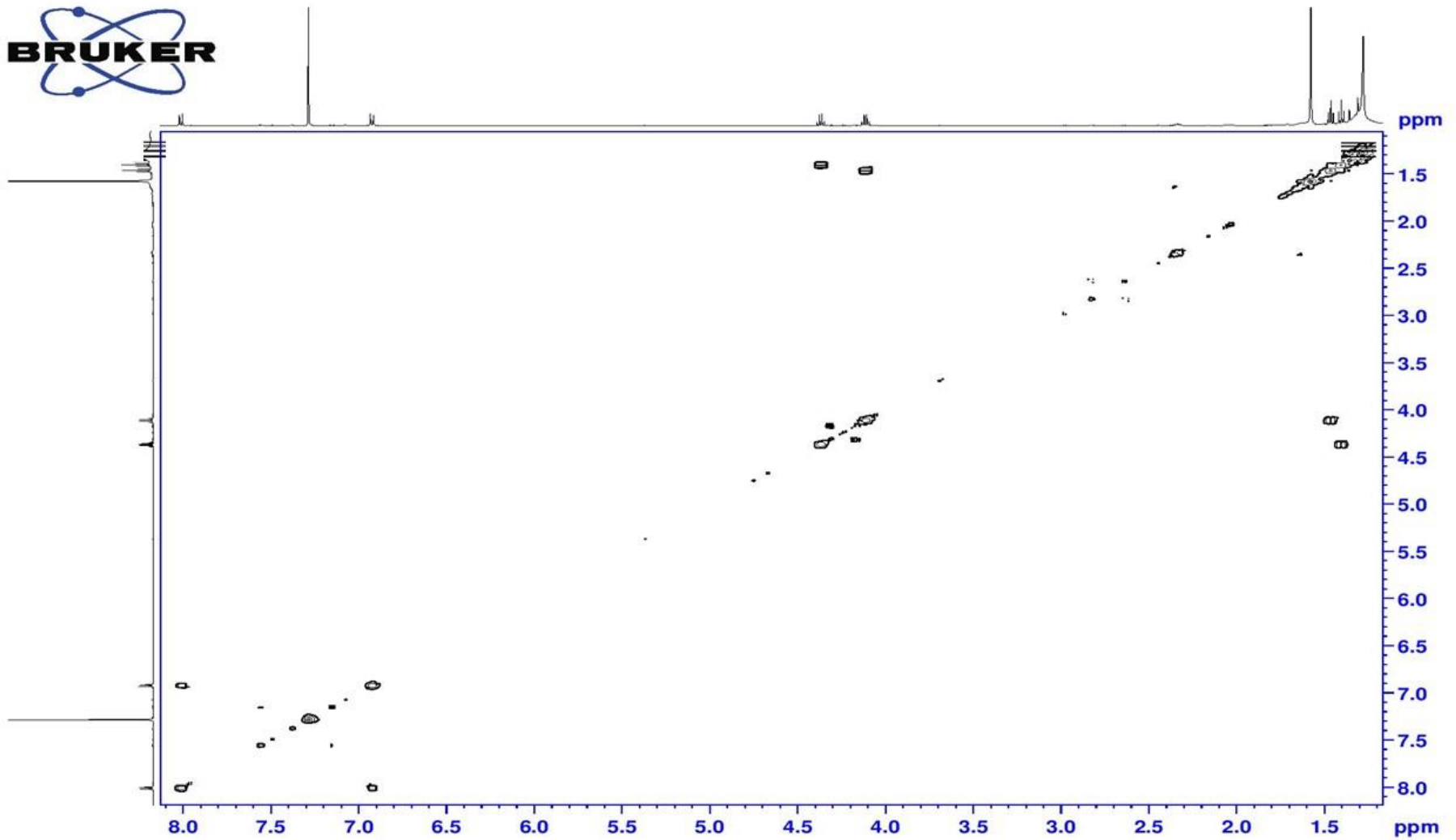
Figure 3.59: COSY spectrum of compound OM5.
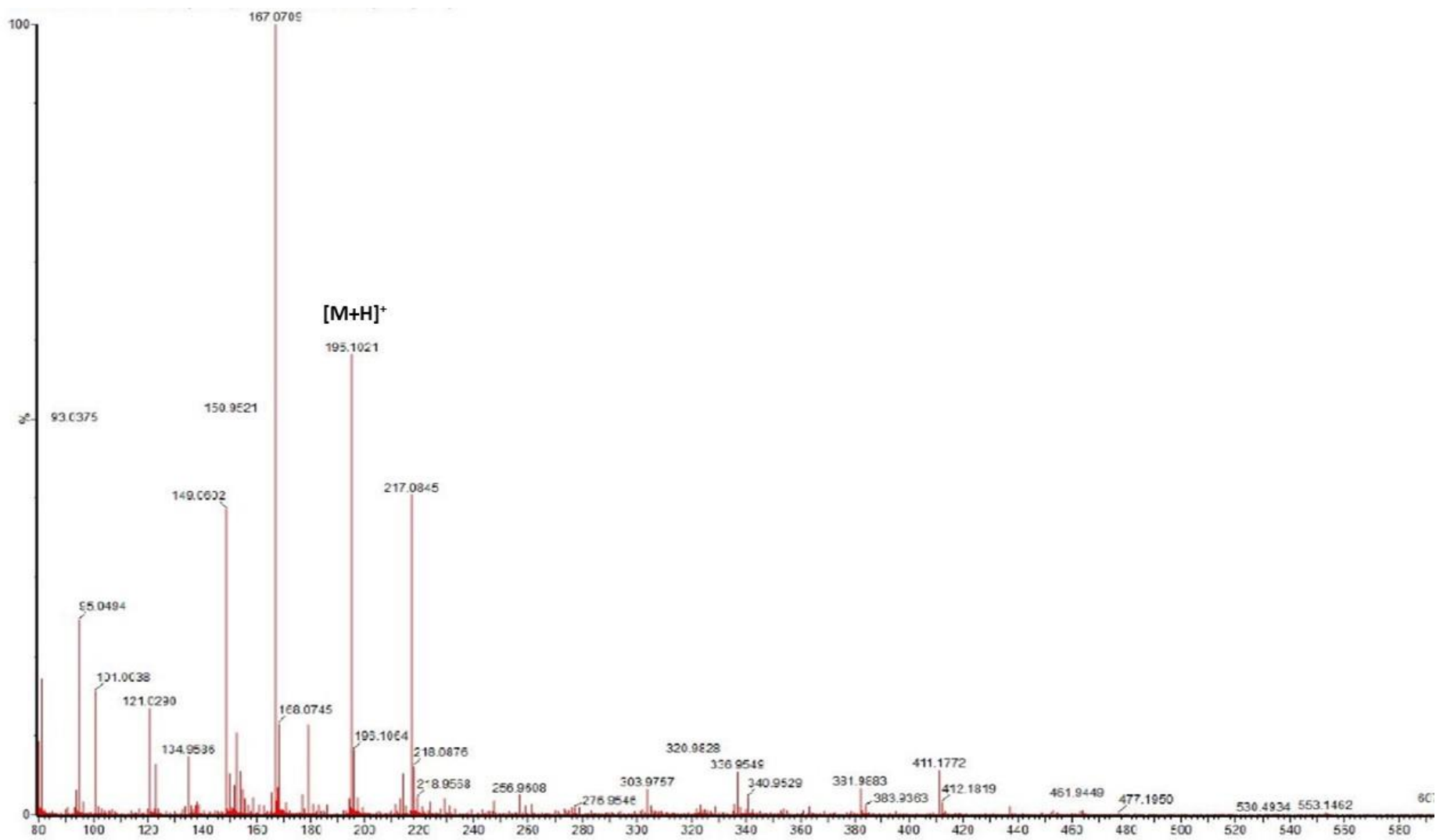
Figure 3.60: ESI-MS spectrum of compound OM5 showing peak ion at *m/z* 195.1021.
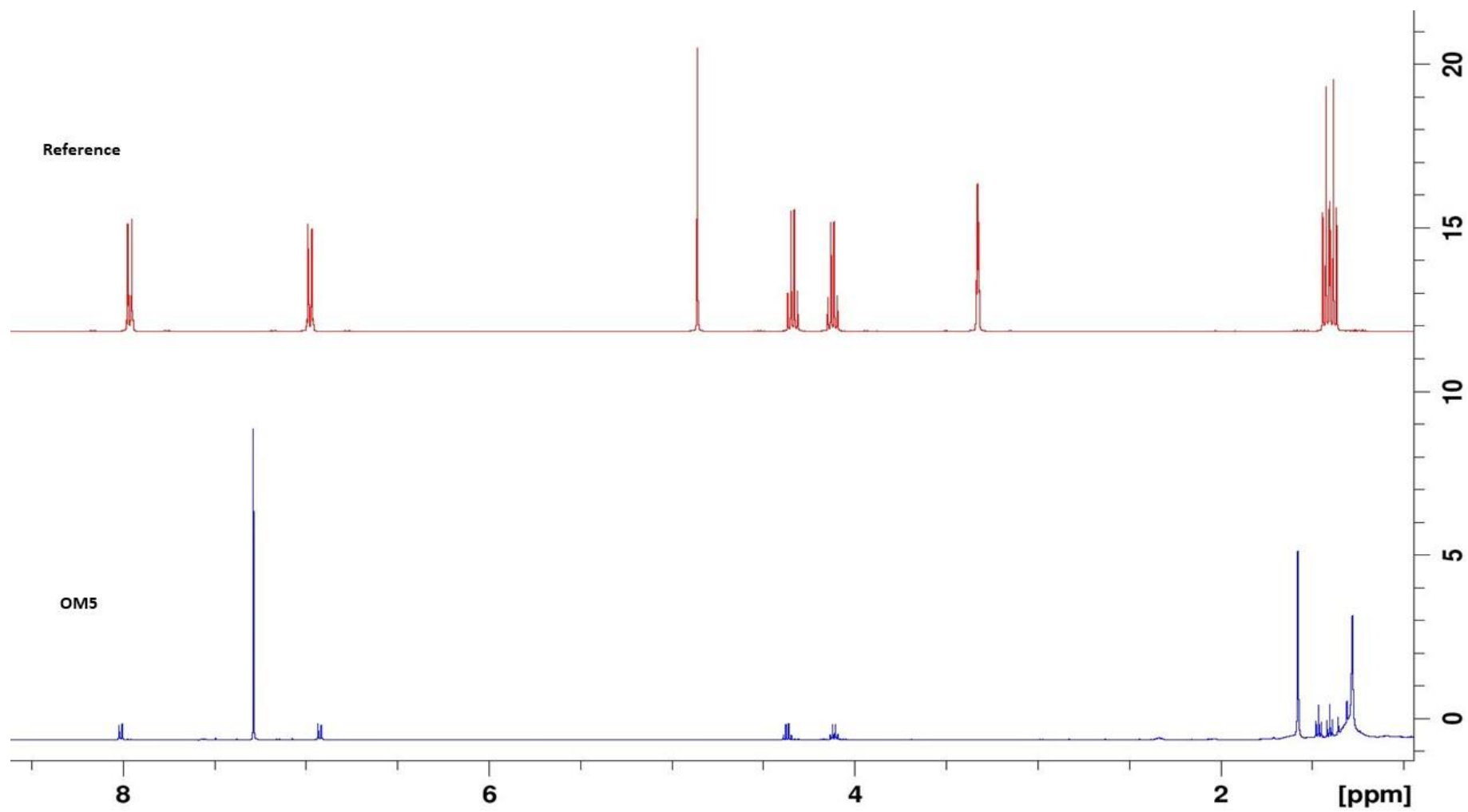
Figure 3.61: Comparison of ^{1}H NMR spectra of the reference (ethyl-4-ethoxybenzoate) and compound OM5.

3.2.6 Compound OM6

Compound **OM6** was obtained as a white powder from the **AR-G2** isolate from the **AR** spring. The methanol extract (1.1 g) of the **AR-G2** isolate was subjected to partitioning chromatography in order to isolate the active compounds **(Figure 3.62)**. Five sub-extracts were collected and the chloroform sub-extract (241.8 mg / 21.98% of the extract) was active based on the disc diffusion assay. The choroform sub-extract was then subjected to NP-SPE to identify the active fractions. Fractions (5, 6 and 7) showed antimicrobial activity. These fractions (102.8 mg / 42.51% of the sub-extract) were collected together and fractionated again using NP-SPE into 12 fractions. Fractions (8 and 9) (54.9 mg / 53.40% of the fraction) were active and applied to prep-NP-TLC with a solvent system of *n*-hexane: ethyl acetate: methanol (80:20:1). A fifth TLC band with an R_f of 0.85 demonstrated activity in the *S. aureus* overlay assay **(Figure 3.63)**. This band gave compound **OM6** (14.62 mg / 26.63% of the fraction), and its structure is shown in **(Figure 3.64)**.
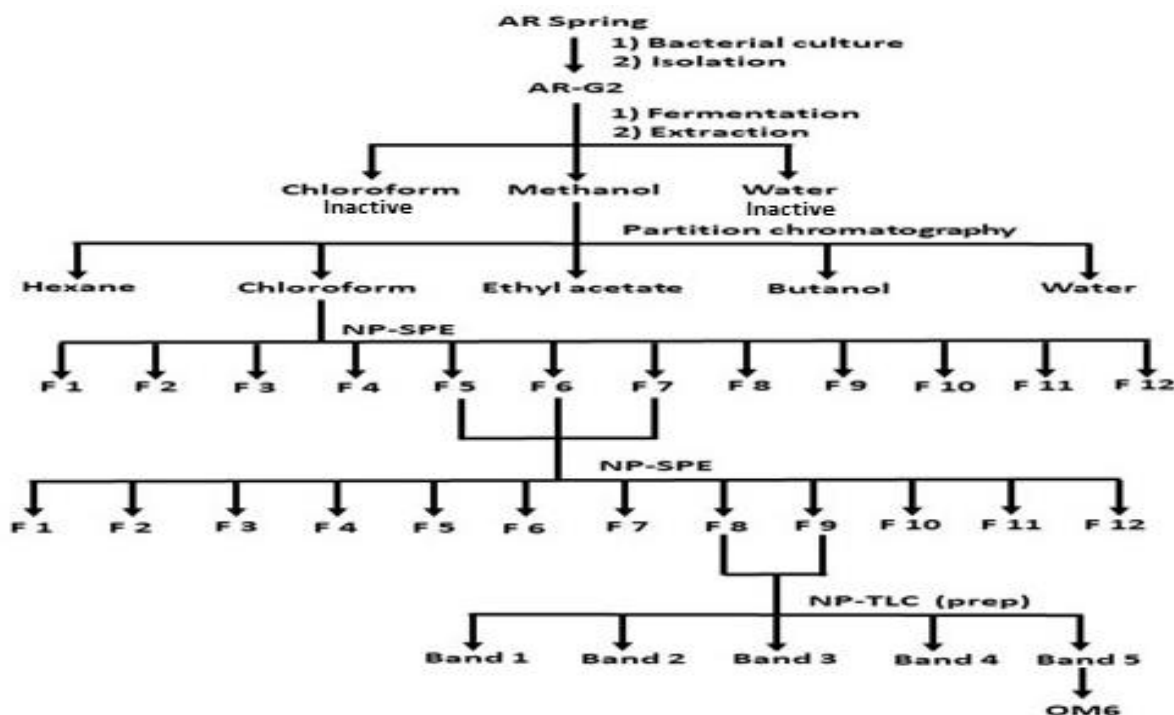
Figure 3.62: Scheme of isolation for compound OM6.

The molecular formula of **OM6** was determined as $C_9H_6O_4$ and the molecular weight of the compound was 178.1413, which was supported by an ion in the HRMS at *m/z* 177.0188 attributed to [M-H]- **(Figure 3.75)**.

The ^1H NMR spectrum **(Figure 3.65)** displayed three olefinic signals; two doublets at δ_H 5.62 (*J*= 7.5 Hz, H-2) and δ_H 7.40 (*J*= 7.5 Hz, H-3), and one singlet at δ_H 7.24 (H-5). Moreover, there was a shielded singlet methyl group at δ_H 1.87 (H_3-9), the hydrogens of which were coupled to an olefinic carbon at C-6 in the HMBC spectrum **(Figure 3.71)**.
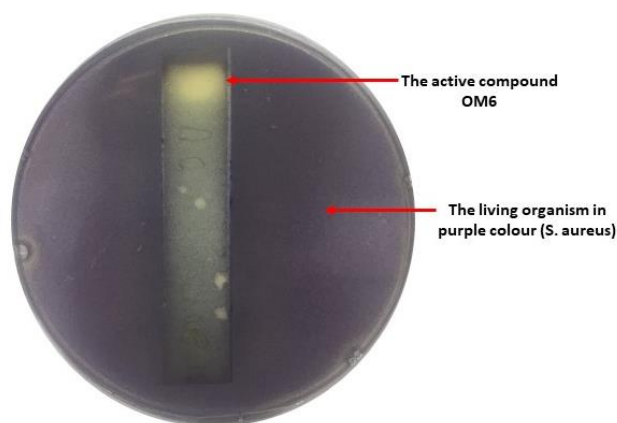
Figure 3.63: Bioautography assay of OM6.

The ^{13}C NMR spectrum **(Figure 3.66)** showed 7 carbon signals in total, from which three were quaternary carbons, based on their absence in the DEPT-135 spectrum, when compared with the broadband decoupled carbon spectrum **(Figure 3.68)**. These quaternary carbons were C-1 (167.6), C-6 (110.4) and C-7 (167.4). Moreover, there were still two quaternary carbons at δ_C 153.5 (C-8) and δ_C 105.1 (C-4), that did not appear in the broadband decoupled ^{13}C NMR spectrum; however, they existed as they were correlated to in the HMBC spectrum. The DEPT-90 **(Figure 3.67)** showed three methine

carbons at δc 139.1 (C-5), δc 143.5 (C-3) and δc 101.7 (C-2). Furthermore, the methyl carbon was observed at δc 12.1 allocated to C-9.

In the HMBC spectrum **(Figures 3.70, 71, 72,** and **73)**, the placement of the carbonyl group at C-1 was supported by a ^2J correlation with the hydrogen H-2 and a ^3J correlation with the hydrogen H-3. The carbonyl group at C-7 was confirmed by a ^3J correlation with the hydrogens of H-5 and H_3-9. Moreover, the position of the methyl group at C-9 was confirmed by a ^3J correlation with the hydrogen H-5. The placement of C-8 was revealed by a ^3J correlation with the hydrogens of H-3 and H-5. In addition, there was a ^3J correlation between H-2 and C-4.
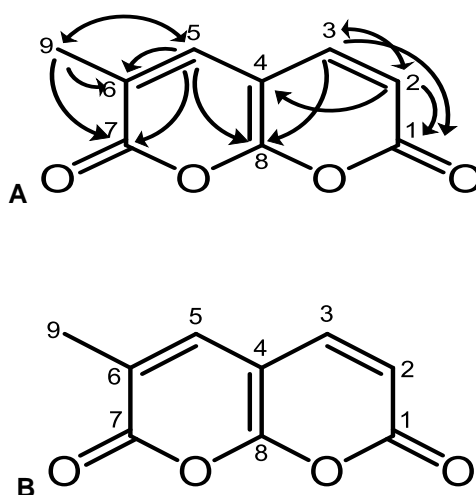
Figure 3.64: The structure of compound OM6.
A: HMBC correlations, **B:OM6** structure.

Further confirmation on the structure of the compound was obtained using FT-IR spectroscopy **(Figure 3.76)**. The FT-IR spectrum was taken by dissolving the compound in methanol and gave a C=O stretching band at 1649 cm^{-1}. There were also bands for alkyl C-H stretching at 2834 cm^{-1} and 2946 cm^{-1}, C-H bending at 1449 cm^{-1} and C-O stretching at 1018 cm^{-1} present in the compound.

In addition, the outcomes of the LC-MS analysis showed that there was a peak at RT: 0.91 with A% = 77.7; this peak gave an ion peak at *m/z* 178.85 [M+H]+ **(Figure 3.77)**, which confirmed the proposed structure.

According to the above data and a SciFinder search, **OM6** was a new compound and identified as 3-methyl-*2H,7H*-pyrano[*2,3-b*]pyran-2,7-dione. The compound has been given the trivial name Wagarin A, to reflect its spring source and the fact that it is a coumarin-like-structure.

Table 3.14: 1H (500 MHz), 13C NMR (125 MHz) and HMBC spectroscopic data of OM6 recorded in CD3OD.

Position	¹H	¹³C	HMBC	
			²*J*	³*J*
C-1	--	167.6	--	--
C-2	5.62 (d)	101.7	C-1, C-3	C-4
C-3	7.40 (d)	143.5	C-1, C-2	C-8
C-4	--	105.1	--	--
C-5	7.24 (s)	139.1	C-6	C-7, C-8, C-9
C-6	--	110.4	--	--
C-7	--	167.4	--	--
C-8	--	153.5	--	--
C-9	1.87 (s)	12.1	C-6	C-5, C-7
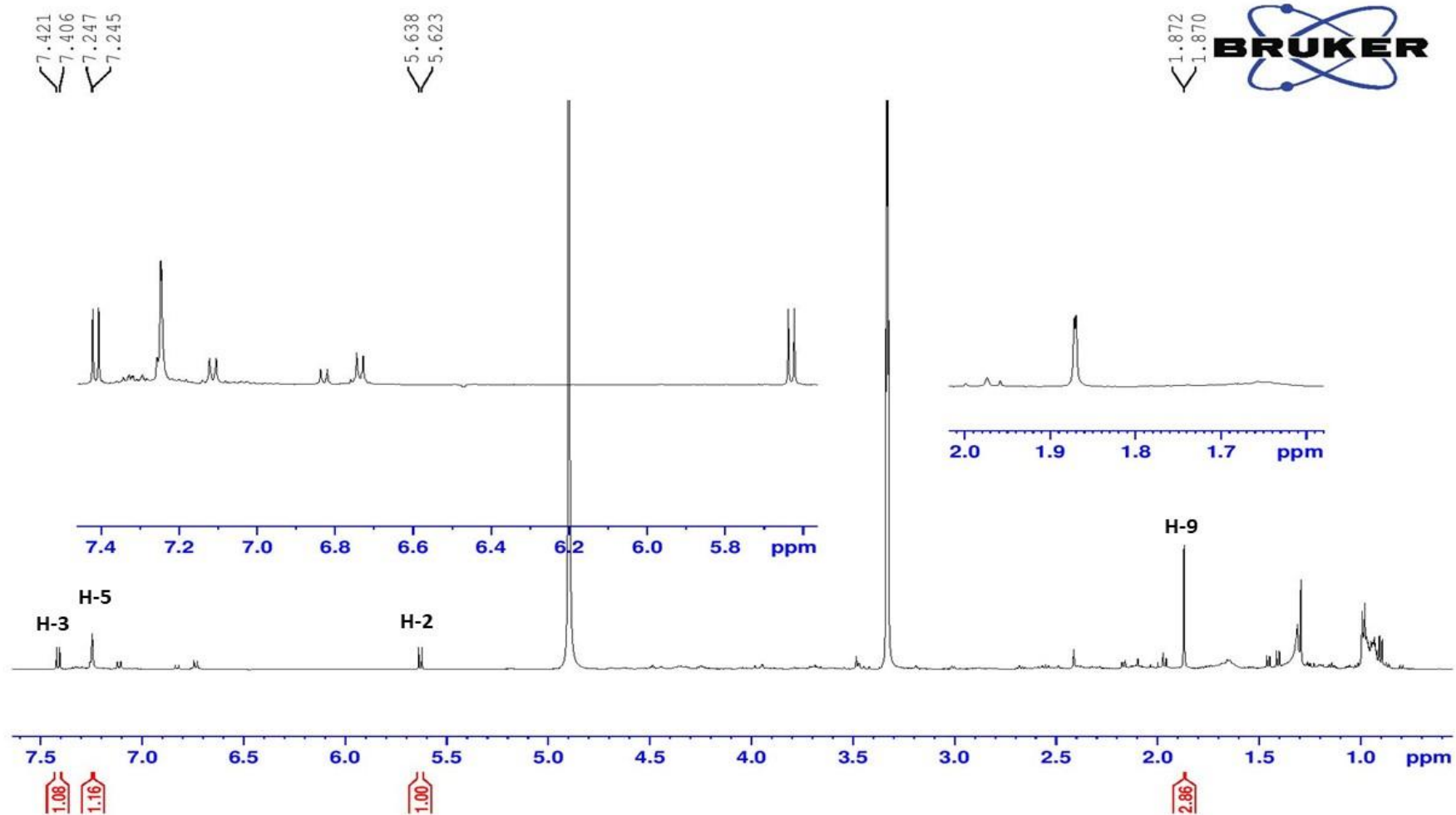
Figure 3.65: ^{1}H NMR spectrum of compound OM6 recorded in CD$_3$OD (500 MHz).
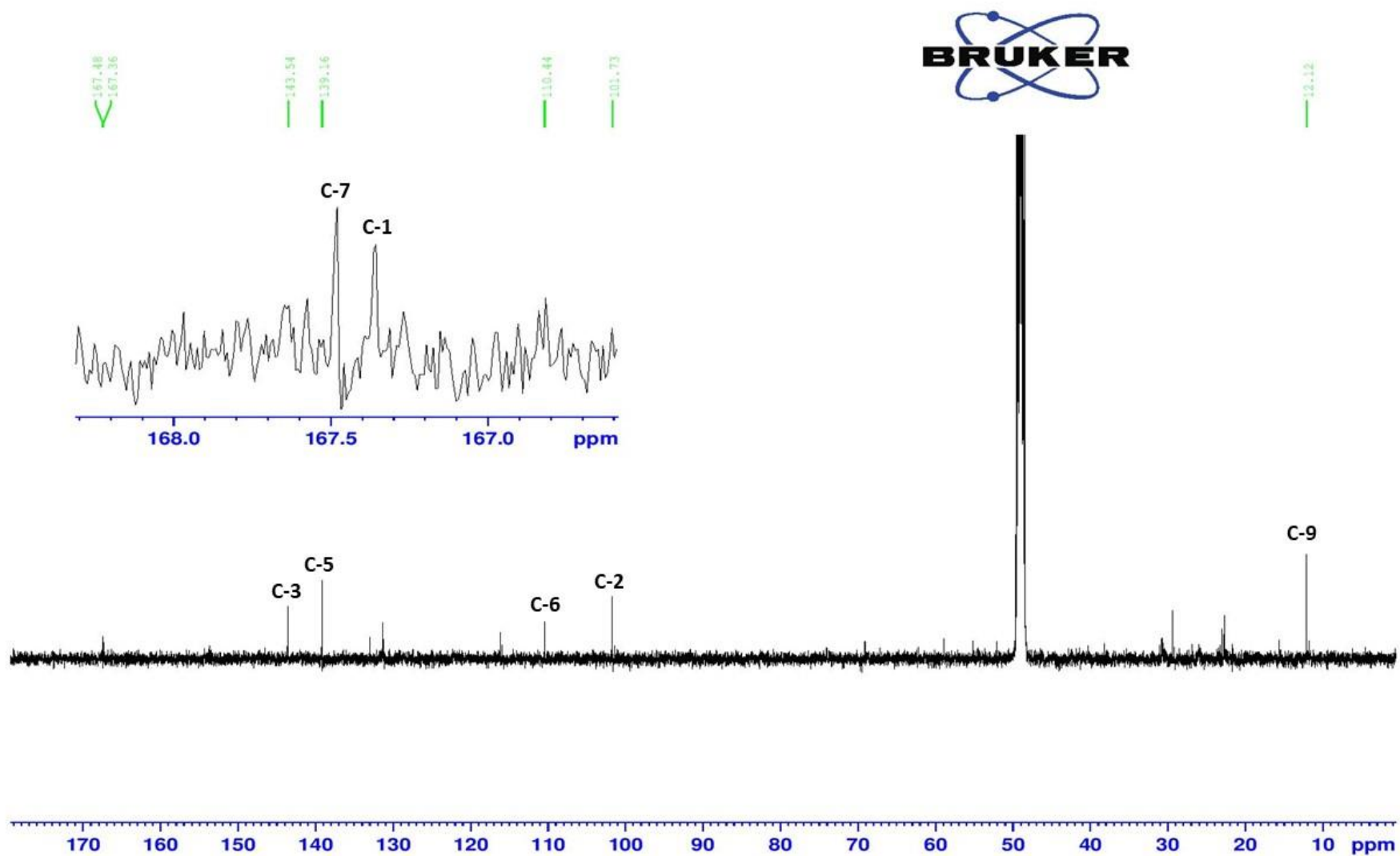
Figure 3.66: ^{13}C NMR spectrum of compound OM6 recorded in CD_3OD (125 MHz).
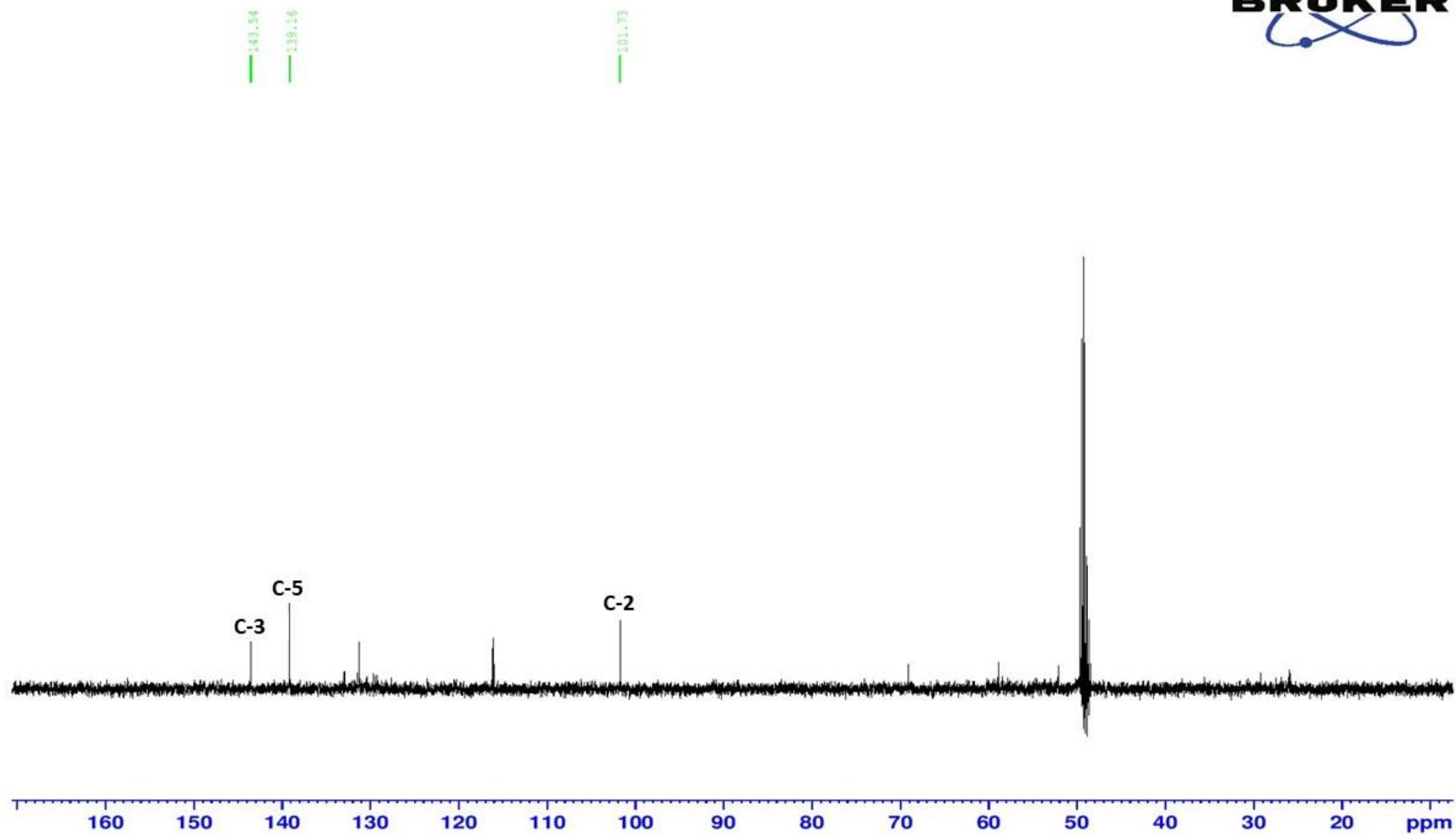
Figure 3.67: DEPT-90 spectrum of compound OM6 recorded in CD₃OD (125 MHz).
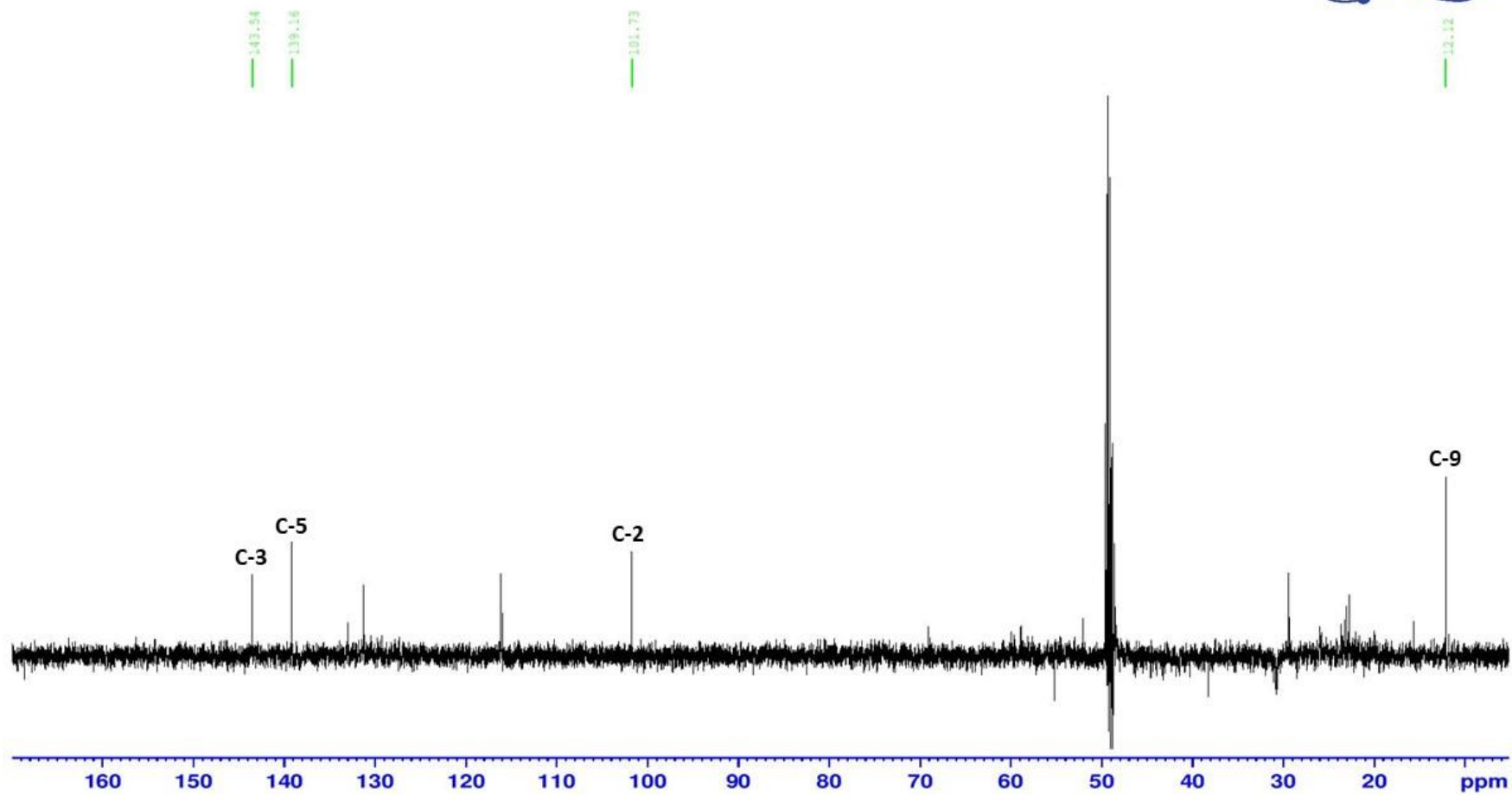
Figure 3.68: DEPT-135 spectrum of compound OM6 recorded in CD₃OD (125 MHz).
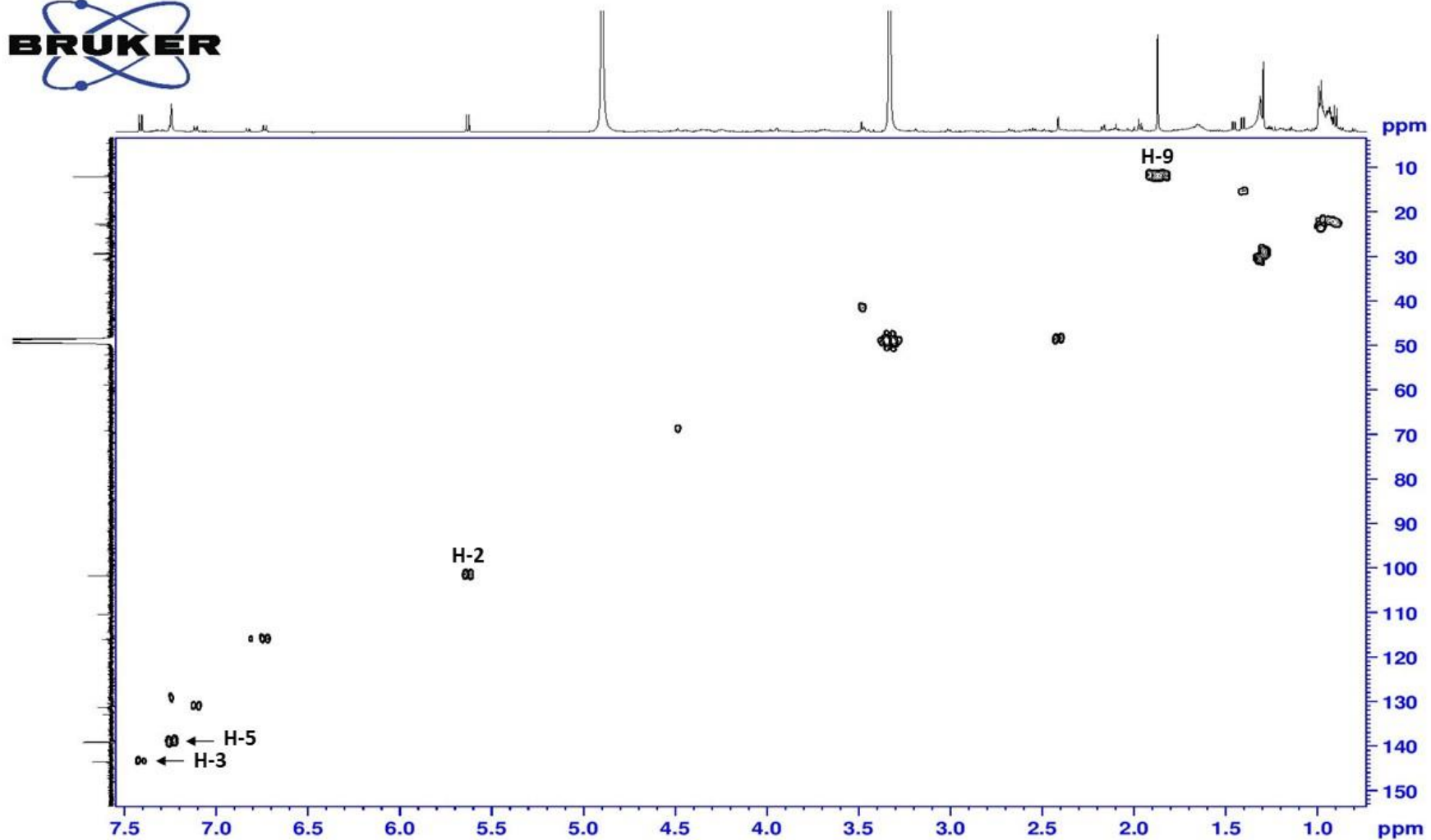
Figure 3.69: HMQC spectrum of compound OM6.
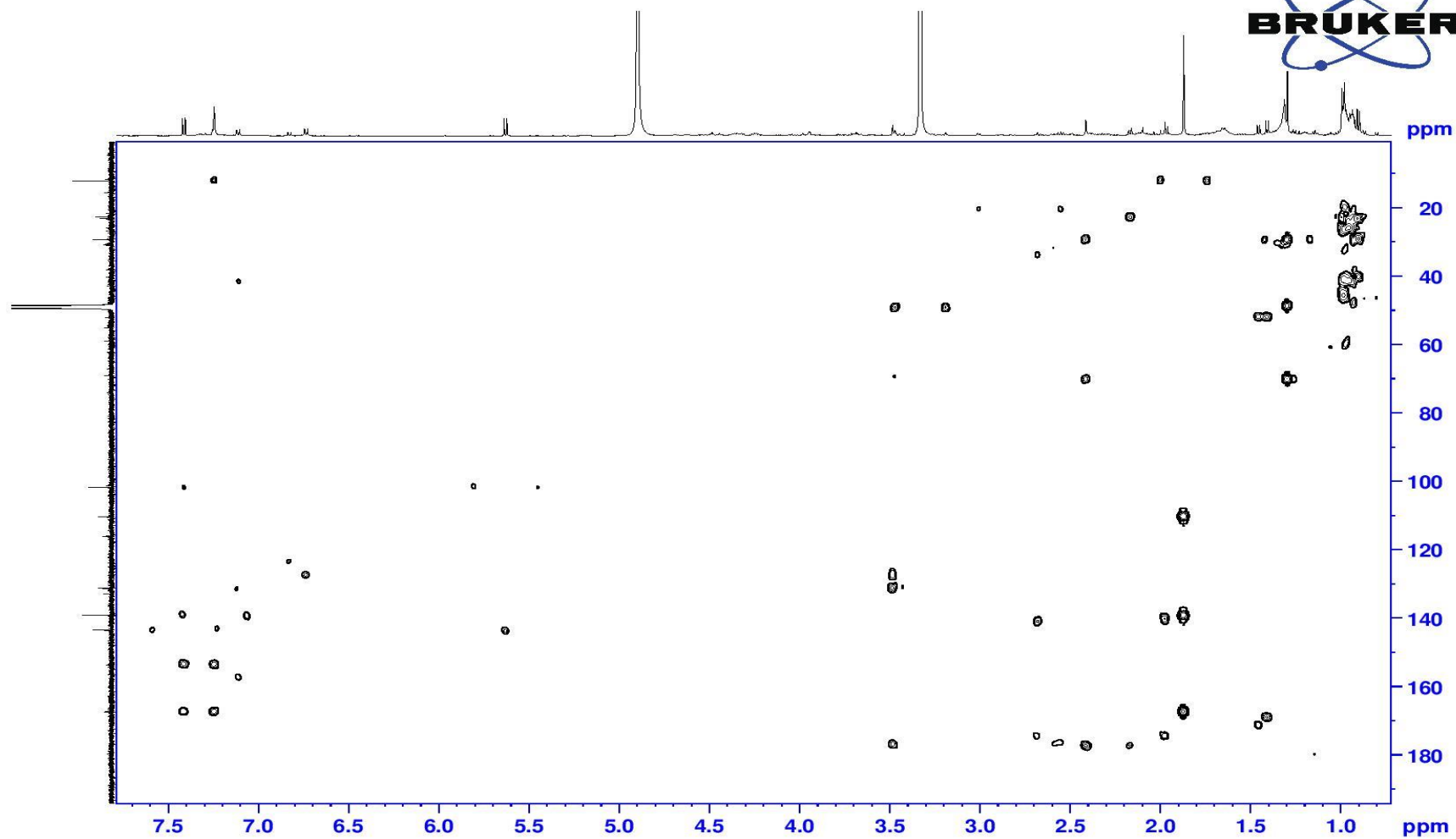
Figure 3.70: HMBC spectrum of compound OM6.
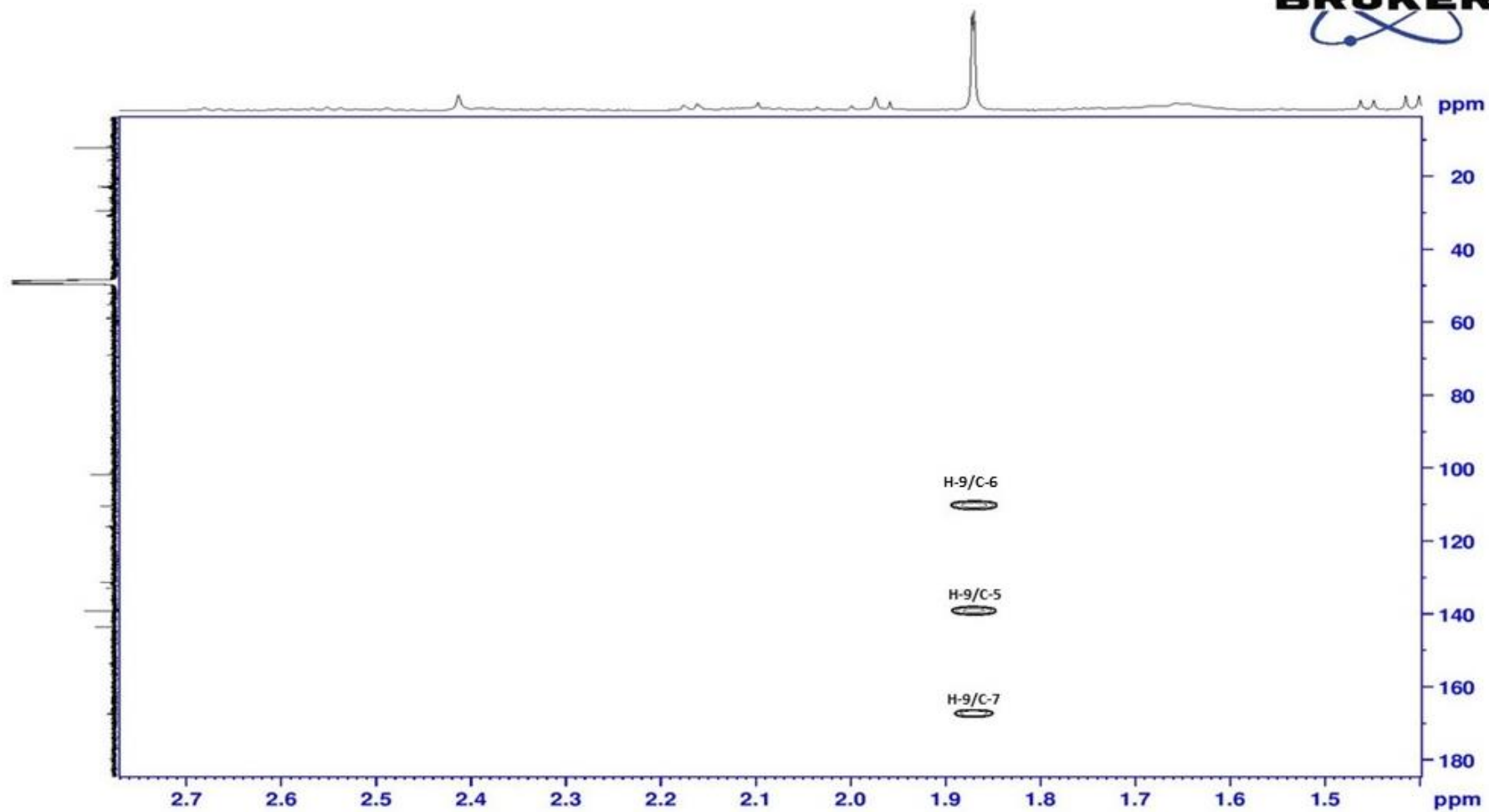
Figure 3.71: HMBC spectrum of compound OM6 (expanded).
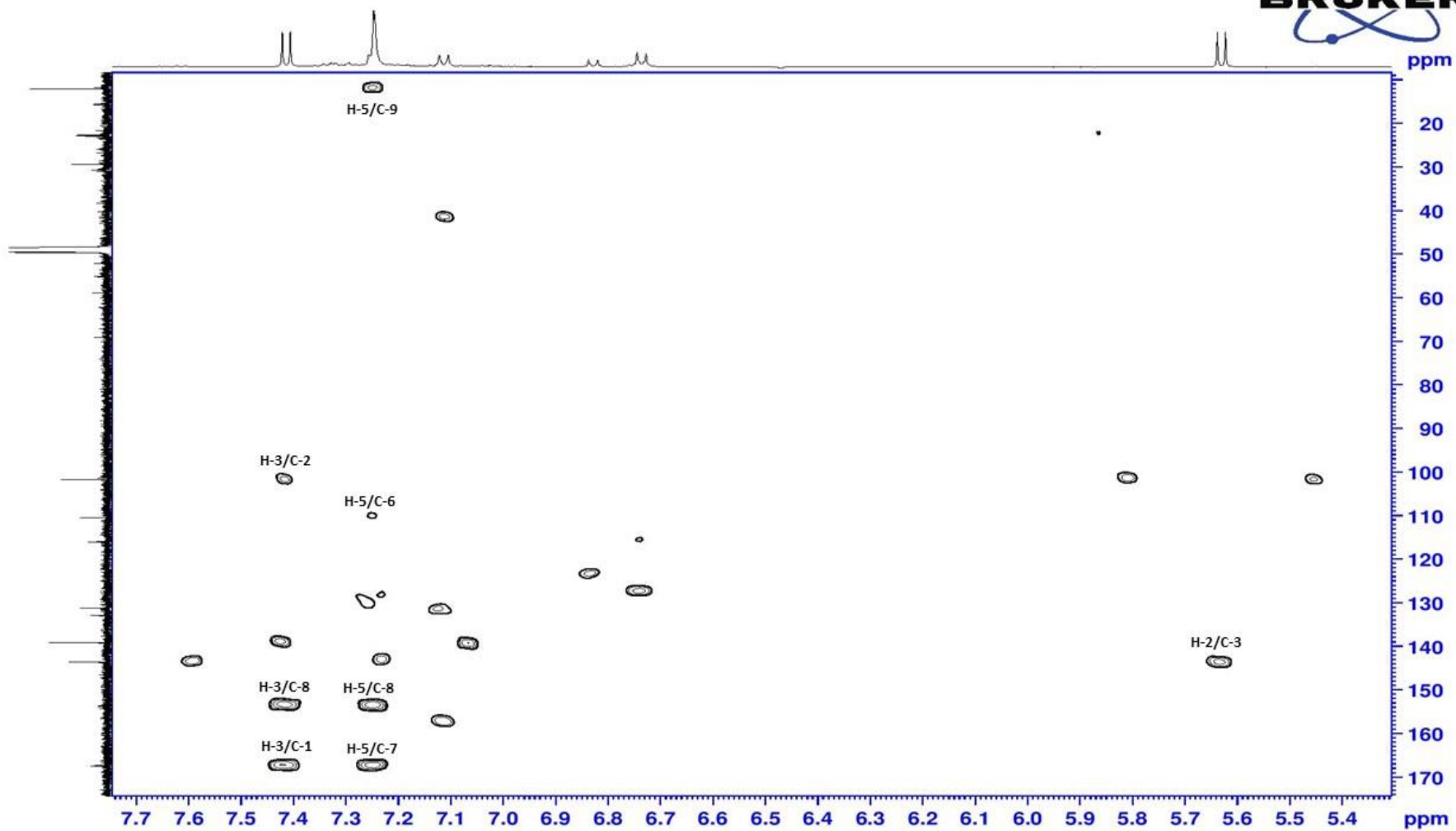
Figure 3.72: HMBC spectrum of compound OM6 (expanded).
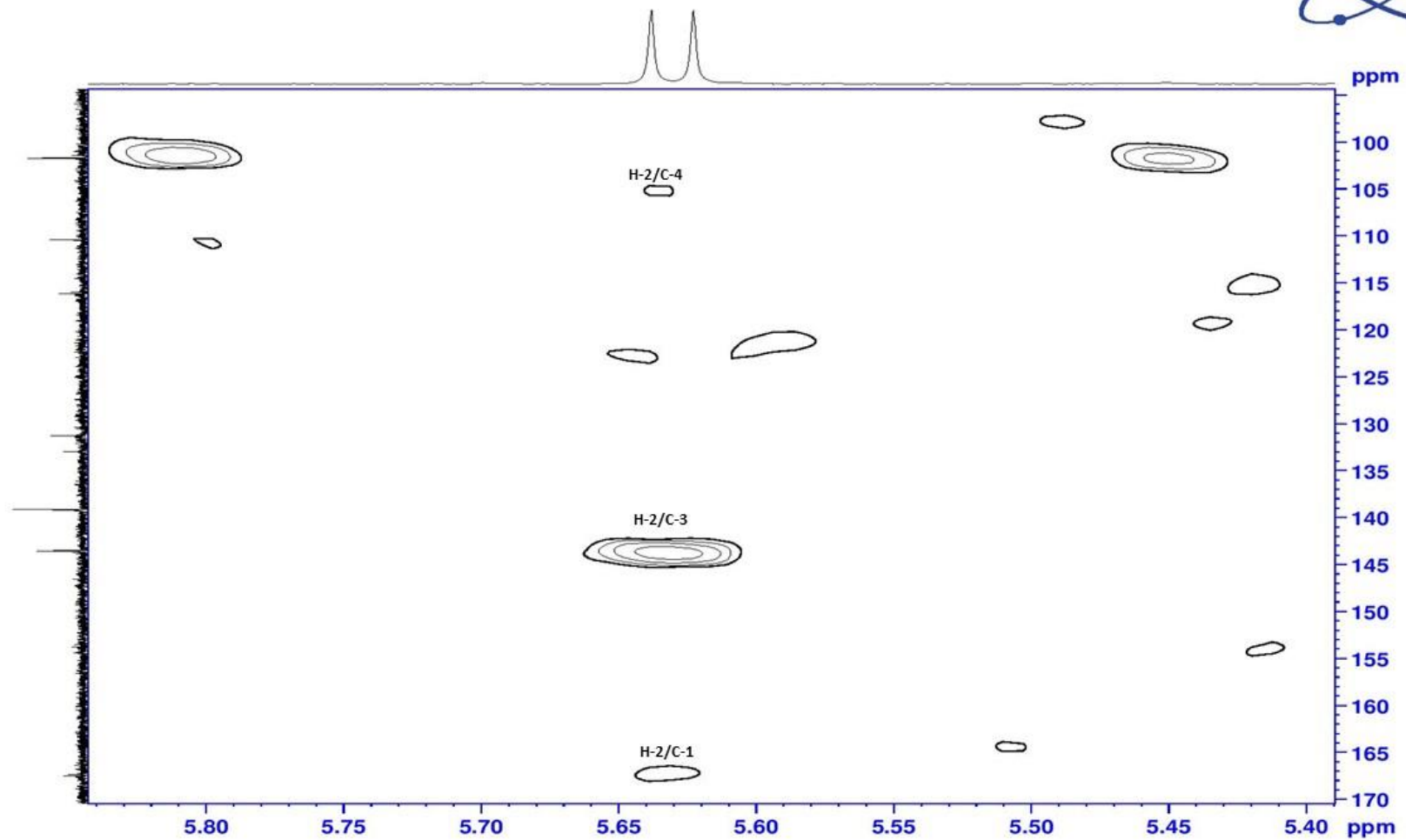
Figure 3.73: HMBC spectrum of compound OM6 (expanded).
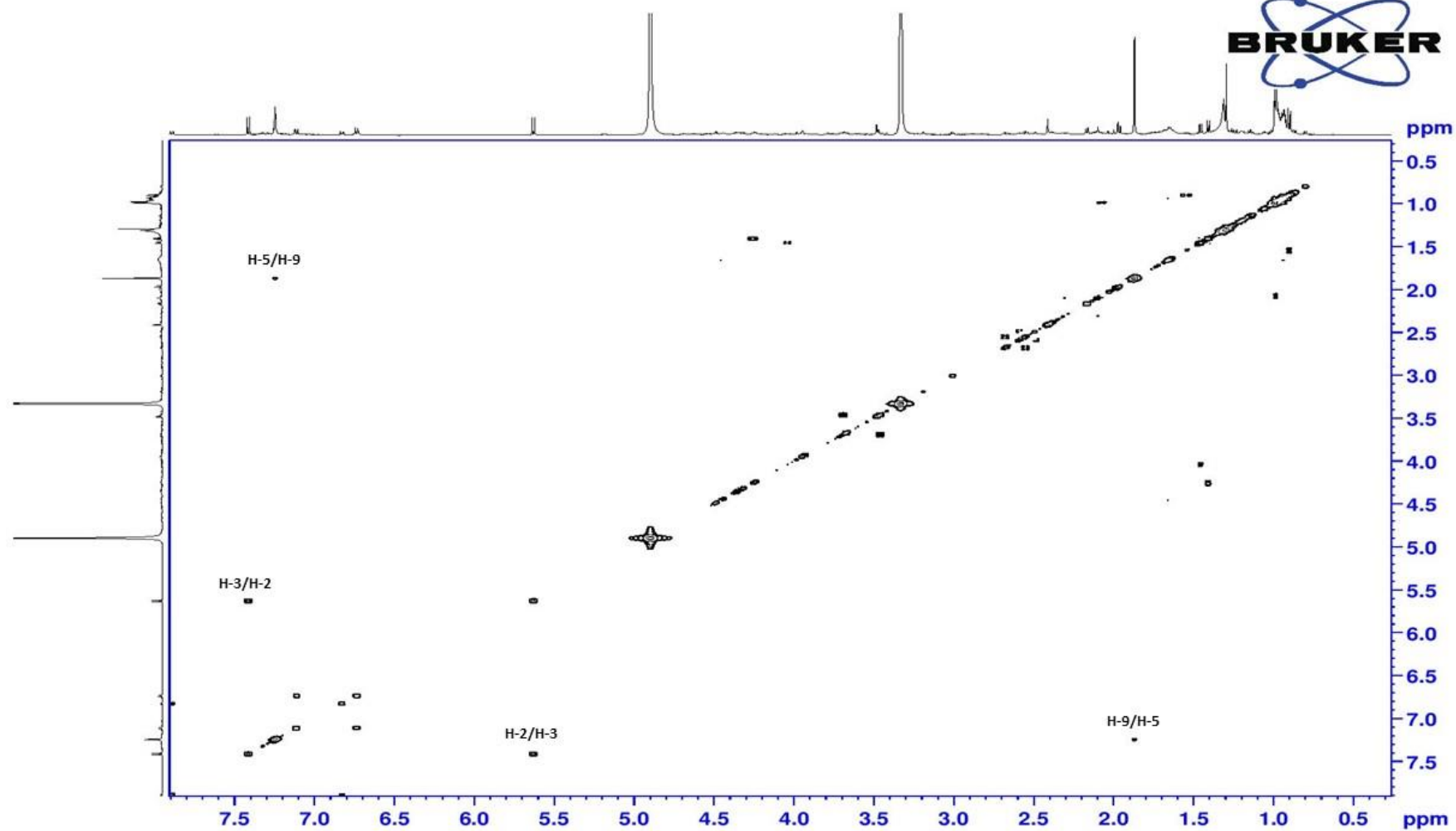
Figure 3.74: COSY spectrum of compound OM6.
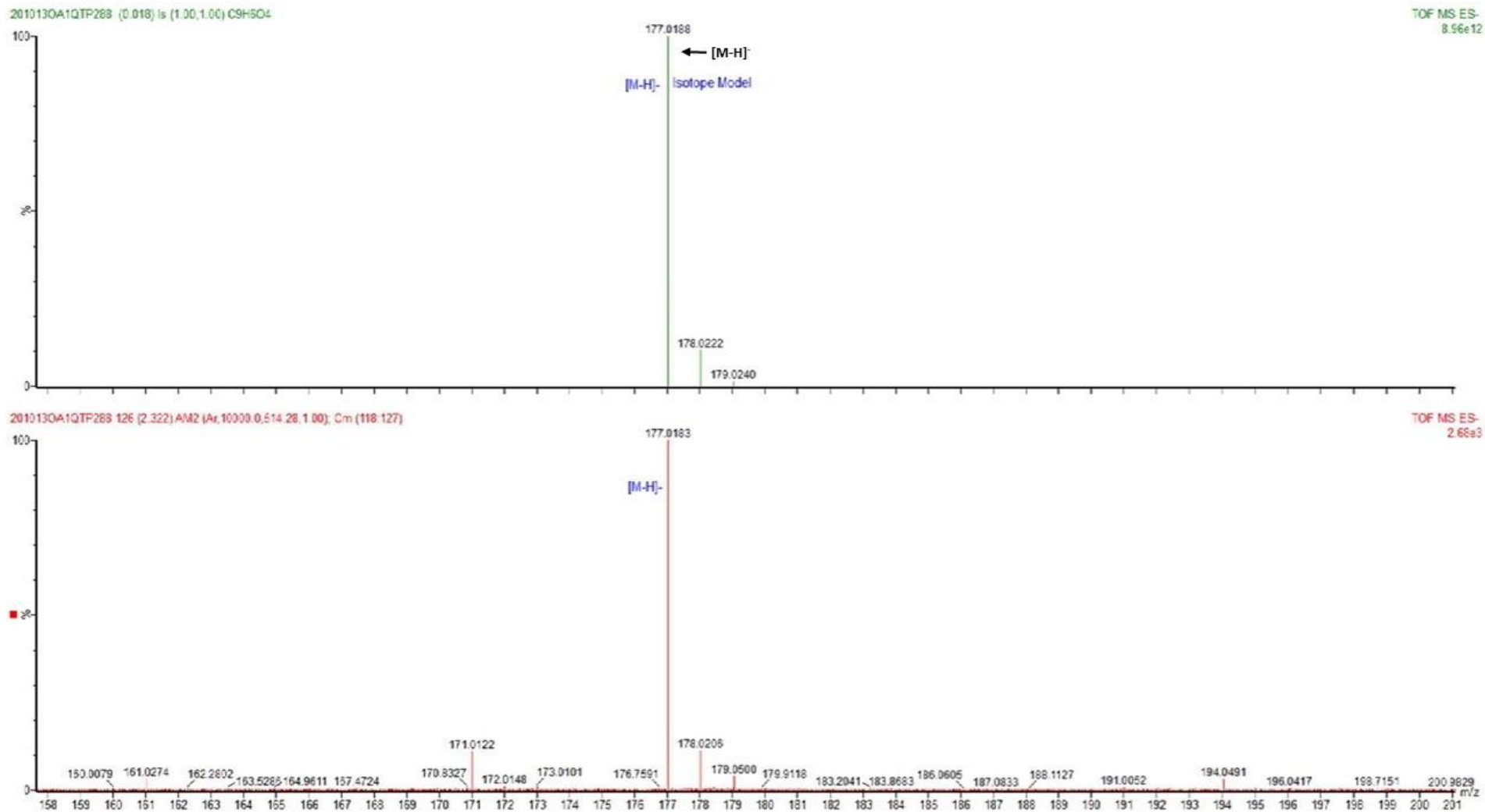
Figure 3.75: HRMS spectrum of compound OM6 showing peak ion at *m/z* 177.0188.
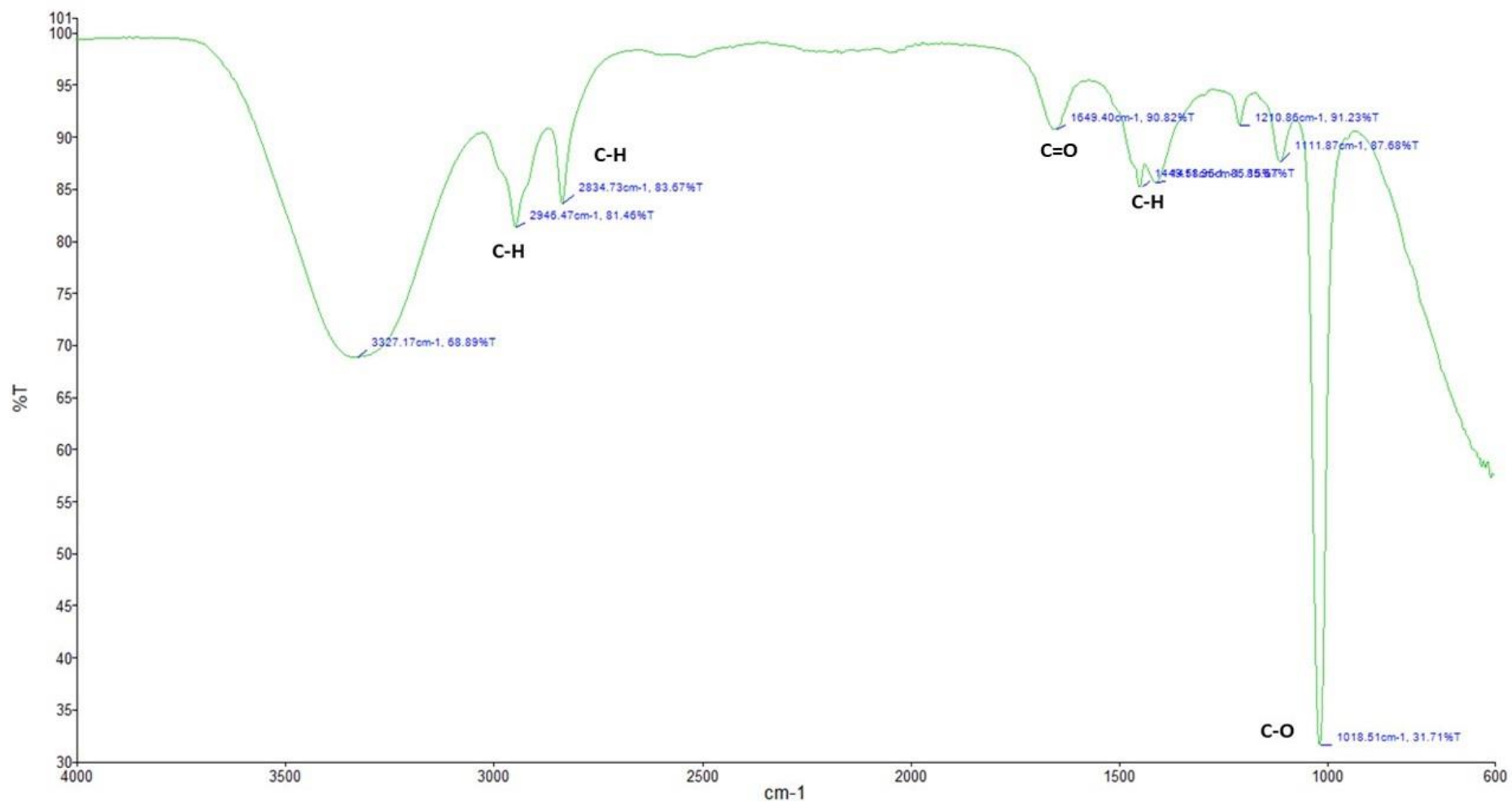
Figure 3.76: FT-IR spectrum of compound OM6.
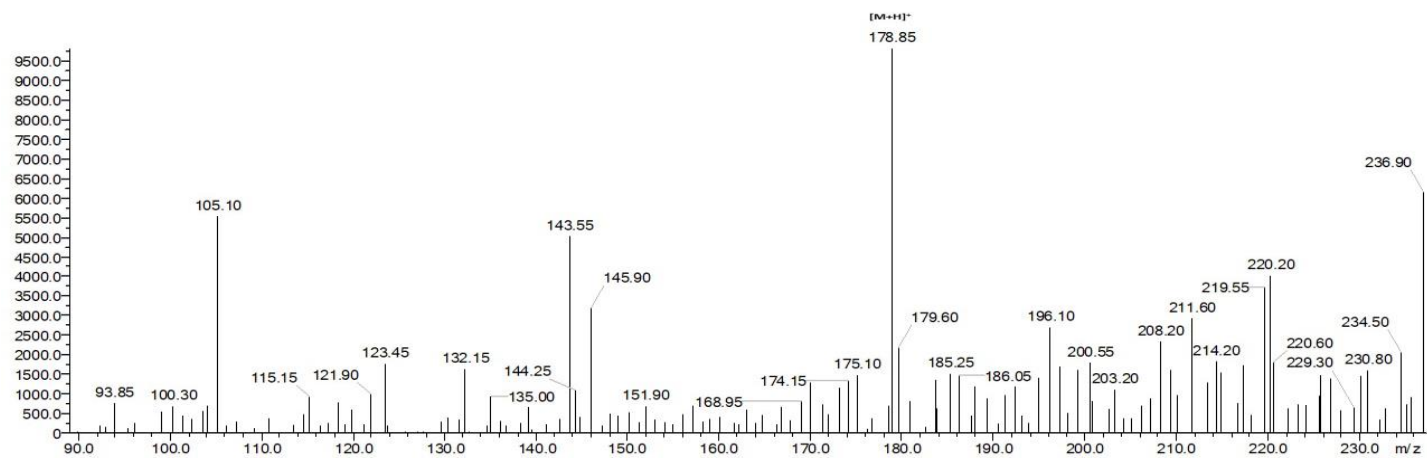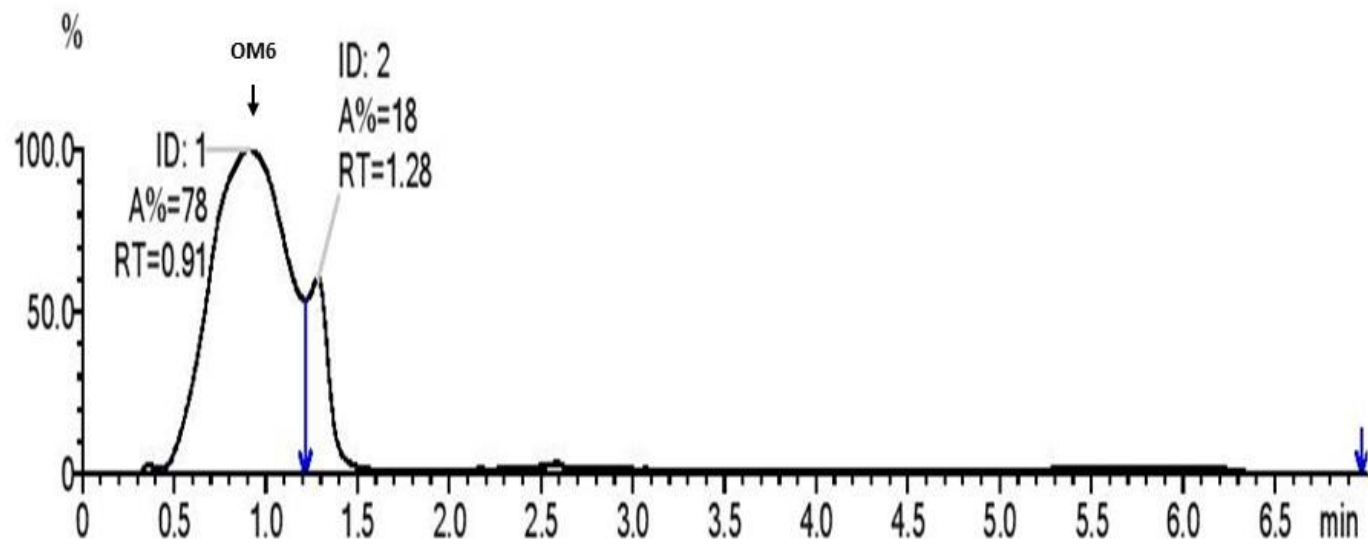
Figure 3.77: LC-MS spectrum of compound OM6 showing peak ion at *m/z* 178.85.

3.2.7 Compound OM7

Compound **OM7** was obtained as a white powder from an isolate **TH-C4** from the **TH** spring. The methanol extract (1.3 g) of the **TH-C4** isolate was subjected to partitioning chromatography to isolate the active compound **(Figure 3.78)**. Five sub-extracts were collected and the ethyl acetate sub-extract (289.3 mg / 22.25% of the extract) was active depending on the disc diffusion assay. The ethyl acetate sub-extract was then subjected to NP-SPE to identify the active fractions. Fractions (8 and 9) exhibited antimicrobial activity. These fractions (99.6 mg / 34.42% of the sub-extract) were collected together and subjected to prep-RP-TLC with a solvent system of chloroform: methanol (90:10). A third band at an R_f of 0.60 illustrated activity against *S. aureus* in the overlay assay. This band gave compound **OM7** (29.6 mg / 29.71% of the fraction), and its structure is shown in **(Figure 3.79).**
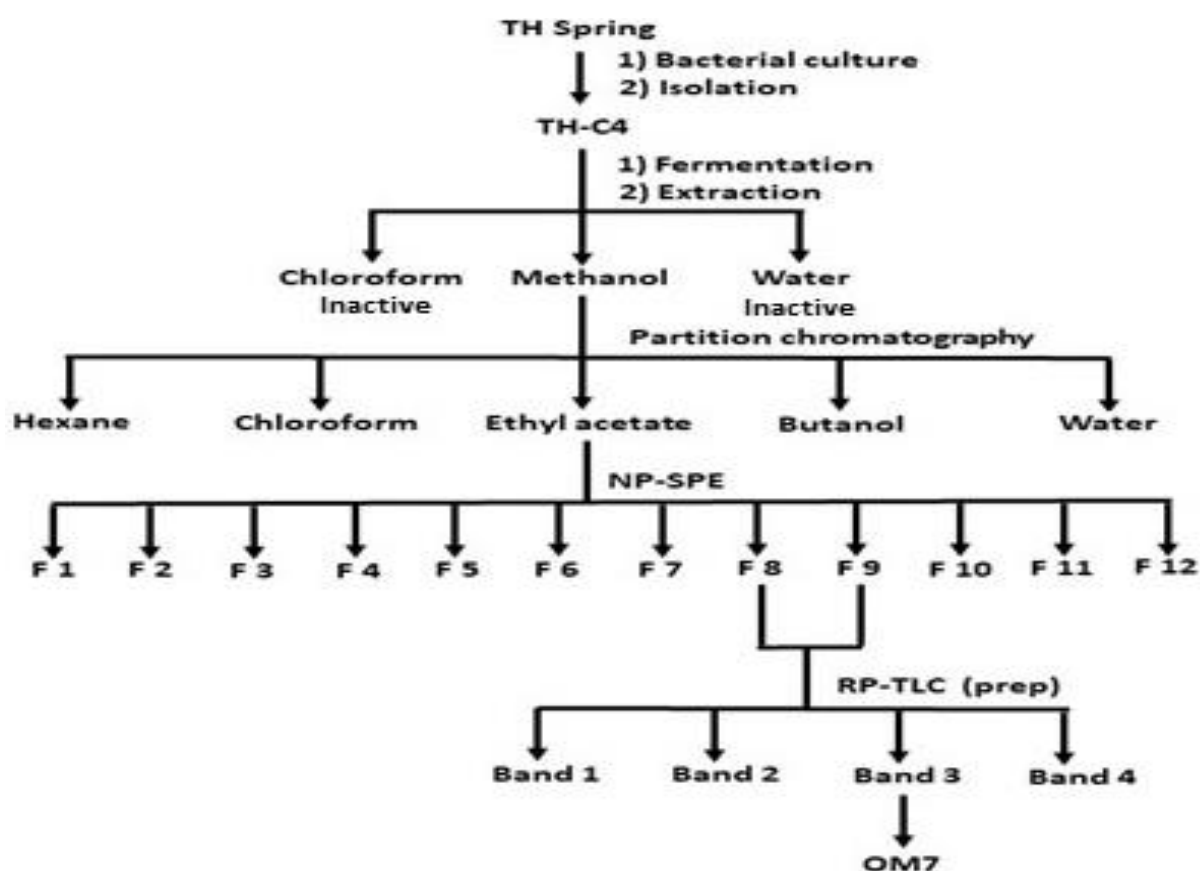
Figure 3.78: Scheme of isolation for compound OM7.

The molecular formula of **OM7** was determined as $C_8H_8O_2$ and the molecular weight of the compound was calculated as 136, which corresponded to an ion in the ESI-MS at *m/z* 135.04 attributable to [M-H]⁻ **(Figure 3.89)**.

The ¹H-NMR spectrum **(Figure 3.80)** showed the deshielded signals of five aromatic protons at δ_H 7.24 (H-4), δ_H 7.28 (H-3, H-5) and δ_H 7.32 (H-2, H-6), indicative of a phenyl ring. Moreover, a methylene hydrogen was observed at δ_H 3.60 (H2-7) and it was slightly deshielded due to its position between an aromatic ring and a carboxylic group.
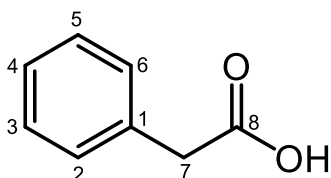
Figure 3.79: The structure of compound OM7.

The ¹³C NMR spectrum **(Figure 3.81)** showed 6 carbon signals in total from which two were quaternary carbons at δ_C 136.3 (C-1) and δ_C 175.9 (C-8) according to the DEPT-135 spectrum **(Figure 3.83)**. Furthermore, a methylene carbon was observed at δ_C 42.2 (C-7). The DEPT-90 spectrum **(Figure 3.82)** showed three methine carbons at δ_C 127.8 (C-4), 129.4 (C-3/C-5) and 130.3 (C-2/C-6). The two aromatic carbons at 2 and 6 positions of the compound appeared as one peak at δ_C 130.3. Similarly, carbons at 3 and 5 positions appeared as one peak at δ_C 129.4.

In the HMBC spectrum **(Figures 3.86** and **87)**, the placement of a carbonyl group at C-8 was revealed by a ^2J correlation with H2-7. Furthermore, the position of the methylene carbon was confirmed by a ^3J correlation with hydrogens of H-2 and H-6 as

well as by a ^4J correlation with hydrogens H-3 and H-5. Coupling between H-3/5 and H$_2$-7 was seen in the COSY spectrum **(Figure 3.88)**.

Further confirmation on the structure of the compound was obtained using FT-IR spectroscopy **(Appendix 2)**. The FT-IR spectrum was taken by dissolving the compound in methanol and the spectrum exhibited a C=O stretching absorption at 1697 cm^{-1}. There were also a broad band for O-H at 3305 cm^{-1}, an alkyl C-H stretching at 2839 cm^{-1} and 2949 cm^{-1}, C-H bending at 1409 cm^{-1} as well as C-O stretching at 1019 cm^{-1}.

Compound **OM7** was therefore identified as benzeneacetic acid, which is commonly known as phenylacetic acid. The ^{1}H and ^{13}C NMR data of this compound are in good agreement with published literature for the phenylacetic acid (Holmes and Lightner, 1995). Furthermore, compound **OM7** was compared to a ^{1}H NMR spectrum of reference phenylacetic acid and it was identical **(Figure 3.90)**.

Table 3.15: ^{1}H (500 MHz), ^{13}C NMR (125 MHz) and HMBC spectroscopic data of OM7 recorded in CD$_3$OD.

Position	^{1}H	^{13}C	HMBC			^{13}C ((CD$_3$)$_2$SO) Holmes and Lightner, 1995
			^2J	^3J	^4J	
C-1	--	136.3	--	--	--	135.0
C-2	7.32	130.3	C-1, C-3	--	--	129.3
C-3	7.28	129.4	--	C-5	C-7	128.1
C-4	7.24	127.8	--	C-2, C-6	--	126.4
C-5	7.28	129.4	--	C-3	C-7	128.1
C-6	7.32	130.3	C-1, C-5	--	--	129.3
C-7	3.60 (s)	42.2	C-1, C-8	C-2, C-6	--	40.4
C-8	--	175.9	--	--	--	172.6

There are numerous studies on the isolation of phenylacetic acid from microbes. For instance, it has been isolated from *Streptomyces zhaozhouensis* (Lacret *et al.*, 2015), *Streptomyces humidus* (Hwang *et al.*, 2001), *Proteus mirabilis* (Erdmann, 1987), *Azospirillum brasilense*, *Enterobacter cloacae*, *Thauera aromatica* and the nitrogen-fixing bacteria *Frankia* (Cook, 2019), *Bacteroides ruminicola, Bacteroides melaninogenicus*

subsp. Macacae, *Clostridium botulinum* type G and in other species of *Clostridium* (Mayrand and Bourgeau, 1982). Moreover, phenylacetic acid has been produced by the fungi such as *Rhizoctonia solani*, *Sporobolomyces roseus* and *Schizophyllum commune* (Cook, 2019). It has also been found in the brown alga, *Undaria pinnatifida* (Cook, 2019). Furthermore, it has been reported that phenylacetic acid was found in some *Bacillus* species. For example, *B. fortis* (Akram *et al*., 2016), *B. megaterium*, *B. cereus* strain HY-3 and *B. subtilis* strain HY-16 (Hwang *et al*., 2001) as well as *B. licheniformis* (Kim *et al*., 2004). Additionally, it has been extracted from some plants such as *Galium aparine* (Goryacha *et al*., 2014).
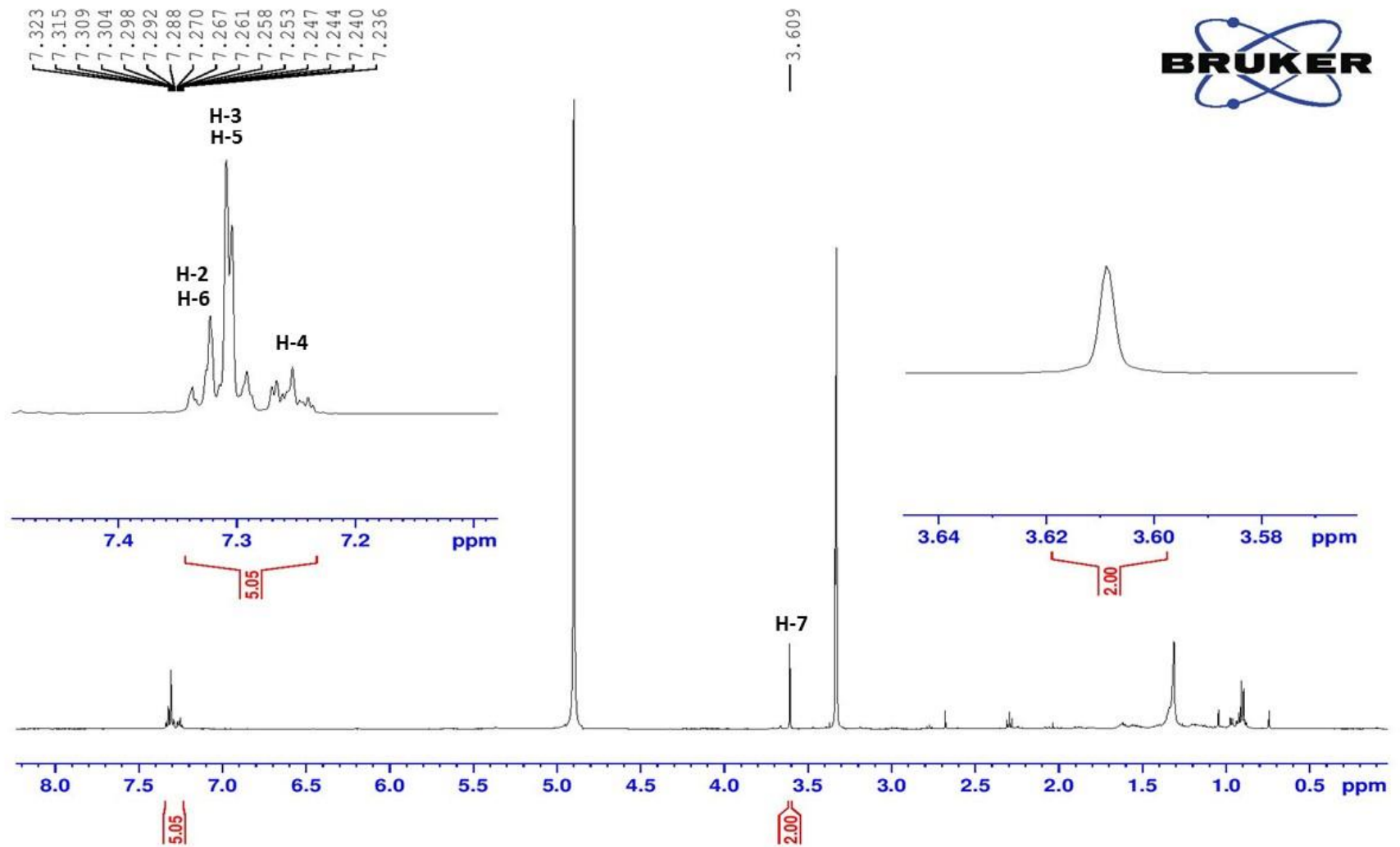
Figure 3.80: ^{1}H NMR spectrum of compound OM7 recorded in CD$_3$OD (500 MHz).
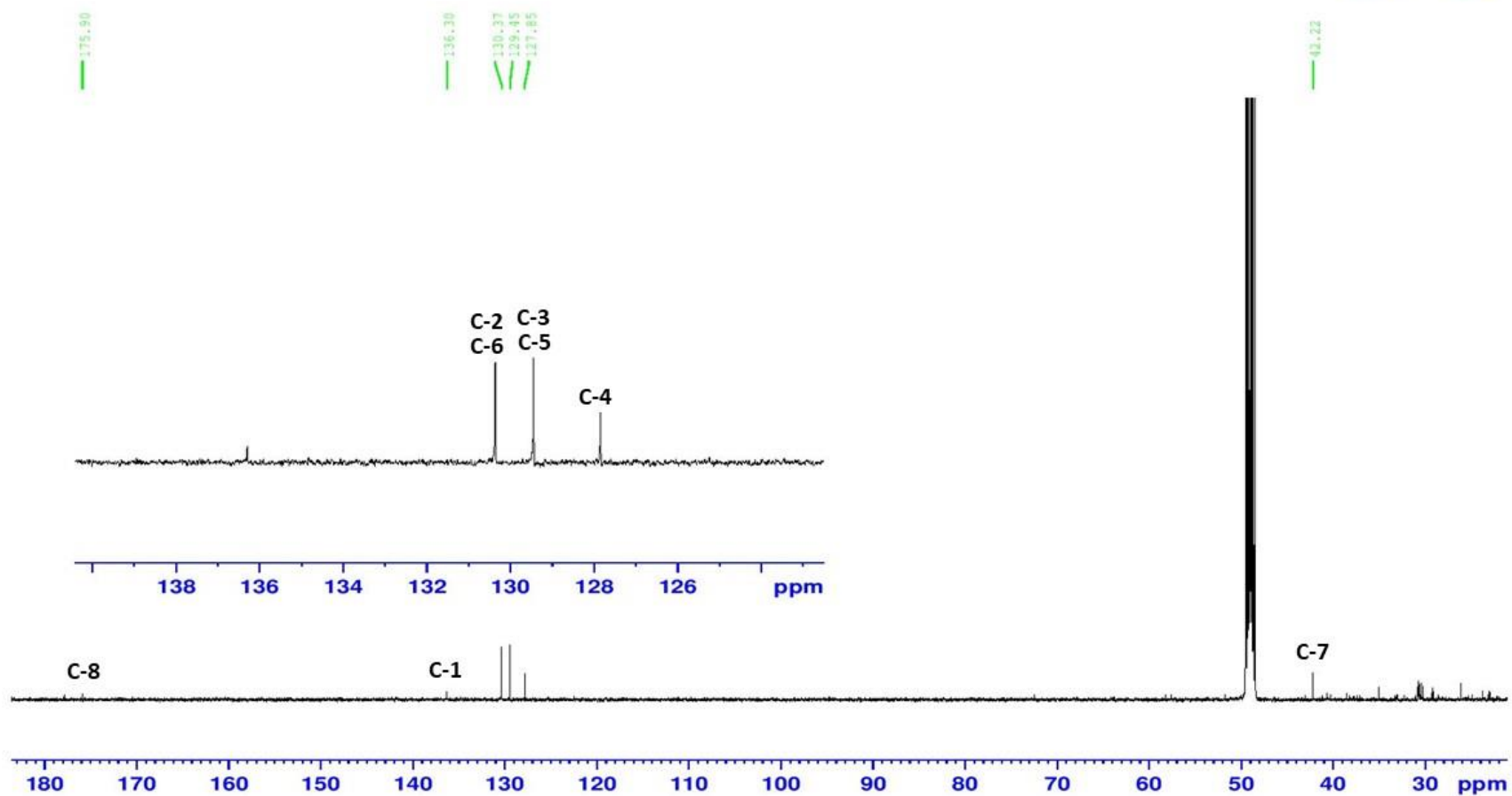
Figure 3.81: ^{13}C NMR spectrum of compound OM7 recorded in CD$_3$OD (125 MHz).
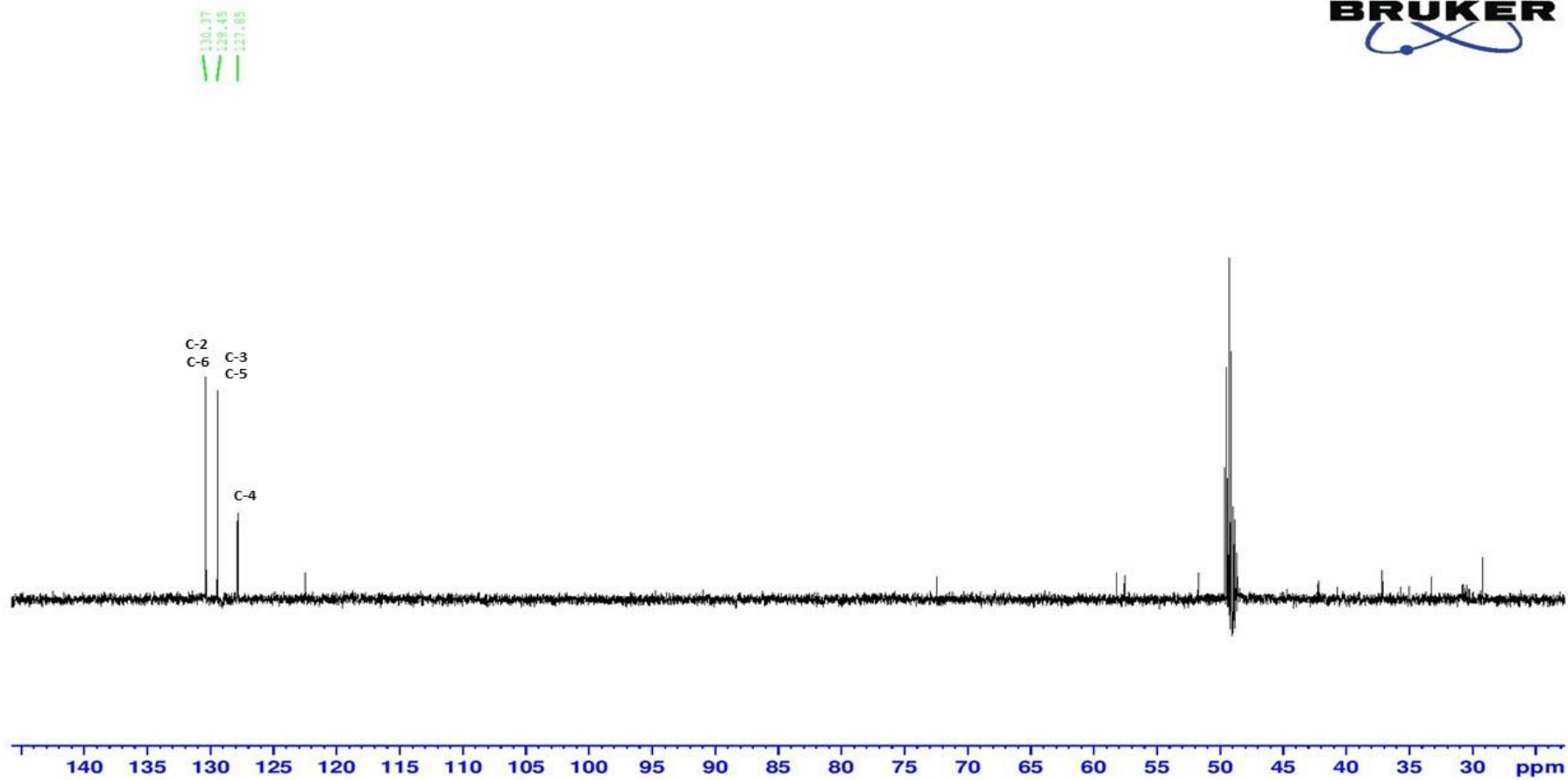
Figure 3.82: DEPT-90 spectrum of compound OM7 recorded in CD$_3$OD (125 MHz).
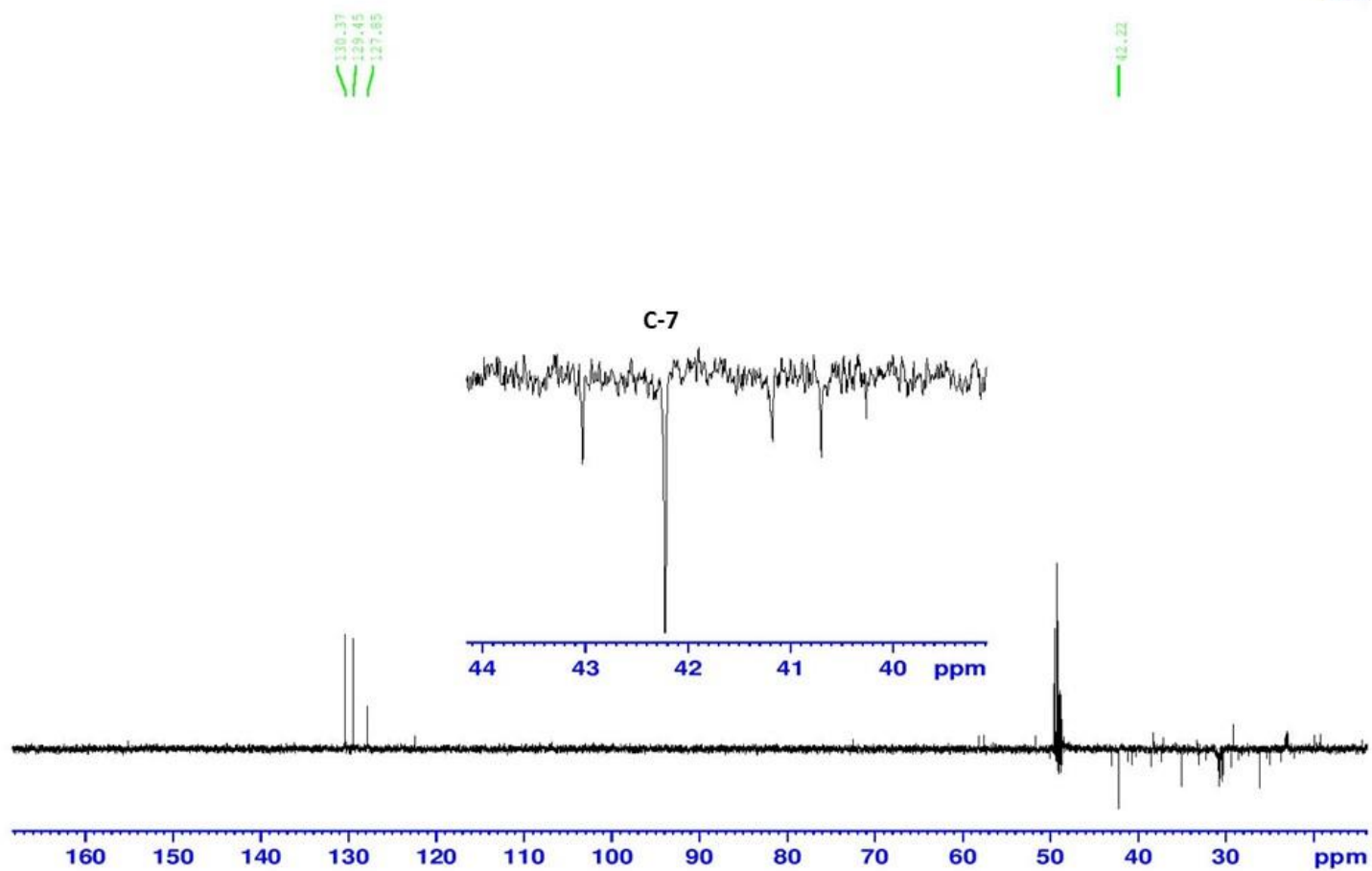
Figure 3.83: DEPT-135 spectrum of compound OM7 recorded in CD₃OD (125 MHz).
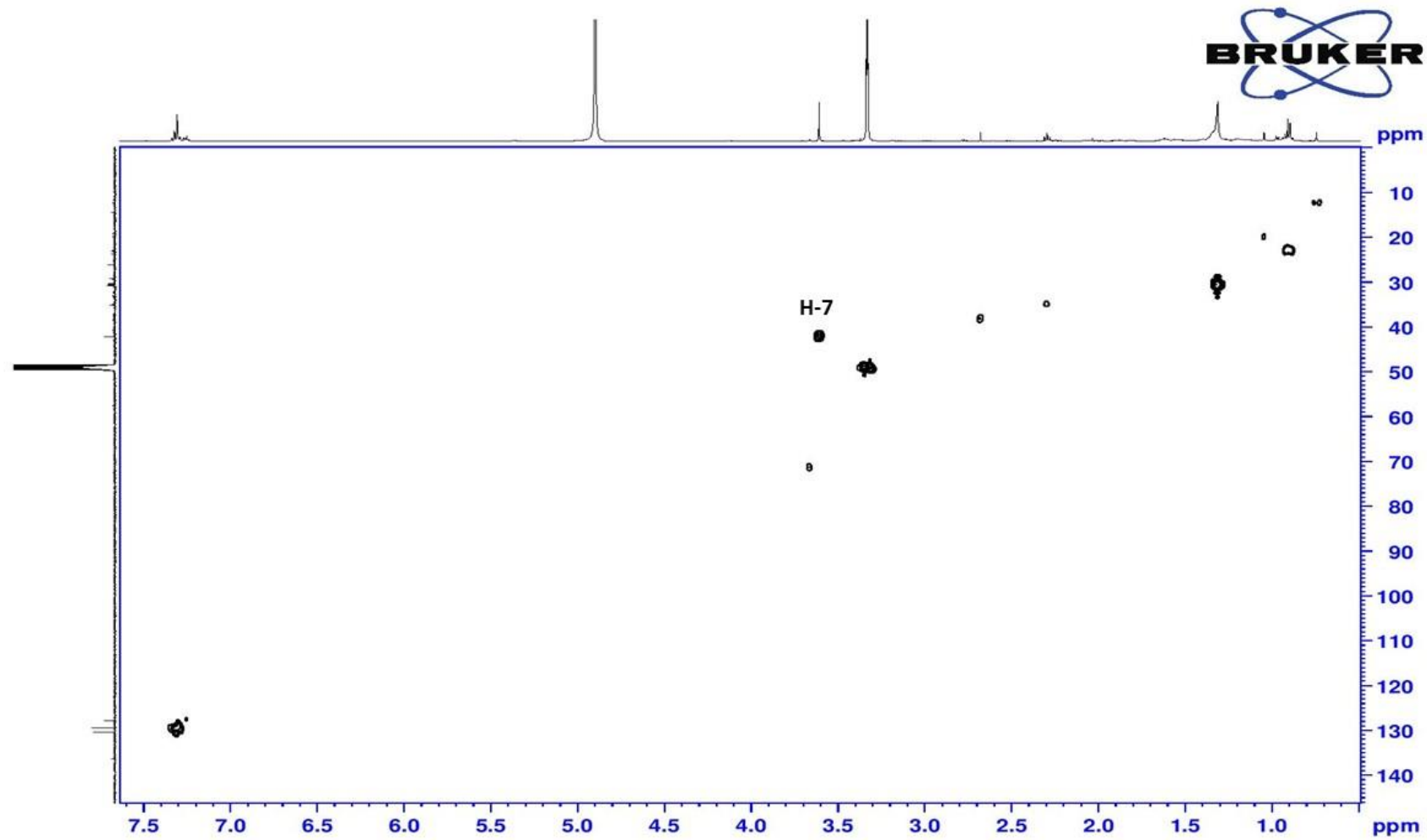
Figure 3.84: HMQC spectrum of compound OM7.
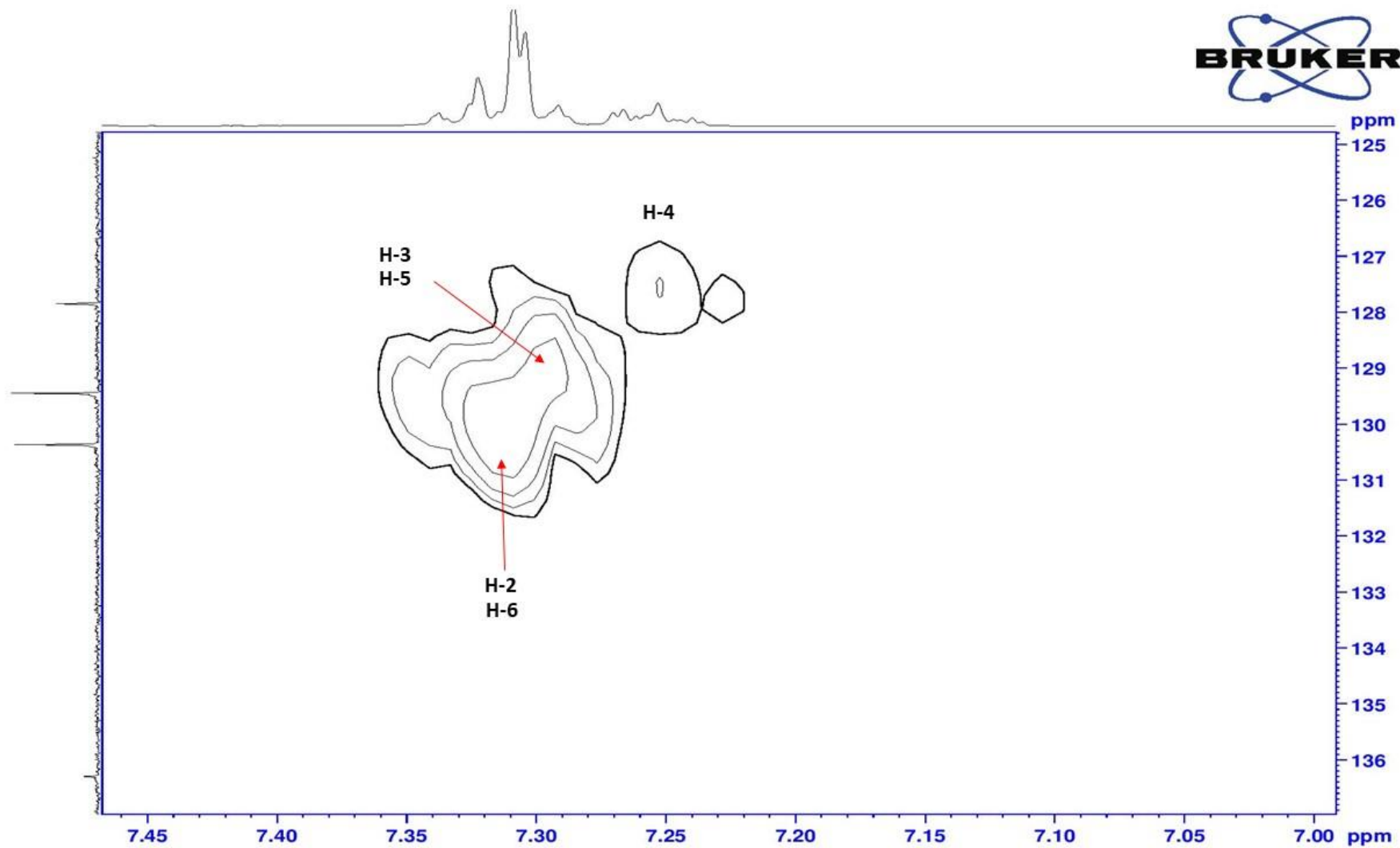
Figure 3.85: HMQC spectrum of compound OM7 (expanded).
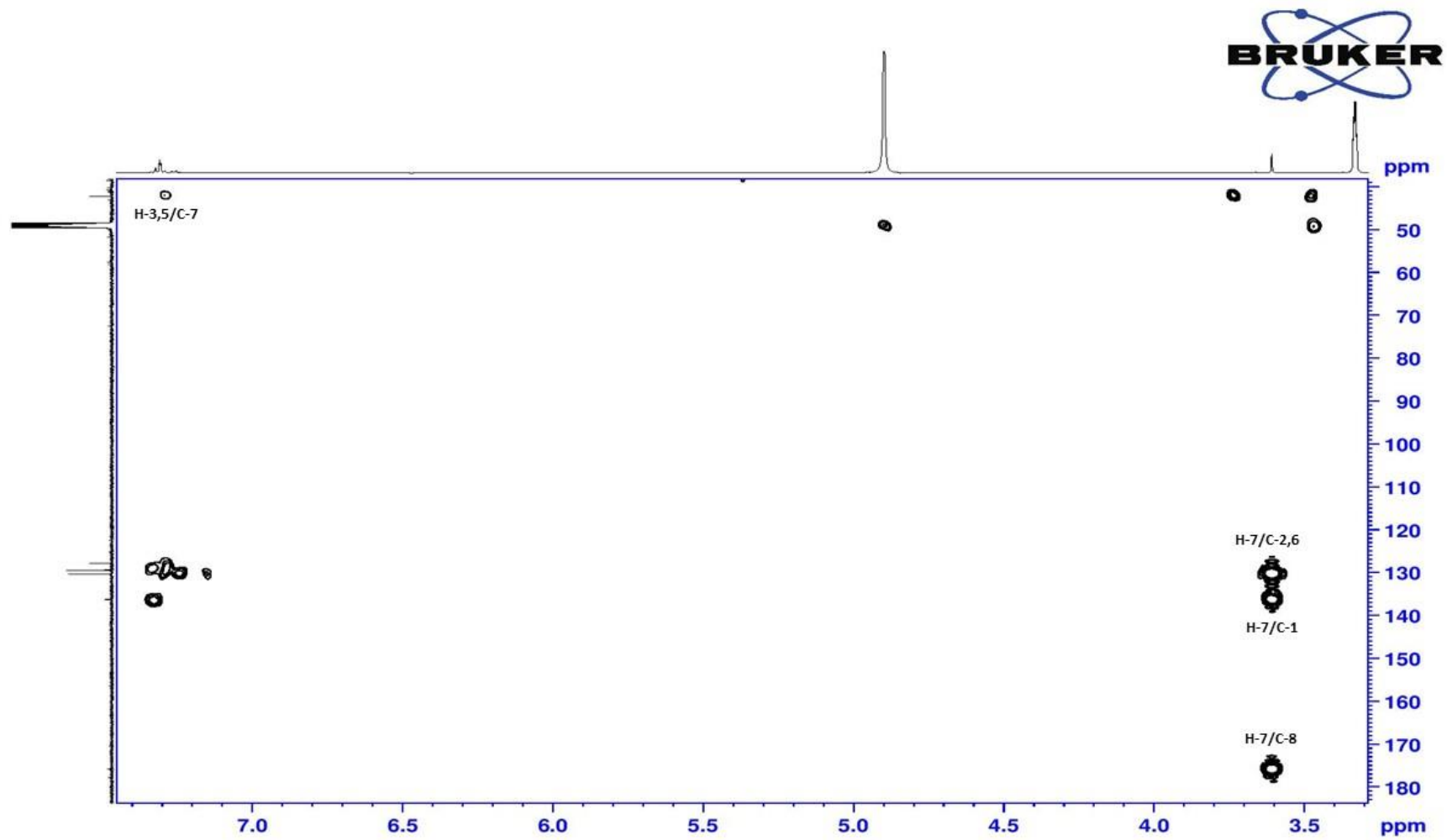
Figure 3.86: HMBC spectrum of compound OM7.
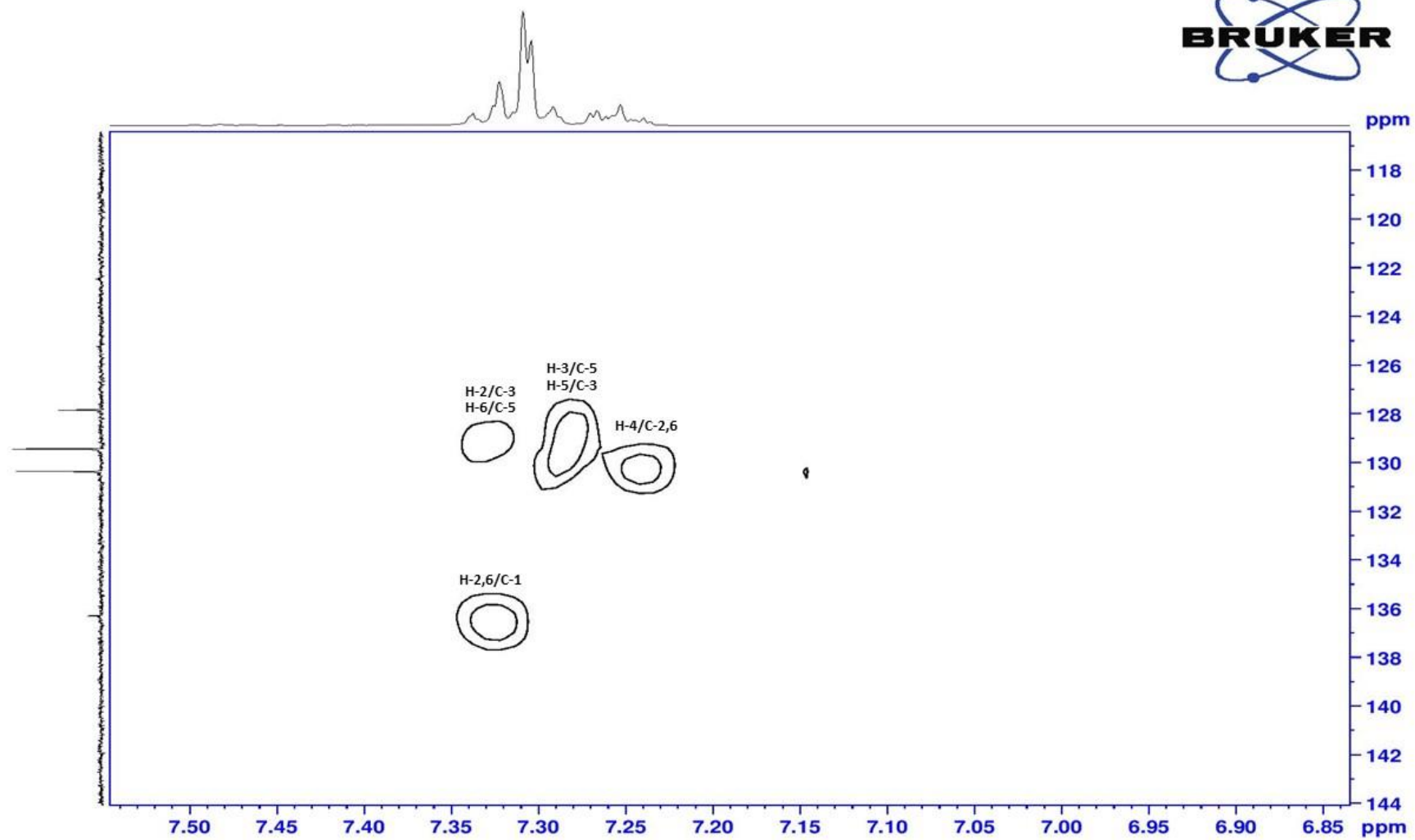
Figure 3.87: HMBC spectrum of compound OM7 (expanded).
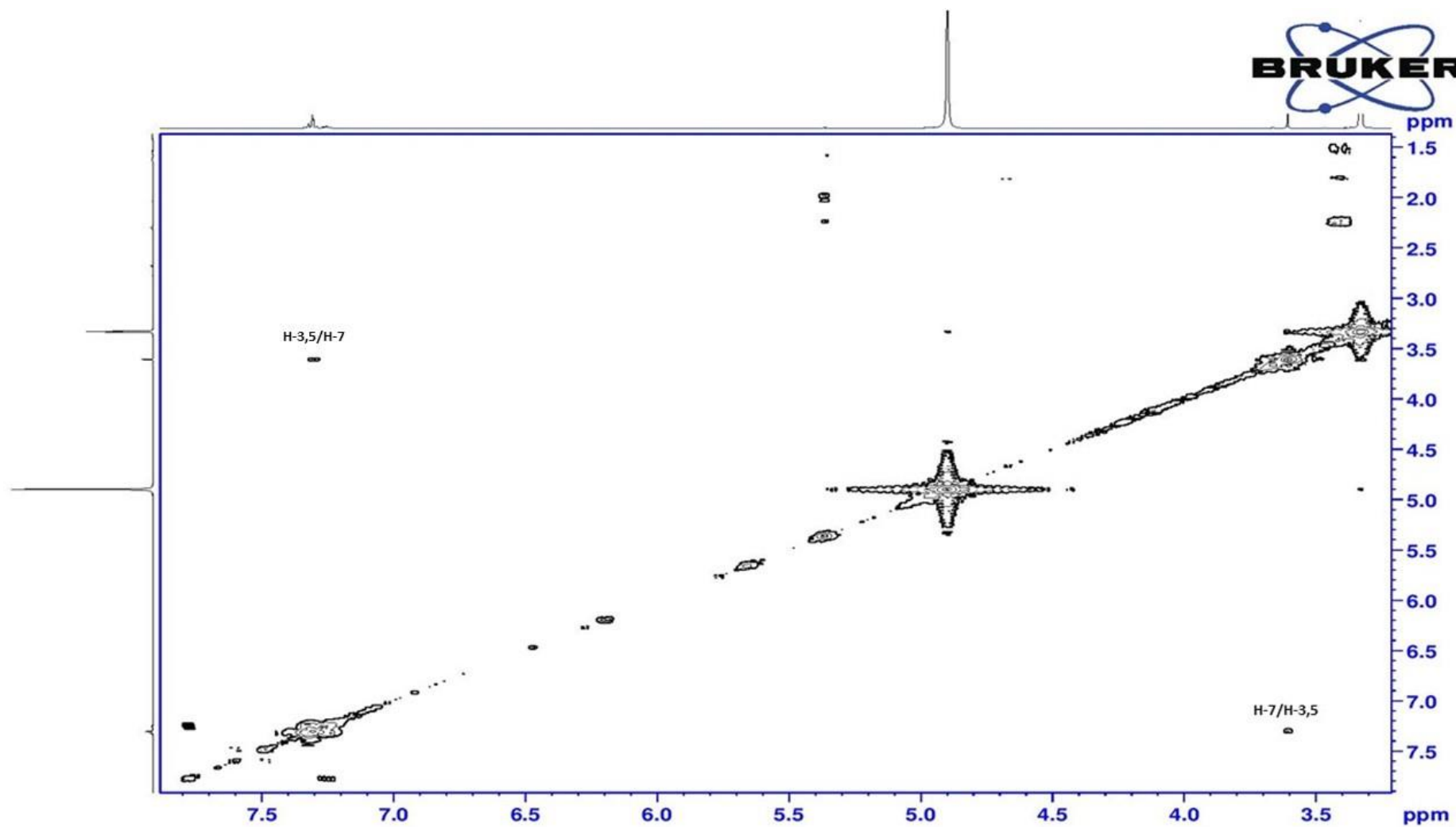
Figure 3.88: COSY spectrum of compound OM7.
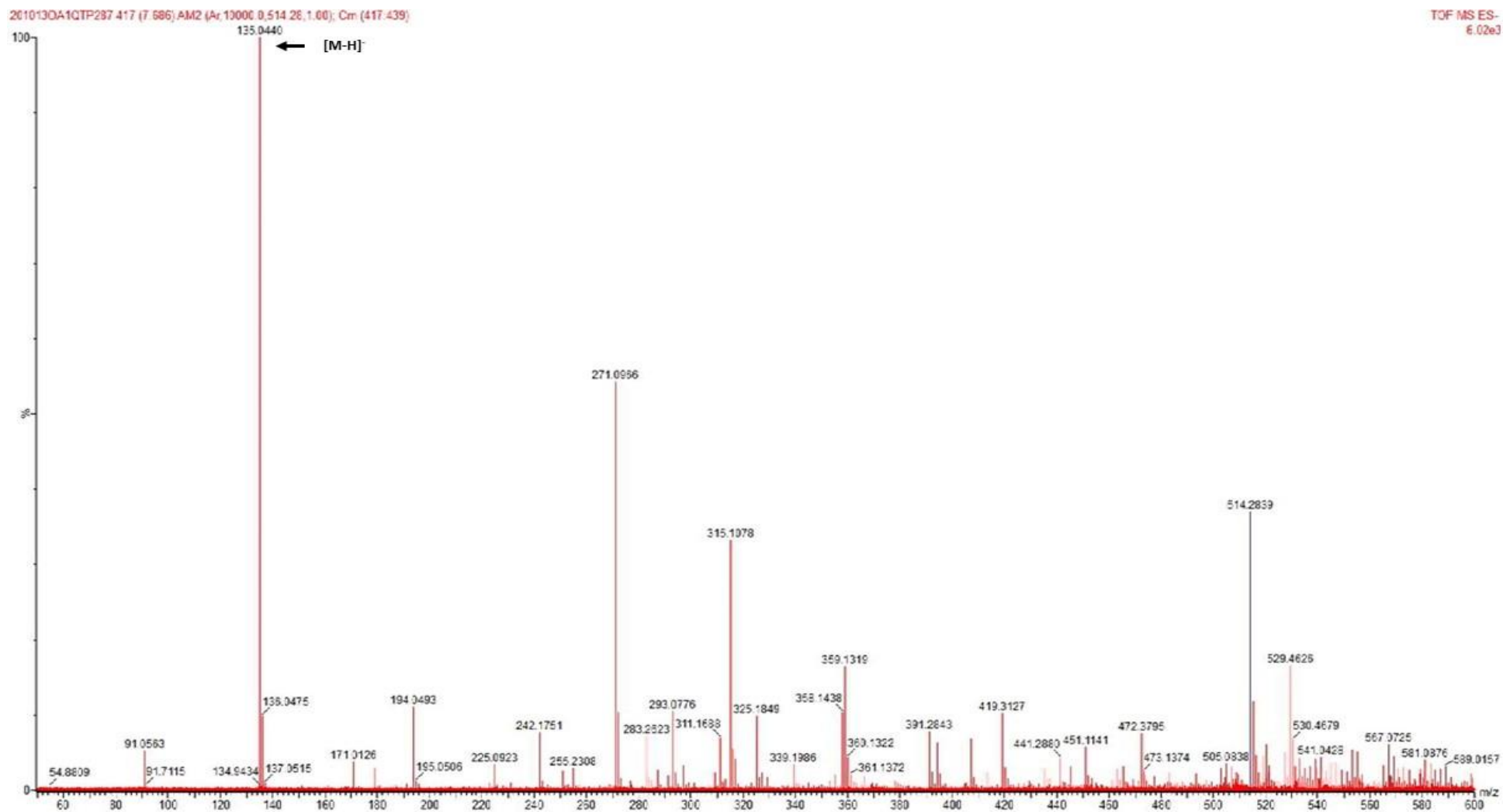
Figure 3.89: ESI-MS spectrum of compound OM7 showing peak ion at *m/z* 135.04.

216

oal-Aug16-2019-4 10 1 C:\Users\Omaish\Desktop'
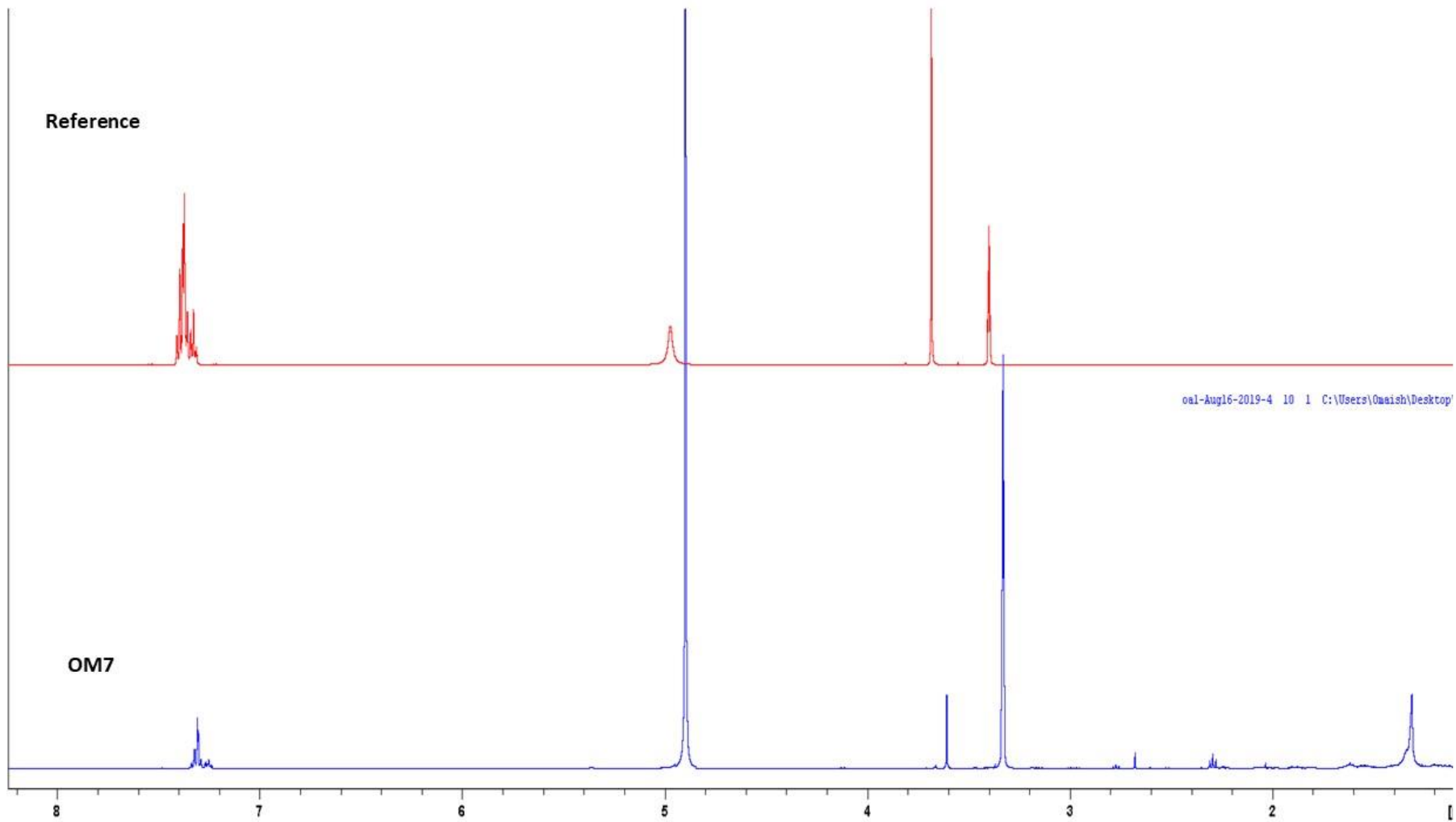
Figure 3.90: Comparison of ¹H NMR spectra of the reference (phenylacetic acid) and compound OM7.

3.3   Biological results

3.3.1 Cross streak assay

Fourteen isolates were subjected to the cross-streak assay in order to identify if they had the ability to inhibit the growth of resistant- and susceptible-strains. Eight bacterial strains were used in this assay. The results are shown below in **(Table 3.16).**

Table 3.16: The zone of inhibition of the cross-streak assay of bacterial isolates in mm.

	S. aureus	SA-1199B	eMRSA-15	XU212	*B. subtilis*	*E. coli*	*P. aeruginosa*	*K. pneumoniae*
AH-D1	3	0	0	1	1	0	0	0
AH-E1	2.5	0	0	2	6	1	0	0
AR-F7	9.5	10	8.5	5	9	0	0	7.5
AR-G2	28	18	11	15	3	1	0	2
GH-C1	16	14	11	2.5	10	5	0	4
GH-C8	14	11	13	14	9	8	0	7
GH-C11	8	10.5	14.5	7.5	9.5	8.5	0	6.5
GH-D4	12	20	23	19	10	7	0	10
GH-D6	14	11	13	19	6	2	0	5
KH-A1	8.5	4.5	7	14	10	0	0	8
KH-B2	18	18	17	18	6	2	0	5
TH-C4	11.5	13	9	11	3	1.5	0	7.5
TH-C8	18	16	15	16	4	1	0	3
TB-A3	23	19	13	15	19	8	0	9

As exhibited in **(Table 3.16)**, the tested isolates illustrated antibacterial activity against resistant- and susceptible-strains, specifically in Gram-positive bacteria. *P. aeruginosa* was the only strain that demonstrated lack of susceptibility to all compounds produced from the isolates. In general, bacterial isolates from the **GH** spring such as **GH-C1, GH-C8** and **GH-C11** showed the highest activity among the other isolates. In contrast, the **AH-D1** isolate showed the lowest activity and was only against Gram-positive organisms. The **AR-G2** and **TB-A3** isolates exhibited the highest activity against *S. aureus* with zones of inhibition of approximately 28 and 23 mm, respectively. Moreover, the **GH-D4** (10 mm) and **TB-A3** (9 mm) isolates showed more activity against *K. pneumoniae* than the other bacterial isolates.

3.3.2 Disc diffusion results

The methanol extracts of 14 isolates were subjected to a disc diffusion assay as an initial step to determine their antibacterial activities **(Table 3.17).** Generally, all isolates were more active against Gram-positive bacteria than Gram-negative microbes. The **AH-D1** isolate was active only against *S. aureus* at 2.5 mm. However, three isolates illustrated weak antibacterial activity against *K. pneumoniae*; these isolates were **GH-C8**, **KH-A1** and **TH-C4**. *P. aeruginosa* was not susceptible to compounds produced by any of the tested isolates. Some bacterial isolates demonstrated weak activity against both *B. subtilis* and *E. coli*. The **KH-A1** isolate showed noteworthy activity against both MRSA and XU212 strains in comparison to the other isolates. On the other hand, the **AR-G2** and **TH-C4** isolates illustrated strong activity toward *S. aureus* with zones of inhibition of 11 and 11.5 mm, respectively.

Table 3.17: The zone of inhibition of the disc diffusion assay of bacterial isolates in mm.

	S. aureus	SA-1199B	eMRSA-15	XU212	*B. subtilis*	*E. coli*	*P. aeruginosa*	*K. pneumoniae*
AH-D1	2.5	0	0	0	0	0	0	0
AH-E1	3	0	1	0	1.5	1	0	0
AR-F7	4	2	2.5	1	1	0	0	0
AR-G2	11	4.5	3	1.5	0	1	0	0
GH-C1	7.5	3	3	0	0	1.5	0	0
GH-C8	9.5	3.5	5.5	4	1.5	2.5	0	1.5
GH-C11	8	4	6.5	2.5	1	1	0	0
GH-D4	6	5.5	7	3.5	2	2	0	0
GH-D6	6.5	2	4.5	2.5	1	0	0	0
KH-A1	8.5	4.5	7	6	2	0	0	1
KH-B2	7.5	2.5	3	1.5	0	1.5	0	0
TH-C4	11.5	3	1.5	1	0	1.5	0	1
TH-C8	5.5	4.5	4.5	2	0	0	0	0
TB-A3	5.5	2.5	3	1	0	1	0	0
Control	23	12	22	13	18	19	19	21

3.3.3 MIC assay results of extracts

The MIC assay was used to assess the activity of methanol extracts for all isolates. **(Table 3.18)** displays the results of these isolates. The extract from the **TH-C4** isolate showed the highest antibacterial activity against the antimicrobial-susceptible- and resistant-

strains in this assay. It was active against all strains except *P. aeruginosa*, which had no susceptibility to extracts from all the 14 isolates tested. Furthermore, there were extracts from two isolates that exhibited mild activity against *K. pneumoniae*; these isolates were **TH-C4** at 256 µg/mL and **GH-C8** at 512 µg/mL. Against *E. coli*, extracts from five isolates showed mild antibacterial activity; **GH-C1**, **GH-C8** and **GH-C11** at 512 µg/mL as well as **AR-G2** and **TH-C4** at 256 µg/mL. In terms of the Gram-positive organisms, all extracts from bacterial isolates demonstrated good activity against *S. aureus,* with some having against MRSA and SA1199B. The extract from the **AH-D1** isolate only demonstrated activity against the standard *S. aureus* strain at 512 µg/mL. In comparison to the control, the results of all tested isolates tended to be mild with the exception of **TH-C4,** which could be considered as moderate activity.

Table 3.18: The results of the MIC assay of methanolic extracts from bacterial isolates in µg/mL.

	S. aureus	**SA-1199B**	**eMRSA-15**	**XU212**	*B. subtilis*	*E. coli*	*P. aeruginosa*	*K. pneumoniae*
AH-D1	512	>512	>512	>512	>512	>512	>512	>512
AH-E1	128	256	128	>512	>512	>512	>512	>512
AR-F7	256	>512	256	512	>512	>512	>512	>512
AR-G2	128	512	256	256	512	256	>512	>512
GH-C1	256	256	512	256	>512	512	>512	>512
GH-C8	128	256	128	512	512	512	>512	512
GH-C11	128	512	256	512	>512	512	>512	>512
GH-D4	512	512	512	>512	>512	>512	>512	>512
GH-D6	256	512	512	>512	>512	>512	>512	>512
KH-A1	256	256	256	512	512	>512	>512	>512
KH-B2	256	512	>512	512	512	>512	>512	>512
TH-C4	128	256	128	128	512	256	>512	256
TH-C8	512	512	512	512	>512	>512	>512	>512
TB-A3	256	512	>512	512	>512	>512	>512	>512
Control	1	16	1	16	1	1	1	1

3.3.4 MIC assay results of isolated compounds

Seven compounds were isolated from six different springs. These compounds were subjected to the MIC assay in order to find out if they had antibacterial activity or not **(Table 3.19)**. According to the findings of the MIC assay, compound **OM6** exhibited the strongest antimicrobial activity compared to the other compounds. It was active against all susceptible-

and resistant-strains except *P. aeruginosa.* Compounds **OM1, OM5** and **OM7** showed mild and (narrow-spectrum activity) against only the Gram-positive bacteria. In contrast, compounds **OM3**, **OM4** and **OM6** illustrated good activity (broad-spectrum activity) toward both Gram-positive and Gram-negative strains. Compounds **OM3** and **OM6** were the only natural products that demonstrated activity against *K. pneumoniae* at approximately 512 μg/mL and 256 μg/mL, respectively. Furthermore, Compound **OM2** was not active against all tested strains.

Table 3.19: The results of the MIC assay of isolated compounds in μg/mL.

	S. aureus	**SA-1199B**	**eMRSA-15**	**XU212**	*B. subtilis*	*E. coli*	*P. aeruginosa*	*K. pneumoniae*
OM1	128	256	256	512	>512	>512	>512	>512
OM2	>512	>512	>512	>512	>512	>512	>512	>512
OM3	128	256	256	512	>512	512	>512	512
OM4	256	256	512	512	512	512	>512	>512
OM5	256	512	512	>512	>512	>512	>512	>512
OM6	128	256	128	256	256	256	>512	256
OM7	128	256	256	512	512	>512	>512	>512
Control	1	16	1	16	1	1	1	1

In comparison with the literature, compound **OM1** (*N*-acetyltryptamine) has been reported to have antibacterial activity against *B. subtilis*, *B. cereus*, *S. aureus*, *E. coli,* MRSA and *Pseudomonas syringae pv. Actinidiae* (Zhang *et al*., 2013). Furthermore, it has been published as an antifungal and antibacterial agent with activity against *Fusarium* spp., *Verticillium dahlia* and the Gram-positive bacterium *Micrococcus luteus* (Mehdi *et al.,* 2009). Moreover, it has been reported that isovaleric acid (compound **OM4**) has antibacterial properties (Hayashida-Soiza *et al*., 2008; Huang *et al*., 2011). For compound **OM5** (ethyl-4-ethoxybenzoate), it has been described as an anti-biofilm agent (Campbell *et al*., 2019). In addition, compound **OM7** (phenylacetic acid) has been shown to demonstrate antibacterial and antifungal activities against *E. coli*, MRSA, *A. fumigatus* and *C. albicans*, (Lacret *et al*., 2015). Moreover, it demonstrated antimicrobial activity against *E. coli* and *Ralstonia solanacearum* (Zhu *et al*., 2011), *S. aureus, E. coli*, *C. albicans*, *Pseudomonas aeruginosa*

and *B. subtilis* (Kim *et al.*, 2004). It has also been found as an antibacterial agent (Erdmann, 1987) and antifungal compound (Hwang *et al.*, 2001).

4 General discussion

The purpose of this study was to discover novel antibiotics and to evaluate their activities against different bacterial strains. As previously discussed, the emergence of bacterial resistance is regarded as a big challenge in this era, as such some antibiotics now lack effectiveness in fighting infectious diseases. As a result, searching for novel antibiotics from different natural sources has increased. In addition, research into how bacteria develop resistance to drugs is being undertaken in order to understand the mechanism of bacterial resistance and find suitable treatments. This project focused on discovering novel antibiotics from hot springs water in Saudi Arabia.

There are several thermal springs in Saudi Arabia and most of them are used by domestic people for curing infectious diseases. For this reason, six different springs were selected to be studied for their antibacterial activities. While, there are several studies on four of these springs, this thesis also reports on two springs, **AH** and **TB**, which have not previously been investigated. In addition, most previous studies have concentrated on the chemical compositions of hot spring water, with a few reporting on the living organisms that reside in these springs. There are limited reports regarding the isolation of antibacterial compounds from microorganisms from these springs, which was the motivation for this study.

Water samples from six different thermal springs from Saudi Arabia were tested in order to find antibiotic-producing bacteria. 43 isolates were discovered from these springs; however, only 14 isolates were selected for further analysis. Generally, the outcomes of the cross-streak assay for these isolates showed that there was antimicrobial activity against most resistant- and susceptible-bacterial strains used in this project. All samples illustrated antibacterial activity against the tested Gram-positive bacteria to a greater extent than

Gram-negative bacteria except for *P. aeruginosa*, which was the only strain that had no inhibition against all isolates. In common, isolates from the **GH** spring had the strongest activity in comparison with the other isolates. For example, the **GH-D4** isolate inhibited the growth of MRSA and SA-1199B at approximately 23 mm and 20 mm from the culture, respectively. However, other isolates from different springs showed less activity. For instance, the zone of inhibition of the **AH-D1** isolate against *B. subtilis* and XU212 was 1 mm.

In terms of antibacterial potential, the **GH-D4, TB-A3** and **AR-G2** isolates demonstrated the highest level of activity against resistant- and susceptible-bacterial strains in comparison with other samples. The **GH-C1**, **GH-C8** and **TH-C8** isolates were in the second position with respect to antibacterial activity. In contrast, the **AH-E1** isolate showed mild activity, whereas the **AH-D1** isolate illustrated very weak activity against only three strains; *S. aureus*, *B. subtilis* and XU212. Care should be taken in interpreting this result; however, as some active compounds may have poor permeability in the agar and be present at a low concentration.

According to the findings of the Gram-stain assay, phylogenetic analysis and 16S rRNA gene sequencing, all isolates were from the genus *Bacillus.* It is known that the *Bacillus* spp. are able to thrive in harsh environments such as thermal springs. A large number of *Bacillus* species have been isolated from different hot springs around the world.

Four different species have been found in Saudi springs based on this project: *B. cereus*, *B. pumilus*, *B. paralicheniformis* and *B. licheniformis*. These results, moreover, were confirmed by the findings of phylogenetic tree analysis that showed all tested isolates had a high percentage of similarity of more than 70% except for two isolates that represented acceptable percentages: **AH-E1** at 69% and **GH-D6** at 67%. The recent species concept is

based on two organisms sharing a DNA–DNA hybridization rate more than 70% (Ludwig and Klenk, 2005).

B. cereus has previously been isolated from the **GH**, **AR** and **KH** springs (Yasir *et al.*, 2019), but this is the first report of this organism being isolated from the **AH** spring. *B. licheniformis* has been discovered from the **TH** (Alrumman *et al.*, 2018) **GH**, **AR** and **KH** springs (Yasir *et al.*, 2019). Again, this is the first time it has been isolated from the **AH** spring. Furthermore, *B. pumilus* and *B. paralicheniformis* have been previously found in the **KH** spring (Yasir *et al.*, 2019). However, discovering them from the **GH**, **TH** and **AR** springs is reported here for the first time.

Seven compounds were isolated from these *Bacillus* spp. Two of which were new compounds and the rest were known. N^1-(*N*, *N*-dimethylcarbamimidoyl)-N^1-methylterephthalamide (**OM3**) was obtained from *B. paralicheniformis* (**GH-C8**) and 3-methyl-*2H*,*7H*-pyrano[*2,3-b*]pyran-2,7-dione (**OM6**) was discovered from *Bacillus paralicheniformis* (**AR-G2**).

By looking at the ^{1}H NMR spectrum of **OM3**, there were major and minor peaks. The major peaks were belonging to the proposed structure (**OM3**), while the minor peaks were thought to be some impurities. Based on the integration of peaks as well as the HMBC and COSY spectra, these minor peaks did not have any connection to the proposed structure. Furthermore, the probability that the activity might belong to the minor compounds was weak because the proposed structure included a guanidine moiety, which is known for its antimicrobial action (Li *et al.*, 2018). Additionally, the LC-MS and MS (high resolution) data confirmed the molecular weight of the proposed structure. Furthermore, by searching in SciFinder, one compound was found to have 84% similarity of **OM3**. This compound is

known as *N*-[(dimethylamino)iminomethyl]-*N*-methyl-Benzamide **(Figure 3.91)**. In general, **OM3** was believed to be new based on the analytical results.
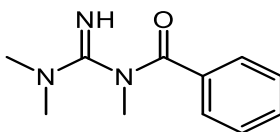
Figure 3.91: Structure of *N*-[(dimethylamino)iminomethyl]-*N*-methyl-Benzamide.

In the same way, the ^{1}H NMR spectrum of **OM6** showed major and minor peaks. The major peaks gave the proposed structure (**OM6**), whereas the minor peaks were believed to be some impurities. According to the integration of peaks and the results of the HMBC and COSY spectra, these minor peaks did not show any linking to the proposed structure. Moreover, the antibacterial activity was thought to belong to the proposed structure because it is classified as pyranpyrandione, which is reported to have antibacterial activity (Goel *et al.*, 2005). Additionally, the proposed structure might consider as a coumarin-like structure, which is known for their antimicrobial actions. Furthermore, the LC-MS and MS (high resolution) data confirmed the molecular weight of the proposed structure. By searching in SciFinder, one compound was found to have 84% similarity of **OM6**. This compound is known as 2*H*,7*H*-Pyrano[2,3-*b*]pyran-2,7-dione **(Figure 3.92).**
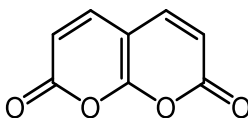
Figure 3.92: Structure of 2*H*,7*H*-Pyrano[2,3-*b*]pyran-2,7-dione.

N-acetyltryptamine (**OM1**) has been found in different organisms such as *Streptomyces* spp. (Lin *et al.*, 2008) and *Intrasporangium* (Okudoh and Wallis, 2012). In *Bacillus* spp., it has been reported that *B. cereus* was able to produce *N*-acetyltryptamine

as a metabolite of tryptamine (Hutzinger, 1969). However, it was reported for the first time to be isolated from *B. pumilus*.

Cholesterol (**OM2**) has previously been found in some bacteria such as *Streptomyces griseus*, *B. megaterium* (Uwajima and Terada, 1976). Some strains of *Streptomyces*, *Bacillus* and *Pseudomonas* form cholesterol esterase that has a pivotal role in the metabolism and absorption of cholesterol in living organisms (Uwajima and Terada, 1976). In this project, cholesterol was isolated from *B. pumilus*. It has been reported that *B. pumilus* has the ability to produce cholesterol oxidase that is capable of degrading cholesterol (Wali *et al*., 2019). In common, cholesterol is naturally found in cell membranes of both animals and bacteria (Palmer, 2004). For this reason, it is normal to isolate cholesterol from bacteria because it is considered an essential content of their cell membrane.

Isovaleric acid (**OM4**) has previously been isolated from some bacteria such as *B. subtilis* (Hong *et al*., 2017) and *Megasphaera hexanoica* spp*. Nov* (Jeon *et al*., 2017). In this study, isovaleric acid was isolated from *B. pumilus* from a Saudi spring, which supports a study that stated that *B. pumilus* was able to produce isovaleric acid (De La Cochetière-Collinet and Larsson, 1984). In general, isovaleric acid and other chemicals like isocaproic and 2-methylbutyric acids are thought to be induced by L-leucine catabolism in anaerobic bacteria (Díaz-Pérez *et al*., 2016).

Ethyl-4-ethoxy benzoate (**OM5**) was isolated from *B. licheniformis* from the **AH** spring. This is consistent with the study of Sharma *et al*., 2010, who isolated the same compound from the same species*.*

This is the first report of phenylacetic acid (**OM7**) being produced from *B. pumilus*. However, it has been isolated from some *Bacillus* spp. such as *B. licheniformis* (Kim *et al*., 2004) and *B. cereus* (Hwang *et al*., 2001). Moreover, it has previously been identified in the

same spring (**TH**), but from a different organism, *Streptomyces* spp. (Al-Dhabi *et al.*, 2019). Phenylacetic acid (also known as benzene acetic acid or α-toluic acid) has drawn the attention of the pharmaceutical industry due to its various biological properties such as antioxidant, anti-inflammatory and antifungal properties as well as its ability to inhibit quorum sensing in *P. aeruginosa* (Musthafa *et al.*, 2012). It has a prevalent distribution in nature and it is formed metabolically from L-phenylalanine (Burkhead *et al.*, 1998). In addition, it is used as a natural flavour compound (Samra *et al.*, 2018) and a plant growth promoter (Cook, 2019).

The MIC findings showed that the tested extracts had antimicrobial potential against all tested organisms except for *P. aeruginosa.* The activity ranged from mild to moderate. For instance, the extract from the **TH-C4** isolate had the highest antibacterial activity; in contrast, the extract from the **AH-D1** isolate only showed activity against the standard *S. aureus* strain; the extract exhibited a high MIC value of 512 µg/mL. For isolated compounds, they showed mild to moderate activity against all organisms evalated except for *P. aeruginosa.* Compound **OM2** exhibited no activity, whilst compound **OM6** exhibited the highest antibacterial activity.

Inspection of the outcomes of the cross-streak assay and disc diffusion and comparing them to MIC values of isolated compounds, the MICs seem to be weak in comparison with the strongest antibacterial action observed for all isolates in the cross-streak assay. This could be attributed to some factors such as the concentration of antibiotics in the agar, their permeability and solubility (the chemical structure of antibiotics) as well as the components of blood agar, which could modify the mobility of antibiotics in the agar. Furthermore, the active constituents might lose activity during chromatographic procedures such as sticking to the silica gel or being oxidized by it. Moreover, some

compounds may work together to give the antibacterial activity in a synergistic fashion, and their separation during the isolation process may lead to mild activity. For example, the fraction 6 of the methanol extract of **KH-B2** strain showed three active bands against *S. aureus* in the overlay assay **(Figure 3.93).**
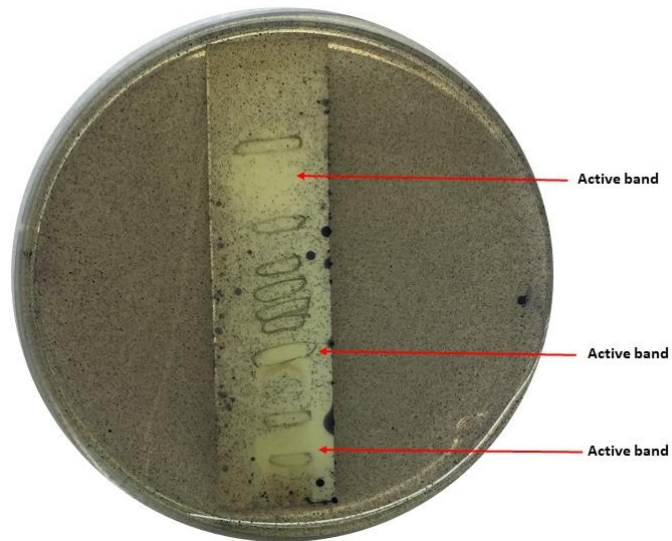
Figure 3.93: The overlay assay of the fraction 6 of KH-B2.

5 Conclusion

In total, 32 water samples were collected from six different hot springs in Saudi Arabia. Several biological and microbiological assays were used to assess the antibacterial activity of samples against antimicrobial-resistant- and susceptible-bacterial strains and to identify the genus and species of the antibiotic-producing bacteria. Moreover, chromatographic and spectroscopic techniques were utilized to isolate the active compounds and to obtain the structural elucidation.

Fourteen antibacterial-producing isolates were isolated from these springs and were identified as *Bacillus paralicheniformis* (6), *Bacillus licheniformis* (2), *Bacillus pumilus* (5) and *Bacillus cereus* (1). Additionally, seven compounds were isolated from these isolates: five of them are known (**OM1**, **OM2**, **OM4**, **OM5** and **OM7**) and two components (**OM3** and **OM6**) are new and may require further evaluation.

The findings of the MIC assay illustrated that all isolated compounds exhibited mild to moderate antibacterial activity against tested strains except **OM2**, which gave no activity. Furthermore, **OM6** was the only compound that showed moderate activity.

6 Future Work

Due to constraints and limitations, some experiments were not performed. Based on this study, it is recommended that future studies be carried out on the following:

Identification of Bacterial Strains

From the 43 bacterial isolates isolated in this project, only 14 isolates were subjected to further analysis. Further work needs to be done on the remaining strains (29 isolates) in order to identify which bacterial family and genus they belong to.

Isolation of Bioactive Compounds

For the 14 isolates, only 6 isolates were subjected to a large-scale fermentation to isolate the active constituents. Further investigation will be required for the remaining isolates (8 isolates) to find out the bioactive compounds.

Identification of Compounds

Some of the compounds isolated in this study were not obtained in sufficient quantity. Consequently, looking for the optimal fermentation method in order to obtain enough quantity of compounds. Furthermore, an additional HPLC purification step might be required to isolate pure samples. Moreover, studies to optimise the activities of the bioactive compounds so that the hits can be further developed as antibacterial leads or as adjuvants against the resistant strains can be performed.

Mechanisms of Action Assays

Further work to understand the mechanism of action of the active agents should also be undertaken in order to discover how each pure compound works in inhibiting bacteria growth.

References

Aanniz, T., Ouadghiri, M., Melloul, M., Swings, J., Elfahime, E., Ibijbijen, J., and Amar, M., 2015. Thermophilic bacteria in Moroccan hot springs, salt marshes and desert soils. *Brazilian Journal of Microbiology*, 46 (2), pp. 443-453.

Abebe, E., Tegegne, B., and Tibebu, S., 2016. A review on molecular mechanisms of bacterial resistance to antibiotics. *European Journal of Applied Science*, 8 (5), pp. 301-310.

Abussaud, M.J., Alanagreh, L. and Abu-Elteen, K., 2013. Isolation, characterization and antimicrobial activity of *Streptomyces* strains from hot spring areas in the northern part of Jordan. *African Journal of Biotechnology*, 12 (51), pp. 7124-7132.

Acharya, T., MG 2013, *Gene Transfer Mechanism in Bacteria and It's types,* photograph, viewed August 2017,<https://microbeonline.com/key-information-regarding-gene-transfer-mechanism-bacteria.

Acharya, T., MG 2013. *Teichoic Acid/Lipoteichoic acid: Characteristics and Medical Importance,* photograph, viewed August 2017, http://microbeonline.com/teichoic-acid-of-gram-positive-bacteria-characteristics-and-medical-importance.

Acharya, T., MG 2013. *Colony Morphology of Bacteria; How to Describe Bacterial Colonies?,* photograph, viewed August 2020, https://microbeonline.com/colony-morphology-bacteria-describe-bacterial-colonies/.

Adiguzel, A., Ozkan, H., Baris, O., Inan, K., Gulluce, M. and Sahin, F., 2009. Identification and characterization of thermophilic bacteria isolated from hot springs in Turkey. *Journal of Microbiological Methods*, *79*(3), pp. 321-328.

Agersø, Y., Bjerre, K., Brockmann, E., Johansen, E., Nielsen, B., Siezen, R., and Zeidan, A. A., 2019. Putative antibiotic resistance genes present in extant *Bacillus licheniformis* and *Bacillus paralicheniformis* strains are probably intrinsic and part of the ancient resistome. *Plos One*, 14 (1), pp. 1-24.

Akram, W., Anjum, T., and Ali, B., 2016. Phenylacetic acid is ISR determinant produced by *Bacillus fortis* IAGS162, which involves extensive re-modulation in metabolomics of tomato to protect against *Fusarium wilt. Frontiers in Plant Science*, 7, pp. 1-12.

Alanis, A.J., 2005. Resistance to antibiotics: are we in the post-antibiotic era?. *Archives of Medical Research*, 36 (6), pp. 697-705.

Al-Dayel, M., 1988. Geothermal resources in Saudi Arabia. *Geothermics*, 17 (2-3), pp. 465-476.

Al-Dhabi, N.A., Esmail, G.A., Duraipandiyan, V., Arasu, M.V. and Salem-Bekhit, M.M., 2016. Isolation, identification and screening of antimicrobial thermophilic *Streptomyces* sp. Al-Dhabi-1 isolated from Tharban hot spring, Saudi Arabia. *Extremophiles*, 20 (1), pp. 79-90.

Al-Dhabi, N. A., Esmail, G. A., Duraipandiyan, V., and Arasu, M. V., 2019. Chemical profiling of *Streptomyces* sp. Al-Dhabi-2 recovered from an extreme environment in Saudi Arabia as a novel drug source for medical and industrial applications. *Saudi Journal of Biological Sciences*, 26 (4), pp. 758-766.

Alexandri, E., Ahmed, R., Siddiqui, H., Choudhary, M. I., Tsiafoulis, C. G., and Gerothanassis, I. P., 2017. High resolution NMR spectroscopy as a structural and analytical tool for unsaturated lipids in solution. *Molecules*, 22 (10), pp.1-72.

Alghadeer, S., Aljuaydi, K., Babelghaith, S., Alhammad, A., and Alarifi, M. N., 2018. Self-medication with antibiotics in Saudi Arabia. *Saudi Pharmaceutical Journal*, 26 (5), pp. 719-724.

Allen, H.K., Donato, J., Wang, H.H., Cloud-Hansen, K.A., Davies, J. and Handelsman, J., 2010. Call of the wild: antibiotic resistance genes in natural environments. *Nature Reviews. Microbiology*, 8 (4), pp. 251-259.

Alrumman, S., Mostafa, Y. S. M., Al-Qahtani, S., and Taha, T. H. T., 2018. Hydrolytic Enzyme Production by Thermophilic Bacteria Isolated from Saudi Hot Springs. *Open Life Sciences*, 13 (1), 470-480.

Alrumman, S. A., Mostafa, Y. S., Al-Qahtani, S. T., Sahlabji, T., and Taha, T. H., 2019. Antimicrobial Activity and GC-MS Analysis of Bioactive Constituents of Thermophilic Bacteria Isolated from Saudi Hot Springs. *Arabian Journal for Science and Engineering*, 44 (1), pp. 75-85.

Alsaleh, M. A., 2017. Natural springs in northwest Saudi Arabia. *Arabian Journal of Geosciences*, 10 (15), pp. 1-13.

Aminov, R., 2017. History of antimicrobial drug discovery: Major classes and health impact. *Biochemical Pharmacology*, 133, pp. 4-19.

Andersson, D.I. and Hughes, D., 2010. Antibiotic resistance and its cost: is it possible to reverse resistance?. *Nature Reviews. Microbiology*, 8 (4), pp. 260-271.

Andreeva, I.S., Morozov, I.V., Pechurkina, N.I., Morozova, O.V., Ryabchikova, E.I., Saranina, I.V., Emel'yanova, E.K., Puchkova, L.I., Torok, T.T., Vlasov, V.V. and Repin, V.E., 2010. Isolation of bacteria of the genus *Paenibacillus* from soil and springs of the Valley of Geysers (Kamchatka). *Microbiology*, 79 (5), pp. 696-704.

Andrianasolo, E. H., Haramaty, L., Rosario-Passapera, R., Vetriani, C., Falkowski, P., White, E., and Lutz, R., 2012. Ammonificins C and D, hydroxyethylamine chromene derivatives from a cultured marine hydrothermal vent bacterium, *Thermovibrio ammonificans*. *Marine Drugs*, 10 (10), pp. 2300-2311.

Antipova, T. V., Zhelifonova, V. P., Baskunov, B. P., Kochkina, G. A., Ozerskaya, S. M., and Kozlovskii, A. G., 2018. Exometabolites the *Penicillium* fungi isolated from various high-latitude ecosystems. *Microbiology*, 87 (5), pp. 642-651.

Athukorala, S. N., Fernando, W. D., and Rashid, K. Y., 2009. Identification of antifungal antibiotics of *Bacillus* species isolated from different microhabitats using polymerase chain reaction and MALDI-TOF mass spectrometry. *Canadian Journal of Microbiology*, 55(9), pp. 1021-1032.

Bal, D., Kraska-Dziadecka, A., Gradowska, W., and Gryff-Keller, A., 2008. Investigation of a wide spectrum of inherited metabolic disorders by 13C NMR spectroscopy. *Acta Biochimica Polonica*, 55 (1), pp. 107-118.

Balcázar, J. L., 2020. Implications of bacteriophages on the acquisition and spread of antibiotic resistance in the environment. *International Microbiology*, pp. 1-5.

Balouiri, M., Sadiki, M., and Ibnsouda, S. K., 2016. Methods for in vitro evaluating antimicrobial activity: A review. *Journal of Pharmaceutical Analysis*, 6 (2), pp. 71-79.

Bartlett, J. M., and Stirling, D. (Eds.)., 2003. *PCR protocols* (Vol. 226). Totowa, NJ: Humana Press. pp. 3

Basahy, A.Y., 1994. Water chemistry of hot springs in Gizan area of Saudi Arabia. *Journal King Saud University*, 6 (1), pp. 23-29.

Battista, J. R., 2016. *Deinococcus–Thermus* Group. *Encyclopedia of Life Sciences*, pp. 1-12. http://www.els.net

Bazuhair, A.S. and Hussein, M.T., 1990. Springs in Saudi Arabia. *Journal King Abdulaziz University Earth Science*, 3, pp. 251-258.

Bazuhair, A. A., Hussein, M. T., and Hamza, M. S., 1990. Comparative hydrochemical study of water springs in Saudi Arabia. *International Journal of Water Resources Development*, 6 (2), pp. 143-150.

Beccaria, M., and Cabooter, D., 2020. Current developments in LC-MS for pharmaceutical analysis. *Analyst*, 145 (4), pp. 1129-1157.

Běhal, V., 2003. Alternative sources of biologically active substances. *Folia Microbiologica*, 48 (5), pp. 563-571.

Bele, A. A., and Khale, A., 2011. An overview on thin layer chromatography. *International Journal of Pharmaceutical Sciences and Research*, 2 (2), pp. 256-267.

Bellisola, G., and Sorio, C., 2012. Infrared spectroscopy and microscopy in cancer research and diagnosis. *American Journal of Cancer Research*, 2 (1), pp. 1-21.

Beveridge, T. J., 2001. Bacterial Cells. *Encyclopedia of Life Sciences,* pp. 1-10. http://www.els.net.

Beveridge, T. J., 2001. Bacterial cell wall. *Encyclopedia of Life Sciences*, pp. 1-7. http://www.els.net.

Bhargav, S., Panda, B. P., Ali, M., and Javed, S., 2008. Solid-state fermentation: an overview. *Chemical and Biochemical Engineering Quarterly*, 22 (1), pp. 49-70.

Bharti, S. K., and Roy, R., 2012. Quantitative 1H NMR spectroscopy. *Trends in Analytical Chemistry*, 35, pp. 5-26.

Binda, E., Marinelli, F., and Marcone, G. L., 2014. Old and new glycopeptide antibiotics: action and resistance. *Antibiotics*, 3 (4), pp. 572-594.

Blair, J.M., Webber, M.A., Baylay, A.J., Ogbolu, D.O. and Piddock, L.J., 2015. Molecular mechanisms of antibiotic resistance. *Nature Reviews. Microbiology*, 13 (1), pp. 42-51.

Bobis, O., Dezmirean, D. S., Tomos, L., Chirila, F., and Marghitas, L. A., 2015. Influence of phytochemical profile on antibacterial activity of different medicinal plants against gram-positive and gram-negative bacteria. *Applied Biochemistry and Microbiology*, 51 (1), pp. 113-118.

Bockstael, K., and Aerschot, A., 2009. Antimicrobial resistance in bacteria. *Open Medicine*, 4 (2), pp. 141-155.

Böhlendorf, B., Bedorf, N., Jansen, R., Trowitzsch-Kienast, W., Höfle, G., Forche, E., and Reichenbach, H., 1996. Antibiotics from gliding bacteria, LXXIII indole and quinoline derivatives as metabolites of tryptophan in myxobacteria. *Liebigs Annalen*, 1996 (1), pp. 49-53.

Bonch-Osmolovskaya, E., 2008. Aquificales. *Encyclopedia of Life Sciences*, pp. 1-7. http://www.els.net.

Bonch-Osmolovskaya, E., 2008. Thermotogales. *Encyclopedia of Life Sciences*, pp. 1-7. http://www.els.net.

Boyle, R., 2017. Eukaryotic origins and the Proterozoic Earth system: A link between global scale glaciations and eukaryogenesis?. *Earth-Science Reviews*, 174, pp. 22-38.

Brack, C., Mikolasch, A., Schlueter, R., Otto, A., Becher, D., Wegner, U., and Schauer, F., 2015. Antibacterial metabolites and bacteriolytic enzymes produced by *Bacillus pumilus* during bacteriolysis of *Arthrobacter citreus*. *Marine Biotechnology*, 17 (3), pp. 290-304.

Bratchkova, A., and Ivanova, V., 2011. Bioactive metabolites produced by microorganisms collected in Antarctica and the Arctic. *Biotechnology and Biotechnological Equipment*, 25 (sup1), pp. 1-7.

Brooks, B. D., and Brooks, A. E., 2014. Therapeutic strategies to combat antibiotic resistance. *Advanced Drug Delivery Reviews*, 78, pp. 14-27.

Burkhead, K. D., Slininger, P. J., and Schisler, D. A., 1998. Biological control bacterium *Enterobacter cloacae* S11: T: 07 (NRRL B-21050) produces the antifungal compound phenylacetic acid in Sabouraud maltose broth culture. *Soil Biology and Biochemistry*, 30 (5), pp. 665-667.

Burns, J., MG 2010, *Hospital Killer: Pseudomonas aeruginosa,* photograph, viewed August 2017,https://microbiologyspring2010.wikispaces.com/Hospital+Killers+Pseudomonas+aeru ginosa

Bush, K., & Bradford, P. A., 2016. β-Lactams and β-lactamase inhibitors: an overview. *Cold Spring Harbor Perspectives in Medicine*, 6 (8), pp. 1-22.

Butler, M. S., Hansford, K. A., Blaskovich, M. A., Halai, R., and Cooper, M. A., 2014. Glycopeptide antibiotics: back to the future. *The Journal of Antibiotics*, 67 (9), pp. 631-644.

Cabezón, E., Ripoll-Rozada, J., Peña, A., De La Cruz, F., and Arechaga, I., 2015. Towards an integrated model of bacterial conjugation. *Federation of European Microbiological Societies Microbiology Reviews*, 39 (1), pp. 81-95.

Cai, H., Archambault, M., and Prescott, J. F., 2003. 16S Ribosomal RNA Sequence—Based Identification of Veterinary Clinical Bacteria. *Journal of Veterinary Diagnostic Investigation*, 15 (5), pp. 465-469.

Calvo, H., Mendiara, I., Arias, E., Gracia, A. P., Blanco, D., and Venturini, M. E., 2020. Antifungal activity of the volatile organic compounds produced by *Bacillus velezensis* strains against postharvest fungal pathogens. *Postharvest Biology and Technology*, 166, pp. 1-10.

Campbell, M., Zhao, W., Fathi, R., Mihreteab, M., and Gilbert, E. S., 2019. *Rhamnus prinoides* (gesho): A source of diverse anti-biofilm activity. *Journal of Ethnopharmacology*, 241, pp. 1-9.

Carattoli, A., 2013. Plasmids and the spread of resistance. *International Journal of Medical Microbiology*, 303 (6-7), pp. 298-304.

Carvalho, I. T., and Santos, L., 2016. Antibiotics in the aquatic environments: a review of the European scenario. *Environment International*, 94, pp. 736-757.

Caulier, S., Nannan, C., Gillis, A., Licciardi, F., Bragard, C., and Mahillon, J., 2019. Overview of the antimicrobial compounds produced by members of the *Bacillus subtilis* group. *Frontiers in Microbiology*, 10 (302), pp. 1-19.

Cava, F., Hidalgo, A. and Berenguer, J., 2009. *Thermus thermophilus* as biological model. *Extremophiles*, 13 (2), pp. 213-231.

Chaudhary, A. S., 2016. A review of global initiatives to fight antibiotic resistance and recent antibiotics՚ discovery. *Acta Pharmaceutica Sinica B*, 6 (6), pp. 552-556.

Chellat, M.F., Raguž, L. and Riedl, R., 2016. Targeting antibiotic resistance. *Angewandte Chemie International Edition*, 55 (23), pp. 6600-6626.

Chen, Y., Liu, M., Chen, S., and Wei, X., 2017. Decreased formation of branched-chain short fatty acids in *Bacillus amyloliquefaciens* by metabolic engineering. *Biotechnology Letters*, 39 (4), pp. 529-533.

Chu, J., Wang, Y., Zhao, B., Zhang, X. M., Liu, K., Mao, L., and Kalamiyets, E., 2019. Isolation and identification of new antibacterial compounds from *Bacillus pumilus*. *Applied Microbiology and Biotechnology*, 103 (20), pp. 8375-8381.

Clardy, J., Fischbach, M. A., and Currie, C. R., 2009. The natural history of antibiotics. *Current Biology*, 19 (11), pp. R437-R441.

Coates, J., 2006. Interpretation of infrared spectra, a practical approach. *Encyclopedia of Analytical Chemistry: Applications, Theory and Instrumentation*, pp. 1-23.

Collins, F. W., O'Connor, P. M., O'Sullivan, O., Rea, M. C., Hill, C., and Ross, R. P., 2016. Formicin–a novel broad-spectrum two-component lantibiotic produced by *Bacillus paralicheniformis* APC 1576. *Microbiology*, 162 (9), pp. 1662-1671.

Cook, S. D., 2019. An historical review of phenylacetic acid. *Plant and Cell Physiology*, 60 (2), pp. 243-254.

Courvalin, P., 2016. Why is antibiotic resistance a deadly emerging disease?. *Clinical Microbiology and Infection*, 22 (5), pp. 405-407.

Cox, G., and Wright, G. D., 2013. Intrinsic antibiotic resistance: mechanisms, origins, challenges and solutions. *International Journal of Medical Microbiology*, 303 (6-7), pp. 287-292.

Cruz-Loya, M., Kang, T. M., Lozano, N. A., Watanabe, R., Tekin, E., Damoiseaux, R., and Yeh, P. J., 2019. Stressor interaction networks suggest antibiotic resistance co-opted from stress responses to temperature. *The International Society for Microbial Ecology Journal*, 13 (1), pp. 12-23.

Dadheech, P.K., Glöckner, G., Casper, P., Kotut, K., Mazzoni, C.J., Mbedi, S. and Krienitz, L., 2013. Cyanobacterial diversity in the hot spring, pelagic and benthic habitats of a tropical soda lake. *FEMS Microbiology Ecology*, 85 (2), pp. 389-401.

Daghrir, R., and Drogui, P., 2013. Tetracycline antibiotics in the environment: a review. *Environmental Chemistry Letters*, 11 (3), pp. 209-227.

Davies, J. and Davies, D., 2010. Origins and evolution of antibiotic resistance. *Microbiology and Molecular Biology Reviews*, 74 (3), pp. 417-433.

Davis, J. A., Kerezsy, A., and Nicol, S., 2017. Springs: conserving perennial water is critical in arid landscapes. *Biological Conservation*, 211, pp. 30-35.

De Bruyn, A., Martin, D. P., and Lefeuvre, P., 2014. Phylogenetic reconstruction methods: an overview. *Molecular Plant Taxonomy*, pp. 257-277.

De la Cochetière-Collinet, M. F., and Larsson, L., 1984. Studies on volatile metabolites of some potentially pathogenic *Bacillus* species, using automated head-space gas chromatography. *Journal of Chromatography B: Biomedical Sciences and Applications*, 305, pp. 178-182.

Decuyper, L., Jukič, M., Sosič, I., Žula, A., D'hooghe, M., and Gobec, S., 2018. Antibacterial and β-lactamase inhibitory activity of monocyclic β-Lactams. *Medicinal Research Reviews*, 38 (2), pp. 426-503.

Desjardins, P., and Conklin, D., 2010. NanoDrop microvolume quantitation of nucleic acids. *Journal of Visualized Experiments*, (45), pp. 1-5.

Devi, P., Wahidullah, S., Rodrigues, C., and Souza, L. D., 2010. The sponge-associated bacterium *Bacillus licheniformis* SAB1: a source of antimicrobial compounds. *Marine Drugs*, 8 (4), pp. 1203-1212.

Dewanjee, S., Gangopadhyay, M., Bhattacharya, N., Khanra, R., and Dua, T. K., 2015. Bioautography and its scope in the field of natural product chemistry. *Journal of Pharmaceutical Analysis*, 5 (2), pp. 75-84.

Dezfully, N. K., and Heidari, A., 2016. Natural bioactive compounds: Antibiotics. *Journal of Fundamental and Applied Sciences*, 8 (2), pp. 674-684.

Díaz-Pérez, A. L., Díaz-Pérez, C., and Campos-García, J., 2016. Bacterial l-leucine catabolism as a source of secondary metabolites. *Reviews in Environmental Science and Bio/Technology*, 15 (1), pp. 1-29.

Dinos, G. P., 2017. The macrolide antibiotic renaissance. *British Journal,* 174, pp. 2967–2983

Dobretsov, S., Abed, R.M., Al Maskari, S.M., Al Sabahi, J.N. and Victor, R., 2011. Cyanobacterial mats from hot springs produce antimicrobial compounds and quorum-sensing inhibitors under natural conditions. *Journal of Applied Phycology*, 23 (6), pp. 983-993.

Dodds, D. R., 2017. Antibiotic resistance: A current epilogue. *Biochemical Pharmacology*, 134, pp. 139-146.

Donachie, W. D., 2002. Binary Fission in Bacteria. *Encyclopedia of Life Sciences*, pp. 1-9. http://www.els.net

Du, Y., Ma, J., Yin, Z., Liu, K., Yao, G., Xu, W., and Wang, C., 2019. Comparative genomic analysis of *Bacillus paralicheniformis* MDJK30 with its closely related species reveals an evolutionary relationship between *B. paralicheniformis* and *B. licheniformis*. *BMC Genomics*, 20 (1), pp. 1-16.

Duan, Y.Y., Ming, H., Dong, L., Yin, Y.R., Zhang, Y., Zhou, E.M., Liu, L., Nie, G.X. and Li, W.J., 2014. *Streptomyces calidiresistens* sp. nov., isolated from a hot spring sediment. *Antonie Van Leeuwenhoek*, 106 (2), pp. 189-196.

Dürre, P., 2015. Clostridia. *Encyclopedia of Life Sciences*, pp. 1-11. http://www.els.net.

Dwivedi, V., Kumari, K., Gupta, S.K., Kumari, R., Tripathi, C., Lata, P., Niharika, N., Singh, A.K., Kumar, R., Nigam, A. and Garg, N., 2015. *Thermus parvatiensis* RLT sp. nov., isolated from a hot water spring, located atop the Himalayan ranges at Manikaran, India. *Indian Journal of Microbiology*, 55 (4), pp. 357-365.

El-Demerdash, A. S., Aggour, M. G., El-Azzouny, M. M., and Abou-Khadra, S. H., 2018. Molecular analysis of integron gene cassette arrays associated multi-drug resistant *Enterobacteriaceae* isolates from poultry. *Cellular and Molecular Biology*, 64 (5), pp. 149-156.

El-Gayar, K. E., Al Abboud, M. A., and Essa, A. M., 2017. Characterization of thermophilic bacteria isolated from two hot springs in Jazan, Saudi Arabia. *Journal of Pure and Applied Microbiology*, 11 (2), pp. 743-752.

Epand, R. M., Walker, C., Epand, R. F., and Magarvey, N. A., 2016. Molecular mechanisms of membrane targeting antibiotics. *Biochimica et Biophysica Acta-Biomembranes*, 1858 (5), pp. 980-987.

Erdmann, G. R., 1987. Antibacterial action of myiasis-causing flies. *Parasitology Today*, 3 (7), pp. 214-216.

Esikova, T. Z., Temirov, Y. V., Sokolov, S. L., and Alakhov, Y. B., 2002. Secondary antimicrobial metabolites produced by thermophilic *Bacillus* spp. strains VK2 and VK21. *Applied Biochemistry and Microbiology*, 38 (3), pp. 226-231.

Fair, R. J., and Tor, Y., 2014. Antibiotics and bacterial resistance in the 21st century. *Perspectives in Medicinal Chemistry*, 6, pp. 25-64.

Favre-Godal, Q., Queiroz, E. F., and Wolfender, J. L., 2013. Latest developments in assessing antifungal activity using TLC-bioautography: a review. *Journal of AOAC International*, 96 (6), pp. 1175-1188.

Feng, X., Liu, X., Luo, Q., and Liu, B. F., 2008. Mass spectrometry in systems biology: an overview. *Mass Spectrometry Reviews*, 27 (6), pp. 635-660.

Fensham, R. J., Silcock, J. L., Powell, O., and Habermehl, M. A., 2016. In search of lost springs: a protocol for locating active and inactive springs. *Groundwater*, 54 (3), pp. 374-383.

Fernandes, P., and Martens, E., 2017. Antibiotics in late clinical development. *Biochemical Pharmacology*, 133, pp. 152-163.

Ferrera, I., and Reysenbach, A. L., 2007. Thermophiles. *Encyclopedia of Life Sciences* pp. 1-9. http://www.els.net

Fields, P. A., 2001. Protein function at thermal extremes: balancing stability and flexibility. *Comparative Biochemistry and Physiology Part A: Molecular and Integrative Physiology*, 129 (2-3), pp. 417-431.

Finley, R. L., Collignon, P., Larsson, D. J., McEwen, S. A., Li, X. Z., Gaze, W. H., and Topp, E., 2013. The scourge of antibiotic resistance: the important role of the environment. *Clinical infectious diseases*, 57 (5), pp. 704-710.

Fotakis, C., Kokkotou, K., Zoumpoulakis, P., and Zervou, M., 2013. NMR metabolite fingerprinting in grape derived products: An overview. *Food Research International*, 54 (1), pp. 1184-1194.

Fontanals, N., Recasens, R. M. M., and Ballarin, F. B., 2010. Overview of the novel sorbents available in solid-phase extraction to improve the capacity and selectivity of analytical determinations. *Contributions to Science*, 6 (2), pp. 199-213.

Friedman, N. D., Temkin, E., and Carmeli, Y., 2016. The negative impact of antibiotic resistance. *Clinical Microbiology and Infection*, 22 (5), pp. 416-422.

Frieri, M., Kumar, K., and Boutin, A., 2017. Antibiotic resistance. *Journal of Infection and Public Health*, 10 (4), pp. 369-378.

Garibyan, L., and Avashia, N., 2013. Research techniques made simple: polymerase chain reaction (PCR). *The Journal of Investigative Dermatology*, 133 (3), pp. 1-4.

Garneau-Tsodikova, S. and Labby, K.J., 2016. Mechanisms of resistance to aminoglycoside antibiotics: overview and perspectives. *Medicinal Chemistry Communications*, 7 (1), pp. 11-27.

Ghernaout, D., and Elboughdiri, N., 2020. Antibiotics resistance in water mediums: background, facts, and trends. *Applied Engineering*, 4 (1), pp. 1-6.

Giampaoli, S., Valeriani, F., Gianfranceschi, G., Vitali, M., Delfini, M., Festa, M.R., Bottari, E. and Spica, V.R., 2013. Hydrogen sulfide in thermal spring waters and its action on bacteria of human origin. *Microchemical Journal*, 108, pp. 210-214.

Gibbons, S., and Udo, E. E., 2000. The effect of reserpine, a modulator of multidrug efflux pumps, on the in vitro activity of tetracycline against clinical isolates of methicillin resistant *Staphylococcus aureus* (MRSA) possessing the tet (K) determinant. *Phytotherapy Research: An International Journal Devoted to Pharmacological and Toxicological Evaluation of Natural Product Derivatives*, 14 (2), pp. 139-140.

Goel, A., Verma, D., and Singh, F. V., 2005. A vicarious synthesis of unsymmetrical meta- and para-terphenyls from 2H-pyran-2-ones. *Tetrahedron letters*, 46 (49), pp. 8487-8491.

Goryacha, O. V., Ilyina, T. V., Kovalyova, A. M., and Kashpur, N. V., 2014. Phytochemical research of *Galium aparine L.* lipophilic complex and study of its antibacterial activity. *The Pharma Innovation* Journal, 3 (1), pp. 7-10.

Gould, K., 2016. Antibiotics: from prehistory to the present day. *Journal of Antimicrobial Chemotherapy*, 71 (3), pp. 572-575.

Grogan, D. W., 2013. Extreme Thermophiles. *Encyclopedia of Life Sciences*, pp. 1-9. http://www.els.net.

Grossman, T. H., 2016. Tetracycline antibiotics and resistance. *Cold Spring Harbor Perspectives in Medicine*, 6 (4), pp. 1-25.

Guerrant, G. O., Lambert, M. A., and Moss, C. W., 1982. Analysis of short-chain acids from anaerobic bacteria by high-performance liquid chromatography. *Journal of Clinical Microbiology*, 16 (2), pp. 355-360.

Hall, J. P., Brockhurst, M. A., and Harrison, E., 2017. Sampling the mobile gene pool: innovation via horizontal gene transfer in bacteria. *Philosophical Transactions of the Royal Society B: Biological Sciences*, 372 (1735), pp. 1-10.

Hao, H., and Starr, D. A., 2019. SUN/KASH interactions facilitate force transmission across the nuclear envelope. *Nucleus*, 10 (1), pp. 73-80.

Hayashida-Soiza, G., Uchida, A., Mori, N., Kuwahara, Y., and Ishida, Y., 2008. Purification and characterization of antibacterial substances produced by a marine bacterium *Pseudoalteromonas haloplanktis* strain. *Journal of Applied Microbiology*, 105 (5), pp. 1672-1677.

Henson, K. E. R., Levine, M. T., Wong, E. A. H., and Levine, D. P., 2015. Glycopeptide antibiotics: evolving resistance, pharmacology and adverse event profile. *Expert Review of Anti-Infective Therapy*, 13 (10), pp. 1265-1278.

Herrero, A., Muro-Pastor, A.M. and Flores, E., 2001. Nitrogen control in cyanobacteria. *Journal of Bacteriology*, 183 (2), pp. 411-425.

Holmes, D. L., and Lightner, D. A., 1995. Synthesis and acidity constants of 13CO2H-labelled mono and dipyrrole carboxylic acids. pKa from 13C-NMR. *Tetrahedron*, 51 (6), pp. 1607-1622.

Holmes, A. H., Moore, L. S., Sundsfjord, A., Steinbakk, M., Regmi, S., Karkey, A., and Piddock, L. J., 2016. Understanding the mechanisms and drivers of antimicrobial resistance. *The Lancet*, 387 (10014), pp. 176-187.

Holzgrabe, U., Deubner, R., Schollmayer, C., and Waibel, B., 2005. Quantitative NMR spectroscopy—applications in drug analysis. *Journal of Pharmaceutical and Biomedical Analysis*, 38 (5), pp. 806-812.

Hong, C., Chen, Y., Li, L., Chen, S., and Wei, X., 2017. Identification of a key gene involved in branched-chain short fatty acids formation in natto by transcriptional analysis and enzymatic characterization in *Bacillus subtilis*. *Journal of Agricultural and Food Chemistry*, 65 (8), pp. 1592-1597.

Huang, C. B., Alimova, Y., Myers, T. M., and Ebersole, J. L., 2011. Short-and medium-chain fatty acids exhibit antimicrobial activity for oral microorganisms. *Archives of Oral Biology*, 56 (7), pp. 650-654.

Huber, R. and Stetter, K. O., 2001. Aquificales. *Encyclopedia of Life Sciences*, pp. 1-6. http://www.els.net

Huber, R., and Stetter, K. O., 2015. Thermotoga. *Bergey's Manual of Systematics of Archaea and Bacteria*, pp. 1-9.

Hussein, M.T. and Loni, O.A., 2011. Major ionic composition of Jizan thermal springs, Saudi Arabia. *Journal of Emerging Trends in Engineering and Applied Sciences*, 2 (1), pp. 190-196.

Hutzinger, O., 1969. *N*-acetyltryptamine: An artifact formed during the extraction of tryptamine. *Analytical Biochemistry*, 30 (1), pp. 153-156.

Hwang, B. K., Lim, S. W., Kim, B. S., Lee, J. Y., and Moon, S. S., 2001. Isolation and in vivo and in vitro antifungal activity of phenylacetic acid and sodium phenylacetate from *Streptomyces humidus. Applied and Environmental Microbiology*, 67 (8), pp. 3739-3745.

Hwang, A. Y., and Gums, J. G., 2016. The emergence and evolution of antimicrobial resistance: Impact on a global scale. *Bioorganic and Medicinal Chemistry*, 24 (24), pp. 6440-6445.

Iino, T., Mori, K., Uchino, Y., Nakagawa, T., Harayama, S. and Suzuki, K.I., 2010. *Ignavibacterium album* gen. nov., sp. nov., a moderately thermophilic anaerobic bacterium isolated from microbial mats at a terrestrial hot spring and proposal of *Ignavibacteria* classis nov., for a novel lineage at the periphery of green sulfur bacteria. *International Journal of Systematic and Evolutionary Microbiology*, 60 (6), pp. 1376-1382.

Ikeda, M., Yagihara, Y., Tatsuno, K., Okazaki, M., Okugawa, S., and Moriya, K., 2015. Clinical characteristics and antimicrobial susceptibility of *Bacillus cereus* blood stream infections. *Annals of Clinical Microbiology and Antimicrobials*, 14 (1), pp. 1-7.

Imhoff, J. F., 2014. Biology of Green Sulfur Bacteria. *Encyclopedia of Life Sciences,* pp. 1-12. http://www.els.net

Imhoff, J. F., 2017. Anoxygenic phototrophic bacteria from extreme environments. In *Modern Topics in the Phototrophic Prokaryotes* (pp. 427-480). Springer, Cham.

Iorio, M., Tocchetti, A., Cruz, J. C. S., Del Gatto, G., Brunati, C., Maffioli, S. I., and Donadio, S., 2018. Novel Polyethers from Screening *Actinoallomurus* spp. *Antibiotics*, 7(2), pp. 1-14.

Izunobi, J. U., and Higginbotham, C. L., 2011. Polymer molecular weight analysis by 1H NMR spectroscopy. *Journal of Chemical Education*, 88 (8), pp. 1098-1104.

Jacobs, A., 2019. Crisis looms in antibiotics as drug makers go bankrupt. *The New York Times*.

Jannasch, H. W., 2017. Isolation of extremely thermophilic, fermentative archaebacteria from deep-sea geothermal sediments. In *Bioprocessing and Biotreatment of Coal* (pp. 417-428). Routledge.

Jeon, B. S., Kim, S., and Sang, B. I., 2017. *Megasphaera hexanoica* sp. nov., a medium-chain carboxylic acid-producing bacterium isolated from a cow rumen. *International Journal of Systematic and Evolutionary Microbiology*, 67 (7), pp. 2114-2120.

Jeong, M. H., Lee, Y. S., Cho, J. Y., Ahn, Y. S., Moon, J. H., Hyun, H. N., and Kim, K. Y., 2017. Isolation and characterization of metabolites from *Bacillus licheniformis* MH48 with antifungal activity against plant pathogens. *Microbial Pathogenesis*, 110, pp. 645-653.

Kaatz, G. W., Seo, S. M., and Ruble, C. A., 1993. Efflux-mediated fluoroquinolone resistance in *Staphylococcus aureus*. *Antimicrobial Agents and Chemotherapy*, 37 (5), pp. 1086-1094.

Khalil, A., 2011. Isolation and characterization of three thermophilic bacterial strains (lipase, cellulose and amylase producers) from hot springs in Saudi Arabia. *African Journal of Biotechnology*, 10 (44), pp. 8834-8839.

Khameneh, B., Diab, R., Ghazvini, K. and Bazzaz, B.S.F., 2016. Breakthroughs in bacterial resistance mechanisms and the potential ways to combat them. *Microbial Pathogenesis*, 95, pp. 32-42.

Khiyami, M. A., Serour, E. A., Shehata, M. M., and Bahklia, A. H., 2012. Thermo-aerobic bacteria from geothermal springs in Saudi Arabia. *African Journal of Biotechnology*, 11 (17), pp. 4053-4062.

Khole, A. M., 2020. Nature's gift natural mineral water springs: A review. *International Journal for Environmental Rehabilitation and Conservation*, pp. 145-154.

Kim, Y., Cho, J. Y., Kuk, J. H., Moon, J. H., Cho, J. I., Kim, Y. C., and Park, K. H., 2004. Identification and antimicrobial activity of phenylacetic acid produced by *Bacillus licheniformis* isolated from fermented soybean, Chungkook-Jang. *Current Microbiology*, 48 (4), pp. 312-317.

Kim, S. H., Lee, C. M., and Kafle, K., 2013. Characterization of crystalline cellulose in biomass: Basic principles, applications, and limitations of XRD, NMR, IR, Raman, and SFG. *Korean Journal of Chemical Engineering*, 30 (12), pp. 2127-2141.

Klales, A., Duncan, J., Nett, E. J., and Kane, S. A., 2012. Biophysical model of prokaryotic diversity in geothermal hot springs. *Physical Review E*, 85 (2), pp. 1-11.

Kolivand, M., and Kolivand, H., 2017. Are antibiotics still the same" Wonder Drugs" they used to be, or will increasing resistance render them useless?. *Journal of Pharmaceutical, Chemical and Biological Sciences*, 5 (3), pp 147-164.

Kourkouta, L., Tsaloglidou, A., Koukourikos, K., Iliadis, C., Plati, P., and Dimitriadou, A., 2018. History of Antibiotics. *Sumerianz Journal of Medical and Healthcare*, 1 (2), pp. 51-54.

Krause, K. M., Serio, A. W., Kane, T. R., and Connolly, L. E., 2016. Aminoglycosides: an overview. *Cold Spring Harbor Perspectives in Medicine*, 6 (6), pp. 1-19.

Krishna, C., 2005. Solid-state fermentation systems—an overview. *Critical Reviews in Biotechnology*, 25 (1-2), pp. 1-30.

Kumar, S., and Varela, M. F., 2013. Molecular mechanisms of bacterial resistance to antimicrobial agents. *Chemotherapy*, 14, pp. 522-534.

Kumar, D. S., and Ray, S., 2014. Fungal lipase production by solid state fermentation-an overview. *Journal of Analytical and Bioanalytical Techniques*, 6 (230), pp. 1-10.

Kumar, A., Alam, A., Rani, M., Ehtesham, N. Z., and Hasnain, S. E., 2017. Biofilms: Survival and defense strategy for pathogens. *International Journal of Medical Microbiology*, 307 (8), pp. 481-489.

Kumar, N., Singh, N., Jaryal, R., Bhandari, C., Singh, J., Thakur, P., & Duhan, A., 2019. Purification, characterization and antibacterial spectrum of a compound produced by *Bacillus cereus* MTCC 10072. *Archives of Microbiology*, 201 (9), pp. 1195-1205.

Kümmerer, K., 2009. Antibiotics in the aquatic environment–a review–part I. *Chemosphere*, 75 (4), pp. 417-434.

Kurosawa, N., Itoh, Y.H. and Itoh, T., 2005. *Thermus kawarayensis* sp. nov., a new member of the genus *Thermus*, isolated from Japanese hot springs. *Extremophiles*, 9 (1), pp. 81-84.

Labed-Zouad, I., Labed, A., Laggoune, S., Zahia, S., Kabouche, A., and Kabouche, Z., 2015. Chemical Compositions and Antibacterial Activity of Four Essential Oils from *Ferula vesceritensis Coss.* and *Dur*. Against Clinical Isolated and Food-Borne Pathogens. *Records of Natural Products*, 9 (4), pp. 518-525.

Lacret, R., Oves-Costales, D., Gómez, C., Díaz, C., De la Cruz, M., Pérez-Victoria, I., and Reyes, F., 2015. New ikarugamycin derivatives with antifungal and antibacterial properties from *Streptomyces zhaozhouensis*. *Marine Drugs*, 13 (1), pp. 128-140.

Lashin, A. and Al Arifi, N., 2012. The geothermal potential of Jizan area, Southwestern parts of   Saudi Arabia. *International Journal of Physical Sciences*, 7 (4), pp. 664-675.

Lashin, A., Al Arifi, N., Chandrasekharam, D., Al Bassam, A., Rehman, S., and Pipan, M., 2015. Geothermal energy resources of Saudi Arabia: country update. In *Proceeding, World Geothermal Congress,* pp. 1-15.

Laxminarayan, R., Duse, A., Wattal, C., Zaidi, A. K., Wertheim, H. F., Sumpradit, N., and Greko, C., 2013. Antibiotic resistance—the need for global solutions. *The Lancet Infectious Diseases*, 13 (12), pp. 1057-1098.

Le Page, G., Gunnarsson, L., Snape, J., and Tyler, C. R., 2017. Integrating human and environmental health in antibiotic risk assessment: a critical analysis of protection goals, species sensitivity and antimicrobial resistance. *Environment Iinternational*, 109, pp. 155-169.

Lebedeva, E.V., Alawi, M., Fiencke, C., Namsaraev, B., Bock, E. and Spieck, E., 2005. Moderately thermophilic nitrifying bacteria from a hot spring of the Baikal rift zone. *FEMS Microbiology Ecology*, 54 (2), pp. 297-306.

Lekunberri, I., Subirats, J., Borrego, C.M. and Balcázar, J.L., 2017. Exploring the contribution of bacteriophages to antibiotic resistance. *Environmental Pollution*, 220, pp. 981-984.

Lele, O.H. and Deshmukh, P.V., 2016. Isolation and characterization of thermophilic *Bacillus* sp. with extracellular enzymatic activities from hot spring of Ganeshpuri, Maharashtra, India. *International Journal of Applied Research ,* 2 (5), pp. 427-430.

Lerminiaux, N. A., and Cameron, A. D., 2019. Horizontal transfer of antibiotic resistance genes in clinical environments. *Canadian Journal of Microbiology*, 65 (1), pp. 34-44.

Levy, S.B., 2002. Active efflux, a common mechanism for biocide and antibiotic resistance. *Journal of Applied Microbiology*, 92, pp. 65S-71S.

Lewis, K., 2017. New approaches to antimicrobial discovery. *Biochemical Pharmacology*, 134, pp. 87-98.

Li, S. F. Y., and Wu, Y. S., 2000. Capillary electrophoresis. *Electrophoresis*, pp. 1176-1187.

Li, L., Tan, J., and Chen, F., 2018. *Bacillus pumilus* strain LYMC-3 shows nematicidal activity against *Bursaphelenchus xylophilus* via the production of a guanidine compound. *Biocontrol Science and Technology*, 28 (12), pp. 1128-1139.

Li, H., Li, L., Chi, Y., Tian, Q., Zhou, T., Han, C., and Zhou, Y., 2020. Development of a standardized Gram stain procedure for bacteria and inflammatory cells using an automated staining instrument. *Microbiology Open*, 9 (9), pp. 1-10.

Liljestrand, J. M., Paju, S., Buhlin, K., Persson, G. R., Sarna, S., Nieminen, M. S., and Pussinen, P. J., 2017. Lipopolysaccharide, a possible molecular mediator between periodontitis and coronary artery disease. *Journal of Clinical Periodontology*, 44 (8), pp. 784-792.

Lin, Z. J., Lu, X. M., Zhu, T. J., Fang, Y. C., Gu, Q. Q., and Zhu, W., 2008. GPR12 Selections of the metabolites from an endophytic *Streptomyces* spp. associated with *Cistanches deserticola*. *Archives of Pharmacal Research*, 31 (9), pp. 1108-1114.

Liu, L., Salam, N., Jiao, J.Y., Jiang, H.C., Zhou, E.M., Yin, Y.R., Ming, H. and Li, W.J., 2016. Diversity of culturable thermophilic Actinobacteria in hot springs in Tengchong, China and studies of their biosynthetic gene profiles. *Microbial Ecology*, 72 (1), pp. 150-162.

Liu, H. Y., Hopping, G. C., Vaidyanathan, U., Ronquillo, Y. C., Hoopes, P. C., and Moshirfar, M., 2019. Polymerase chain reaction and its application in the diagnosis of infectious keratitis. *Medical Hypothesis, Discovery and Innovation in Ophthalmology*, 8 (3), pp. 152-155.

Llamas, A. M., Ojeda, C. B., and Rojas, F. S., 2007. Process analytical chemistry—application of mass spectrometry in environmental analysis: an overview. *Applied Spectroscopy Reviews*, 42 (4), pp. 345-367.

Lobanovska, M., and Pilla, G., 2017. Focus: drug development: penicillin's discovery and antibiotic resistance: lessons for the future?. *The Yale Journal of Biology and Medicine*, 90 (1), PP. 135-145.

Logan, N. A., and Vos, P. D., 2015. *Bacillus. Bergey's Manual of Systematics of Archaea and Bacteria*, pp. 1-163.

Ludwig, W., and Klenk, H. P., 2005. Overview: a phylogenetic backbone and taxonomic framework for procaryotic systematics. *Bergey's Manual of Systematic Bacteriology,* pp. 49-66.

Luxminarayan, L., Sharma, N., Viswas, A., and Khinchi, M. P., 2017. A Review on chromatography techniques. *Asian Journal of Pharmaceutical Research and Development*, 5 (2), pp.1-8.

MacGowan, A., and Macnaughton, E., 2017. Antibiotic resistance. *Medicine*, 45 (10), pp. 622-628.

Mahajan, G. B., and Balachandran, L., 2017. Sources of antibiotics: Hot springs. *Biochemical Pharmacology*, 134, pp. 35-41.

Mahrous, E. A., and Farag, M. A., 2015. Two dimensional NMR spectroscopic approaches for exploring plant metabolome: A review. *Journal of Advanced Research*, 6 (1), pp. 3-15.

Mak, K. K., and Pichika, M. R., 2019. Artificial intelligence in drug development: present status and future prospects. *Drug Discovery Today*, 24 (3), pp. 773-780.

Malanovic, N., and Lohner, K., 2016. Gram-positive bacterial cell envelopes: The impact on the activity of antimicrobial peptides. *Biochimica et Biophysica Acta-Biomembranes*, 1858 (5), pp. 936-946.

Maldonado, M. C., Corona, J., Gordillo, M. A., and Navarro, A. R., 2009. Isolation and partial characterization of antifungal metabolites produced by *Bacillus* spp. IBA 33. *Current Microbiology*, 59 (6), pp. 646-650.

Manitchotpisit, P., Bischoff, K. M., Price, N. P., and Leathers, T. D., 2013. *Bacillus* spp. produce antibacterial activities against lactic acid bacteria that contaminate fuel ethanol plants. *Current Microbiology*, 66 (5), pp. 443-449.

Manivasagan, P., Venkatesan, J., Sivakumar, K., and Kim, S. K., 2014. Pharmaceutically active secondary metabolites of marine actinobacteria. *Microbiological Research*, 169 (4), pp. 262-278.

Mărghitaş, L., Dezmirean, D., Chirilă, F., Fiţ, N., and Bobiş, O., 2011. Antibacterial activity of different plant extracts and phenolic phytochemicals tested on *Paenibacillus larvae* bacteria. *Scientific Papers Animal Science and Biotechnologies*, 44 (2), pp. 94-99.

Margolin, W., 2014. Binary Fission in Bacteria. *Encyclopedia of Life Sciences*, pp. 1-14. http://www.els.net.

Marquis, R. E., & Gerhardt, P., 2001. Bacterial endospores. *Encyclopedia of Life Sciences*, pp. 1-6. http://www.els.net.

Marti, E., Variatza, E., & Balcazar, J. L., 2014. The role of aquatic ecosystems as reservoirs of antibiotic resistance. *Trends in Microbiology*, 22 (1), pp. 36-41.

Martinez, J. L., 2014. General principles of antibiotic resistance in bacteria. *Drug Discovery Today: Technologies*, 11, pp. 33-39.

Martinez-Klimova, E., Rodríguez-Peña, K., and Sánchez, S., 2017. Endophytes as sources of antibiotics. *Biochemical Pharmacology*, 134, pp. 1-17.

Mayer, C., 2012. Bacterial cell wall recycling. *Encyclopedia of Life Sciences,* pp. 1-14. http://www.els.net.

Mayrand, D., and Bourgeau, G., 1982. Production of phenylacetic acid by anaerobes. *Journal of Clinical Microbiology*, 16 (4), pp. 747-750.

McCoy, L. S., Xie, Y., and Tor, Y., 2011. Antibiotics that target protein synthesis. *Wiley Interdisciplinary Reviews: RNA*, 2 (2), pp. 209-232.

Meerwein, M., Tarnutzer, A., Böni, M., Van Bambeke, F., Hombach, M., and Zinkernagel, A. S., 2020. Increased azithromycin susceptibility of multidrug-resistant gram-negative bacteria on RPMI-1640 agar assessed by disk diffusion testing. *Antibiotics*, 9 (5), pp. 218-227.

Mehdi, R. B. A., Shaaban, K. A., Rebai, I. K., Smaoui, S., Bejar, S., and Mellouli, L., 2009. Five naturally bioactive molecules including two rhamnopyranoside derivatives isolated from the *Streptomyces sp.* strain TN58. *Natural Product Research*, 23 (12), pp. 1095-1107.

Meletis, G., 2016. Carbapenem resistance: overview of the problem and future perspectives. *Therapeutic Advances in Infectious Disease*, 3 (1), pp. 15-21.

Mendo, S., Faustino, N. A., Sarmento, A. C., Amado, F., and Moir, A. J., 2004. Purification and characterization of a new peptide antibiotic produced by a thermotolerant *Bacillus licheniformis* strain. *Biotechnology Letters*, 26 (2), pp. 115-119.

Ming, H., Duan, Y.Y., Guo, Q.Q., Yin, Y.R., Zhou, E.M., Liu, L., Li, S., Nie, G.X. and Li, W.J., 2015. *Meiothermusroseus* sp. nov., a thermophilic bacterium isolated from a geothermal area. *Antonie Van Leeuwenhoek*, 108 (4), pp. 897-905.

Mohamed, Z.A., 2008. Toxic cyanobacteria and cyanotoxins in public hot springs in Saudi Arabia. *Toxicon*, 51 (1), pp. 17-27.

Morar, M., and Wright, G. D., 2010. The genomic enzymology of antibiotic resistance. *Annual Review of Genetics*, 44, pp. 25-51.

Mumtaz, M. Z., Barry, K. M., Baker, A. L., Nichols, D. S., Ahmad, M., Zahir, Z. A., and Britz, M. L., 2019. Production of lactic and acetic acids by *Bacillus* sp. ZM20 and *Bacillus cereus* following exposure to zinc oxide: A possible mechanism for Zn solubilization. *Rhizosphere*, 12, pp. 1-10.

Mundt, S., Kreitlow, S., and Jansen, R., 2003. Fatty acids with antibacterial activity from the cyanobacterium *Oscillatoria redekei* HUB 051. *Journal of Applied Phycology*, 15 (2-3), pp. 263-267.

Murphy, B. T., Jensen, P. R., and Fenical, W., 2012. The chemistry of marine bacteria. *Handbook of Marine Natural Products*, 1, pp. 153-189.

Mury, S. P., and Popham, D. L., 2014. Bacterial Endospores. *Encyclopedia of Life Sciences*, pp. 1-8. http://www.els.net.

Musthafa, K. S., Sivamaruthi, B. S., Pandian, S. K., and Ravi, A. V., 2012. Quorum sensing inhibition in *Pseudomonas aeruginosa* PAO1 by antagonistic compound phenylacetic acid. *Current Microbiology*, 65 (5), pp. 475-480.

Mweetwa, L. L., Adiukwu, P. C., Tshiamo, K. O., Kenaope, T., Nthusang, T., and Oluwabusola, E. T., 2021. Evaluation of factors fuelling global antimicrobial resistance and its economic and clinical burden. *African Journal of Microbiology Research*, 15 (3), pp. 125-131.

Nagia, M. M., Shaaban, M., Abdel-Aziz, M. S., El-Zalabani, S. M., and Hanna, A. G., 2012. Secondary metabolites and bioactivity of two fungal strains. *Egyptian Pharmaceutical Journal*, 11 (1), pp. 16-21.

Narayanan, S., Ramesh, S., Priya, V. V., and Gayathri, R., 2017. MSA and Phylogenetic Analysis of ABC Transporter from Bacterial Species Causing Apical Periodontitis. *Journal of Pharmaceutical Sciences and Research*, 9 (7), pp. 1217-1219.

Nguyen, F., Starosta, A. L., Arenz, S., Sohmen, D., Dönhöfer, A., and Wilson, D. N., 2014. Tetracycline antibiotics and resistance mechanisms. *Biological Chemistry*, 395 (5), pp. 559-575.

Nicolaou, K. C., and Rigol, S., 2018. A brief history of antibiotics and select advances in their synthesis. *The Journal of Antibiotics*, 71 (2), pp. 153-184.

Nigam, A., Gupta, D., and Sharma, A., 2014. Treatment of infectious disease: beyond antibiotics. *Microbiological Research*, 169 (9-10), pp. 643-651.

Okudoh, V. I., and Wallis, F. M., 2012. Enhanced recovery and identification of a tryptamine-related antibiotic produced by *intrasporangium* N8 from KwaZulu-Natal, South Africa. *Tropical Journal of Pharmaceutical Research*, 11 (5), pp. 729-737.

Oliverio, A. M., Power, J. F., Washburne, A., Cary, S. C., Stott, M. B., and Fierer, N., 2018. The ecology and diversity of microbial eukaryotes in geothermal springs. *The International Society for Microbial Ecology journal*, 12 (8), pp. 1918-1928.

O'Neill, M., McPartlin, J., Arthure, K., Riedel, S., and McMillan, N. D., 2011. Comparison of the TLDA with the Nanodrop and the reference Qubit system. *Journal of Physics-Conference Series*, 307 (1), pp1-6.

O'Neill, K., Brocks, D., and Hammell, M. G., 2020. Mobile genomics: tools and techniques for tackling transposons. *Philosophical Transactions of the Royal Society B*, 375 (1795), pp. 1-13.

Oren, A., 2009. Microbial Diversity. *Encyclopedia of Life Sciences*, pp. 1-9. http://www.els.net.

Orfali, R., and Perveen, S., 2019. New bioactive metabolites from the Thermophilic fungus *Penicillium* spp. isolated from Ghamiqa hot spring in Saudi Arabia. *Journal of Chemistry*, 2019, pp 1-7.

Overmann, J., 2007. Green sulfur bacteria *Encyclopedia of Life Sciences*, pp. 1-8. http://www.els.net.

Overmann, J., 2008. Green nonsulfur bacteria. *Encyclopedia of Life Sciences*, pp. 1-10. http://www.els.net.

Palinska, K. A., 2008. Cyanobacteria. *Encyclopedia of Life Sciences,* pp. 1-11. http://www.els.net.

Palmer, M., 2004. Cholesterol and the activity of bacterial toxins. *FEMS Microbiology Letters*, 238 (2), pp. 281-289.

Panda, A.K., Bisht, S.S., DeMondal, S., Kumar, N.S., Gurusubramanian, G. and Panigrahi, A.K., 2014. *Brevibacillus* as a biological tool: a short review. *Antonie Van Leeuwenhoek*, 105 (4), pp. 623-639.

Parasuraman S., Anish R., Balamurugan S., Muralidharan S., Kumar, K. J., and Vijayan, V., 2014. An overview of liquid chromatography-mass spectroscopy instrumentation. *Pharmaceutical Methods,* 5, (2), pp. 47-55.

Papke, R.T., Ramsing, N.B., Bateson, M.M. and Ward, D.M., 2003. Geographical isolation in hot spring cyanobacteria. *Environmental Microbiology*, 5 (8), pp. 650-659.

Perry, J. A., Westman, E. L., and Wright, G. D., 2014. The antibiotic resistome: what's new?. *Current Opinion in Microbiology*, 21, pp. 45-50.

Pidot, S. J., Coyne, S., Kloss, F., and Hertweck, C., 2014. Antibiotics from neglected bacterial sources. *International Journal of Medical Microbiology*, 304 (1), pp. 14-22.

Pitt, J. J., 2009. Principles and applications of liquid chromatography-mass spectrometry in clinical biochemistry. *The Clinical Biochemist Reviews*, 30 (1), pp. 19-34.

Plotka, M., Kapusta, M., Dorawa, S., Kaczorowska, A. K., and Kaczorowski, T., 2019. Ts2631 endolysin from the extremophilic *Thermus scotoductus* bacteriophage vB_Tsc2631 as an antimicrobial agent against Gram-negative multidrug-resistant bacteria. *Viruses*, 11 (7), pp. 1-15.

Poddar, A., and Das, S. K., 2018. Microbiological studies of hot springs in India: a review. *Archives of Microbiology*, 200 (1), pp. 1-18.

Poirel, L., Jayol, A., and Nordmann, P., 2017. Polymyxins: antibacterial activity, susceptibility testing, and resistance mechanisms encoded by plasmids or chromosomes. *Clinical Microbiology Reviews*, 30 (2), pp. 557-596.

Poole, K., 2002. Mechanisms of bacterial biocide and antibiotic resistance. *Journal of Applied Microbiology*, 92, pp. 55S-64S.

Popjak, G., Edmond, J., Anet, F. A., and Easton Jr, N. R., 1977. Carbon-13 NMR studies on cholesterol biosynthesized from [13C] mevalonates. *Journal of The American Chemical Society*, 99 (3), pp. 931-935.

Purro, M., Qiao, J., Liu, Z., Ashcraft, M., and Xiong, M. P., 2018. Desferrioxamine: gallium-pluronic micelles increase outer membrane permeability and potentiate antibiotic activity against *Pseudomonas aeruginosa*. *Chemical Communications*, 54 (99), pp. 13929-13932.

Ramalingam, A. J., 2015. History of antibiotics and evolution of resistance. *Research Journal of Pharmacy and Technology*, 8 (12), pp. 1719-1724.

Ramos, M. A. D. S., Da Silva, P. B., Spósito, L., De Toledo, L. G., Bonifácio, B. V., Rodero, C. F., and Bauab, T. M., 2018. Nanotechnology-based drug delivery systems for control of microbial biofilms: a review. *International Journal of Nanomedicine*, 13, pp. 1179-1213.

Rathee, D., Rathee, S., Rathee, P., Deep, A., Anandjiwala, S. and Rathee, D., 2011. HPTLC densitometric quantification of stigmasterol and lupeol from *Ficus religiosa*. *Arabian Journal of Chemistry*, 8, pp. 366-371.

Rather, I. A., Kim, B. C., Bajpai, V. K., and Park, Y. H., 2017. Self-medication and antibiotic resistance: Crisis, current challenges, and prevention. *Saudi Journal of Biological Sciences*, 24 (4), pp. 808-812.

Rehman, S. and Shash, A., 2005. Geothermal resources of Saudi Arabia–Country update report. *Proceedings World Geothermal Congress,* pp. 1-7

Reygaert, W. C., 2018. An overview of the antimicrobial resistance mechanisms of bacteria. *AIMS Microbiology*, 4 (3), pp. 482-501.

Roberts, M. C., and Schwarz, S., 2017. Tetracycline and chloramphenicol resistance mechanisms. In *Antimicrobial Drug Resistance* (pp. 231-243). Springer, Cham.

Robinson, T.P., Bu, D.P., Carrique-Mas, J., Fèvre, E.M., Gilbert, M., Grace, D., Hay, S.I., Jiwakanon, J., Kakkar, M., Kariuki, S. and Laxminarayan, R., 2016. Antibiotic resistance is the quintessential One Health issue. *Transactions of The Royal Society of Tropical Medicine and Hygiene*, 110 (7), pp. 377-380.

Roca, I., Akova, M., Baquero, F., Carlet, J., Cavaleri, M., Coenen, S., and Kahlmeter, G., 2015. The global threat of antimicrobial resistance: science for intervention. *New Microbes and New Infections*, 6, pp. 22-29.

Rodríguez-Rojas, A., Rodríguez-Beltrán, J., Couce, A., and Blázquez, J., 2013. Antibiotics and antibiotic resistance: a bitter fight against evolution. *International Journal of Medical Microbiology*, 303 (6-7), pp. 293-297.

Rogers, K. and Kadner R. J., MG 2017, *Bacteria,* photograph, viewed August 2017, https://www.britannica.com/science/bacteria

Rolain, J. M., Abat, C., Jimeno, M. T., Fournier, P. E., and Raoult, D., 2016. Do we need new antibiotics?. *Clinical Microbiology and Infection*, 22 (5), pp. 408-415.

Rossolini, G.M., Arena, F., Pecile, P. and Pollini, S., 2014. Update on the antibiotic resistance crisis. *Current Opinion in Pharmacology*, 18, pp. 56-60.

Roe, M.T. and Pillai, S.D., 2003. Monitoring and identifying antibiotic resistance mechanisms in bacteria. *Poultry Science*, 82 (4), pp. 622-626.

Salem, M.M.E., Ayesh, A.M., Gomaa, M.N.E.D. and Abouwarda, A.M., 2016. Isolation, and identification of thermophilic bacteria from Al-Laith hot springs and detection of their ability to produce protease enzyme, *American-Eurasian Journal Agriculture and Environment Science*, 16 (7), pp. 1227-1236.

Samra, S., Tokovenko, B., Kaszubowska, M., Makitrynskyy. R., Alali, A., Schmidt, Y., Welle, E., Gross, S., Paululat, T., Luzhetskyy, A., and Bechthold, A., 2018. Insight into *Saccharothrix espanaensis* Grown in Different Media: Transcriptome and Natural Product Analysis. *Natural Products Chemistry Research*, 6 (5), pp. 1-10.

Sanders, E. R., 2012. Aseptic laboratory techniques: plating methods. *Journal of Visualized Experiments*, (63), pp. 1-18.

Sarhan, M. A., and Alamrri, S., 2014. Characterization and Identification of Moderately Thermophilic Bacteria Isolated from Jazan Hot Springs in Saudi Arabia. *Egyptian Academic Journal of Biological Sciences, G. Microbiology*, 6 (1), pp. 67-75.

Satyanarayana, T., Raghukumar, C., and Shivaji, S., 2005. Extremophilic microbes: Diversity and perspectives. *Current Science*, 89 (1), pp. 78-90.

Sawasdee, N., Chaveerach, A., Tanee, T., Suwannakud, K. S., Ponkham, P., and Sudmoon, R., 2019. *Sauropus* species containing eudesmin and their DNA profile.. *Asian Journal of Agriculture and Biology*, 7 (3), pp. 412-422.

SCENIHR, 2009. Assessment of the antibiotic resistance effects of biocides. *Eur. Comm. Consum. Prot. DG.*, *2009*.

Schirra, H. J., and Craik, D. J., 2008. Overview of NMR in the Pharmaceutical Sciences. *Modern Magnetic Resonance*, pp. 1195-1202.

Seiple, I. B., Zhang, Z., Jakubec, P., Langlois-Mercier, A., Wright, P. M., Hog, D. T., and Myers, A. G., 2016. A platform for the discovery of new macrolide antibiotics. *Nature*, 533 (7603), pp. 338-345.

Sekhon, B. S., 2011. An overview of capillary electrophoresis: pharmaceutical, biopharmaceutical and biotechnology applications. *Journal of Pharmaceutical Education and Research*, 2 (2), pp. 1-36.

Sem, D. S., and Pellecchia, M., 2001. NMR in the acceleration of drug discovery. *Current Opinion in Drug Discovery and Development*, 4 (4), pp. 479-492.

Shaikh, S., Fatima, J., Shakil, S., Rizvi, S. M. D., and Kamal, M. A., 2015. Antibiotic resistance and extended spectrum beta-lactamases: Types, epidemiology and treatment. *Saudi Journal of Biological Sciences*, 22 (1), pp. 90-101.

Shakhatreh, M. A. K., Jacob, J. H., Hussein, E. I., Masadeh, M. M., Obeidat, S. M., Abdul-salam, F. J., and Abd Al-razaq, M. A., 2017. Microbiological analysis, antimicrobial activity, and heavy-metals content of Jordanian Ma'in hot-springs water. *Journal of Infection and Public Health*, 10 (6), pp. 789-793.

Sharma, P. K., Goel, M., Dureja, P., and Uniyal, P. L., 2010. Isolation and identification of secondary metabolites from hexane extract of culture filtrate of *Bacillus licheniformis* MTCC 7445. *Archives of Phytopathology and Plant Protection*, 43 (16), pp. 1636-1642.

Shao, S., Hu, Y., Cheng, J., and Chen, Y., 2018. Research progress on distribution, migration, transformation of antibiotics and antibiotic resistance genes (ARGs) in aquatic environment. *Critical Reviews in Bbiotechnology*, 38 (8), pp. 1195-1208.

Shively, J. M., Cannon, G. C., Heinhorst, S., Bryant, D. A., DasSarma, S., Bazylinski, D., and Dahl,   C., 2011. Bacterial and archaeal inclusions. *Encyclopedia of Life Sciences*, pp. 1-14. http://www.els.net.

Shivlata, L. and Satyanarayana, T., 2015. Thermophilic and alkaliphilic Actinobacteria: biology and potential applications. *Frontiers in Microbiology*, 6, pp. 1-29.

Shriniwas, P. P., and Subhash, T. K., 2017. Antioxidant, antibacterial and cytotoxic potential of silver nanoparticles synthesized using terpenes rich extract of *Lantana camara L.* leaves. *Biochemistry and Biophysics Reports*, 10, pp. 76-81.

Siddique, H., 2019. Bangladeshi Medicinal Plants: Ethnopharmacology, Phytochemistry and Anti-Staphylococcal Activity (Doctoral dissertation, University of East London).

Simmler, C., Napolitano, J. G., McAlpine, J. B., Chen, S. N., and Pauli, G. F., 2014. Universal quantitative NMR analysis of complex natural samples. *Current Opinion in Biotechnology*, 25, pp. 51-59.

Simpson, A. J., Simpson, M. J., and Soong, R., 2018. Environmental nuclear magnetic resonance spectroscopy: an overview and a primer. *Analytical Chemistry*, 90, pp. 628−639

Singh, R. K., Tiwari, S. P., Rai, A. K., and Mohapatra, T. M., 2011. Cyanobacteria: an emerging source for drug discovery. *The Journal of Antibiotics*, 64 (6), pp. 401-412.

Singh, S. B., Young, K., and Silver, L. L., 2017. What is an "ideal" antibiotic? Discovery challenges and path forward. *Biochemical Pharmacology*, 133, pp. 63-73.

Singh, B. P., Ghosh, S., and Chauhan, A., 2021. Development, dynamics and control of antimicrobial-resistant bacterial biofilms: a review. *Environmental Chemistry Letters*, pp. 1-11.

Sinha, R. P., and Häder, D. P., 2008. UV-protectants in cyanobacteria. *Plant Science*, 174 (3), pp. 278-289.

Skandalis, N., Maeusli, M., Papafotis, D., Miller, S., Lee, B., Theologidis, I., and Luna, B., 2021. Environmental Spread of Antibiotic Resistance. *Antibiotics*, 10 (6), pp. 640-654.

Smith, A. C., and Hussey, M. A., 2005. Gram stain protocols. *American Society for Microbiology*, 1, pp. 1-9.

Soto, S. M., 2013. Role of efflux pumps in the antibiotic resistance of bacteria embedded in a biofilm. *Virulence*, 4 (3), pp. 223-229.

Spanò, A., Laganà, P., Visalli, G., Maugeri, T. L., and Gugliandolo, C., 2016. In vitro antibiofilm activity of an exopolysaccharide from the marine thermophilic *Bacillus licheniformis* T14. *Current Microbiology*, 72 (5), pp. 518-528.

Stal, L. J., 2012. Cyanobacterial mats and stromatolites. In *Ecology of Cyanobacteria II* (pp. 65-125). Springer, Dordrecht.

Stanton, T. B., 2013. A call for antibiotic alternatives research. *Trends in Microbiology*, 21 (3), pp. 111-113.

Stetter, K.O., 2006. Hyperthermophiles in the history of life. *Philosophical Transactions of the Royal Society of London B: Biological Sciences*, 361 (1474), pp. 1837-1843.

Stuart, B., 2000. Infrared spectroscopy. *Kirk-Othmer Encyclopedia of Chemical Technology*, 14, pp. 1-20.

Sumi, C. D., Yang, B. W., Yeo, I. C., and Hahm, Y. T., 2015. Antimicrobial peptides of the genus *Bacillus*: a new era for antibiotics. *Canadian Journal of Microbiology*, 61 (2), pp. 93-103.

Szymanska-Chargot, M., and Zdunek, A., 2013. Use of FT-IR spectra and PCA to the bulk characterization of cell wall residues of fruits and vegetables along a fraction process. *Food Biophysics*, 8 (1), pp. 29-42.

Tang, S.S., Apisarnthanarak, A. and Hsu, L.Y., 2014. Mechanisms of β-lactam antimicrobial resistance and epidemiology of major community-and healthcare-associated multidrug-resistant bacteria. *Advanced Drug Delivery Reviews*, 78, pp. 3-13.

Tahir, A. A., Barnoh, N. F. M., Yusof, N., Said, N. N. M., Utsumi, M., Yen, A. M., and Sugiura, N., 2019. Microbial diversity in decaying oil palm empty fruit bunches (OPEFB) and isolation of lignin-degrading bacteria from a tropical environment. *Microbes and Environments*, pp. 1-8.

Tanwar, J., Das, S., Fatima, Z., and Hameed, S., 2014. Multidrug resistance: an emerging crisis. *Interdisciplinary Perspectives on Infectious Diseases*, 2014, pp. 1-7.

Tendulkar, S. R., Saikumari, Y. K., Patel, V., Raghotama, S., Munshi, T. K., Balaram, P., and Chattoo, B. B., 2007. Isolation, purification and characterization of an antifungal molecule produced by *Bacillus licheniformis* BC98, and its effect on phytopathogen Magnaporthe grisea. *Journal of Applied Microbiology*, 103 (6), pp. 2331-2339.

Thabit, A. K., Crandon, J. L., and Nicolau, D. P., 2015. Antimicrobial resistance: impact on clinical and economic outcomes and the need for new antimicrobials. *Expert Opinion on Pharmacotherapy*, 16 (2), pp.159-177.

Toma, A., and Deyno, S., 2015. Overview on mechanisms of antibacterial resistance. *International Journal of Research in Pharmacy and Biosciences*, 2 (1), pp. 27-36.

Tomar, R. S., Sharma, P., Sharma, A., and Mishra, R., 2015. Assessment and evalution of methods used for antimicrobial activity assay: an overview. *World Journal of Pharmaceutical Research*, 4 (5), pp. 907-934.

Trabelsi, L., Mnari, A., Abdel-Daim, M. M., Abid-Essafi, S., and Aleya, L., 2016. Therapeutic properties in Tunisian hot springs: first evidence of phenolic compounds in the cyanobacterium Leptolyngbya sp. biomass, capsular polysaccharides and releasing polysaccharides. *BMC Complementary and Alternative Medicine*, 16 (1), pp. 515.

Trujillo, M. E., 2016. Actinobacteria. *Encyclopedia of Life Sciences*, pp. 1-16. http://www.els.net.

Tuan, C. D., Huong, D. T. M., Ngan, T. B., Quyen, V. T., Brian, M., Van Minh, C., and Van Cuong, P., 2017. Secondary metabolites from *Micromonospora* sp.(G044). *Vietnam Journal of Science and Technology*, 55 (3), pp. 251-257.

Tusgul, S., Prod'hom, G., Senn, L., Meuli, R., Bochud, P. Y., and Giulieri, S. G., 2017. *Bacillus cereus* bacteraemia: comparison between haematologic and nonhaematologic patients. *New Microbes and New Infections*, 15, pp. 65-71.

Tyrrell, C., Burgess, C. M., Brennan, F. P., and Walsh, F., 2019. Antibiotic resistance in grass and soil. *Biochemical Society Transactions*, 47 (1), pp. 477-486.

Urban, P. L., 2016. Quantitative mass spectrometry: an overview. *Philosophical Transactions of The Royal Society A,* pp. 1-5.

Urbieta, M. S., Donati, E. R., Chan, K. G., Shahar, S., Sin, L. L., and Goh, K. M., 2015. Thermophiles in the genomic era: biodiversity, science, and applications. *Biotechnology Advances*, 33 (6), pp. 633-647.

Uwajima, T., and Terada, O., 1976. Production of cholesterol esterase by *Pseudomonas fluorescens*. *Agricultural and Biological Chemistry*, 40 (8), pp. 1605-1609.

Valverde, A., Tuffin, M., and Cowan, D. A., 2012. Biogeography of bacterial communities in hot springs: a focus on the actinobacteria. *Extremophiles*, 16 (4), pp. 669-679.

Van-Hoek, A.H., Mevius, D., Guerra, B., Mullany, P., Roberts, A.P. and Aarts, H.J., 2011. Acquired antibiotic resistance genes: an overview. *Frontiers in Microbiology*, 2, pp. 1-27.

Velho-Pereira, S., and Kamat, N. M., 2011. Antimicrobial screening of actinobacteria using a modified cross-streak method. *Indian Journal of Pharmaceutical Sciences*, 73 (2), pp. 223-228.

Vinokurova, N. G., Ozerskaya, S. M., Zhelifonova, V. P., and Adanin, V. M., 2000. Taxonomic position and nitrogen-containing secondary metabolites of the fungus *Penicillium vitale* pidoplichko et bilai apud bilai. *Microbiology*, 69 (3), pp. 343-346.

Volk, R.B. and Furkert, F.H., 2006. Antialgal, antibacterial and antifungal activity of two metabolites produced and excreted by cyanobacteria during growth. *Microbiological Research*, 161 (2), pp. 180-186.

Voytas, D., 2000. Resolution and recovery of large DNA fragments. *Current Protocols in Molecular Biology,* pp.1-9.

Vullo, D., De Luca, V., Scozzafava, A., Carginale, V., Rossi, M., Supuran, C.T. and Capasso, C., 2013. The alpha-carbonic anhydrase from the thermophilic bacterium *Sulfurihydrogenibium yellowstonense* YO3AOP1 is highly susceptible to inhibition by sulfonamides. *Bioorganic and Medicinal Chemistry*, 21 (6), pp. 1534-1538.

Wagner, R., and Berger, S., 1998. ACCORD–HMBC: a superior technique for structural elucidation. *Magnetic Resonance in Chemistry*, 36 (S1), pp. S44-S46.

Wali, H., Rehman, F. U., Umar, A., and Ahmed, S., 2019. Cholesterol degradation and production of extracellular cholesterol oxidase from *Bacillus pumilus* W1 and *Serratia marcescens* W8. *BioMed Research International*, 2019, pp. 1-9.

Wang, Q., Cen, Z., and Zhao, J., 2015. The survival mechanisms of thermophiles at high temperatures: an angle of omics. *Physiology*, 30 (2), pp. 97-106.

Wedge, D. E., and Nagle, D. G., 2000. A new 2D-TLC bioautography method for the discovery of novel antifungal agents to control plant pathogens. *Journal of Natural Products*, 63 (8), pp. 1050-1054.

Wencewicz, T. A., 2016. New antibiotics from Nature's chemical inventory. *Bioorganic and Medicinal Chemistry*, 24 (24), pp. 6227-6252.

Williams, R. A. D., 2021. The genus *Thermus*. In *Thermophilic Bacteria* (pp. 51-62). CRC Press.

Wilson, Z. E., and Brimble, M. A., 2009. Molecules derived from the extremes of life. *Natural Product Reports*, 26 (1), pp. 44-71.

Wishart, D., 2005. NMR spectroscopy and protein structure determination: applications to drug discovery and development. *Current Pharmaceutical Biotechnology*, 6 (2), pp. 105-120.

Wright, G. D., and Poinar, H., 2012. Antibiotic resistance is ancient: implications for drug discovery. *Trends in Microbiology*, 20 (4), pp. 157-159.

Wrighton, K. C., Agbo, P., Warnecke, F., Weber, K. A., Brodie, E. L., DeSantis, T. Z., and Coates, J. D., 2008. A novel ecological role of the Firmicutes identified in thermophilic microbial fuel cells. *The ISME journal, 2* (11), pp. 1146-1156.

Woo, C. B., Kang, H. N., and Lee, S. B., 2014. Molecular cloning and anti-fungal effect of endo-β-1, 3-glucanase from *Thermotoga maritima*. *Food Science and Biotechnology*, 23 (4), pp. 1243-1246.

Woodford, N., 2005. Biological counterstrike: antibiotic resistance mechanisms of Gram-positive cocci. *Clinical Microbiology and Infection*, 11, pp. 2-21.

Wu, Y., 2000. The use of liquid chromatography–mass spectrometry for the identification of drug degradation products in pharmaceutical formulations. *Biomedical Chromatography*, 14 (6), pp. 384-396.

Wu, C., Zhu, H., Van Wezel, G. P., and Choi, Y. H., 2016. Metabolomics-guided analysis of isocoumarin production by *Streptomyces* species MBT76 and biotransformation of flavonoids and phenylpropanoids. *Metabolomics*, 12 (5), pp. 1-11..

Yan, H., Yun, J., Ai, D., Zhang, W., Bai, J., and Guo, J., 2018. Two novel cationic antifungal peptides isolated from *Bacillus pumilus* HN-10 and their inhibitory activity against *Trichothecium roseum*. *World Journal of Microbiology and Biotechnology*, 34 (21), pp. 1-10.

Yasir, M., Qureshi, A. K., Khan, I., Bibi, F., Rehan, M., Khan, S. B., and Azhar, E. I., 2019. Culturomics-based taxonomic diversity of bacterial communities in the hot springs of Saudi Arabia. *OMICS: A Journal of Integrative Biology*, 23 (1), pp. 17-27.

Yılmaz, Ç., and Özcengiz, G., 2017. Antibiotics: Pharmacokinetics, toxicity, resistance and multidrug efflux pumps. *Biochemical Pharmacology*, 133, pp. 43-62.

Young, K. D., 2010. Bacterial cell wall. *Encyclopedia of Life Sciences*, pp. 1-10. http://www.els.net.

Young, K. D., 2011. Peptidoglycan. *Encyclopedia of Life Sciences*, pp. 1-11. http://www.els.net.

Zaffiri, L., Gardner, J., and Toledo-Pereyra, L. H., 2012. History of antibiotics. From salvarsan to cephalosporins. *Journal of Investigative Surgery*, 25 (2), pp. 67-77.

Zhang, W., Wei, S., Zhang, J., and Wu, W., 2013. Antibacterial activity composition of the fermentation broth of *Streptomyces djakartensis* NW35. *Molecules*, 18 (3), pp. 2763-2768.

Zheng, W., Sun, W., and Simeonov, A., 2018. Drug repurposing screens and synergistic drug-combinations for infectious diseases. *British Journal of Pharmacology*, 175 (2), pp. 181-191.

Zhou, S. Y., Hu, Y. J., Meng, F. C., Qu, S. Y., Wang, R., Andersen, R. J., and Chen, M., 2018. Bacillamidins A–G from a Marine-Derived *Bacillus pumilus. Marine Drugs*, 16 (9), pp. 1-11.

Zhu, Y. J., Zhou, H. T., Hu, Y. H., Tang, J. Y., Su, M. X., Guo, Y. J., and Liu, B., 2011. Antityrosinase and antimicrobial activities of 2-phenylethanol, 2-phenylacetaldehyde and 2-phenylacetic acid. *Food Chemistry*, 124 (1), pp. 298-302.

Appendix 1: NMR and MS spectra of compound OM2
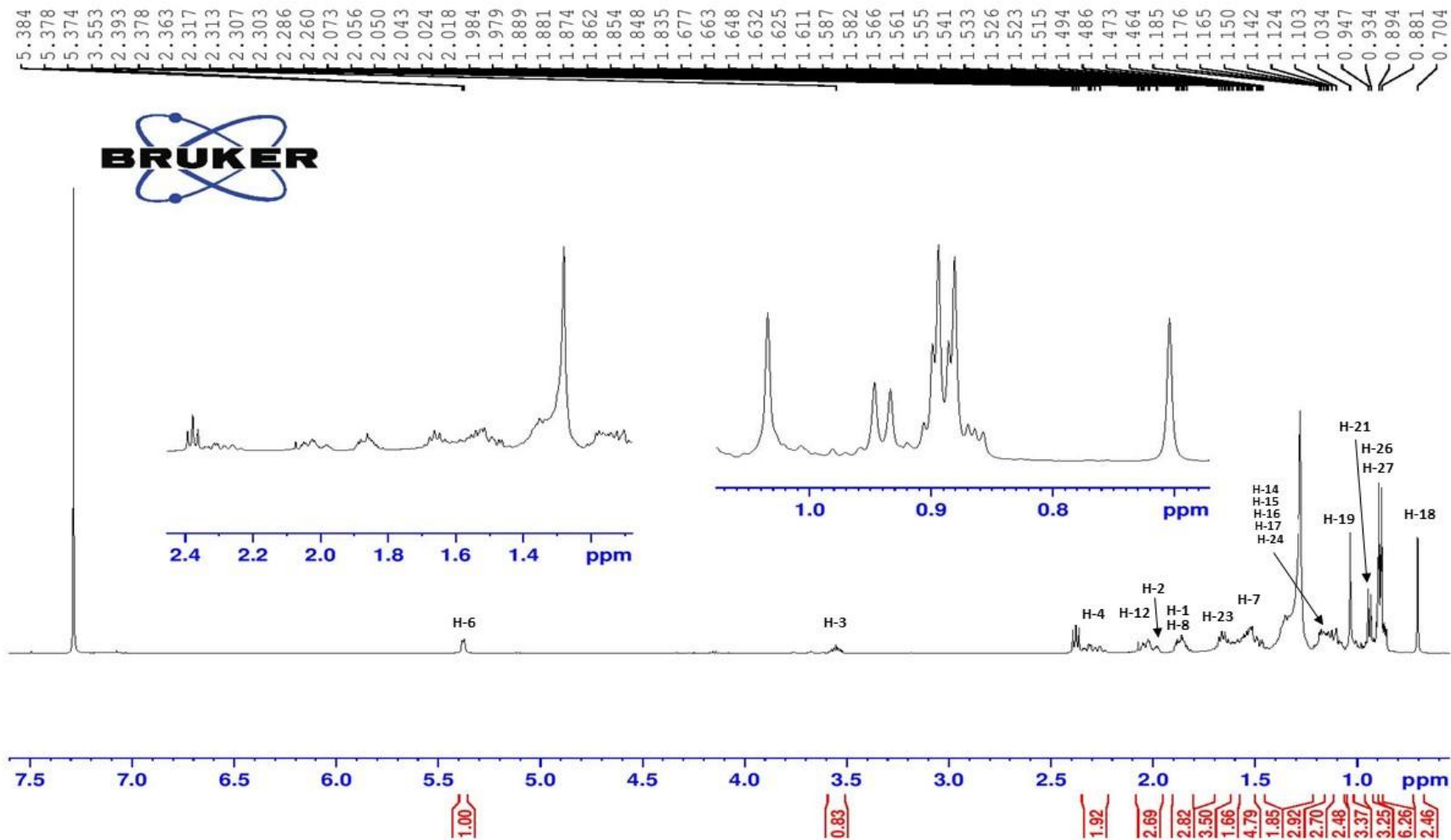
^{1}H NMR spectrum of compound OM2 recorded in CDCl$_3$ (500 MHz).
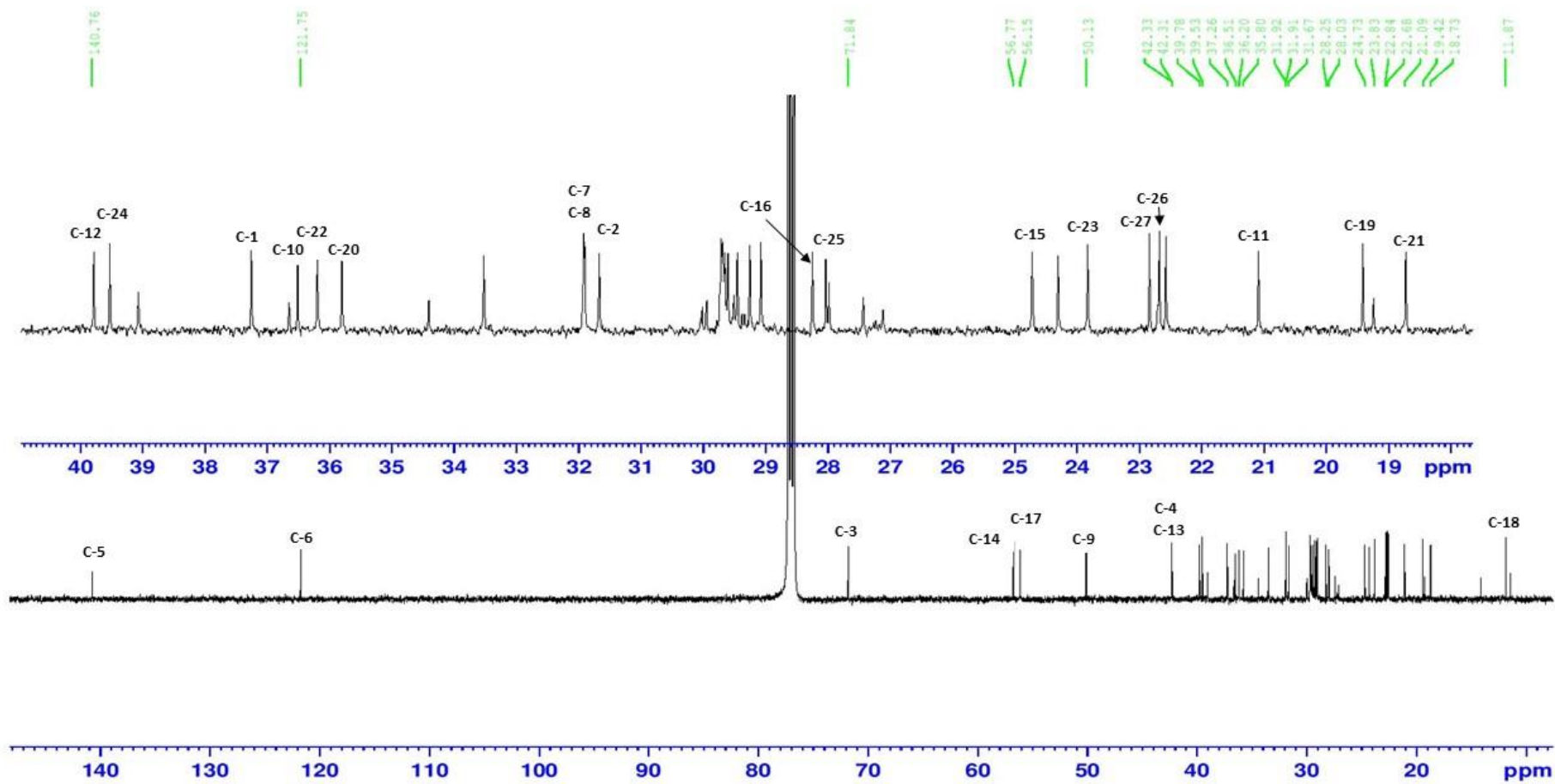
^{13}C NMR spectrum of compound OM2 recorded in CDCl$_3$ (125 MHz).
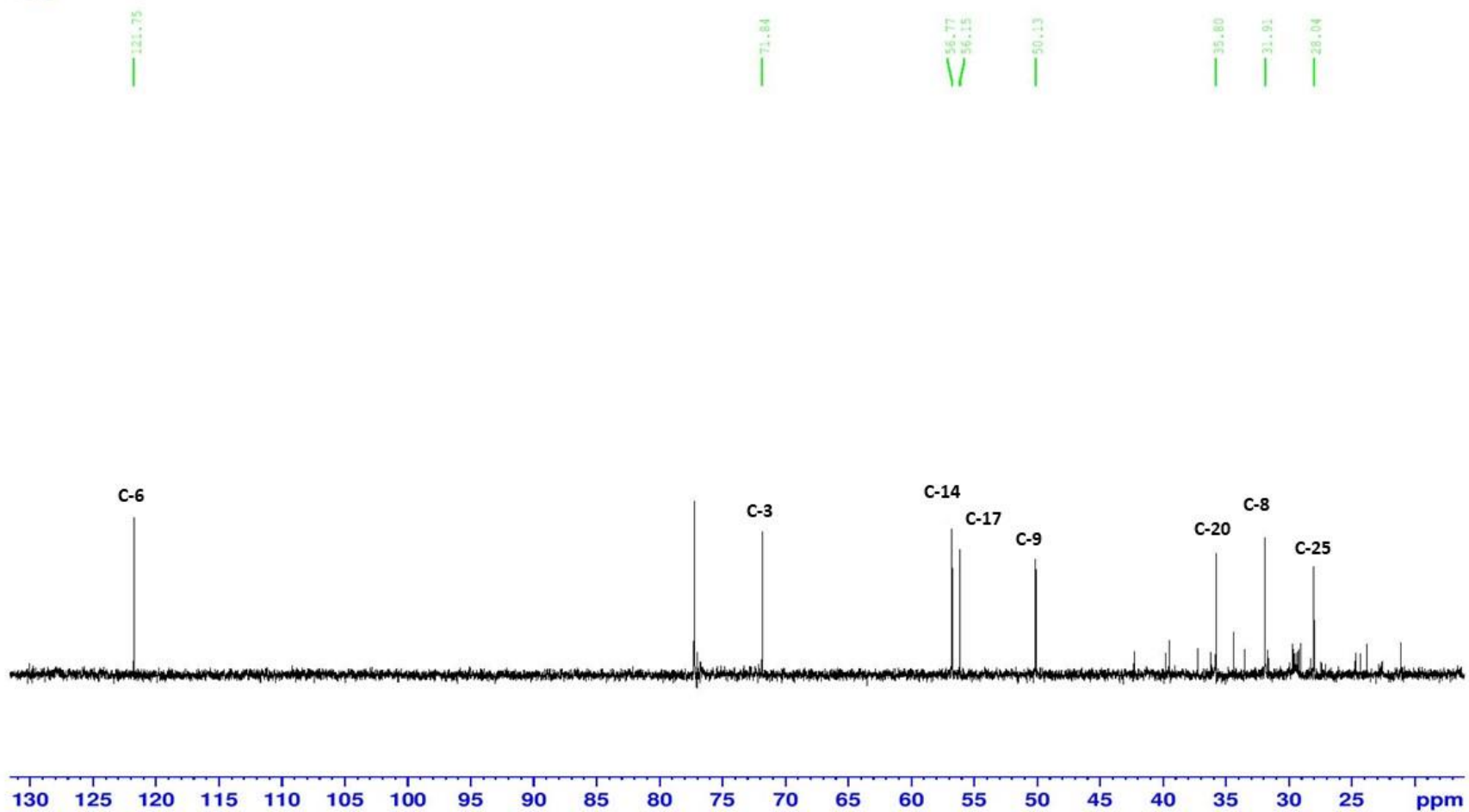
DEPT-90 spectrum of compound OM2 recorded in CDCl₃ (125 MHz).
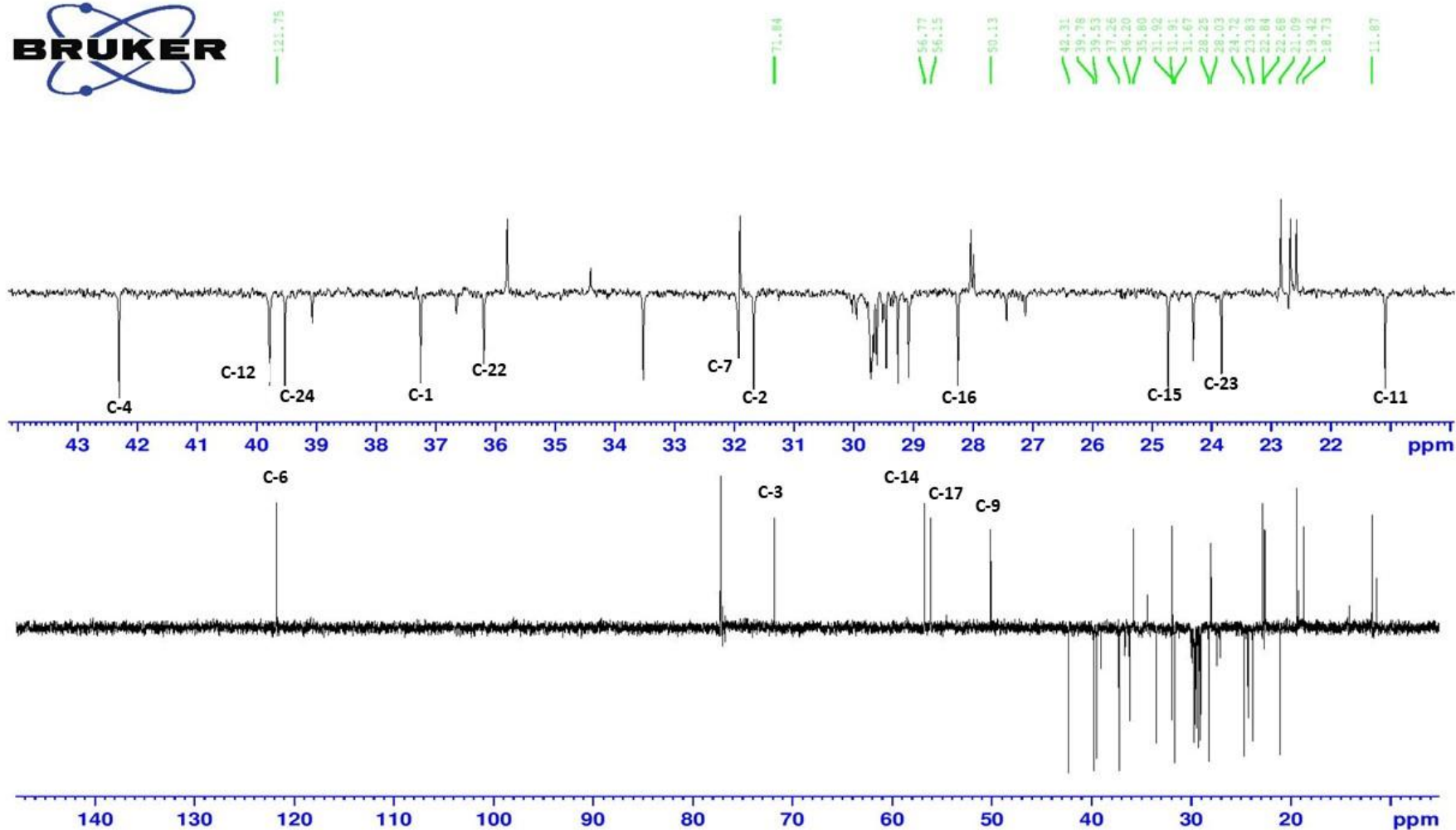
DEPT-135 spectrum of compound OM2 recorded in CDCl₃ (125 MHz).
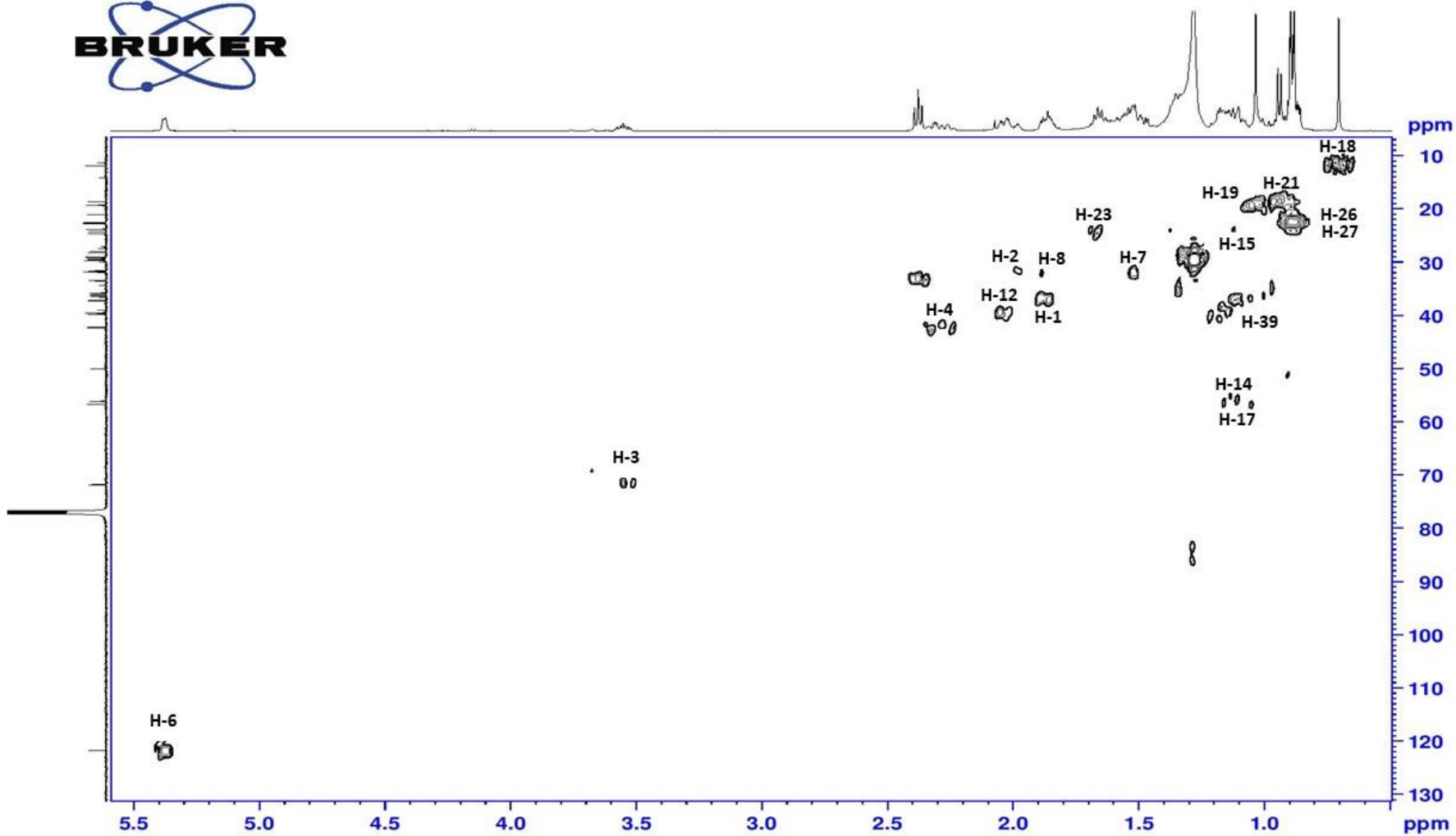
HMQC spectrum of compound OM2.
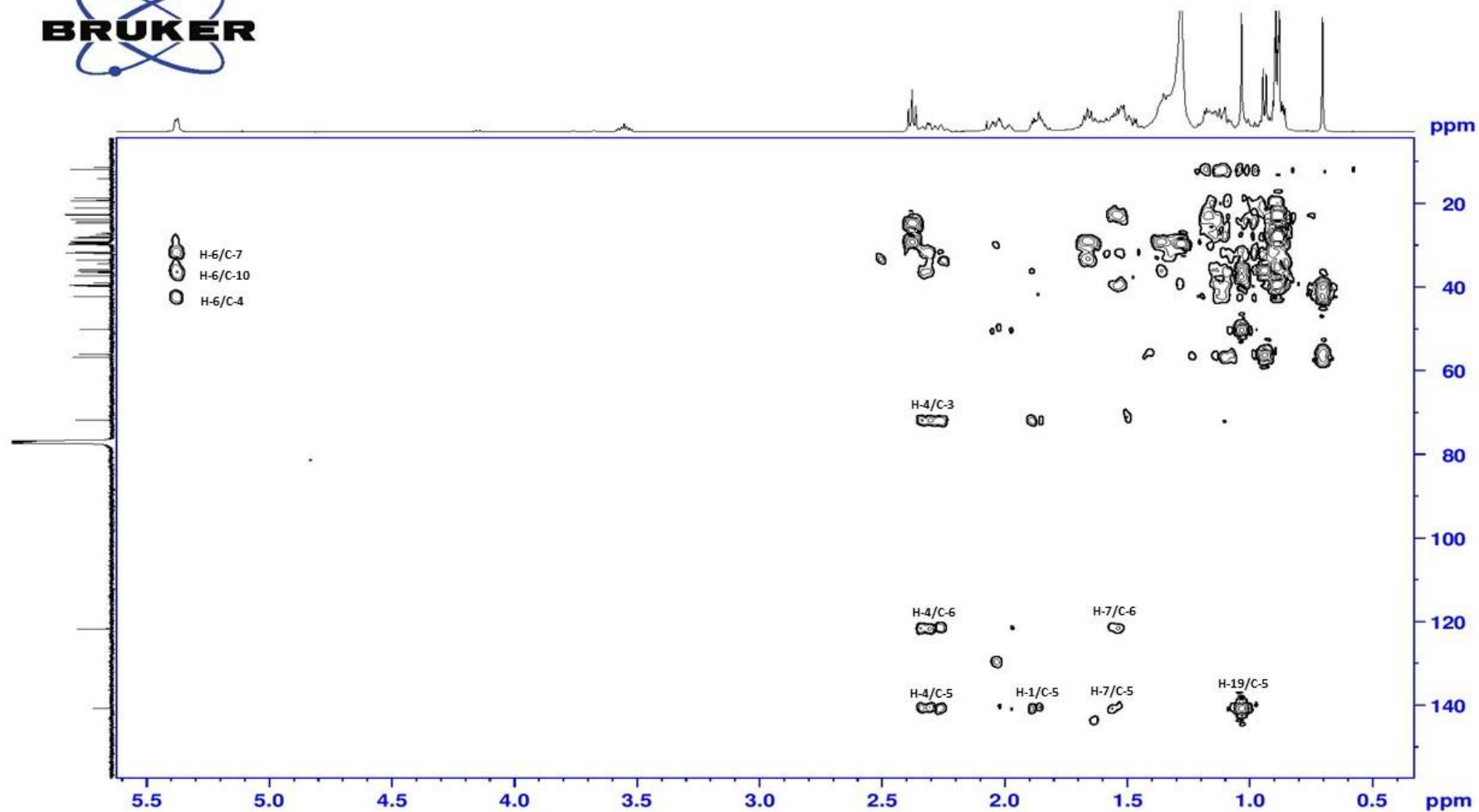
HMBC spectrum of compound OM2.
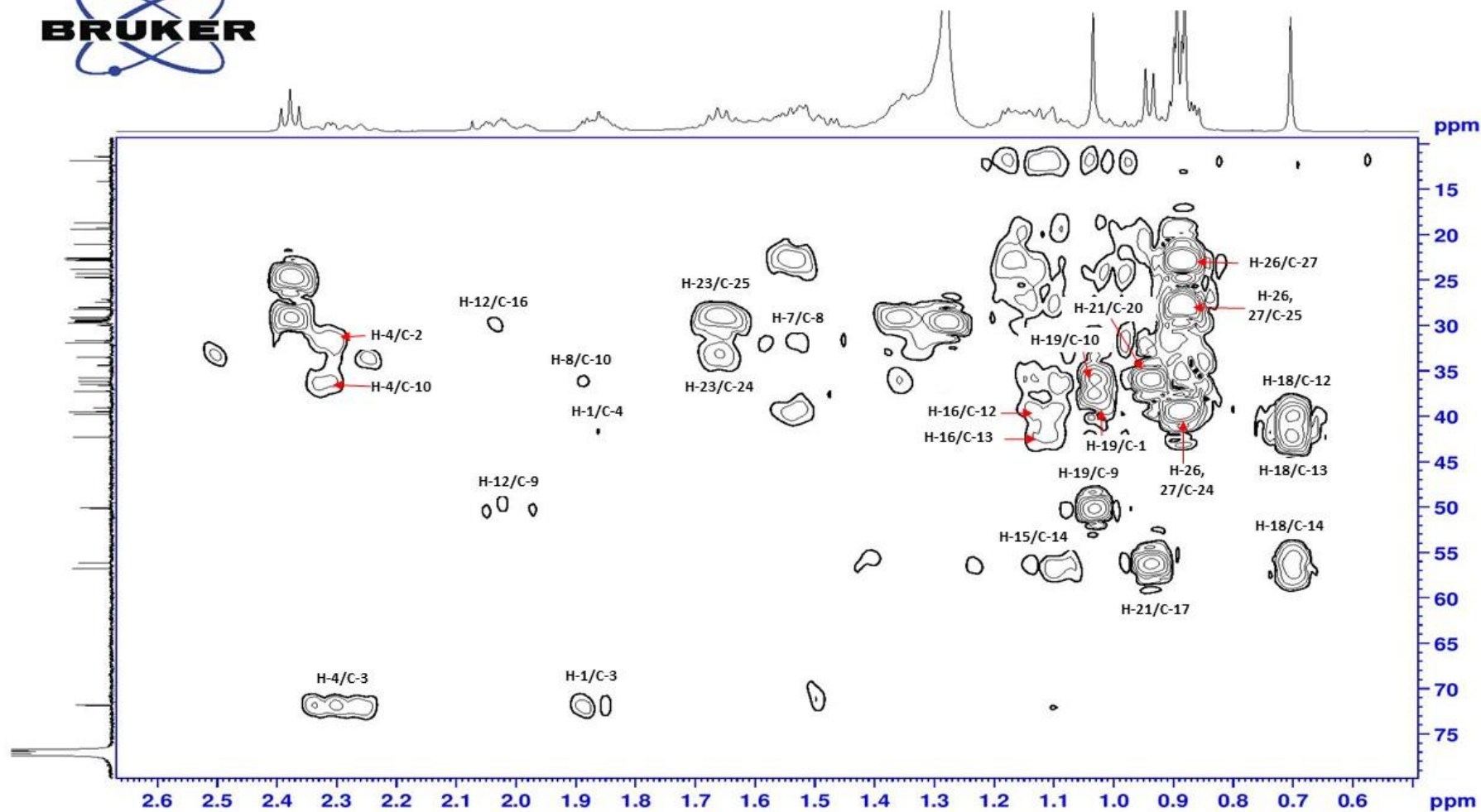
HMBC spectrum of compound OM2 (expanded).
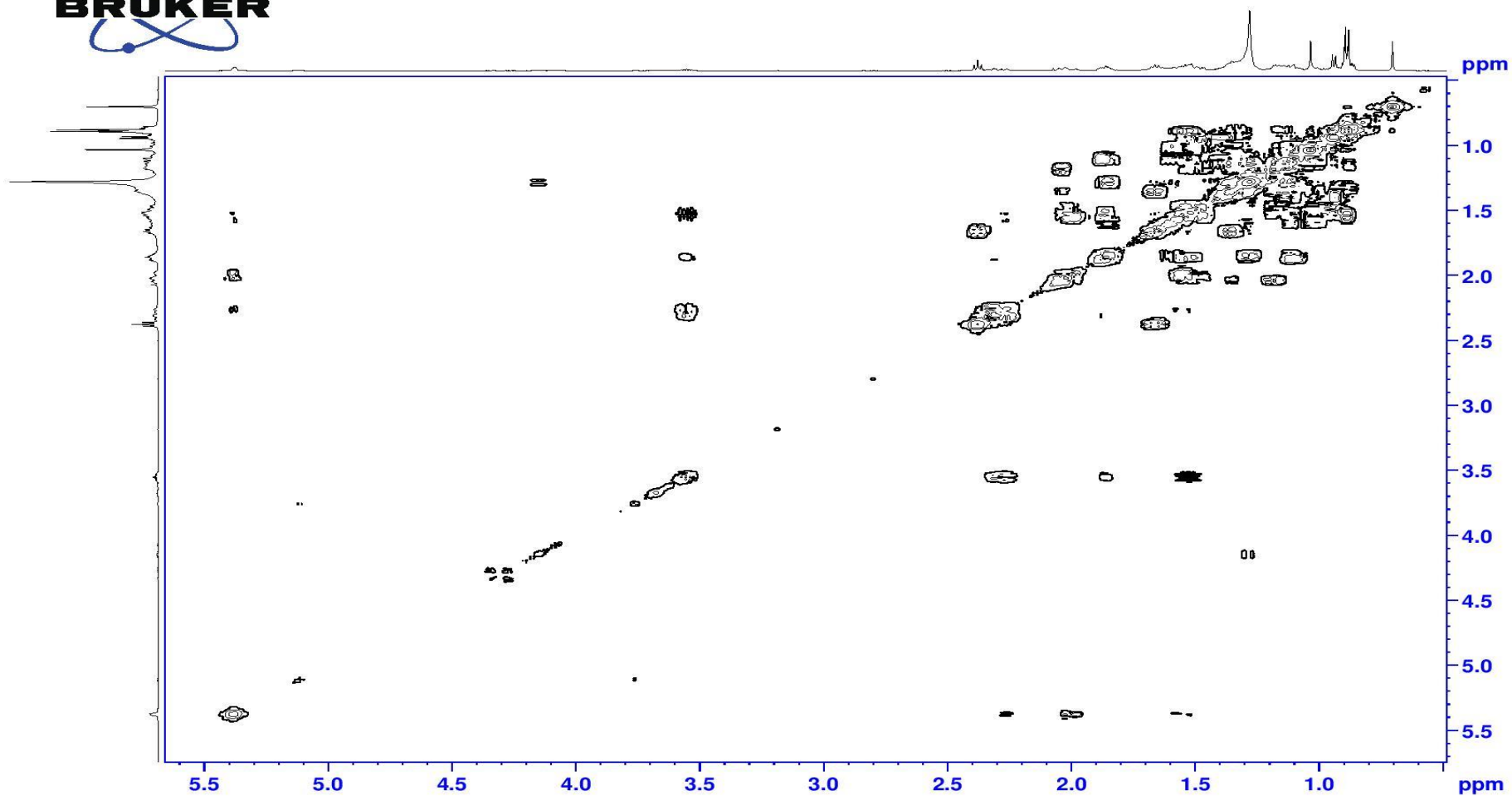
COSY spectrum of compound OM2.
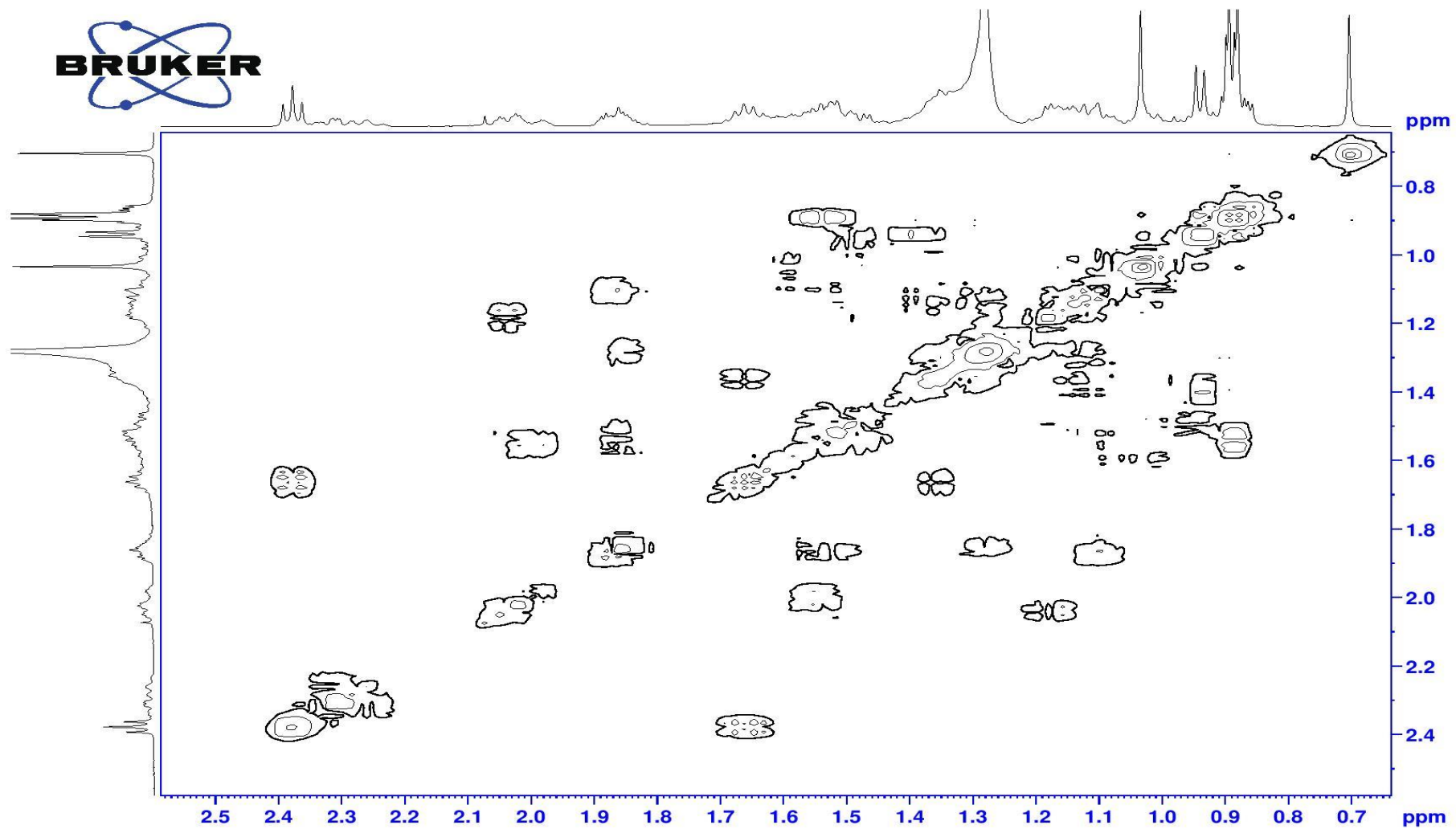
COSY spectrum of compound OM2 (expanded).
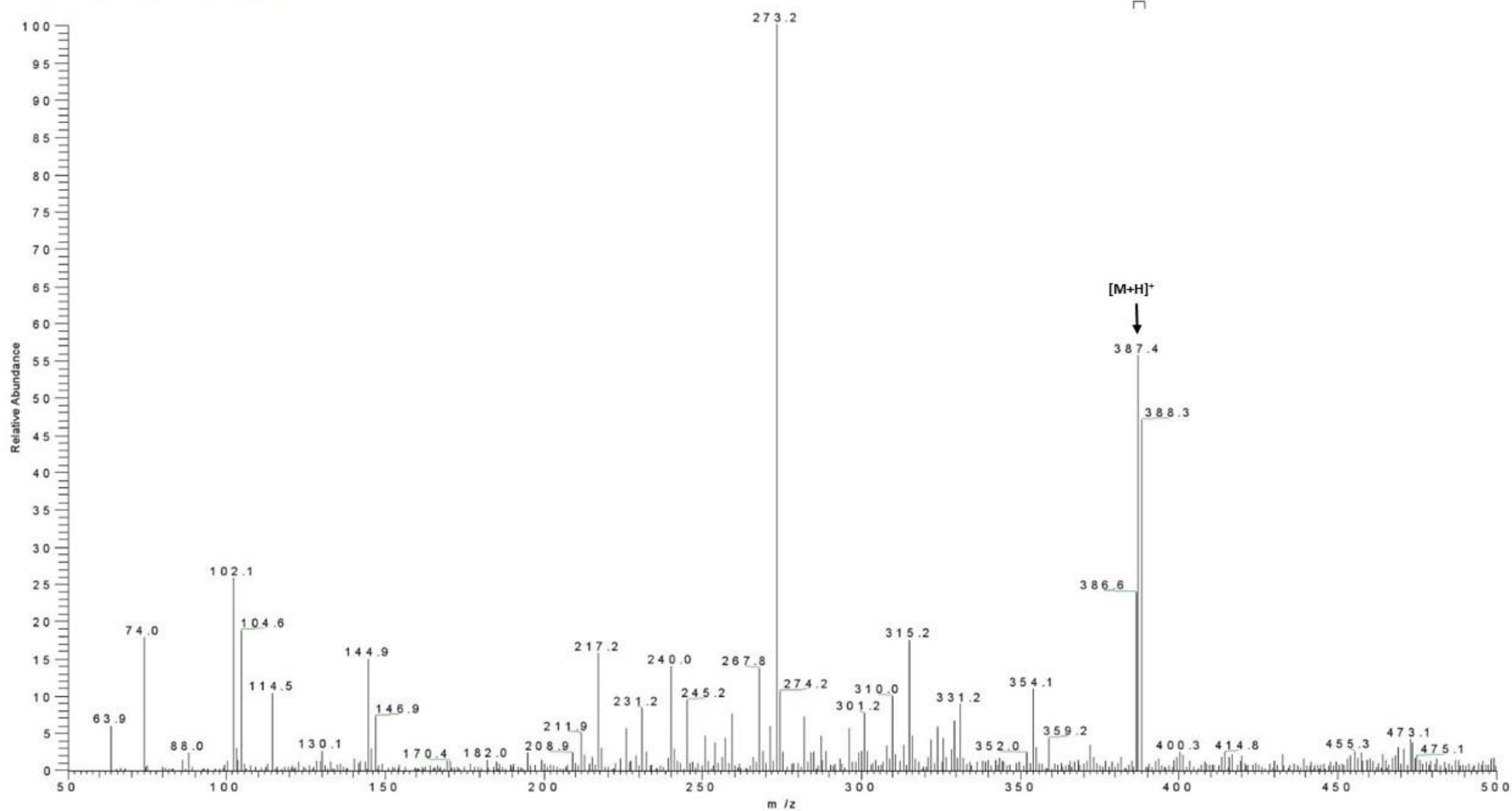
ESI-MS spectrum of compound OM2 showing peak ion at *m/z* 387.4.
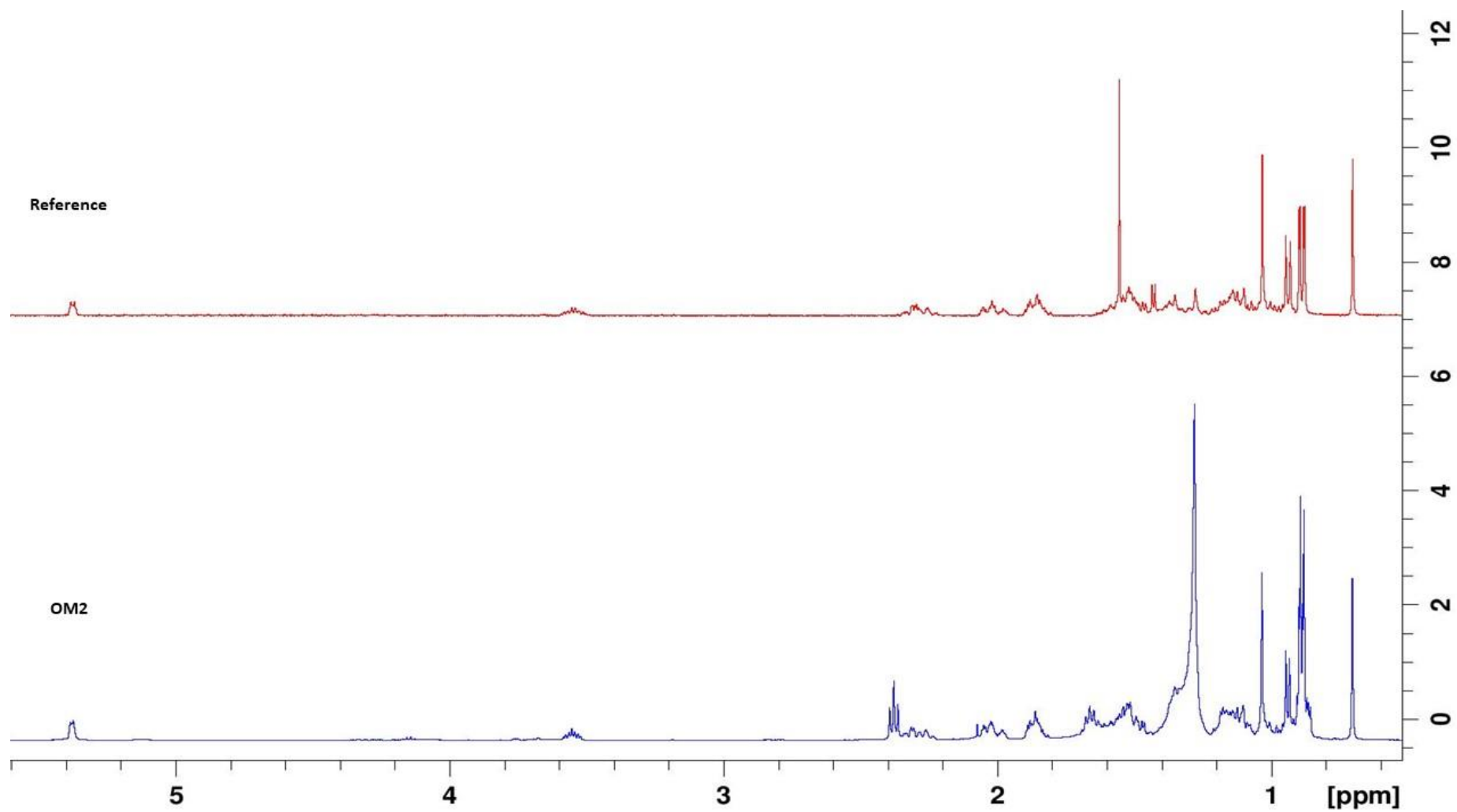
Comparison of ¹H NMR spectra of the reference (cholesterol) and compound OM2.

Appendix 2: IR spectra of isolated compounds.
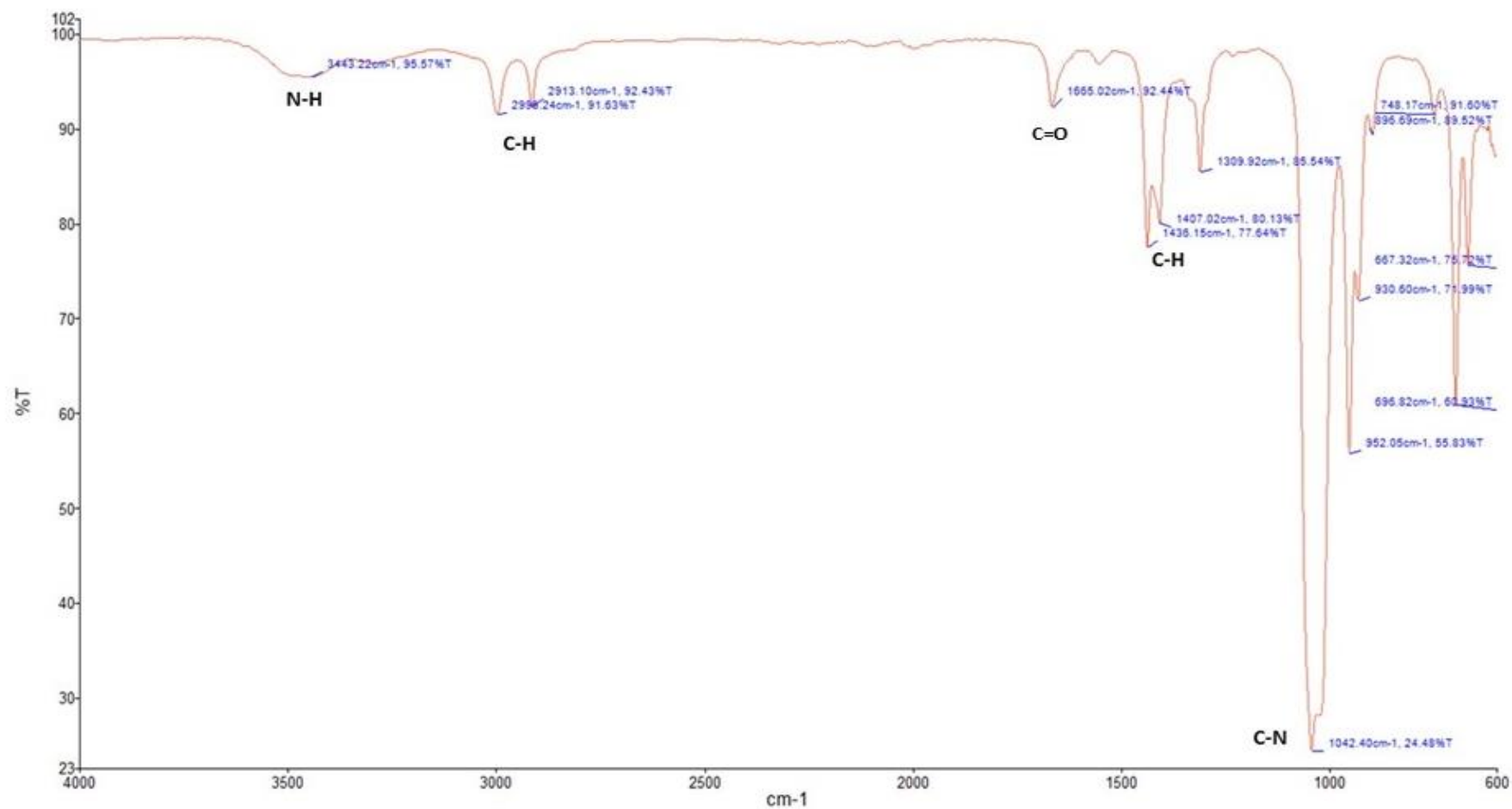
FT-IR spectrum of compound OM1.
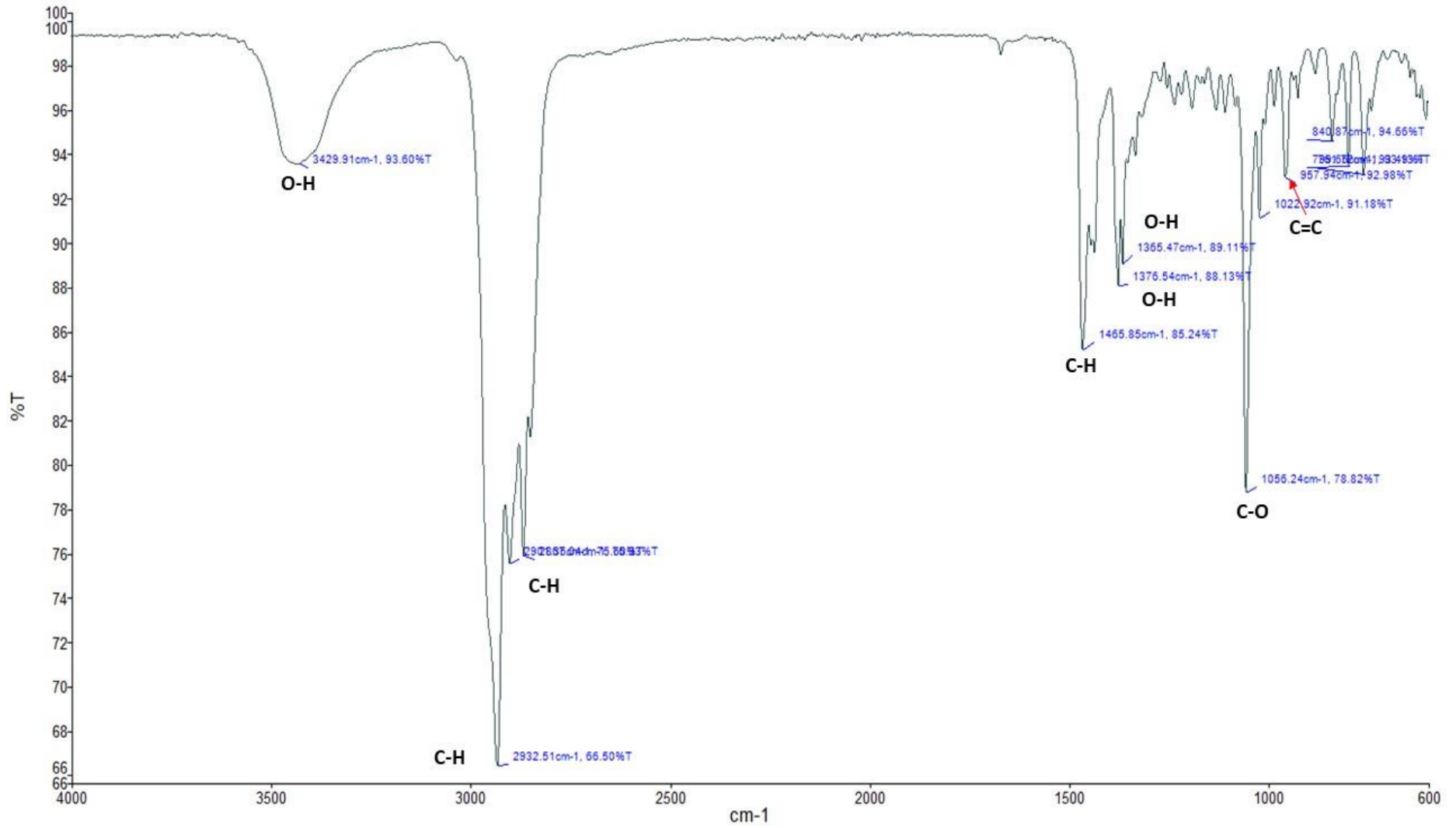
FT-IR spectrum of compound OM2.
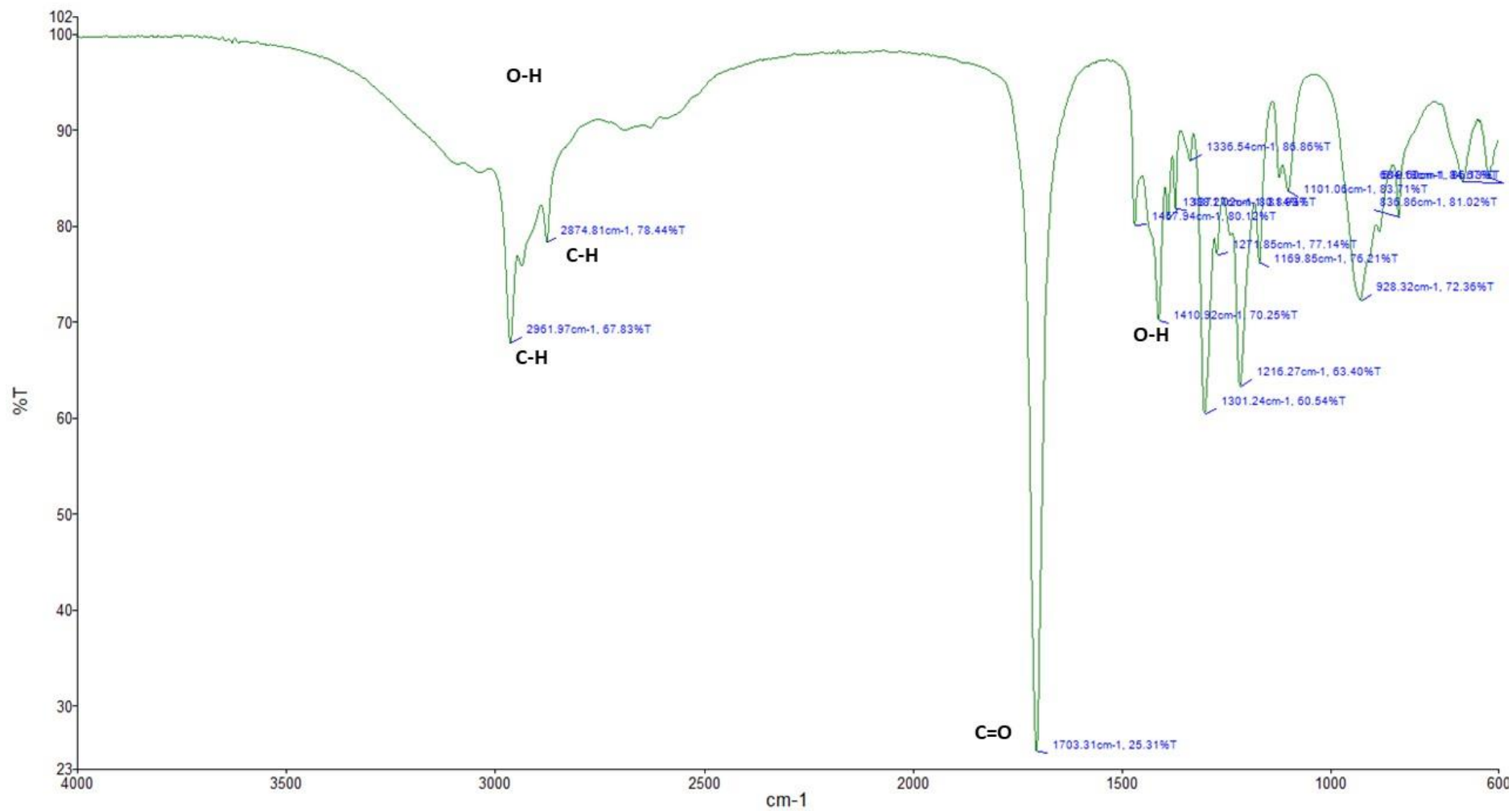
FT-IR spectrum of compound OM4.
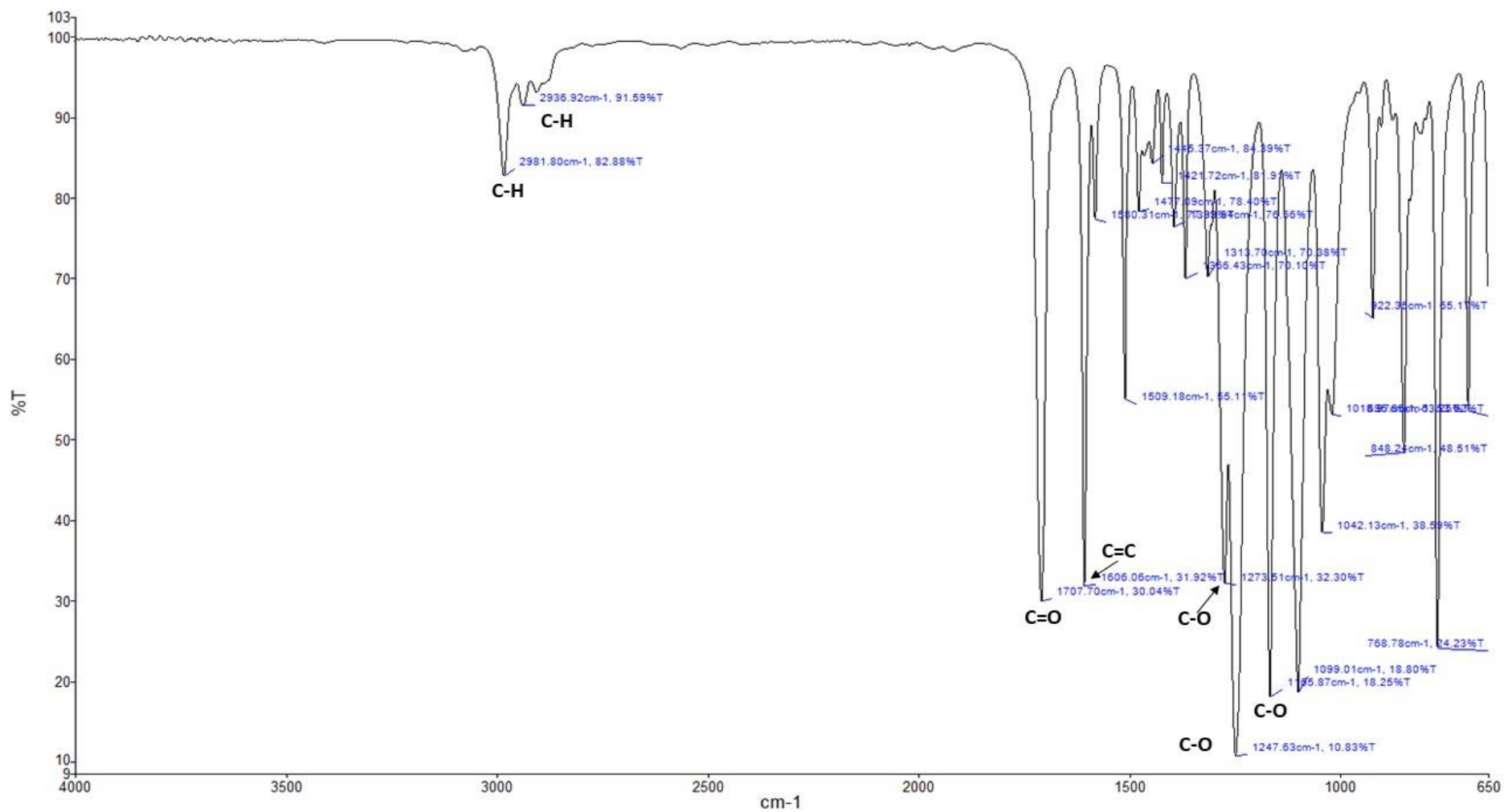
FT-IR spectrum of compound OM5.

FT-IR spectrum of compound OM7.